Efficient Ways to Valorize Biomass into Sugars & Furans: Study on the Properties of SAPO's & Metal Oxide Catalysts

A Thesis Submitted to AcSIR
For the Award of the Degree of

DOCTOR OF PHILOSOPHY
in
CHEMISTRY

By

Prasenjit Bhaumik

(Enrollment No. 10CC11J26007)

Under the guidance of

Dr. Paresh Laxmikant Dhepe

Catalysis & Inorganic Chemistry Division
CSIR-National Chemical Laboratory
Pune- 411 008, India

October, 2014

राष्ट्रीय रासायनिक प्रयोगशाला
(वैज्ञानिक तथा औद्योगिक अनुसंधान परिषद)
डॉ. होमी भाभा रोड, पुणे - 411 008. भारत
NATIONAL CHEMICAL LABORATORY
(Council of Scientific & Industrial Research)
Dr. Homi Bhabha Road, Pune - 411008. India

CERTIFICATE

Certified that the work comprised in the thesis entitled "**Efficient ways to valorize biomass into sugars & furans: study on the properties of SAPO's & metal oxide catalysts**" submitted by **Mr. Prasenjit Bhaumik**, for the award of the degree of **Doctor of Philosophy in Chemistry** to the **Academy of Scientific & Innovative Research (AcSIR)**, New Delhi, was carried out by him under my supervision/guidance at Catalysis & Inorganic Chemistry Division, CSIR-National Chemical Laboratory, Pune-411008, India. Such materials as has been obtained from other sources have been duly acknowledged in the thesis.

October, 2014

Dr. Paresh L. Dhepe
(Research Guide)
Senior Scientist, CSIR-NCL, Pune, India
Assistant Professor, AcSIR, New Delhi, India

Communications Channels ☎ +91 20 25902000 +91 20 25893300 +91 20 25893400 Fax +91 20 25902601 (Director) +91 20 25902660 (Admin.) +91 20 25902639 (Business Development) URL : www.ncl-india.org

Declaration by the candidate

I hereby declare that the thesis entitled **"Efficient ways to valorize biomass into sugars & furans: study on the properties of SAPO's & metal oxide catalysts"** submitted for the award of the degree of ***Doctor of Philosophy in Chemistry*** to the **Academy of Scientific & Innovative Research (AcSIR)**, New Delhi, has been carried out by me at Catalysis & Inorganic Chemistry Division, CSIR-National Chemical Laboratory, Pune-411008, India, under the supervision of Dr. Paresh L. Dhepe. The work is original and has not been submitted as a part or full by me for any degree or diploma to this or any other university.

October, 2014

Prasenjit Bhaumik

(Enrollment No. 10CC11J26007)

Dedicated to.....

My
Sweet Sister
&
Parents

For their warmest love, encouragement, endless support and happiness

ACKNOWLEDGEMENTS

First and foremost, it is my great pleasure to express my utmost gratitude to my research supervisor, Dr. Paresh Laxmikant Dhepe. I feel very lucky and honored that I have conducted my doctoral study under his supervision. His invaluable guidance, constant support, numerous discussion and constructive suggestions for not only in science but also to be a sensible and responsible human being nourished throughout my doctoral study. His continuous support and encouragements enlighten the path to pursue my future career goal in science. His wide knowledge, logical way of thinking and understanding has provided me a good basis for the present thesis. I salute his supporting attitude that has always led me to think and work independently and do something constructive for the science and personal life. I sincerely thank for his care and affection that I received from him in the entire period. He taught me the art of writing papers, how to put forth convincingly the main hypothesis and its successful demonstration, the use of the most appropriate words to convey the exact meaning, and so on. Finally, all I can offer him is my promise to strive hard to live up to the standards that he has set.

I am thankful to Dr. Nandini Devi for the stimulating discussions, valuable suggestions and constant encouragement and support. I convey my sincere gratitude to Dr. T. Raja, Dr. C. V. V. Satyanarayana, Dr. S. Umbarkar, Dr. C. S. Gopinath, Dr. N. M. Gupta and Dr. A. K. Kinage for helping me in every possible way.

I would like to express my thanks to my DAC committee members Dr. D. S. Reddy, Dr. A. A. Kelkar, Dr. Nandini Devi and AcSIR coordinator Dr. C. G. Suresh for their valuable suggestions and guidance during my research work.

I wish to convey my sincere gratitude to Dr. A. P. Singh, Head, Catalysis Division for not only providing the divisional facilities for use but also for helpful stimulating discussion and personal help whenever required.

I am indebted to Dr. S. P. Mirajkar, Dr. (Mrs) S. Deshpande, Ms. Samuel Violet, Mr. R. K. Jha, Mr. Purushottaman, Mr. Madhu, Dr. Tejas, Mr. Gholap, Mr. Ketan, Mr. Naren, Mr. Anuj, Mr. Pandiraj, Mr. Pankaj and all other scientific and non-scientific staff of the division and NCL for their valuable help and cooperation.

I am especially thankful to Dr. R. K. Jain (Head, Central Pulp & Paper Research Institute) for his help in analysis crop waste composition. I am very thankful to Dr. R. K. Jain's group; Dhermander, Diwakar, Sandip, Chetna, Priyanka and Vipin, it was my pleasure to work with them.

I would like to thank all my colleagues and lab mates (former and present) for their helpful hand and cheerful attitude that had made my work very easy and enjoyable. I should mention Dr. Ramakanta Sahu and Dr. Atul Prashar for their continuous support and help in each and every moment of my life. I specially thank all the present lab mates Deepa, Anup, Babasaheb, Sandip,

Richa, Manisha and Himani for their presence in all aspects of my Ph. D. career. I would like to acknowledge Anupam da, who gave me support since first time I came to NCL for the Ph. D. interview. I am thankful to him for his support and friendship throughout my Ph. D. life. I would like to thank Jijil, Rajesh, Soumya, Leena, Sourik, Monojit, Sumona, Priti, Anish, Sanjay, Atul, Nishita, Kanna, Hanmant, Sumit, Pavan, Joby, Debdatta, Bhogesh, Shrikanth, Devraji, Priyanka, Prajitha, Manoj, Raju, Anjani, Anji, Brijesh, Bihag, Nagraju, Sharath for their help and support during my doctoral study. I would like to acknowledge Debashis da, Sujit da, Anal da, Pati da, Munmun di, Partha da, Sumanta da, Krishanu da, Shyam da, Achinta da, Subha di, Arijit, Subhadip, Tamas da, Chandan da, Sanjiv da, Pravat da, Kanak da, Mrinmoy da, Arpan da, Arya da, Sudhansu da, Himadri, Saibal, Soumen, Jagadish, Ramkrishna, Jhumur, Anup, Arunava, Bikash, Tanaya, Barun and the entire Bengali group at GJ Hostel and many more in NCL for their support and friendship throughout my staying in NCL. A special thanks to Deepak, Manu, Rupa and Soumen for their help in making my week-days and weekend enjoyable. My deep thanks to my earlier roommate Deepak Jadhav, from whom I received great support and encouragement during my doctoral studies. I have spent a great and enjoyable time with my some special friends Christy, Asha, Sanil, Nuthan, Nanda, Nidhina, Deepthi, Ajay and Tanushree. I truly believe they will be very successful in the future.

I want to acknowledge my entire school teachers for their help in nurturing my mind towards higher education. I also would like to thank Prof. Tapan Kumar Mondal (former Principal, Panskura Banamali College), Prof. Pulakesh Bera (Panskura Banamali College), Prof. Pradyut Kumar Bera (Panskura Banamali College), Prof. Soumitra Mondal (Panskura Banamali College) and all other professor from my B.Sc. and M.Sc. study, who really nourished my interest in Chemistry.

I gratefully acknowledge University Grant Commission (UGC), New Delhi for providing me a research fellowship and Academy of Scientific & Innovative Research (AcSIR) for registering me for the Ph. D. degree. I would like to acknowledge director, CSIR-NCL for providing me with infrastructure and facilities, and allowing me to carry out research work in this prestigious institute, CSIR-National Chemical Laboratory, Pune.

Finally, I owe an enormous debt of gratitude to my parents and my sweet sister for their love, support, tremendous patience, trust and encouragement.

Prasenjit Bhaumik

CONTENTS

Chapter 1: *General Introduction & Literature Survey*

Chapter 2: *Catalyst Synthesis, Characterization Techniques & Catalytic Methods*

Chapter 3: *Structured Catalysts: Stable, Recyclable SAPO's for the Efficient Synthesis of C_5 Sugars & Furfural from Crop Wastes*

Chapter 4: *Amorphous Catalysts: SiO_2 & ZrO_2 Supported Metal Oxides in the Conversion of Crop Wastes to C_5 Sugars & Furfural*

Chapter 5: *One-Pot Synthesis of 5-Hydroxymethylfurfural from Biomass Derived C_6 Carbohydrates*

Chapter 6: *Summary & Conclusions*

Appendix

LIST OF SCHEMES

Chapter 1

Chapter 3

Chapter 4

Chapter 5

Chapter 6

LIST OF FIGURES

Chapter 1

Chapter 2

Chapter 3

Chapter 4

Chapter 5

Chapter 6

LIST OF TABLES

Chapter 1

Chapter 2

Chapter 3

Chapter 4

Chapter 5

ABBREVIATIONS

ALPO	Aluminophosphate
AHM	Ammonium heptamolybdate
AMT	Ammonium metatungstate hydrate
AR	Analytic Reagent
BA	Brönsted acid
BHMF	2,5-bis(hydroxymetyl)furan
CHA	Chabazite and Cyclohexyl amine
DFF	2,5-diformylfuran
DMF	2,5-dimethylfuran
DMSO	Dimethyl sulfoxide
DP	Degree of Polymerization
DPA	Di-*n*-propyl amine
EDX	Energy Dispersive X-ray
E. N.	Electronegativity
FAS	Ferrous Ammonium Sulfate
FDCA	2,5-furan dicarboxylic acid
FID	Flame Ionization Detector
FSM	Folded Sheet Mesoporous/Material
GC	Gas Chromatograph
GVL	γ-valerolactone
Hβ	Beta zeolite (H-form)
HMF	5-hydroxymethylfurfural
HMFC	5-hydroxymethyl 2-furancarboxylic acid
HMOR	Mordenite (H-form)
HPA	Heteropoly acid
HPLC	High Performance Liquid Chromatography
HT	Hydrotalcite
HTC	Hydrothermal carbonization
HUSY	Ultra Stable Zeolite Y (H-form)
HZSM	Zeolite Socony Mobil (H-form)
ICP-OES	Inductively Coupled Plasma-Optical Emission Spectroscopy
IR	Infra-Red
LA	Lewis acid

LCA	Life Cycle Assessment
MAS	Magic Angle Spinning
MCM	Mobil Corporation/Composite Mesoporous/Material
MIBK	Methyl *iso*-butyl ketone
NMR	Nuclear Magnetic Resonance
OD	Oven Dried
PHL	Pre Heated Liquid
RB flask	Round Bottom flask
RID	Refractive Index Detector
RT	Room Temperature
SAPO	Silicoaluminophosphate
SBA	Santa Barbara Amorphous
SDA	Structure Directing Agent
SEM	Scanning Electron Microscopy
SG	Sol-Gel
SGO	Sulfonated graphene oxide
TAPPI	Technical Association of the Pulp and Paper Industry
TEM	Transmission Electron Microscopy
TEOS	Tetraethyl orthosilicate
TGA	Thermal Gravimetric Analysis
THF	Tetrahydrofuran
TPD	Temperature Programmed Desorption
USDA	United States Department of Agriculture
US DOE	United States Department of Energy
UV-Vis	Ultra Violet-Visible
WI	Wet-Impregnation
XPS	X-Ray Photoelectron Spectroscopy
XRD	X-Ray Diffraction
ZDCT	Zero Day Crystallization Time
2DCT	2 Days Crystallization Time
4DCT	4 Days Crystallization Time
7DCT	7 Days Crystallization Time

Abstract of Thesis

Introduction

In the green chemistry aspects, replacement of dwindling non-renewable fossil reserves with sustainable renewable resource, biomass is necessary to secure the society need of chemicals as well as to protect our environment from global warming. Moreover, it is estimated that the worldwide production of plant derived non-edible (lignocelluloses) biomass including agricultural and forest residues is ca. 1.8×10^{12} tones.[1] In view of this it would be natural that researchers are looking at biomass for the synthesis of chemicals.[2] However, to minimize food crisis, it will be preferable to use non-edible biomass such as woody or lignocellulosic biomass to synthesize chemicals. The lignocellulosic biomass are mainly made up of cellulose (ca. 45%; polymer of β-1,4-D-glucose), hemicellulose (ca. 25%; polymer of C_5 and C_6 sugars) and lignin (ca. 20%; aromatic polymer) with some minor ingredients such as nutrients, proteins and wax.[3,4]

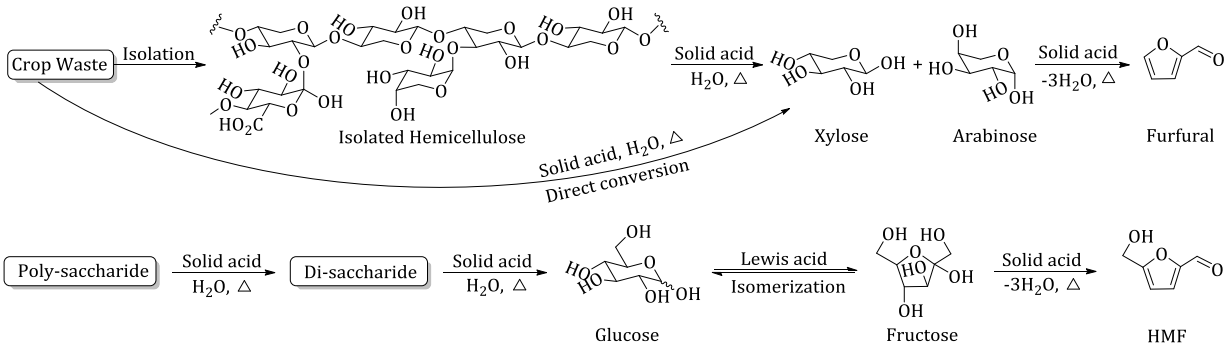

Scheme 1. Synthesis of furfural and HMF from various substrates using solid acid catalyst.

The hydrolysis of polysaccharides (cellulose and hemicelluloses) can yields monosaccharides (C_6 and C_5 sugars) which in turn upon dehydration reaction can yield industrially very important chemical, 5-hydroxymethylfurfural (HMF) and furfural (Scheme 1).[3,5,6] Hence in my work synthesis of sugars (C_5 & C_6) and furans (HMF & furfural) from lignocellulosic biomass was undertaken.

Excluding introduction chapter my thesis is divided into 5 chapters which discuss the details on synthesis of various solid acid catalysts, characterizations, catalytic details, reaction results for synthesis of sugars and furans from biomass, catalyst structure-activity correlations, overall summary and novelty of work.

Statement of Problem

There are several issues with the current available reports for the synthesis of sugars (C_5 and C_6) and furans (HMF and furfural). Those are mentioned below.

- Use of homogeneous acid catalyst: face serious drawbacks such as difficulty in recovering the catalyst, environmental issues, toxicity, corrosiveness etc.[7,8]
- Use of edible sugars: may create food crisis in society.[5,6]
- Use of multiple reactors for biomass processing; need additional set-up.[9,10]
- Low yield and selectivity for desired products.[5,11]
- Purification of desired product.[5,11]
- Stability of catalyst: to obtain recyclable activity.[5,11,12]

Based on the above mentioned drawbacks, it is essential to develop a methodology for the synthesis of sugars and furans from lignocelluloic biomass in a one-pot process. Also, for this process stable solid acid catalysts need to be developed to obtain better catalytic activity and recyclability of catalysts. Moreover, it is essential to develop a simpler strategy to isolate desired product in pure form.

Methodology Used

- Synthesis of acidic hydrothermally stable structured silicoaluminophosphate (SAPO) catalysts (SAPO-44, SAPO-46, SAPO-5, SAPO-11) by hydrothermal method.

- Synthesis of amorphous supported metal oxide catalysts having acidic properties using various metals (W, Mo, Ga, P, B), supports (SiO_2, ZrO_2) and synthesis methods (wet-impregnation, sol-gel).
- Detail characterizations of all the catalysts using XRD, NMR, IR, Raman, XPS, TPD-NH_3, N_2 sorption, ICP-OES, UV-Vis, SEM, TEM, TGA techniques.
- Detail composition analysis of collected seven crop wastes (bagasse: 3 types, rice husk: 3 types, wheat straw: 1 type).
- Use of all the catalysts for synthesis of sugars and furans from isolated hemicelluloses, crop wastes and C_6 carbohydrates.
- Purification methodology for furans from reaction mixture

Sample Results

Structured SAPO's and other solid acid catalysts (zeolites, resins, Nb_2O_5) are screened for the synthesis of C_5 sugars & furfural from isolated hemicelluloses and crop wastes.[13,14] In an efficient one-pot methodology, at 170°C and in presence of water+toluene (1:2 *v/v*), the best active catalyst SAPO-44 converts either isolated hemicelluloses or pentosan part of un-purified crop wastes (bagasse, rice husk & wheat straw) into extraordinarily high yields of furfural (82-93%). Influence of hydrophilic property of catalyst in reaction system is shown where due to higher hydrophilicity, SAPO-44 tends to remain in water layer and hence, stay separated from the formed furfural extracted in organic layer which lessens

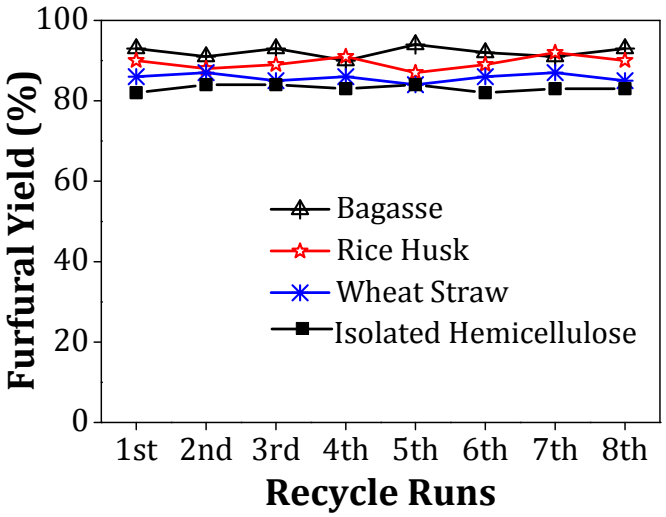

Fig. 1 Recycle study of SAPO-44 catalyst for furfural synthesis from various substrates. SAPO-44 (0.05 g), water+toluene (1:2 *v/v*), 170°C, 10/8

side reactions. Presence of optimized strong acid sites in SAPO-44 allows it to provide higher catalytic activity in reaction.[15] Due to higher hydrothermal stability, SAPO-44 showed a constant recycle activity minimum up to 8th runs with all the substrates (Fig. 1). Formed furfural was easily isolated with 79% yield in purest form (confirmed with NMR analysis) after simply evaporation of toluene. Various physico-chemical characterizations for both fresh and spent SAPO-44 are described to enlighten its stability. Hence, it can be concluded that successful use of stable structured catalyst, SAPO-44 for the efficient conversion of crop wastes into furfural is attained.

Various amorphous supported metal oxide catalysts having Lewis acidity are evaluated for the synthesis of C_5 sugars and furfural. Amongst all the catalysts evaluated, 10 *wt*% WO_3/SiO_2 (SG) showed maximum furfural yield of 72-86% directly from isolated hemicelluloses and pentosan part of un-purified crop wastes (Fig. 2).[16,17] Higher activity for WO_3/SiO_2 (SG) catalyst is explained in terms of higher acid strength of catalyst as determined by Hammett function calculation. Moreover, it is revealed that SiO_2 supported catalysts showed superior performance than the ZrO_2 supported ones and that catalysts prepared by SG method exhibited better activity compared to WI method in the synthesis of furfural. Further, all the substrates were used for recycling experiment in presence of WO_3/SiO_2 (SG) and the results showed a constant catalytic activity. Several characterizations were demonstrated to assure catalyst stability under reaction conditions. Finally, it can be concluded that the purpose of using amorphous (non-structured) supported metal oxides was successfully achieved as it showed high activity as well as stability.

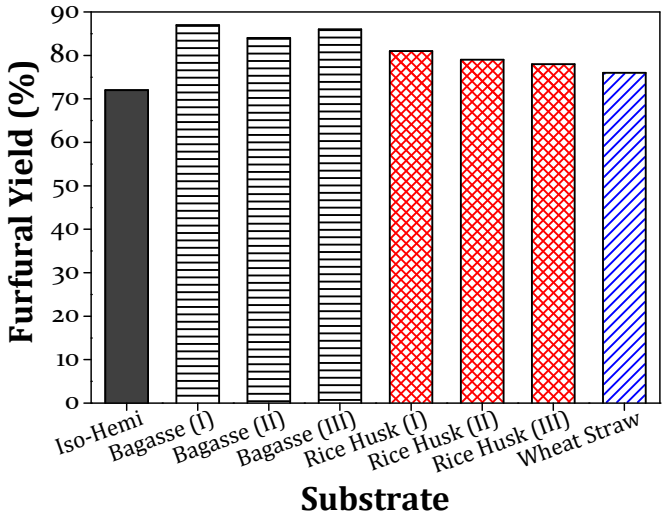

Fig. 2 One-pot synthesis of furfural from various substrates. WO_3/SiO_2 (SG) (0.05 g), water+toluene (1:2 *v/v*), 170°C, 10/8 h.

Table 1 One-pot conversion of mono-, di- and polysaccharide into HMF using SAPO-44 catalyst.

Substrate	Reaction Time (h)	Conversion (%)	Fructose Yield (%)	Glucose Yield (%)	HMF Yield (%)
Fructose	1	89	-	6	78
Glucose	4	83	13	-	67
Maltose	4	ca. 99	9	5	57
Cellobiose	6	ca. 99	5	7	56
Starch	6	ca. 99	7	15	68

Reaction conditions: substrate (10 *wt*%), 175°C, water+MIBK (1:5 *v/v*).

Structured SAPO's were evaluated further for the synthesis of HMF from one-pot conversion of mono-, di- and poly-saccharide in water+MIBK at 175°C.[18,19] Higher hydrophilic SAPO-44 having both Brönsted and Lewis acid sites allows high HMF yield from all the substrates (Table 1). Repeated reaction with SAPO-44 showed a marginal decrease in HMF yields up to 3rd run and afterwards constant activity was observed up to 5th run however, HMF selectivity remained similar (80-88%). Studies on the catalyst characterizations revealed that SAPO-44 undergoes slight modifications in its structure. However, ICP-OES data suggests that Al and/or P are not leached out in the solution indicating that change in local environment around elements is possible. The influence of acid amount, type of acid site etc. on the catalytic activity is discussed and found out that strong acid sites are required to boost the HMF yields.

References

(1) Fan, L. T.; Gharpuray, M. M.; Lee, Y. H. *Cellulose Hydrolysis*; Springer Berlin Heidelberg: Berlin, 1987; Vol. 3.

(2) Lucia-Lucian, A.; Argyropoulos-Dimitris, S.; Adamopoulos, L.; Gaspar-Armindo, R. In *Materials, Chemicals, and Energy from Forest Biomass*; American Chemical Society: 2007; Vol. 954, p 2.

(3) Kobayashi, H.; Fukuoka, A. *Green Chem.* **2013**, *15*, 1740.

(4) Maki-Arvela, P.; Salmi, T.; Holmbom, B.; Willfor, S.; Murzin, D. Y. *Chem. Rev.* **2011**, *111*, 5638.

(5) Hu, L.; Zhao, G.; Hao, W.; Tang, X.; Sun, Y.; Lin, L.; Liu, S. *RSC Adv.* **2012**, *2*, 11184.
(6) Dutta, S.; De, S.; Saha, B.; Alam, M. I. *Catal. Sci. Technol.* **2012**, *2*, 2025.
(7) Lima, S.; Neves, P.; Antunes, M. M.; Pillinger, M.; Ignatyev, N.; Valente, A. A. *Appl. Catal. A: Gen.* **2009**, *363*, 93.
(8) Binder, J. B.; Blank, J. J.; Cefali, A. V.; Raines, R. T. *ChemSusChem* **2010**, *3*, 1268.
(9) Gurbuz, E. I.; Gallo, J. M. R.; Alonso, D. M.; Wettstein, S. G.; Lim, W. Y.; Dumesic, J. A. *Angew. Chem. Int. Ed.* **2013**, *52*, 1270.
(10) Kusema, B. T.; Hilmann, G.; Maki Arvela, P.; Willfor, S.; Holmbom, B.; Salmi, T.; Murzin, D. *Catal. Lett.* **2011**, *141*, 408.
(11) Rosatella, A. A.; Simeonov, S. P.; Frade, R. F. M.; Afonso, C. A. M. *Green Chem.* **2011**, *13*, 754.
(12) Sahu, R.; Dhepe, P. L. *ChemSusChem* **2012**, *5*, 751.
(13) Bhaumik, P.; Dhepe, P. L. *ACS Catal.* **2013**, *3*, 2299.
(14) Bhaumik, P.; Dhepe, P. L. *RSC Adv.* **2014**, *4*, 26215.
(15) Bhaumik, P.; Dhepe, P. L. *Manuscript under revision* **2014**.
(16) Bhaumik, P.; Kane, T.; Dhepe, P. L. *Catal. Sci. Technol.* **2014**, *4*, 2904.
(17) Bhaumik, P.; Dhepe, P. L. *Manuscript in preparation* **2014**.
(18) Bhaumik, P.; Dhepe, P. L. *RSC Adv.* **2013**, *3*, 17156.
(19) Bhaumik, P.; Deepa, A. K.; Kane, T.; Dhepe, P. L. *J. Chem. Sci.* **2014**, *126*, 373.

CHAPTER-1

GENERAL INTRODUCTION & LITERATURE SURVEY

1.1 Introduction to Topic

Chemicals play a major role in our daily life. Our regular personal and other uses carry a remarkable collection of commonly used chemicals in the form of detergents, cosmetics, paints, adhesives, lubricants, fabrics, pesticides, pharmaceutical drugs, vitamins, plastic items etc. Also presently, a huge amount of transportation fuel is used to make our life more comfortable. As per the current technology, most of the chemicals (approximate 96%)[1] are produced from fossil feedstocks such as coal, crude oil and natural gas since those are mainly consists of carbon, backbone of organic chemicals. Fossil feedstock is formed by natural processes such as anaerobic decomposition of buried dead organisms over a long period of time (millions of years) under very high temperatures and pressures. Most of the chemicals are produced via fossil feedstock gasification processes to form syngas ($CO + H_2$) which is further transformed into various other chemicals. Another way of producing chemicals is the petroleum refinery process. The projection by the experts suggests that fossil reserves have limited availability and hence, those can be used up to a certain period of time (crude oil: 42 years, natural gas: 63 years, coal: 159 years).[2] However, these predictions are strictly based on the current global fossil reserves and current global consumption, and those may change depending upon several factors such as finding of new stock, consumption rate of fossil feedstocks, quality of fossil feedstocks etc.[2] Nevertheless, it can be said that those may not be available in sufficient amount in future to cater our increasing demand for chemicals. Another drawback of fossil feedstocks is its fluctuating price. The crude oil price fluctuation data provided by U. S. Energy Information Administration[3] is plotted in Fig. 1.1 and it shows the increasing cost of crude oil. Furthermore, in the same report it is also predicted that crude oil price will continue to increase over the time of period. The continuous increase in fossil feedstocks price will lead to the increase in the cost of useful chemicals which might be a real problem in future. Moreover, while processing of fossil feedstocks to chemicals, CO_2 that is trapped in the form of fossil feedstocks is released in the atmosphere which creates global warming.

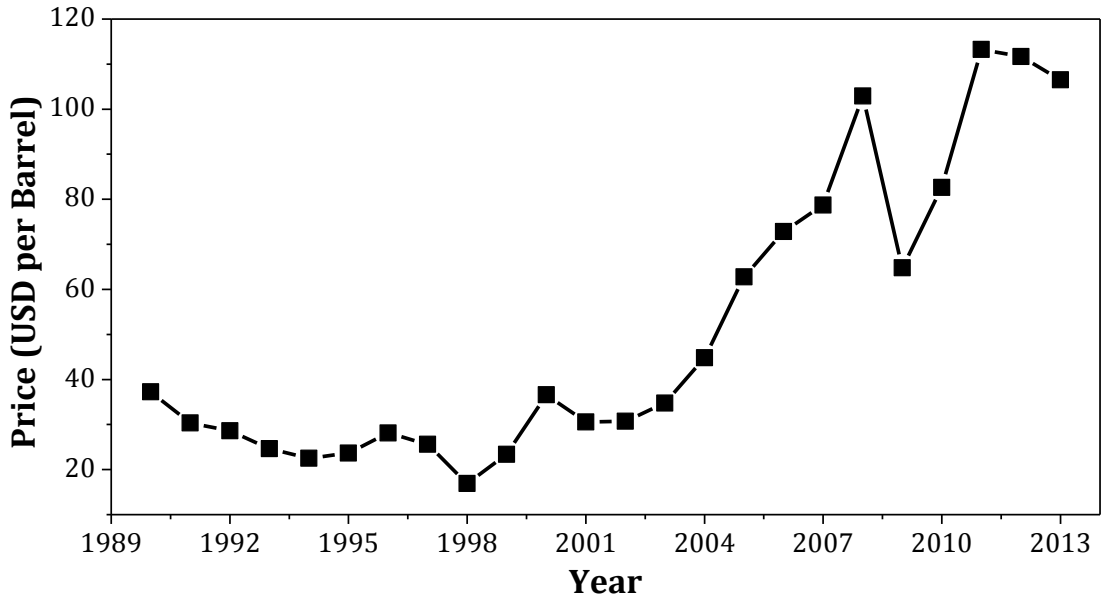

Fig. 1.1. Year-wise cost fluctuation of crude oil as per U. S. Energy Information Administration database.[3]

Considering all the problems associated with the use of fossil feedstocks and to provide a sustainable future technology, a renewable, inexpensive and abundantly available biomass can serve as an alternative feedstock for the synthesis of chemicals. As per the U.S. Department of Energy (DOE) and the U.S. Department of Agriculture (USDA) report[4] use of biomass can offer three major purposes;

1) Reduce the need for fossil resource import since most of the countries don't have sufficient fossil reserves.

2) Support for the growth of agriculture, forestry and rural economies.

3) Foster major new domestic industries – bio-refinery – making chemicals, fuels and other products.

Hence, it is now clear that to fulfil our demand of chemicals in future, we need to be dependent on renewable resource, biomass instead of using non-renewable resource, fossil feedstocks.

1.2. Overview of Biomass and its Applicability

Biomass is generally defined as any living or recently living material on earth. In view of potentiality of biomass (as discussed before), it is obvious that the researchers are looking at biomass as the future source for the synthesis of chemicals.[5] Biomass is generally classified as plant derived and animal derived. Depending on the edibility to humans, the plant derived biomass is again classified into 2 types namely; edible and non-edible. The edible biomass is a food material such as rice, potato, cereals, wheat, corn etc. which is mainly consists of starch. Starch is made up of several α-D-glucose units (C_6 sugar) connected together via α-1→4 glycosidic linkages (linear) to form amylase and via α-1→4 glycosidic linkages (linear) along with α-1→6 glycosidic linkages (branched) to form amylopectin part of starch (Fig. 1.2).

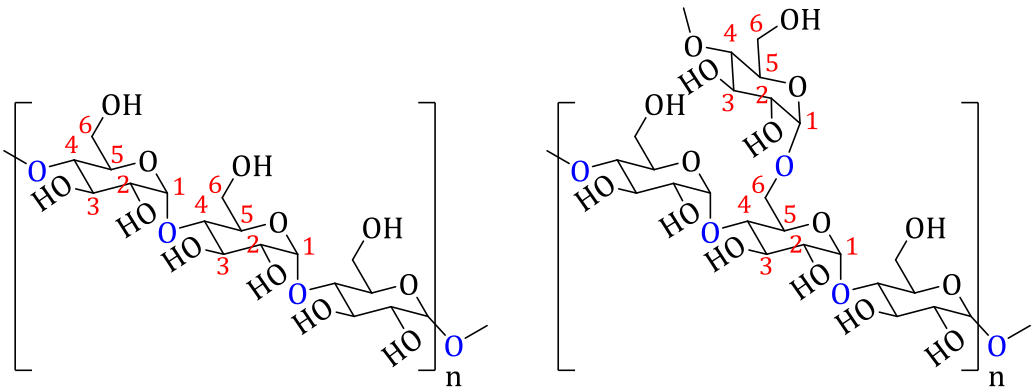

Fig. 1.2. Structure of starch.

Another category of plant derived biomass is non-edible biomass which is typically called as lignocellulosic biomass / lignocellulosic material / lignocellulose. The lignocellulosic biomass is mainly made up of cellulose (ca. 45%), hemicellulose (ca. 25%), and lignin (ca. 20%) with some minor ingredients such as nutrients (micro: boron, copper, iron, chloride, manganese, molybdenum and zinc; macro: nitrogen, phosphorous, potassium, calcium, magnesium and sulfur), proteins and wax (Fig. 1.3).[6,7] Cellulose is a homopolysaccharide made up of several β-D-glucose units connected together via β-1→4 glycosidic linkages and the hemicellulose is a heteropolysaccharide and is typically made up of C_5 (D-xylose, L-arabinose) and C_6 sugars (glucose, glucuronic acid or its 4-*O*-methyl ether, galactose etc.) (Fig. 1.3). On the other hand lignin is made

up of several aromatic monomers (*p*-coumeryl alcohol, coniferyl alcohol and sinapyl alcohol) joined together via β-*O*-4, α-*O*-4, 4-*O*-5, β-β, β-5, 5-5, β-1 etc. linkages (Fig. 1.3). The other type of plant derived biomass is, kitchen garbage or generally known as municipal solid waste which is considered to be available in plenty. Besides this, use of animal derived biomass like chitin, chitosan can also be explored for the synthesis of chemicals.[8]

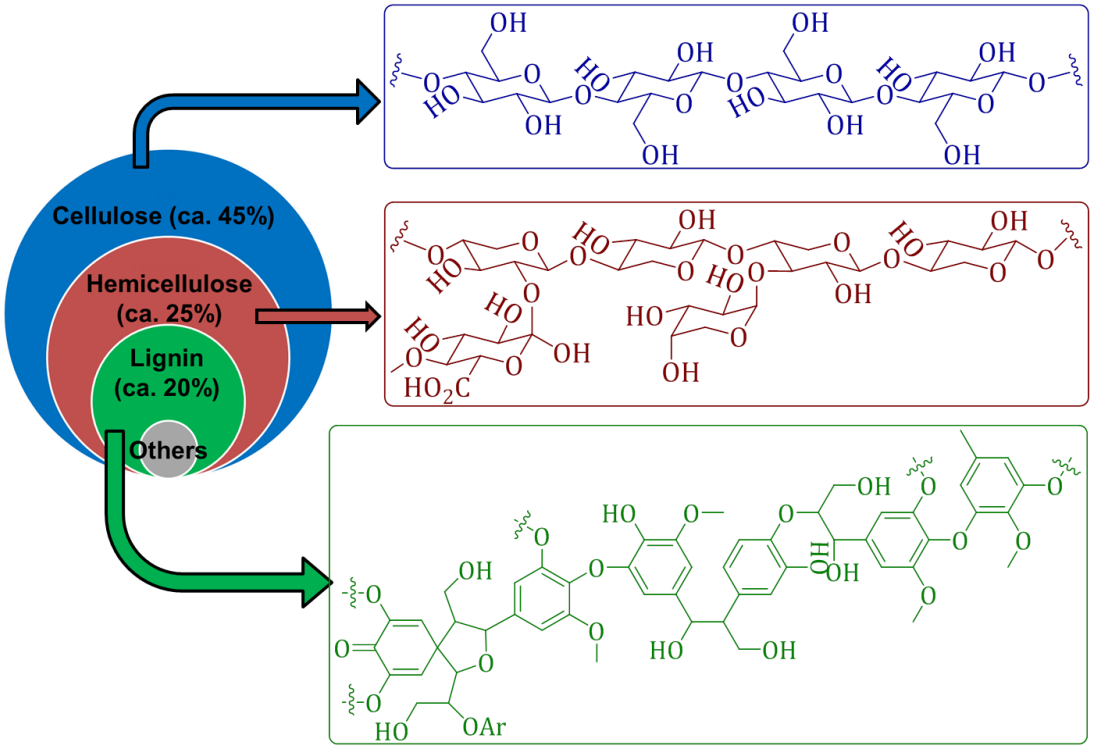

Fig. 1.3. Composition of lignocellulosic biomass and the structures of different components.

From the above discussions it is clear that the biomass feedstocks are composed of various sugars, sugars derivatives and aromatics those can be converted into various useful chemicals. So, it is important to develop methodology for the biomass conversion into chemicals in an efficient pathway. As seen, both plant and animal derived biomass can be converted into chemicals however; until now, mainly efforts are diverted in the development of conversion methodologies for the plant derived biomass. Again, in plant derived biomass, both of its edible and non-edible parts can be converted into various chemicals. However, it is preferable to process non-edible biomass (lignocellulose) since, use of edible biomass to synthesize chemicals may create food crisis in society.

Moreover, it is projected that the worldwide production of plant derived non-edible (lignocellulose) biomass including agricultural and forest residues is enormous and vaguely estimated to be around 1.8×10^{12} tones.[9] This database suggests that if an efficient methodology is developed for the lignocellulose conversion into chemicals, it will be very significant.

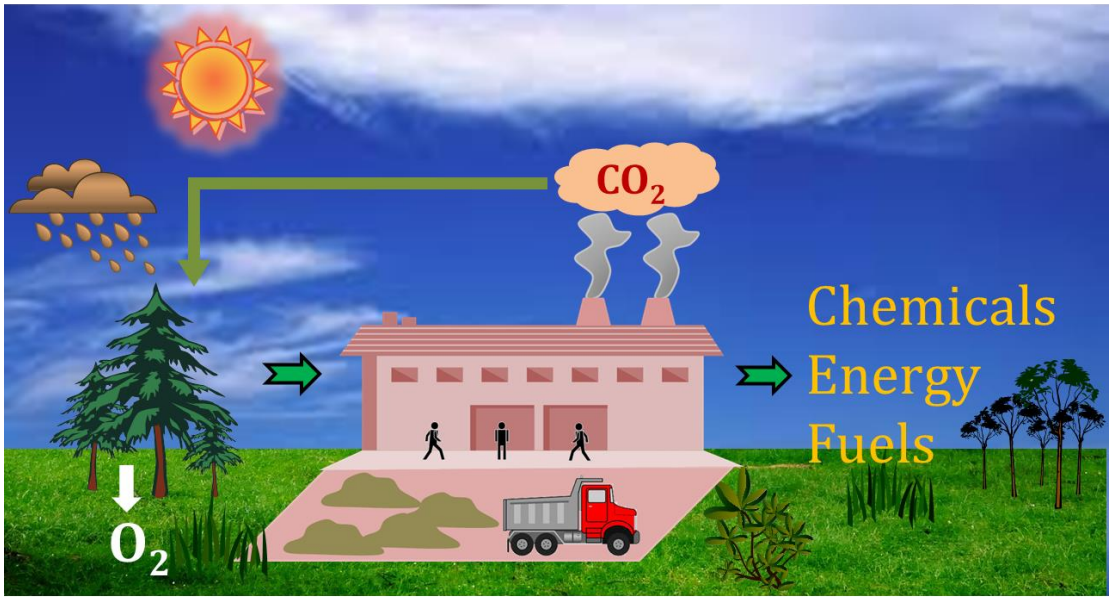

Fig. 1.4. Bio-refinery pathway for conversion of biomass.

Biomass conversion into value added chemicals can be operated via "bio-refinery process" which is defines as 'bio-refining is the sustainable processing of biomass into a spectrum of marketable products and energy" by International Energy Agency (IEA) Bioenergy Task 42.[10] Basically, bio-refinery process integrates biomass conversion processes and equipment to produce chemicals, energy and fuels. In this methodology, biomass (preferably lignocelluloses) is processed in industry to the formation of various products. Since, chemicals are made up of carbon, upon utilization those releases CO_2 in atmosphere. The released CO_2 is then immediately integrated into plants (living biomass) through photosynthesis process in the presence of sunlight and water. Now, again the same plant biomass (lignocelluloses) can be used for chemical synthesis via bio-refinery pathway. Therefore, it can be seen that use of lignocellulosic biomass allows re-utilization of carbon in a cyclic way (carbon neutral process) which eventually, reduces CO_2 in atmosphere i.e. reduction of global warming. The whole

process is illustrated in Fig. 1.4. In contrast, in case of fossil feedstock, a millions of years are required for the natural transformation of plants into fossil resources and in the due time excess of CO_2 will be released in atmosphere which ultimately causes global warming. Hence, use of biomass instead of fossil resources may reduce one of the current major society problem, global warming.

1.3. Biomass Conversion Technology

Since, it is now recognized that lignocelluloses can be converted into chemicals, it would be interesting to be aware of the known methods for this processing. Researchers have developed various conversion technologies for biomass into chemicals which are summarized below.

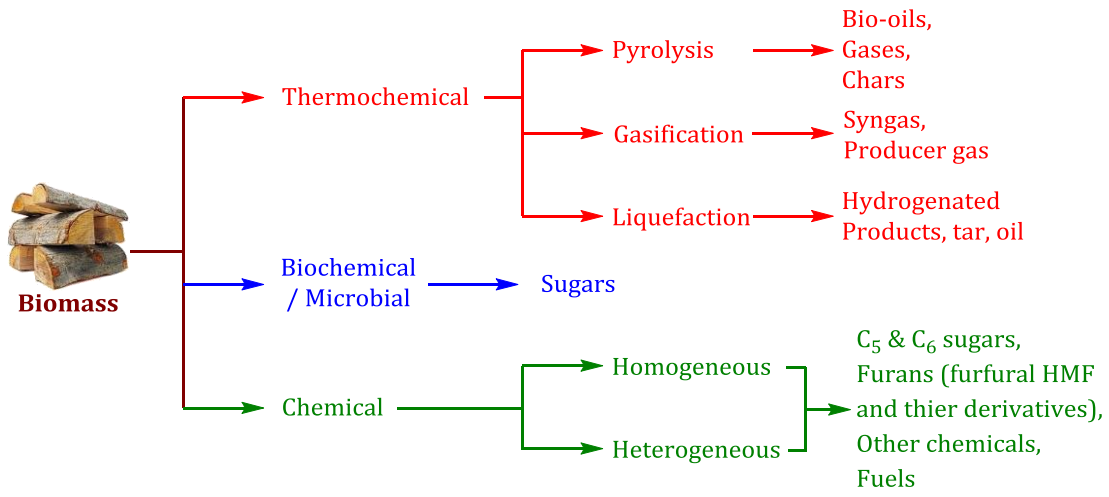

Fig. 1.5. Illustration of biomass conversion technologies.

Generally, three types of biomass conversion technologies are reported *viz.* thermochemical, biochemical and chemical (Fig. 1.5). Thermochemical processes (pyrolysis, gasification and liquefaction) are guided by thermal degradation of biomass into gas, bio-oil and char; and those generally require high temperatures and high pressures.[11,12] In pyrolysis method, biomass is heated in absence of oxygen / air at moderate temperatures (400-600°C) to produce gases, bio-oils and chars. Gasification reactions of biomass are carried out in the presence controlled amount of oxygen and/or steam at >750°C to yield syngas (CO +H_2) (used in transportation fuel production) and producer gas (CO + N_2) (fuel for diesel engine). This method is more

energy efficient compared to combustion process (heating of biomass in presence of sufficient oxygen) because gasification produces syngas which has more potentiality. Liquefaction is a process where biomass is hydrogenated or thermally decomposed under high pressure at 300-400°C. The main purpose of this process is to reduce the C/O ratio and to improve C/H ratio in products those have high calorific value. Moreover, use of precious metal catalysts (gasification process), generation of ash, large amount of char formation due to inefficient burning, deactivation of catalyst due to high temperature & carbon deposition and requirement of special design of reactor to sustain at high temperature & pressure are the major drawbacks for thermochemical processes.

Biochemical or microbial processes transform biomass into sugars via hydrolysis reaction using several enzymes (cellulase, β-glycosidase, endo- and exo-xylanase, β-xylosidase, *p*-coumeric acid esterase etc.).[13-15] It is well-known that individual enzymes are very selective for the formation of a specific chemical. However, biochemical methods face various problems such as high cost of enzymes, recovery of enzymes and products etc.

Chemical conversion methods of biomass are generally carried out in presence of organic or inorganic chemical substance in small amount, called as catalysts. Catalyst is a substance which can alter the rate of a chemical reaction without modifying the overall standard Gibbs free energy change in the reaction. Use of catalysts generally reduces the operating temperature for biomass conversion processes for the formation of chemicals. Moreover, use of catalysts allows the efficient utilization of biomass for the synthesis of chemicals compared to thermochemical processes. Catalysts can be homogeneous and heterogeneous in nature. Homogeneous catalysts such as mineral acids, mineral bases, soluble metal chlorides, acidic ionic liquids etc. are used for biomass conversion into several chemicals.[16-21] Nevertheless, use of homogeneous catalysts face serious drawbacks such as difficulty in the recovery of catalyst, environmental issues, toxicity, corrosiveness etc. Considering these problems, it can be anticipated that the use of heterogeneous catalysts may overcome these problems since those are typically non-corrosive, easily recoverable and environmentally friendly. The concept of heterogeneous catalysts was first introduced by Faraday in 1834 where he

showed that the combination of hydrogen and oxygen to form water was possible at room temperature in presence of platinum electrode.[22] After this discovery, several other researchers also developed many heterogeneous catalyzed processes for the chemical transformations. Moreover, in recent times, several heterogeneous catalysts are used for the biomass conversion through hydrolysis, hydrogenation, dehydration, hydrogenolysis, oxidation, condensation reaction etc.[6,23-29] From these reported processes it is understood that the use of heterogeneous catalysts in biomass conversion into chemicals is highly promising. However, selection of a catalyst and reaction parameters (temperature, time, solvent, pressure etc.) is very important to achieve an efficient biomass conversion processes.

As discussed above, though, various biomass conversion technologies are available in literature yet, in terms of efficient use of biomass and to have environment friendly operating process, it is preferable to use chemical transformation methods using heterogeneous catalysts. It is shown in Fig. 1.3 that lignocelluloses are mainly consists of polymers of various sugars, sugar derivatives and aromatics. Among those, cellulose and hemicellulose are carbohydrate polymers and hence can be hydrolyzed in presence of heterogeneous catalysts having acidic properties (known as solid acid catalysts) to produce several sugars such as glucose, xylose, arabinose, galactose etc. which are very well-known for their applications.[6,7,20,30-32] In presence of solid acid catalysts, those sugars can be further dehydrated (dehydrocyclization / cyclodehydration) into formation of furan derivative, 5-hydroxymethylfurufral (HMF) and furfural. Several other chemical transformations of sugars and furans are also reported by researchers.[6,7,20,31-34] Furthermore, lignin (aromatic polymer) can also be converted into aromatic monomers in presence of solid acid catalysts.[23] Hence, it is safe to claim that chemical transformation of lignocellulosic biomass in presence of solid acid catalyst can produce several value-added chemicals. Nevertheless, considering the fact that I have extensively worked on the synthesis of furans (furfural and HMF) below I will summarize importance of these chemicals. Moreover, I will also discuss about the known methods for the synthesis of furans.

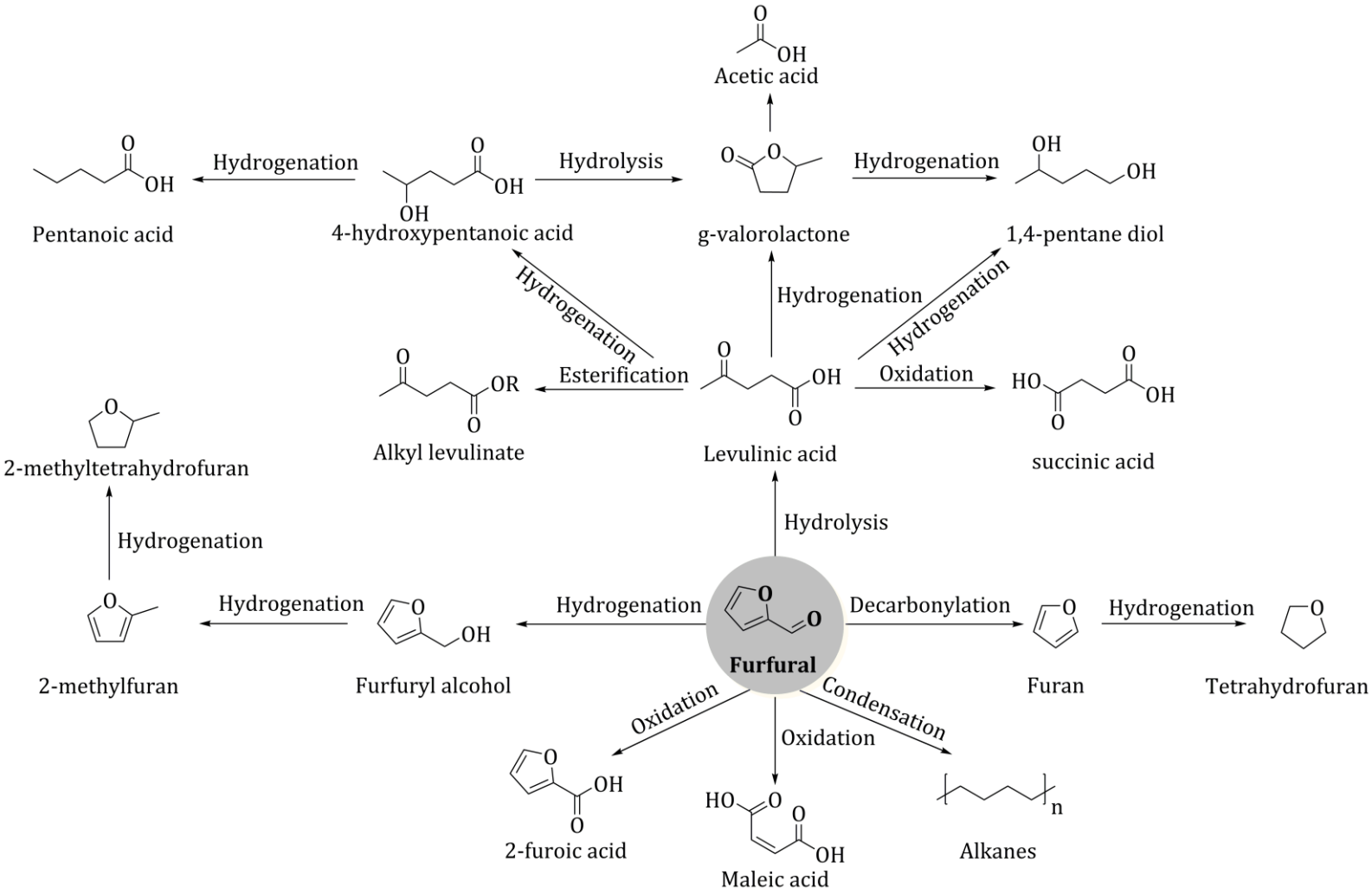

Fig. 1.6. Applications of furfural as a platform chemical for the synthesis of several other chemicals.

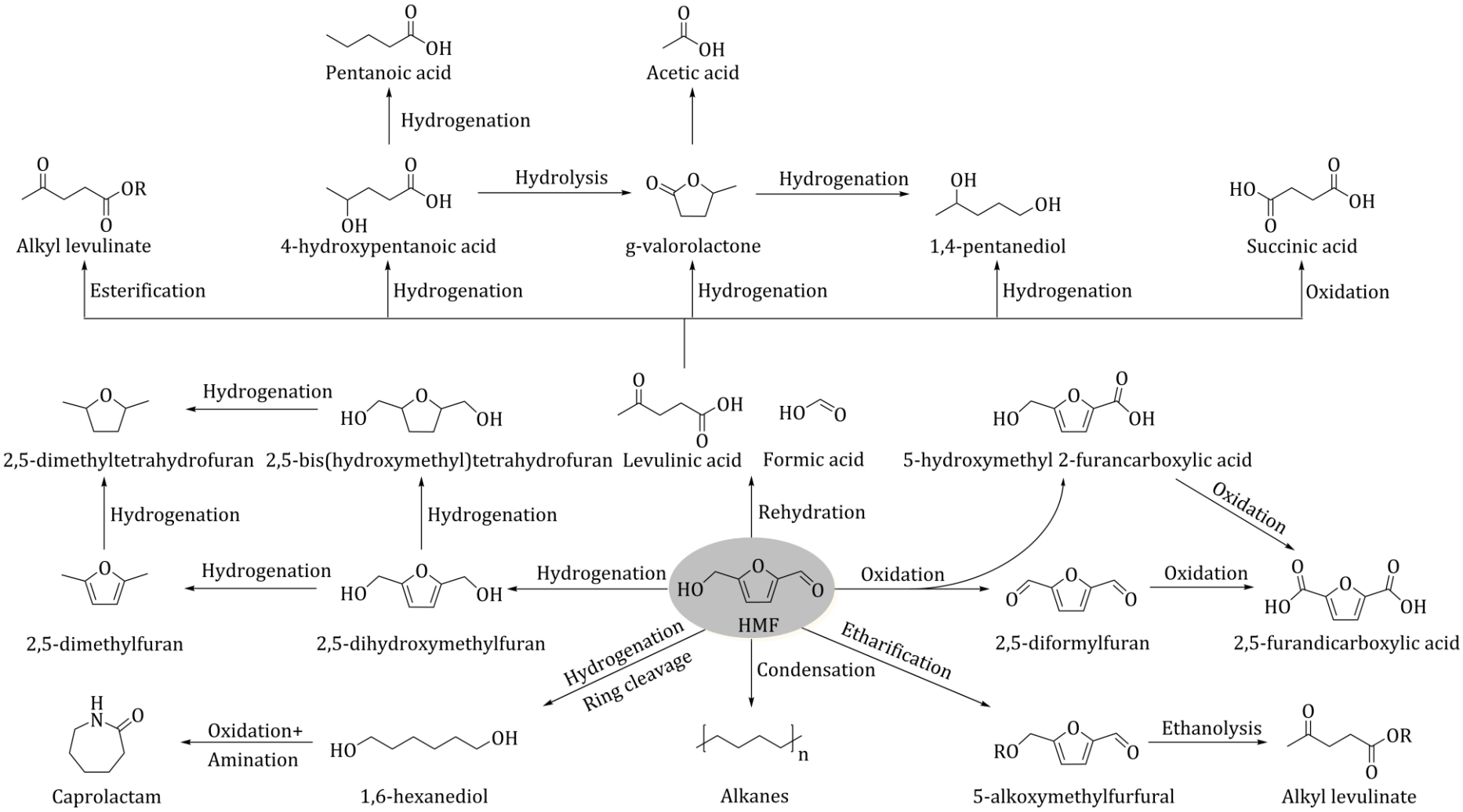

Fig. 1.7. Applications of HMF as a platform chemical for the synthesis of several other chemicals.

1.4. Applications of Furan Chemicals

It is well known that furfural has numerous industrial uses and those are shown in Fig. 1.6. It can undergo hydrogenation reaction to produce furfuryl alcohol, 2-methylfuran and 2-methyltetrahydrofuran which can be further used as solvent, alternative fuel, flavoring agent and in manufacture of resin, adhesives, wetting agents etc.[35,36] Similarly, via Aldol condensation reaction furfural transforms into alkanes which are used as transportation fuel.[26,37] Other important chemicals, furoic acid and maleic acid also can be synthesized from oxidation reaction of furfural which are used in nylon preparation, optic technologies, food products as flavoring agent, in synthesis of several fine chemicals etc..[38,39] Besides this, vapour phase decarbonylation reaction of furfural produces furan which can be further used as a platform chemicals in synthesis of various other chemicals.[40] Furfural hydrolysis produces levulinic acid which also can be used in synthesis of various other chemicals.[41] Furthermore, furfural can also be used as a non-petroleum based renewable solvent.[35]

Similarly, HMF also has a wide range of industrial applications as shown in Fig. 1.7. Oxidation reactions of HMF produces 2,5-furan dicarboxylic acid (FDCA), 2,5-diformylfuran (DFF) and 5-hydroxymethyl 2-furancarboxylic acid (HMFC) and those can be further used as alternative to terephthalic acid in manufacture of polyamide, polyurethane and polyester, in synthesis of diamine and Schiff bases etc..[42,43] HMF transformed into 2,5-dimethylfuran (DMF) 2,5-bis(hydroxymetyl)furan (BHMF), 2,5-bis(hydroxymethyl)tetrahydrofuran, 2,5-dimethyltetrahydrofuran via hydrogenation reactions.[44,45] These products have several uses as transportation fuel, in manufacture of polyurethane foam and polyester etc. via Aldol condensation reactions, HMF transforms into long chain alkanes which are further used as transportation fuel.[26,37] Moreover, ring hydrogenation of HMF is possible to produce 1,6-hexanediol which has applications in production of plastic and various chemicals.[46,47] Hydrolysis of HMF yields formic acid and levulinic acid which can be used as platform chemical to synthesize various other chemicals.[48,49] Moreover, HMF undergoes etherification reaction to yield 5-alkoxymethylfurfural, a potential diesel additive which further converted to alkyl levulinate which has several applications as fine chemical, solvent additive etc..[50,51]

Considering the importance of furans, in the last couple of years researchers are devoting lot of efforts in developing newer efficient methods for their synthesis using heterogeneous catalysts. Before discussing much more details on catalytic processes here, I am summarizing some common type of solid acid catalysts and their properties which are used in biomass conversion reactions.

1.5. Solid Acid Catalyst

As discussed earlier in this chapter, to surmount the problems with homogeneous catalysts, in recent years, researchers have developed several types of solid acid catalysts for the synthesis of sugars and/or furans from biomass conversion. In Table 1.1, some of the important solid catalyst properties are briefly summarized.

Heteropoly acids (HPA) are mainly made of heteroatoms *viz.* W and Mo as a major constituent and those can have several structures such as Keggin, Dawson, Waugh and Anderson based on synthesis conditions and elements.[52] HPA with Keggin structure is reported as stable compared to others. Protonated form of phosphotungstic acid ($H_3PW_{12}O_{40}$) is a homogeneous acid catalyst but to make it heterogeneous, two pathways are chosen by the researchers; 1) incorporation of larger Cs^+ ions in place of proton and 2) supporting $H_3PW_{12}O_{40}$ on MCM-41 (siliceous material).[52,53] Another type of solid acid catalyst is ion-exchanged resin. Amberlyst resins are made up of styrene divinylbenzene copolymer with sulfonic group functionalization. Commonly used Amberlyst catalysts are Amberlyst-15 and Amberlyst-70 and the basic difference between those are in acid amount (4.7 mmol/g and 2.5 mmol/g, respectively).[54,55] In comparison, Nafion resin (Nafion NR-50) and silica supported Nafion resin (Nafion SAC-13) have less amount of acid sites (0.9 mmol/g and 0.17 mmol/g, respectively).[52] Various siliceous material such as FSM-16 (Folded Sheet Mesoporous/Material),[56] MCM-41 (Mobil Corporation/Composite Mesoporous/Material)[57] and SBA-15 (Santa Barbara Amorphous)[58] have definite channel structure and hence, these materials are attracting lot of attention for their use in catalysis. When mesoporous silica materials (MCM-41 and SBA-15) are functionalized with sulfonic acid group, those can act as solid acid catalysts.[59-61] Aluminosilicate (zeolite) materials are also well known as structured solid acid catalysts. The properties of HZSM-5 (Zeolite Soconyl Mobil), HMOR

(Mordenite), HUSY (Faujasite) and Hβ (Beta) are shown in Table 1.1.[62,63] Sulfonated graphene oxide (SGO) prepared from graphene (G) via sulfonation is also available as solid acid catalysts due to its acid sites.[64] Moreover, properties of some of the metal oxide catalysts having acidic nature are also summarized in Table 1.1.[52,65,66]

Table 1.1. Physicochemical properties of solid acid catalysts.

Entry No.	Type	Catalyst	Acid amount (mmol/g)	Surface area (m^2/g)	Ref.
1	Heteropoly acid (HPA)	$H_3PW_{12}O_{40}$	1.0	-	52
2		$Cs_{2.5}H_{0.5}PW_{12}O_{40}$	0.15	128	52
3		34% $H_3PW_{12}O_{40}$ /MCM-41	-	713	53
4	Resin	Amberlyst-15	4.7	53	54
5		Amberlyst-70	2.5	36	55
6		Nafion NR-50	0.9	0.02	52
7		Nafion SAC-13	0.17	200	52
8	Silica	MCM-41	0.0	833	59
9		MCM-41-SO_3H	0.7	438	59
10		H-MCM-22 (Si/Al=24)	0.2	333	60
11		SBA-15	0.0	765	61
12		SBA-15-SO3H	1.5	747	61
13	Zeolite	HZSM-5 (Si/Al=11.5)	1.0	425	62, 63
14		HMOR (Si/Al=10)	1.2	500	62, 63
15		HUSY (Si/Al=15)	0.6	780	62, 63
16		Hβ (Si/Al=19)	0.9	710	62, 63
17	Carbon	Graphene (G)	0.2	128	64
18		Graphene oxide (GO)	2.0	318	64
19		Sulfonated graphene oxide (SGO)	1.7	680	64
20	Metal oxide	SO_4^{2-}/ZrO_2	2.5	75	65
21		Nb_2O_5	0.31	131	52
22		16% Nb_2O_5/MCM-41	0.06	880	66

Although, all these solid catalysts consist of acid sites however, the types of acid sites present in those catalysts are not similar. It is known that solid acid catalysts consist of two types of acid sites namely, Brönsted and Lewis. Brönsted acid center is defined as a proton donating site in catalyst and Lewis acid center in catalyst is defined as a site where electron pair is accepted. In Fig. 1.8, I have presented the typical acid sites present in these solid acid catalysts. Heteropoly acids, resins, sulfonated mesoporous silica and sulfonated carbon comprise of Brönsted acid sites however, metal oxides and zeolites have both Brönsted and Lewis acid sites.

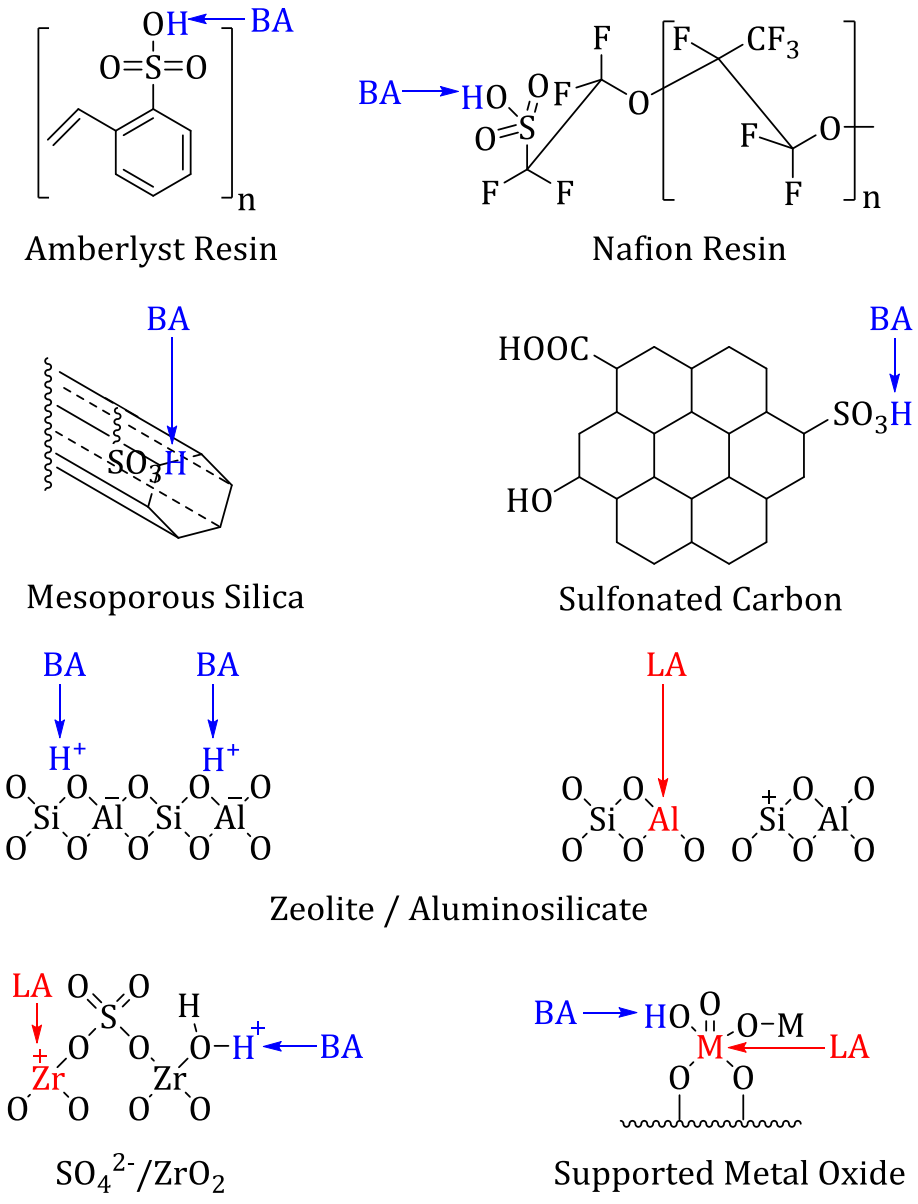

Fig. 1.8. Typical acid sites in solid acid catalysts; 'BA' indicates Brönsted acid sites and 'LA' indicates Lewis acid sites.

From the above discussions, it is now understood that processing of biomass might be possible in presence of solid acid catalyst. Moreover, it is anticipated that very important chemicals, sugars and/or furans (furfural and HMF) can be synthesized from biomass using solid acid catalysts via hydrolysis-dehydration reaction. Considering this point, below I am discussing some of the important literature reports which show the synthesis of furans using solid acid catalysts.

1.6. Recent Processes on Furfural Synthesis from Carbohydrates

As per the current technology, industrial scale furfural synthesis is based on the use of mineral acid, H_2SO_4 as a catalyst and the typical furfural production varied in the range of 4-70%.[67-73] The details about the industrial processes for the furfural production are summarized in Table 1.2. However, as suggested earlier, to offer environment friendly and sustainable technology, solid acid catalysts need to be used instead of homogeneous acid catalysts. As per the current reports, the major primary sources for furfural production are xylose and arabinose those can be obtained by hydrolysis of hemicellulose (a component of lignocellulose). Further, the supply of hemicellulose is possible from various plant-derived biomasses such as crop waste, wood, food waste etc. Moreover, hemicellulose is the second largest available plant-derived poly-saccharide after cellulose and hence, it can be used as a substrate for synthesis of either C_5 sugars or furfural. Scheme 1.1 illustrates the possibility of formation of final product, furfural in a stepwise conversion of raw feedstock (lignocelluloses).

Recently, several researchers have tried the synthesis of furfural using solid acid catalysts however; here mainly I am summarizing some reports which will give a glimpse of all the works done in this filed in recent past.

Table 1.2. Summary of industrial processes available for furfural production.

Entry no.	Company (plant started)	Mode of operation	Substrate	Catalyst	Solvent	Operating *T* (°C)	Furfural yield (%)	Co-products	Ref.
1.	Quaker Oats (1921)	batch/ continuous	oat hulls, bagasse	H_2SO_4	water	153-200, steam	<50	-	67, 68
2.	Biofine Incorporated (1990)	continuous	paper sludge and waste residue	H_2SO_4	water	190-200	70	formic acid, levulinic acid, char	69
3.	Lignol Innovation Corp. (2001)	continuous	wood chips	H_2SO_4	ethanol	180	ca. 4	xylose, glucose, lignin	70
4.	Westpro modified Huaxia Technology (2004)	fixed bed reactor with continuous dynamic refining	corn cob	H_2SO_4	water	160-165	35-50	acetic acid, acetone, methanol, levulinic acid	68, 71
5.	Vedernikovs Technology (2006)	continuous	wood chips	H_2SO_4	water	188	75	acetic acid, ethanol	72
6.	SupraYield®, now owned by PSM Biorefinery (2009)	continuous	bagasse	H_2SO_4	water	240	50-70	acetic acid	68, 73

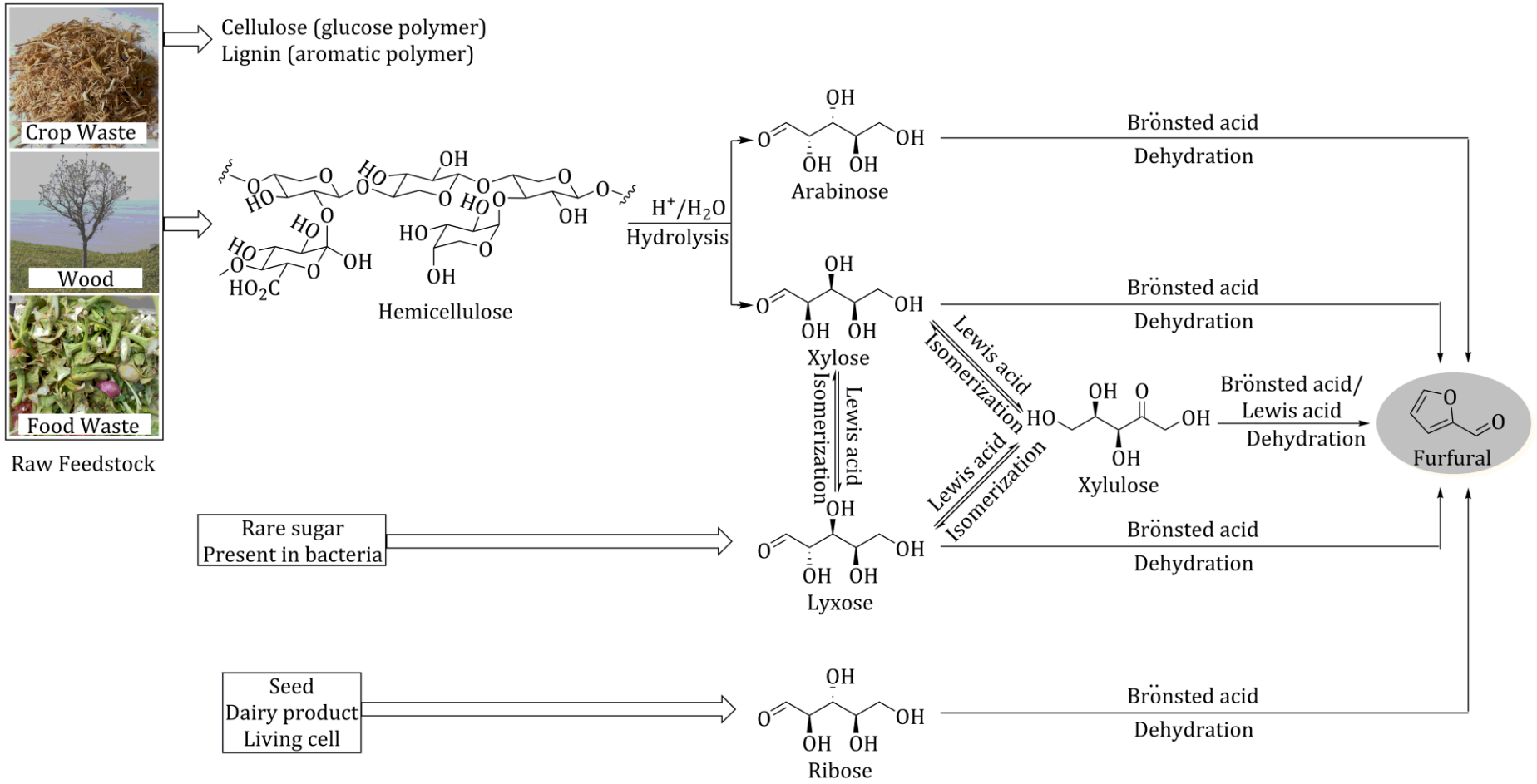

Scheme 1.1. Pathway for furfural synthesis from various feedstocks.

1.6.1. Use of Xylose as Substrate

Mainly, xylose is used as a substrate for the synthesis of furfural through dehydrocyclization reaction in presence of solid acid catalysts. Various Brönsted acid catalysts are used for the processing of xylose into furfural. As discussed in earlier section (section 1.5), to make homogeneous phosphotungstic acids (heteropoly acid, HPA) catalyst heterogeneous, researcher either partially replaced the protons by larger size Cs^+ ions or HPA is anchored on mesoporous silica.[53,74] These two heterogeneous HPA catalysts were studied in presence of either DMSO or water + toluene solvent system to yield 33-45% furfural. Among the two solvent systems, DMSO showed better activity and it was suggested that slightly better activity in DMSO solvent system is due to stabilization of the intermediate cation formed during xylose transformation through solvation and thereby prevents condensation product formation between furfural and cationic intermediate. Another possibility might be due to catalytic influence of DMSO solvent through simultaneous activation of –OH group at C2 position in fructose by electrophilic interaction of sulfur center of DMSO and hydrogen abstraction from C1 position of fructose by nucleophilic interaction of oxygen center of DMSO as explained in case of HMF synthesis.[75] Although, DMSO showed better activity yet, the major problem with DMSO is low solubility of sugars in this solvent and separation of reaction products/unreacted substrate from it because of very high boiling point (189°C). Moreover, the stability of HPA is a serious problem while use of those as a catalyst. Further, various resin catalysts such as Amberlyst-15, Amberlyst-70, Nafion-117 and Nafion SAC-13 having strong acidity were also studied for xylose conversion into furfural (yield = 60-78%) reaction.[59,76,77] Acidic mesoporous silica prepared by either sulfonic group functionalization or incorporation of aluminimum in silica framework of MCM-41 and SBA-15 were also checked and 50-86% furfural yields were achieved from xylose.[59-61,78,79]

Recently, a new reaction pathway for the furfural synthesis from xylose via xylulose (xylo-ketose) formation is projected in presence of base catalysts.[80] In this strategy, use of solid base (hydrotalcite, HT) isomerizes xylose into xylulose (xylo-ketose) and further in presence of solid acid catalyst (Amberlyst-15) xylulose undergoes dehydration reaction to form furfural (37%). Lately, it is suggested that the same phenomenon of xylose isomerization to xylulose can be directed by Lewis acidic catalyst

(Fig. 1.9).[81,82] Sn-beta zeolite having Lewis acid properties can isomerize xylose into xylulose (18.4%) in water and additional use of Amberlyst-15 catalyst gave dehydration reaction of xylulose to form 5% furfural.[81] Moreover, it is suggested in literature that xylose to furfural formation is guided by different pathway in presence of Brönsted and Lewis acid catalysts. Additionally, it is proved that the presence of Lewis acid catalyst in reaction system reduces the activation energy barrier of xylose to furfural formation reaction [Ea (xylose to xylulose) = 15.5 kcal/mol, r.d.s. and Ea (xylulose to furfural) = 23.1 kcal/mol] compared to Brönsted acid catalyzed reaction (Ea ~ 30-32 kcal/mol).[31,82,83]

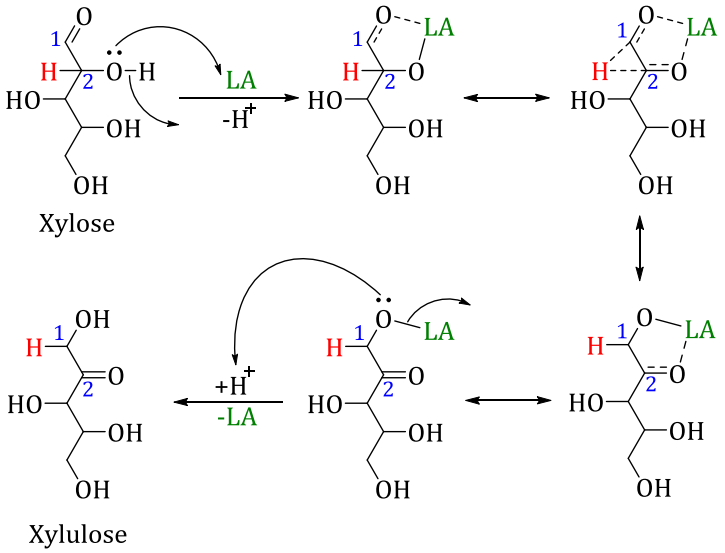

Fig. 1.9. Mechanism for Lewis acid catalyzed isomerization of xylose into xylulose.

Several other researches were also studied various metal oxide, sulfated metal oxide and supported metal oxide catalysts having both Lewis acid and Brönsted acid properties for xylose conversion into furfural (31-60%).[66,84-87] Another report shows the use of sulfonated graphene oxide catalyst for 62% furfural formation from xylose.[64] Later, H-form of various zeolites (ZSM-5, MOR, BEA) and dealuminated zeolite were used by researchers for the conversion of xylose into furfural (41-98%).[76,79,88-91]

1.6.2. Use of Lignocelluloses as Substrate

Although, several reports are available (discussed above) on the synthesis of furfural from sugar monomer xylose using solid acid catalysts but the use of sugars may create problem since those are food material. Moreover, to obtain sugars from lignocelluloses, separate processing (hydrolysis) of lignocellulose is required. Hence, it is preferable to

use abundant and inexpensive lignocellulose material directly for the synthesis of furfural in order to develop a sustainable future technology.

In literature, few of the reports are available for the direct conversion of lignocellulose or hemicellulose (part of lignocellulose) into C_5 sugars and furfural using solid acid catalysts. One report shows the hydrolysis of corn cob (lignocellulose consists of cellulose 34.6%, xylan 26.9%, arabinose 3.6%, others 34.9%) into sugar monomers in presence of sulfonated carbon.[92] Xylan (polysaccharide made up of xylose + arabinose), arabinogalactan (polysaccharide made up of arabinose + galactose) were also used as substrates for the synthesis of sugar monomers by undergoing hydrolysis reactions using various solid acid catalysts such as sulfonated biochar,[93] smopex-101 (fibrous non-porous catalyst bearing sulfonic acid group on poly-ethylene graft poly-styrene),[94] zeolites (Hβ, HUSY, HMOR)[30,95] and resins.[96] In these reported processes, although, significant amount of C_5 sugar formation is achieved but with consideration of more applicability later, researchers are tried to synthesize furfural directly via hydrolysis-dehydration reaction. For the first time, our group presented a solid acid catalyzed process for the direct conversion of hemicellulose / xylan (part of lignocellulose) into C_5 sugars and furfural in one-pot method.[30,63] The selectivity of product (sugars and furfural) was shown to be dependent on the solvent system. Using water as a solvent system, processing of isolated hemicellulose produced mainly C_5 sugars (41%) with less amount of furfural (12%) over HUSY (Si/Al = 15) catalyst at 170°C.[30] The activity of various other catalysts such as zeolites (HMOR, Hβ), K10 clay, Al incorporated mesoporous silica (Al-MCM-41), Cs-HPA, γ-Al_2O_3, Nb_2O_5 was also tested and it was found that those were less active compared to HUSY. Later under similar reaction conditions, conversion of untreated bagasse (lignocellulose; containing cellulose, hemicellulose & lignin) was also tried with three different zeolites; HUSY (Si/Al = 15), HMOR (Si/Al = 10), Hβ (Si/Al = 19) using water as solvent and the similar activities were observed for all the zeolites (oligomers = 29-36%, C_5 sugars = 60±4% and furfural = 3±2%). Improvement in furfural yield was shown by changing the solvent system from water only to water + organic (biphasic) where organic phase extracts furfural from water phase and thereby enhances furfural yields by minimizing side reactions.[63] Use of water + toluene, water + MIBK and water + *p*-xylene in 1:1 *v/v* ratio yields almost similar furfural (ca. 55%) directly from bagasse in presence of HUSY catalyst at 170°C.

Although, a methodology is developed for direct conversion of lignocellulose or part of lignocellulose into sugars and furfural however, under the reaction conditions, structured zeolite catalysts underwent morphological changes (proved with the help of XRD, NMR, ICP and TPD-NH_3) and thereby showed poor recyclability. Another report shows conversion of xylan into xylose (28%) and furfural (18%) in water + toluene solvent system in presence of solid acid catalyst, Al-TUD-1 at 170°C.[97] In another report, conversion of wood chips (lignocellulose) into furfural via sugar formation was shown using two reactors.[76] Basically, in the first reactor, deconstruction of wood chips into mainly C_5 sugars and soluble oligomers (PHL) is shown in hot water (170°C) and in the next reactor, PHL was processed in presence of HMOR catalyst at 175°C in water + γ-valerolactone (GVL) solvent for the formation of maximum of 74% furfural.

From the above discussions, it is now understood that for the synthesis of sugars and furfural directly from lignocelluloses faces some drawbacks such as stability of catalysts, low and selective yields of product etc. Hence, there is a possibility to modify the catalytic system by developing stable solid acid catalyst and by adjusting reaction parameters to improve yields and selectivity.

1.7. Recent Processes on HMF Synthesis from Carbohydrates

As described in revised US-DOE report,[98] HMF is one of the top value-added chemical can be derived from biomass and hence, I am summarizing the latest developments in the synthesis of HMF reported in recent times. As per the recent report, only one commercial process is known for the production of HMF.[99] From January 2014, AVA Biochem Facility, Switzerland has started the industrial production of HMF from renewable biomass using modified hydrothermal carbonization (HTC) process.[99] The method is based on the technology developed by Karlsruhe Institute of Technology (KIT) researchers.

For the synthesis of HMF, researchers have mainly used fructose as substrate. However, several other substrates such as mono-saccharide (glucose), di-saccharides (maltose: α-D-glucose dimer, cellobiose: β-D-glucose dimer and sucrose: dimer of glucose and fructose) and poly-saccharides (starch: α-D-glucose polymer, cellulose: β-D-glucose polymer and inulin: fructose polymer) are also can be used for the synthesis of HMF. A stepwise conversion of poly-saccharide into HMF via di-saccharide and mono-saccharide is illustrated in Scheme 1.2.

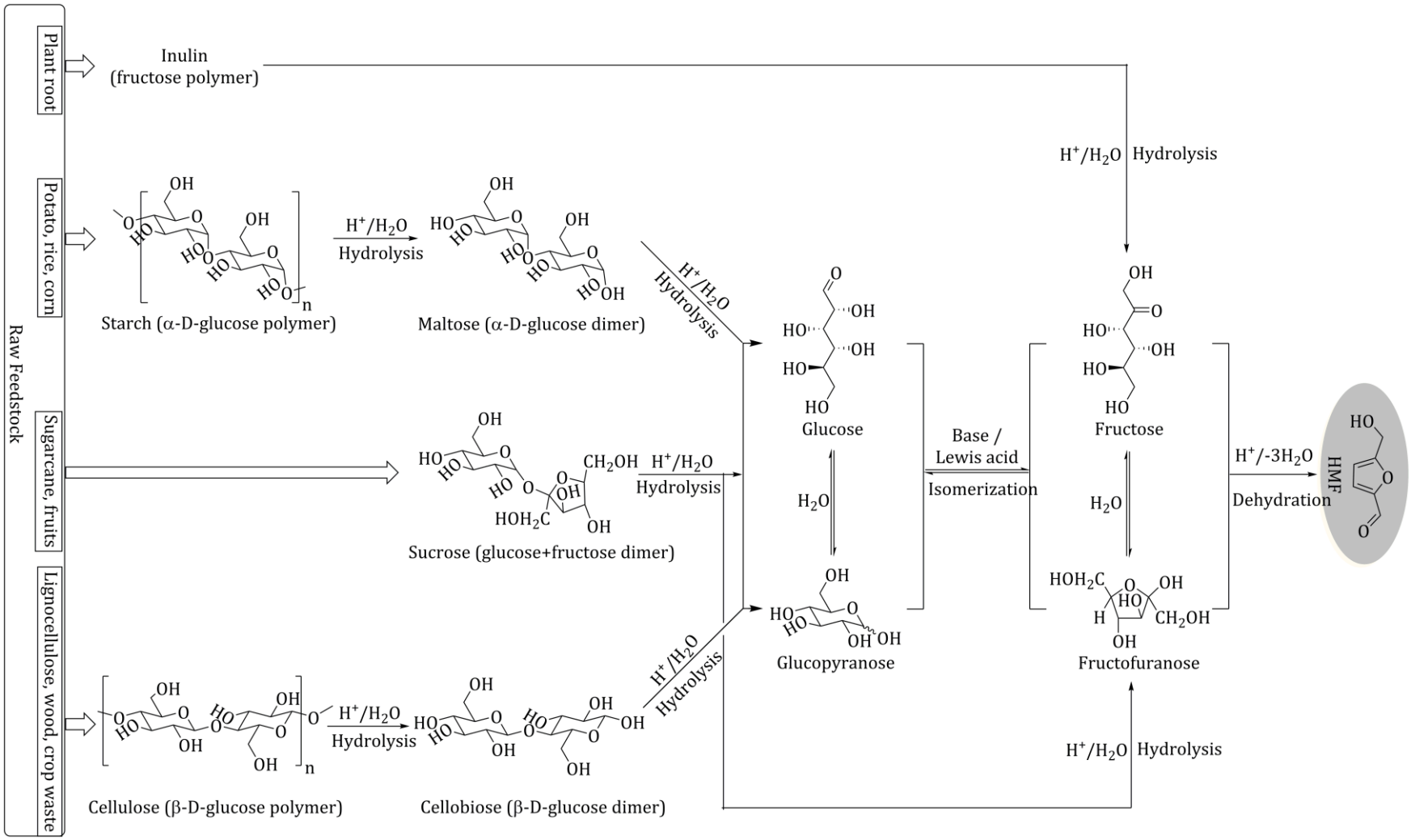

Scheme 1.2. Pathway for HMF synthesis from various feedstocks.

1.7.1. Use of Fructose as Substrate

Fructose is widely used substrate for the synthesis of HMF because this ketonic C_6 mono-saccharide can easily undergo acid catalyzed dehydration reaction (removal of three water molecule) to yield HMF. The mechanistic pathway for fructose dehydration into HMF is shown in Fig. 1.10. Here, mainly I am summarizing the solid acid catalyzed processes for HMF synthesis. Since in water, both substrate and product are soluble, water is mainly used as a reaction media.[32,33,100] However, use of water alone as a solvent allows the rehydration reaction of HMF to form formic and levulinic acid.[33] Additionally, separation and purification of HMF from reaction mixture (water) containing unreacted fructose and formed rehydration by-products is a challenge. To surmount these problems, recently, a range of organic and biphasic solvent systems based methods for the HMF synthesis from fructose are tried.

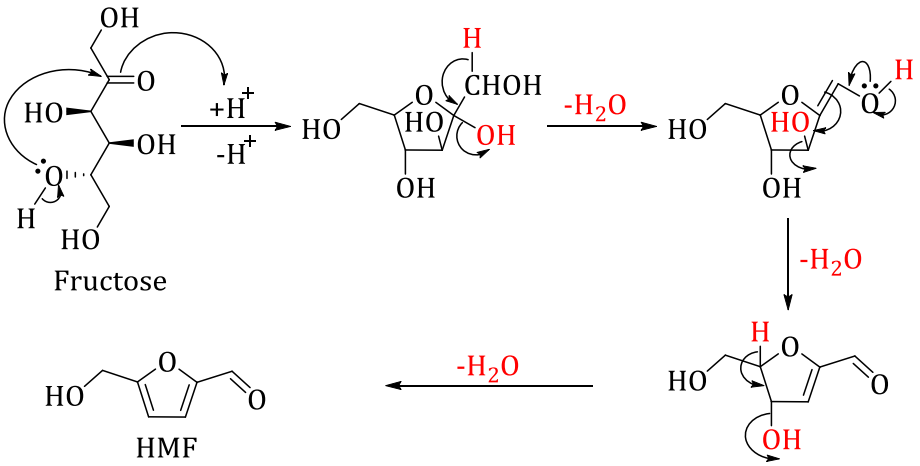

Fig. 1.10. Mechanism for fructose dehydration into HMF in presence of acid catalysts.

Powdered form of Amberlyst-15 resin catalyst was tried in presence of DMSO solvent for fructose conversion into 100% yields of HMF.[101] However use of other solvent system such as isopropyl alcohol, tetrahydrofuran (THF), water + methyl *iso*-butyl ketone (MIBK) provides less HMF yield (45-48%).[102-104] The higher yields in DMSO solvent can be explained due to catalytic influence of DMSO. Even though, such a high yield of HMF is obtained yet, high boiling point of DMSO (189°C) makes the separation of HMF (BP = 114-116°C) from solvent a challenging and energy consuming task and hence, it suggests that use of low boiling solvent might be preferable. Dowex 50wx8-100 resin catalyst was used in presence of water + acetone and acetone + DMSO

solvent system and 73-90% HMF yield was reported.[105,106] Various solid heteropolyacids such as $Cs_{2.5}H_{0.5}PW_{12}O_{40}$ and $Ag_3PW_{12}O_{40}$ were also checked for fructose conversion in presence of water + MIBK solvent to yield 74-78% HMF.[104,107] Various sulfonated and phosphorylated carbons were also used as catalyst to yield 43-98% HMF from fructose conversion.[108-111] Use of sulfonic acid functionalized mesoporous materials were shown in the conversion of fructose yields 45-81% HMF.[112-114] Several zeolite catalysts *viz.* HMOR, HZSM-5, Hβ, boron incorporated zeolite (B-TUD-1) were also shown as catalyst to yield 45-74% HMF from fructose in water + MIBK solvent.[115-117] Anatage titanium oxide (TiO_2), zirconia (ZrO_2), niobium oxide (Nb_2O_5), niobium phosphate, sulfated zirconia, tungsten oxide supported on zirconia etc. were also used as solid acid catalyst in fructose conversion into HMF (12-88%).[104,118-123]

From the above results and discussions it is apparent that, solid acids catalyzed fructose dehydration reactions to yield HMF are well studied. However, fructose is not abundant in nature and to obtain it in pure form from various substrates, costly processing is involved and so, it cannot be used for the sustainable production of HMF. This problem can be surmounted if a methodology is developed for the direct processing of other abundantly available feedstocks.

1.7.2. Use of Other Substrates

As per the literature reports HMF can be synthesized from various other substrates such as glucose, maltose, cellobiose, inulin, starch and cellulose (Scheme 1.2). However, most of the catalytic systems which show promising results in fructose dehydration into HMF remain unsuccessful to convert glucose into HMF. The fundamental reason behind this is the preferable availability of most stable pyranose form of glucose in water phase i.e. a lower fraction of open chain glucose is available in solution to offer lower enolization reaction which is the rate determining step for HMF synthesis.[124,125] Furthermore, formation of HMF from glucose is a two-step process; where glucose has to be first isomerized into fructose preferably in presence of base (through Lobry de Bruyn–van Ekenstein transformation) and later, fructose dehydrates into HMF in presence of acids. For this reason, to carry out reaction in a single pot, both basic and acidic catalysts are required to be used which may partially neutralize the catalytic system leading to lower HMF yields. In other way, two separate reactors can be used for

the conversion of glucose into fructose and fructose in to HMF reactions individually. By understanding practical problems and requirements in using glucose instead of fructose, in recent times, remarkable efforts in this area using both homogeneous and heterogeneous catalysts were undertaken and here, I am summarizing the solid acid catalyzed methods for HMF synthesis.

Several solid base catalysts such as alkali metal exchanged zeolites, hydrotalcite (HT), basic ZrO_2 and metallosilicates were reported for the isomerization of glucose into fructose.[126-130] Combined use of HT and Amberlyst-15 catalysts was also shown to convert 73% glucose into 42% HMF with some amount of intermediate products; anhydroglucose and fructose.[131,132] Moreover, to overcome the problem of using base catalysts in reaction in recent time, use of Lewis acidic catalyst was shown to convert glucose into fructose via 1, 2 hydride shift mechanism (similar as shown in case of xylose in Fig. 1.9).[133-135] Based on this development several Lewis acid catalysts are designed for one-pot conversion of glucose into HMF. Combination of Lewis acid (LA) catalyst, Sn-beta or Ti-beta and Brönsted acid (BA) catalyst, HCl was studied to achieve maximum of 57% HMF yield directly from 79% glucose conversion.[136] In this method, LA is responsible for isomerization reaction and BA catalyst is mainly responsible for the fructose dehydration reaction. Later, under microwave heating, use of mesoporous TiO_2 nanoparticles having Lewis acid sites was studied but the HMF yields presented were very less (25-37%).[137] Sn-W mixed metal oxide catalyst was known to yield moderate amount of HMF (48%) from glucose conversion but the process required very long reaction time (18h).[138]

In addition to use of glucose as substrate for HMF synthesis, very few reports are available on the use of di-saccharides and poly-saccharides. Maltose and cellobiose were used in presence of TiO_2 nanoparticles to yield only 14-19% HMF.[137] Combination of HT + Amberlyst-15 was also used for cellobiose conversion to yield 35% of HMF.[132] Utilization of Sn-W oxide catalyst was shown to yield 39% of HMF from cellobiose.[138] Sn-W oxide was used as a catalyst for starch conversion to yield 41% HMF but it took very long time (36 h).[138] Moreover, a study on the direct use of lignocellulosic waste (cassava waste) containing 60% starch, 16% cellulose, 5% hemicellulose and 19% lignin as a substrate was carried out in the presence of sulfonated carbon based catalyst and a maximum of 30% HMF yield was reported.[139]

1.8. Drawbacks of Earlier Processes and Motivation of Work

Although, several processes are reported for the synthesis of sugars and furans (furfural and HMF) in presence of solid acid catalysts however, most of the processes face a major problem i.e. un-stability of catalyst. Moreover, critical view on most of these processes emphasizes some other drawbacks associated with these methods such as use of edible sugars (xylose, fructose and glucose), low product yields and selectivity, difficulty in product isolation in pure form, use of multiple reactors etc.

Structured catalyst zeolite (HUSY) was shown as very active catalyst in furfural synthesis directly from either isolated hemicellulose or bagasse (raw biomass).[63] Looking at the results it can be said that this process may serve better in developing future technology since abundantly available raw biomass was used directly. However, a major problem with the reported structured zeolite catalyst was that, under the reaction conditions deformation of zeolite morphology (structure) was seen.[63] This in turn showed decrease in the activity in recycle runs. These results emphasize the fact that though direct (one-pot) conversion of hemicellulose is possible to obtain furfural but still there is a need to develop stable catalyst which can show similar activity in repeated runs. For the development of new stable catalysts, synthesis of either structurally more stable catalysts or amorphous (no definite channel structure) catalysts can be undertaken. It is reported in the literature that structured silicoaluminophosphate (SAPO) catalysts are hydrothermally more stable (600°C under 20% steams)[140] compared to zeolites (aluminosilicate) (HMOR: ca. 240°C under 20% steams[141]). However, it is more important to understand the phenomenon why SAPO catalysts are hydrothermally more stable compared to zeolite. To understand this fact I have calculated the bond lengths of phosphorous-oxygen, silicon-oxygen and aluminum-oxygen bonds using Chem3D Pro 13.0 software (after minimization of energy). These calculations suggest that the phosphorous-oxygen bond lengths (P-O: 1.59 Å, P=O: 1.49 Å) are smaller in PO_4 unit however, Si-O bond length (1.64 Å) and Al-O bond length (1.83 Å) are larger in SiO_4 and AlO_4 units respectively. The similar data is also reported in literature [P-O: 1.63 Å, P=O: 1.50 Å, Si-O: 1.60 Å, Al-O: 1.76 Å].[142,143] Moreover, due to shorter bond length, PO_4 unit has higher energy (16.4 kcal/mol) compared to SiO_4 unit (9.99 kcal/mol) and AlO_4 unit (7.01 kcal/mol) having larger bonds, as calculated using Chem3D Pro 13.0 software (after minimization of energy). Hence, incorporation of

shorter P-O bonds (higher force constant) in aluminosilicate (zeolite) framework to form SAPO framework, it becomes more stable catalyst.[144] In another category, if metal oxides are incorporated on amorphous support material it will form amorphous catalyst which having acidic properties can catalyze reactions. Moreover, from literature reports it is understood that use of raw biomass directly may provide sustainable future technology. Hence, seven types of crop wastes (raw biomass) namely, bagasse (3 types), rice husk (3 types) and wheat straw (1 type) were collected from various regions of India (detail sources were described in section 2.6, chapter 2) and used as substrate without any pre-treatment.

SAPO materials can have various structure types depending on the synthesis procedure, molar gel compositions of precursors and hydrothermal treatment conditions. Here, in this work, four SAPO materials *viz.* SAPO-44, SAPO-46, SAPO-5 and SAPO-11 will be used and hence their structure types are shown in Fig. 1.11. The International Zeolite Association (IZA) database[145] is used for discussion of SAPO catalyst structure. SAPO-44 has 'Chabazite (CHA)' morphology. CHA framework was first described by von Born in 1772. It has a 3-dimentional (3D) channel system with 'R-3m' space group. The T atom ring size in CHA morphology consists of 8, 6 and 4 membered ring. CHA has a framework structure consisting of a stacked sequence of 6-rings in the order of AABBCC which forms double 6-rings at each apex of the pseudo-rhombic unit cell. The pseudo-rhombohedra CHA single crystals looks like almost cube shaped morphology.

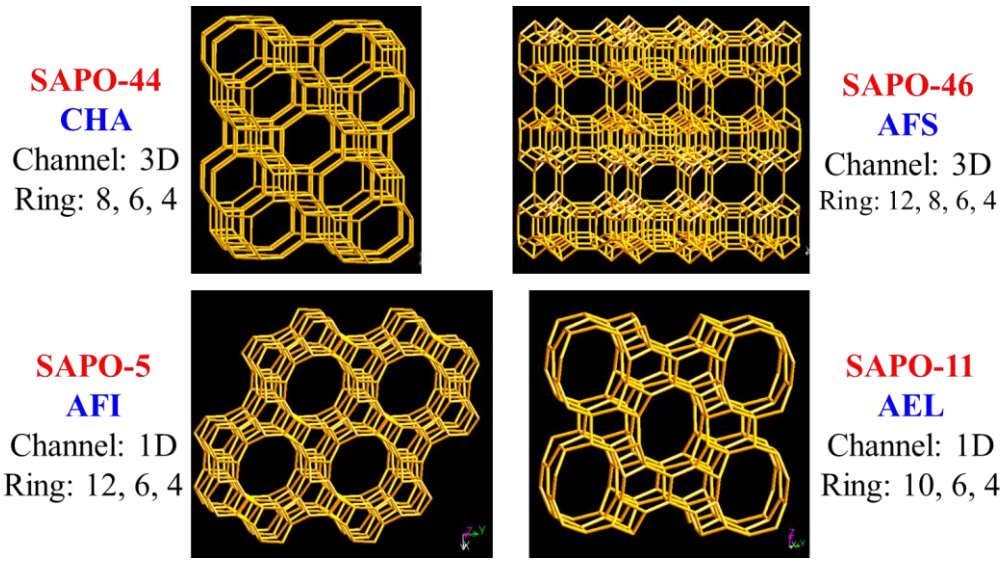

Fig. 1.11. Structure type of SAPO catalysts.

SAPO-46 has 'AFS' morphology which shows a 3-dimentional (3D) channel system with 'P6$_3$/mcm' space group. The T atom ring size in AFS morphology consists of 12, 8, 6 and 4 membered ring.

SAPO-5 has 'AFI' morphology which has a 1-dimentional (1D) channel system with 'P6$_3$/mcm' space group. The T atom ring size in AFI morphology consists of 12, 6 and 4 membered ring.

SAPO-11 has 'AEL' morphology which shows a 1-dimentional (1D) channel system with 'Imma' space group. The T atom ring size in AEL morphology consists of 10, 6 and 4 membered ring.

The type of acid sites present in SAPO's and supported metal oxide catalysts are shown in Fig. 1.12. Similar like aluminosilicate (zeolite) material, in SAPO's, the charge imbalance in material framework is satisfied by attachment of protons to the bridging oxygen atom (Fig. 1.12) which is principally assigned as Brönsted acid site. The Lewis acid sites in SAPO catalysts are the tri coordinated Al center as shown in Fig 1.12.

Furthermore, supported metal oxide catalysts may consists M=O, M-OH, M-O-M and M-O-support bonds (Fig. 1.12). This possibility was proved earlier and also in this study using IR (Infra-Red) spectra analysis (from more detail please see section 2.5.3, chapter 2). So, in case of supported metal oxides, metal center can act as Lewis acid site due to its available vacant orbitals. Moreover, the –OH group attached to metal center can donate proton and act as Brönsted acid center.

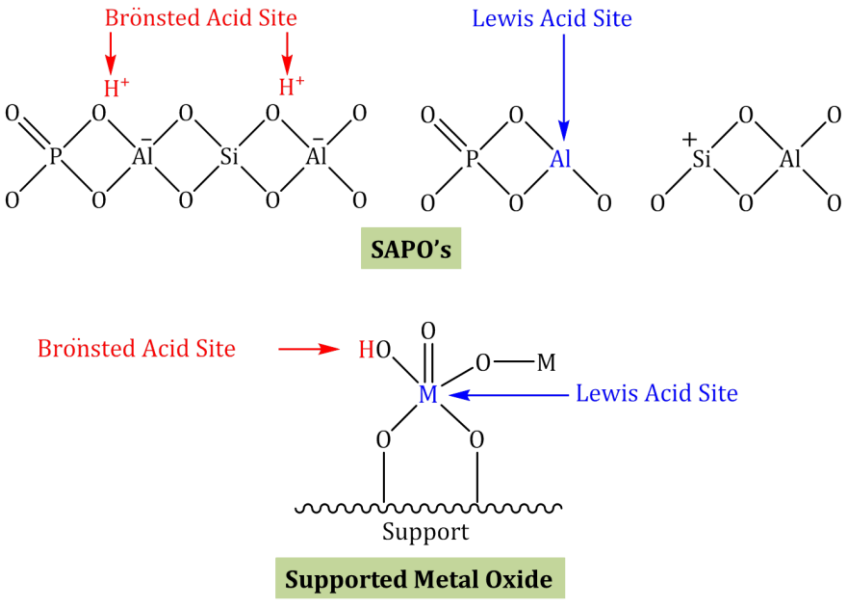

Fig. 1.12. Brönsted and Lewis acid sites in SAPO's and supported metal oxide catalysts.

1.9. Objectives and Scope of the Thesis

Considering the importance of conversion of biomass, especially lignocellulosic biomass (containing hemicelluloses, cellulose, lignin) into chemicals and after understanding the problems associated with the current processes for the synthesis of furan chemicals (furfural and HMF) it is necessary to develop new catalytic systems for the one-pot conversion of poly-saccharides and sugars into furans. Hence, to provide an efficient method along with development of new catalysts following objectives were set for my Ph.D work,

- Development of efficient methods for the one-pot conversion of plant-derived poly-saccharides into sugars and furans.

  - ☑ *Literature shows that plant-derived poly-saccharides (hemicellulose, starch) are inexpensive and largely available. Additionally, it is shown above that sugars and furans (furfural, HMF) have various industrial applications. Therefore, it is preferable to convert these poly-saccharides into value-added chemicals using solid acid catalysts.*

- Exploration of new stable solid acid catalysts.

  - ☑ *It is presented earlier that structured solid acid catalysts (zeolite) are not stable under reaction conditions. But, to develop sustainable methodology for biomass conversion catalysts needed to be stable. In this view point, two strategies will be undertaken for the development of stable solid acid catalysts such as, 1) synthesis of structured SAPO catalysts having higher hydrothermal stability than zeolites and 2) synthesis of amorphous supported metal oxide catalysts, since those do not have any definite structural properties (pore diameter, pore volume) may prove to be stable under reaction conditions.*

- To ensure high yields of furan compounds.

  - ☑ *As discussed above, most of the methods fail to provide high, selective yields for furans (furfural, HMF) from conversion of plant biomass (hemicellulose, starch). Considering this issue, efforts will be diverted to optimize the reaction conditions so that maximum possible yields for furans along with sugars can be achieved.*

- Employment of crop wastes without any pre-treatment for the selective conversion of hemicellulose.

  - ☑ *It is highly appreciative if plant-derived lignocellulosic biomass (crop waste) can be directly converted into value-added chemicals without undergoing any pre-treatment. This will nullify the step for the isolation of hemicelluloses and will also allow for the development of a catalyst which can withstand various impurities present in substrate. Efforts to be put forth for the complete analysis of crop wastes by TAPPI method which will allow knowing impurities and actual composition of substrates.*

- Establish the correlation between catalyst property and activity.

  - ☑ *Various physico-chemical characterization methods will be used to understand the properties of catalysts. This may help in proper understanding of influence of catalyst parameters those play major role in the reactions. Spent catalysts will be subjected for the characterization to help understand catalysts structure after used.*

1.10. Outline of the Thesis

The thesis is divided into six chapters and the key contents from all the chapters are outlined below.

Chapter 1 provides the overview of the work area, about biomass and biomass conversion technologies. Effort is given to understand the problems in this topic and based on that my plan of work is highlighted. Moreover, the recent developed solid acid catalyzed processes for the biomass conversion into valuable chemical, sugars and furans (furfural and HMF) are studied thoroughly to understand possibility of modification in these methods. Later, the properties of the typical solid acid catalysts along with their acid sites used in these processing are summarized. Finally, the drawbacks of the recent developed processes are understood and based on the problems my objective of work are discussed.

Chapter 2 presents the detailed synthesis procedures of all the solid acid catalysts. The physico-chemical characterization methods and data obtained with all the

catalysts are thoroughly discussed. Furthermore, it is shown that seven types of crop wastes (bagasse, rice husk and wheat straw) were collected from various regions of India and those were thoroughly characterized. The details of catalytic methods, analysis methods and calculations are also documented.

Chapter 3 describes the use of structured SAPO catalysts and other solid acid catalysts (zeolites, resins, Nb_2O_5) for the synthesis of C_5 sugars and furfural. The use of both isolated hemicelluloses (softwood and hardwood) and un-purified crop wastes (bagasse, rice husk and wheat straw) as substrate is demonstrated in presence of best active catalyst, SAPO-44. Effects of various reaction parameters are studied to establish the optimum conditions for achieving best possible yields. Further, a very high and recyclable furfural yield is presented from all the substrates. Later, an easy isolation methodology for furfural in pure form is demonstrated. Various physico-chemical characterizations for both fresh and spent SAPO-44 are described to enlighten its stability.

Chapter 4 deals with the use of various amorphous supported metal oxide catalysts having Lewis acidity for the synthesis of C_5 sugars and furfural from either isolated hemicelluloses or crop wastes. Amongst all the catalysts evaluated, 10 wt% WO_3/SiO_2 (SG) catalyst is presented as the best catalyst for the production of highest amount of furfural from all the substrates in several recycle runs. To understand the better catalytic activity of WO_3/SiO_2 (SG) compared to other supported metal oxides, various characterization techniques are used. Furthermore, several reaction parameters are optimized to obtain best possible furfural formation. Importantly, several characterizations are demonstrated to assure catalyst stability under reaction conditions.

Chapter 5 describes the one-pot synthesis of HMF from various carbohydrates such as mono-saccharide (fructose, glucose), di-saccharide (maltose, cellobiose) and poly-saccharide (starch) using SAPO catalysts. Best active catalyst SAPO-44 shows very high yields of HMF with very high selectivity from all the substrates. Repeated reaction with SAPO-44 shows a marginal decrease in HMF yields and this change in catalytic activity is due to slight morphological modification in SAPO-44 via reposition of

elements in its structure. Further, the influence of acid amount, type of acid site etc. on the catalytic activity is discussed.

In chapter 6 overall works is summarized and novelty of this work is discussed.

1.11. References

(1) Raymond, L. R.; Deming, C. P.; Nichols, M. W. *Facing the hard truths about energy: a comprehensive view to 2030 of global oil and natural gas*, National Petroleum Council, 2007.
(2) Keim, W. In *Methanol: The Basic Chemical and Energy Feedstock of the Future*; Bertau, M., Offermanns, H., Plass, L., Schmidt, F., Wernicke, H. J., Eds.; Springer-Verlag: Berlin, Heidelberg, 2014, p 421.
(3) Conti, J.; Holtberg, P.; Napolitano, S.; Schaal, A. M. *International Energy Outlook 2014: World Petroleum and Other Liquid Fuels*, U.S. Energy Information Administration, DOE/EIA-0484(2014), September 2014.
(4) Perlack, R. D.; Wright, L. L.; Turhollow, A. F.; Graham, R. L. *Biomass as feedstock for a bioenergy and bioproducts industry: the technical feasability of a billion-ton annual supply*, Oak Ridge National Laboratory, 2005.
(5) Lucia-Lucian, A.; Argyropoulos-Dimitris, S.; Adamopoulos, L.; Gaspar-Armindo, R. In *Materials, Chemicals, and Energy from Forest Biomass*; Argyropoulos, D. S., Ed.; American Chemical Society: 2007; Vol. 954, p 2.
(6) Kobayashi, H.; Fukuoka, A. *Green Chem.* **2013**, *15*, 1740.
(7) Maki-Arvela, P.; Salmi, T.; Holmbom, B.; Willfor, S.; Murzin, D. Y. *Chem. Rev.* **2011**, *111*, 5638.
(8) Sitanggang, A. B.; Sophia, L.; Wu, H. S. *Int. Food Res. J.* **2012**, *19*, 393.
(9) Fan, L. T.; Gharpuray, M. M.; Lee, Y. H. *Cellulose Hydrolysis*; Springer Berlin Heidelberg: Berlin, 1987; Vol. 3, p 1.
(10) Morais, A.; Bogel-Lukasik, R. *Sustainable Chem. Processes* **2013**, *1*, 18.
(11) Tanger, P.; Field, J. L.; Jahn, C. E.; DeFoort, M. W.; Leach, J. E. *Front. Plant Sci.* **2013**, *4*, 218.
(12) Damartzis, T.; Zabaniotou, A. *Renewable Sustainable Energy Rev.* **2011**, *15*, 366.
(13) Chen, W. Y.; Seiner, J.; Suzuki, T.; Lackner, M.; Mahalaxmi, S.; Williford, C. In *Handbook of Climate Change Mitigation*; Chen, W. Y., Seiner, J., Suzuki, T., Lackner, M., Eds.; Springer US: 2012, p 965.
(14) Himmel, M. E.; Baker, J. O.; Overend, R. P. In Pretreatment of Lignocellulosic Biomass; McMillan, J. D., Ed.; American Chemical Society: USA, 1994; Vol. 566., p 292.
(15) Kumar, R.; Singh, S.; Singh, O. *J. Ind. Microbiol. Biotechnol.* **2008**, *35*, 377.
(16) Wyman, C. E.; Decker, S. R.; Himmel, M. E.; Brady, J. W.; Skopec, C. E.; Viikari, L. *Chapter 43: Hydrolysis of cellulose and hemicellulose*; 2nd ed.; CRC Press: USA, 2004.
(17) Karimi, K.; Kheradmandinia, S.; Taherzadeh, M. J. *Biomass Bioenergy* **2006**, *30*, 247.
(18) Jin, F.; Enomoto, H. *Energy Environ. Sci.* **2011**, *4*, 382.
(19) Brandt, A.; Grasvik, J.; Hallett, J. P.; Welton, T. *Green Chem.* **2013**, *15*, 550.
(20) Zhou, C. H.; Xia, X.; Lin, C. X.; Tong, D. S.; Beltramini, J. *Chem. Soc. Rev.* **2011**, *40*, 5588.
(21) Matsagar, B. M.; Dhepe, P. L. *Catal. Sci. Technol.* **2014**, *DOI: 10.1039/C4CY01047G*.
(22) Robertson, A. J. B. *Platinum Metals Rev.* **1983**, *27*, 31.
(23) Deepa, A. K.; Dhepe, P. L. *RSC Adv.* **2014**, *4*, 12625.
(24) Alonso, D. M.; Wettstein, S. G.; Dumesic, J. A. *Chem. Soc. Rev.* **2012**, *41*, 8075.

(25) Dutta, S.; De, S.; Saha, B.; Alam, M. I. *Catal. Sci. Technol.* **2012**, *2*, 2025.
(26) Huber, G. W.; Chheda, J. N.; Barrett, C. J.; Dumesic, J. A. *Science* **2005**, *308*, 1446.
(27) Deepa, A. K.; Dhepe, P. L. *ChemPlusChem* **2014**, *DOI: 10.1002/cplu.201402145*.
(28) Tathod, A.; Kane, T.; Sanil, E. S.; Dhepe, P. L. *J. Mol. Catal. A: Chem.* **2014**, *388-389*, 90.
(29) Tathod, A. P.; Dhepe, P. L. *Green Chem.* **2014**, *DOI: 10.1039/C4GC01264J*.
(30) Dhepe, P. L.; Sahu, R. *Green Chem.* **2010**, *12*, 2153.
(31) Climent, M. J.; Corma, A.; Iborra, S. *Chem. Rev.* **2011**, *111*, 1072.
(32) Gallezot, P. *Chem. Soc. Rev.* **2012**, *41*, 1538.
(33) Rosatella, A. A.; Simeonov, S. P.; Frade, R. F. M.; Afonso, C. A. M. *Green Chem.* **2011**, *13*, 754.
(34) Saha, B.; Abu-Omar, M. M. *Green Chem.* **2014**, *16*, 24.
(35) Lange, J. P.; van der Heide, E.; van Buijtenen, J.; Price, R. *ChemSusChem* **2012**, *5*, 150.
(36) Stevens, J. G.; Bourne, R. A.; Twigg, M. V.; Poliakoff, M. *Angew. Chem. Int. Ed.* **2010**, *49*, 8856.
(37) Dedsuksophon, W.; Faungnawakij, K.; Champreda, V.; Laosiripojana, N. *Bioresour. Technol.* **2011**, *102*, 2040.
(38) Verdeguer, P.; Merat, N.; Gaset, A. *Appl. Catal. A: Gen.* **1994**, *112*, 1.
(39) Shi, S.; Guo, H.; Yin, G. *Catal. Commun.* **2011**, *12*, 731.
(40) Zhang, W.; Zhu, Y.; Niu, S.; Li, Y. *J. Mol. Catal. A: Chem.* **2011**, *335*, 71.
(41) Hu, X.; Song, Y.; Wu, L.; Gholizadeh, M.; Li, C. Z. *ACS Sustainable Chem. Eng.* **2013**, *1*, 1593.
(42) Sahu, R.; Dhepe, P. L. *React. Kinet., Mech. Catal.* **2014**, *112*, 173.
(43) Gupta, N. K.; Nishimura, S.; Takagaki, A.; Ebitani, K. *Green Chem.* **2011**, *13*, 824.
(44) Roman-Leshkov, Y.; Barrett, C. J.; Liu, Z. Y.; Dumesic, J. A. *Nature* **2007**, *447*, 982.
(45) Thananatthanachon, T.; Rauchfuss, T. B. *ChemSusChem* **2010**, *3*, 1139.
(46) Buntara, T.; Noel, S.; Phua, P. H.; Melian-Cabrera, I.; de Vries, J. G.; Heeres, H. J. *Angew. Chem. Int. Ed.* **2011**, *50*, 7083.
(47) Tuteja, J.; Choudhary, H.; Nishimura, S.; Ebitani, K. *ChemSusChem* **2014**, *7*, 96.
(48) Yaaaini, N.; Amin, N. A. S.; Asmadi, M. *Bioresour. Technol.* **2012**, *116*, 58.
(49) Chen, H.; Yu, B.; Jin, S. *Bioresour. Technol.* **2011**, *102*, 3568.
(50) Balakrishnan, M.; Sacia, E. R.; Bell, A. T. *Green Chem.* **2012**, *14*, 1626.
(51) Demolis, A.; Essayem, N.; Rataboul, F. *ACS Sustainable Chem. Eng.* **2014**, *2*, 1338.
(52) Dhepe, P. L.; Fukuoka, A. In *Bottom-up Nanofabrication: Supramolecules, Self-Assemblies, and Organized Films*; Ariga, K., Nalwa, H. S., Eds.; American Scientific Publisher: Valencia, 2009; Vol. 5, p 365.
(53) Dias, A. S.; Pillinger, M.; Valente, A. A. *Micro. Meso. Mater.* **2006**, *94*, 214.
(54) Dow Water & Process Solutions; http://www.dow.com/products/market/infrastructure/product-line/amberlyst-polymeric-catalysts/product/amberlyst-15dry/.
(55) Dow Water & Process Solutions; http://www.dow.com/products/product/amberlyst-70/.
(56) Inagaki, S.; Fukushima, Y.; Kuroda, K. *J. Chem. Soc., Chem. Commun.* **1993**, 680.
(57) Kresge, C. T.; Leonowicz, M. E.; Roth, W. J.; Vartuli, J. C.; Beck, J. S. *Nature* **1992**, *359*, 710.
(58) Zhao, D.; Feng, J.; Huo, Q.; Melosh, N.; Fredrickson, G. H.; Chmelka, B. F.; Stucky, G. D. *Science* **1998**, *279*, 548.
(59) Dias, A. S.; Pillinger, M.; Valente, A. A. *J. Catal.* **2005**, *229*, 414.
(60) Antunes, M. M.; Lima, S. R.; Fernandes, A.; Pillinger, M.; Ribeiro, M. F.; Valente, A. A. *Appl. Catal. A: Gen.* **2012**, *417-418*, 243.

(61) Shi, X.; Wu, Y.; Yi, H.; Rui, G.; Li, P.; Yang, M.; Wang, G. *Energies* **2011**, *4*, 669.
(62) Zeolyst International; http://www.zeolyst.com/our-products.aspx.
(63) Sahu, R.; Dhepe, P. L. *ChemSusChem* **2012**, *5*, 751.
(64) Lam, E.; Chong, J. H.; Majid, E.; Liu, Y.; Hrapovic, S.; Leung, A. C. W.; Luong, J. H. T. *Carbon* **2012**, *50*, 1033.
(65) Saravanan, K.; Tyagi, B.; Bajaj, H. C. *Catal. Sci. Technol.* **2012**, *2*, 2512.
(66) Garcia-Sancho, C.; Sadaba, I.; Moreno-Tost, R.; Merida-Robles, J.; Santamaria-Gonzalez, J.; Lopez-Granados, M.; Maireles-Torres, P. *ChemSusChem* **2013**, *6*, 635.
(67) Brownlee, H. J.; US002140572; Ed.; Quaker Oats Co.: USA, 1938.
(68) The chemistry and technology of furfural and its many by-products; Zeitsch, K. J., Ed.; Elsevier: Amsterdam, 2000; Vol. 13.
(69) Fitzpatrick, S. W.; US004897497; Ed.; Biofine Incorporated (Wilmington, DE): USA, 1990.
(70) Pan, X.; Gilkes, N.; Kadla, J.; Pye, K.; Saka, S.; Gregg, D.; Ehara, K.; Xie, D.; Lam, D.; Saddler, J. Biotechnol. Bioeng. 2006, 94, 851-861.
(71) Win, D. T. Aust. J. Technol. 2005, 8, 185-190.
(72) Gravitis, J.; Vedernikov, N.; Zandersons, J.; Kokorevics, A. In Chemicals and Materials from Renewable Resources; American Chemical Society: 2001; Vol. 784, p 110-122.
(73) Zeitsch, K. J.; US006743928; International Furan Technology (PTY) Limited (Kwa Zulu Natal, ZA), Ed.; Steiner, Philipp Daniel, S. Afr.: USA, 2004.Brownlee, H. J.; Quaker Oats Co. : 1938.
(74) Dias, A. S.; Lima, S.; Pillinger, M.; Valente, A. A. *Carbohydr. Res.* **2006**, *341*, 2946.
(75) Amarasekara, A. S.; Williams, L. D.; Ebede, C. C. *Carbohydr. Res.* **2008**, *343*, 3021.
(76) Gurbuz, E. I.; Gallo, J. M. R.; Alonso, D. M.; Wettstein, S. G.; Lim, W. Y.; Dumesic, J. A. *Angew. Chem. Int. Ed.* **2013**, *52*, 1270.
(77) Lam, E.; Majid, E.; Leung, A. C. W.; Chong, J. H.; Mahmoud, K. A.; Luong, J. H. T. *ChemSusChem* **2011**, *4*, 535.
(78) Agirrezabal-Telleria, I.; Requies, J.; Guemez, M. B.; Arias, P. L. *Appl. Catal. B: Env.* **2014**, *145*, 34.
(79) Lima, S. R.; Pillinger, M.; Valente, A. A. *Catal. Commun.* **2008**, *9*, 2144.
(80) Takagaki, A.; Ohara, M.; Nishimura, S.; Ebitani, K. *Chem. Lett.* **2010**, *39*, 838.
(81) Choudhary, V.; Pinar, A. B.; Sandler, S. I.; Vlachos, D. G.; Lobo, R. F. *ACS Catal.* **2011**, *1*, 1724.
(82) Choudhary, V.; Sandler, S. I.; Vlachos, D. G. *ACS Catal.* **2012**, *2*, 2022.
(83) Weingarten, R.; Cho, J.; Conner, J. W. C.; Huber, G. W. *Green Chem.* **2010**, *12*, 1423.
(84) Suzuki, T.; Yokoi, T.; Otomo, R.; Kondo, J. N.; Tatsumi, T. *Appl. Catal. A: Gen.* **2011**, *408*, 117.
(85) Li, H.; Deng, A.; Ren, J.; Liu, C.; Wang, W.; Peng, F.; Sun, R. *Catal. Today* **2014**, *234*, 251.
(86) Zhang, J.; Lin, L.; Liu, S. *Energy Fuels* **2012**, *26*, 4560.
(87) Dias, A. S.; Lima, S. R.; Carriazo, D.; Rives, V.; Pillinger, M.; Valente, A. A. *J. Catal.* **2006**, *244*, 230.
(88) Ferreira, L. R.; Lima, S. R.; Neves, P.; Antunes, M. M.; Rocha, S. M.; Pillinger, M.; Portugal, I.; Valente, A. A. *Chem. Eng. J.* **2013**, *215-216*, 772.
(89) O'Neill, R.; Ahmad, M. N.; Vanoye, L.; Aiouache, F. *Ind. Eng. Chem. Res.* **2009**, *48*, 4300.
(90) You, S. J.; Park, E. D. *Micro. Meso. Mater.* **2014**, *186*, 121.
(91) Lessard, J.; Morin, J. F.; Wehrung, J. F.; Magnin, D.; Chornet, E. *Top. Catal.* **2010**, *53*, 1231.
(92) Jiang, Y.; Li, X.; Wang, X.; Meng, L.; Wang, H.; Peng, G.; Wang, X.; Mu, X. *Green Chem.* **2012**, *14*, 2162.
(93) Ormsby, R.; Kastner, J. R.; Miller, J. *Catal. Today* **2012**, *190*, 89.

(94) Kusema, B. T.; Hilmann, G.; Maki Arvela, P.; Willfor, S.; Holmbom, B.; Salmi, T.; Murzin, D. *Catal. Lett.* **2011**, *141*, 408.
(95) Fabaa, L.; Kusema, B. T.; Murzina, E. V.; Tokarev, A.; Kumar, N.; Smeds, A.; Diaz, E.; Ordonez, S.; Maki-Arvela, P.; Willfor, S.; Salmi, T.; Murzin, D. Y. *Micro. Meso. Mater.* **2014**, *189*, 189.
(96) Cara, P. D.; Pagliaro, M.; Elmekawy, A.; Brown, D. R.; Verschuren, P.; Shiju, N. R.; Rothenberg, G. *Catal. Sci. Technol.* **2013**, *3*, 2057.
(97) Lima, S. R.; Antunes, M. M.; Fernandes, A.; Pillinger, M.; Ribeiro, M. F.; Valente, A. A. *Molecules* **2010**, *15*, 3863.
(98) Bozell, J. J.; Petersen, G. R. *Green Chem.* **2010**, *12*, 539.
(99) AVA Biochem, Switzerland; http://www.ava-biochem.com/pages/en/products/description.php.
(100) Dashtban, M.; Gilbert, A.; Fatehi, P. *RSC Adv.* **2014**, *4*, 2037.
(101) Shimizu, K.; Uozumi, R.; Satsuma, A. *Catal. Commun.* **2009**, *10*, 1849.
(102) Zhu, H.; Cao, Q.; Li, C.; Mu, X. *Carbohydr. Res.* **2011**, *346*, 2016.
(103) Lai, L.; Zhang, Y. *ChemSusChem* **2011**, *4*, 1745.
(104) Zhao, Q.; Wang, L.; Zhao, S.; Wang, X.; Wang, S. *Fuel* **2011**, *90*, 2289.
(105) Qi, X.; Watanabe, M.; Aida, T. M.; Smith, R. L. *Green Chem.* **2008**, *10*, 799.
(106) Qi, X.; Watanabe, M.; Aida, T. M.; Smith, R. L. *Ind. Eng. Chem. Res.* **2008**, *47*, 9234.
(107) Fan, C.; Guan, H.; Zhang, H.; Wang, J.; Wang, S.; Wang, X. *Biomass Bioenergy* **2011**, *35*, 2659.
(108) Wang, J.; Ren, J.; Liu, X.; Lu, G.; Wang, Y. *AIChE J.* **2013**, *59*, 2558.
(109) Qi, X.; Guo, H.; Li, L.; Smith, R. L. *ChemSusChem* **2012**, *5*, 2215.
(110) Kim, B.; Antonyraj, C. A.; Kim, Y. J.; Kim, B.; Shin, S.; Kim, S.; Lee, K. Y.; Cho, J. K. *Ind. Eng. Chem. Res.* **2014**, *53*, 4633.
(111) Villa, A.; Schiavoni, M.; Fulvio, P. F.; Mahurin, S. M.; Dai, S.; Mayes, R. T.; Veith, G. M.; Prati, L. *J. Energy Chem.* **2013**, *22*, 305.
(112) Tucker, M. H.; Crisci, A. J.; Wigington, B. N.; Phadke, N.; Alamillo, R.; Zhang, J.; Scott, S. L.; Dumesic, J. A. *ACS Catal.* **2012**, *2*, 1865.
(113) Alamillo, R.; Crisci, A. J.; Gallo, J. M. R.; Scott, S. L.; Dumesic, J. A. *Angew. Chem. Int. Ed.* **2013**, *52*, 10349.
(114) Guo, X.; Cao, Q.; Jiang, Y.; Guan, J.; Wang, X.; Mu, X. *Carbohydr. Res.* **2012**, *351*, 35.
(115) Moreau, C.; Durand, R.; Razigade, S.; Duhamet, J.; Faugeras, P.; Rivalier, P.; Ros, P.; Avignon, G. *Appl. Catal. A: Gen.* **1996**, *145*, 211.
(116) Ordomsky, V. V.; van der Schaaf, J.; Schouten, J. C.; Nijhuis, T. A. *J. Catal.* **2012**, *287*, 68.
(117) Ranoux, A.; Djanashvili, K.; Arends, I. W. C. E.; Hanefeld, U. *RSC Adv.* **2013**, *3*, 21524.
(118) Kourieh, R.; Rakic, V.; Bennici, S.; Auroux, A. *Catal. Commun.* **2013**, *30*, 5.
(119) Qi, X.; Watanabe, M.; Aida, T. M.; Smith Jr, R. L. *Catal. Commun.* **2008**, *9*, 2244.
(120) Zhang, Y.; Wang, J.; Ren, J.; Liu, X.; Li, X.; Xia, Y.; Lu, G.; Wang, Y. *Catal. Sci. Technol.* **2012**, *2*, 2485.
(121) Stosic, D.; Bennici, S.; Rakis, V.; Auroux, A. *Catal. Today* **2012**, *192*, 160.
(122) Kuo, C. H.; Poyraz, A. S.; Jin, L.; Meng, Y.; Pahalagedara, L.; Chen, S. Y.; Kriz, D. A.; Guild, C.; Gudz, A.; Suib, S. L. *Green Chem.* **2014**, *16*, 785.
(123) Qi, X.; Guo, H.; Li, L. *Ind. Eng. Chem. Res.* **2011**, *50*, 7985.
(124) Wang, T.; Nolte, M. W.; Shanks, B. H. *Green Chem.* **2014**, *16*, 548.
(125) Hu, L.; Zhao, G.; Hao, W.; Tang, X.; Sun, Y.; Lin, L.; Liu, S. *RSC Adv.* **2012**, *2*, 11184.
(126) Moreau, C.; Durand, R.; Roux, A.; Tichit, D. *Appl. Catal. A: Gen.* **2000**, *193*, 257.

(127) Lecomte, J.; Finiels, A.; Moreau, C. *Starch - Starke* **2002**, *54*, 75.
(128) Watanabe, M.; Aizawa, Y.; Iida, T.; Aida, T. M.; Levy, C.; Sue, K.; Inomata, H. *Carbohydr. Res.* **2005**, *340*, 1925.
(129) Watanabe, M.; Aizawa, Y.; Iida, T.; Nishimura, R.; Inomata, H. *Appl. Catal. A: Gen.* **2005**, *295*, 150.
(130) Lima, S. R.; Dias, A. S.; Lin, Z.; Brandao, P.; Ferreira, P.; Pillinger, M.; Rocha, J.; Calvino-Casilda, V.; Valente, A. A. *Appl. Catal. A: Gen.* **2008**, *339*, 21.
(131) Tuteja, J.; Nishimura, S.; Ebitani, K. *Bull. Chem. Soc. Japan* **2012**, *85*, 275.
(132) Takagaki, A.; Ohara, M.; Nishimura, S.; Ebitani, K. *Chem. Commun.* **2009**, 6276.
(133) Moliner, M.; Roman-Leshkov, Y.; Davis, M. E. *Proc. Nat. Acad. Sci.* **2010**, *107*, 6164.
(134) Roman-Leshkov, Y.; Moliner, M.; Labinger, J. A.; Davis, M. E. *Angew. Chem. Int. Ed.* **2010**, *49*, 8954.
(135) Choudhary, V.; Pinar, A. B.; Lobo, R. F.; Vlachos, D. G.; Sandler, S. I. *ChemSusChem* **2013**, *6*, 2369.
(136) Nikolla, E.; Roman□Leshkov, Y.; Moliner, M.; Davis, M. E. *ACS Catal.* **2011**, *1*, 408.
(137) Saikat, D.; Sudipta, D.; Astam, K. P.; Manickam, S.; Asim, B.; Basudeb, S. *Appl. Catal. A: Gen.* **2011**, *409-410*, 133.
(138) Yamaguchi, K.; Sakurada, T.; Ogasawara, Y.; Mizuno, N. *Chem. Lett.* **2011**, *40*, 542.
(139) Daengprasert, W.; Boonnoun, P.; Laosiripojana, N.; Goto, M.; Shotipruk, A. *Ind. Eng. Chem. Res.* **2011**, *50*, 7903.
(140) Lok, B. M.; Messina, C. A.; Patton, R. L.; Gajek, R. T.; Cannan, T. R.; Flanigen, E. M. *J. Am. Chem. Soc.* **1984**, *106*, 6092.
(141) Lutz, W.; Toufar, H.; Kurzhals, R.; Suckow, M. *Adsorption* **2005**, *11*, 405.
(142) http://www.wiredchemist.com/chemistry/data/bond_energies_lengths.html.
(143) Jones, J. *Acta Crystallographica Section B* **1968**, *24*, 355.
(144) Ashtekar, S.; Chilukuri, S. V. V.; Chakrabarty, D. K. *J. Phy. Chem.* **1994**, *98*, 4878.
(145) Nimlos, M. R.; Qian, X.; Davis, M.; Himmel, M. E.; Johnson, D. K. *J. Phy. Chem. A* **2006**, *110*, 11824.

CHAPTER-2

CATALYST SYNTHESIS, CHARACTERIZATION TECHNIQUES & CATALYTIC METHODS

2.1. Introduction

As discussed in the introduction chapter, conversion of lignocellulose into C_5 sugars C_6 sugars, furfural and 5-hydroxymethylfurfural (HMF) is very important and also it will be preferable if solid acid based methodology is developed for this transformation. Moreover, it is also suggested in the introduction chapter that development of stable solid acid catalyst is necessary. To develop stable solid acid catalyst, two strategies were undertaken *viz.* synthesis of structured silicoaluminophosphates (SAPO's) which are already known in literature as more hydrothermally stable[1] than zeolites and amorphous (no uniform pore structure) supported metal oxide catalysts which doesn't have uniform pore structure, might remain stable while using. This property will help in achieving stable catalytic activity in repeated runs.

In this chapter, the details on synthesis procedure of catalysts, characterization methods and catalytic methods will be discussed. In structured catalyst, various SAPO's such as SAPO-44, SAPO-5, SAPO-11 and SAPO-46 were synthesized. As per the literature reports, SAPO materials chosen in this study have different physical properties such as structure type, acid amount, acid sites, surface area, pore diameter etc. and therefore it would be interesting to evaluate their activity in the synthesis of furans. Along with structured catalysts, various amorphous catalysts such as supported metal oxides were also synthesized. Various metals such as tungsten, molybdenum, gallium, boron and phosphorous were used for supported metal oxide catalysts synthesis since those metal oxides show acidity. It is well-known in literature that although, the metals are the main active component in catalyst however, due to less surface area and less thermal stability (leading to formation of bigger particles which are inactive to carry out reactions) those are not preferable to use alone.[2] Therefore, it is necessary to support these active centers (metals) on thermally stable and porous materials to provide mechanical strength to catalysts and effective dispersion of metals. In this work, silica and zirconia materials were used as a support for the synthesis of supported metal oxide catalysts. The purpose of using silica as support material was basically due to its high surface area (395 m^2/g) which may allow effective dispersion of active centers (metals) on catalyst. Another material, zirconia having less surface area (82 m^2/g) compared to silica (395 m^2/g) was chosen as support to check whether surface area of support material has any

influence on synthesis of better active catalyst. Moreover, from literature it is understood that combination of silica and tungsten/molybdenum may form silicotungstic acid/silicomolybdic acid (heteropoly acid) type species[3] which can provide additional acid sites in catalysts. But, the similar type of species (heteropoly acid) is not possible with other commonly used supports (zirconia, ceria, titania, alumina). Considering these possibilities, in this work, silica and zirconia materials were tried as support. The supported metal catalysts were prepared by two methods namely, wet-impregnation (WI) and sol-gel (SG). In WI method of catalyst preparation, metals (active centers) are physically/chemically adsorbed on the surface of support via support-metal interaction.[4] So WI method can provide a catalyst having almost all the active centers (metals) exposed on surface and hence, those may show better catalytic activity. However, in some cases, support-metal interaction becomes so weak that the catalyst active sites (metals) are prone to leached out in solution while used. Moreover, due to weak bonding between supports and metals, under the reaction conditions, the metal centers come closer and forms bigger metal particles which are inactive.[4] Considering these problems with WI methods, another synthesis technique, SG was also tried. In SG methods, the precursors for synthesis of support material and metal precursors are mixed together under the synthesis conditions and hence, metal centers are incorporated into the structure of silica uniformly which provides structural stability in the catalysts.[4] Later, all those synthesized catalysts were characterized thoroughly with the help of several physico-chemical methods and details on the results are discussed in this chapter. In this work these solid acid catalysts were chosen since literature provides several successful organic transformations using them[5-12] and furthermore, till now these catalysts are not investigated for biomass conversion into chemicals.

Additionally, as discussed earlier, use of real biomass (without separation of its components) and selective conversion of its particular component would be always preferred for the synthesis of chemicals and hence various raw biomass (crop wastes: bagasse, rice husk and wheat straw) were collected from different regions of India. Further, to check the stability and ability of various solid acid catalysts developed in this work those were used as substrate for synthesis of chemicals. However, before carrying out reactions with these substrates, those were characterized by TAPPI method and the details on this method and results are discussed in this chapter.

Table 2.1. Summary on the materials used in the synthesis of SAPO's and supported metal oxides.

Sr. No.	Chemical Name	Molecular Formula	CAS No.	Supplier	Purity (%)
1.	Pseudoboehmite (Grade: MCI-1524)	Al_2O_3	24623-77-6	Marathwada Chemical Industries Pvt. Ltd, India	65-78; Al_2O_3
2.	Aluminium isopropoxide	$Al[OCH(CH_3)_2]_3$	555-31-7	Loba Chemie, India	98
3.	Fumed silica (0.007 μm)	SiO_2	112945-52-5	Aldrich, USA	>99
4.	Silica sol (Ludox AS-40)	SiO_2	7631-86-9	Aldrich, USA	40; SiO_2
5.	Ortho phosphoric acid	H_3PO_4	7664-38-2	Fisher Scientific, Germany	85
6.	Phosphorous acid	H_3PO_3	13598-36-2	Loba Chemie, India	98
7.	Cyclohexyl amine (CHA)	$C_6H_{13}N$	108-91-8	Spectrochem, India	99
8.	Di-*n*-propyl amine (DPA)	$[(CH_3CH_2CH_2]_2NH$	142-84-7	Spectrochem, India	99
9.	Tetraethyl orthosilicate (TEOS)	$Si(OC_2H_5)_4$	78-10-4	Aldrich, USA	98
10.	Zirconyl nitrate hydrate	$ZrO(NO_3)_2{\cdot}xH_2O$	14985-18-3	Loba Chemie, India	99
11.	Ammonia solution	NH_3	1336-21-6	Rankem, India	25; NH_3
12.	Ammonium metatungstate hydrate (AMT)	$(NH_4)_6H_2W_{12}O_{40}{\cdot}xH_2O$	12333-11-8	Aldrich, USA	≥66.5
13.	Ammonium heptamolybdate tetrahydrate (AHM)	$(NH_4)_6Mo_7O_{24}{\cdot}4H_2O$	12054-85-2	Loba Chemie, India	99
14.	Gallium nitrate hydrate	$Ga(NO_3)_3{\cdot}xH_2O$	69365-72-6	Acros Organics, USA	99.99

Sr. No.	Chemicals	Molecular Formula	CAS No.	Supplier	Purity (%)
15.	Tri-n-butyl borate	$[CH_3(CH_2)_3]_3B$	688-74-4	Alfa Aesar, USA	98
16.	Di-ammonium hydrogen phosphate	$(NH_4)_2HPO_4$	7783-28-0	Loba Chemie, India	>99
17.	Ethanol	C_2H_5OH	64-17-5	Analytical Reagents, India	99.9
18.	Ethylene glycol	$HOCH_2CH_2OH$	107-21-1	s. d. fine, India	99
19.	Hydrochloric acid	HCl	7647-01-0	Loba Chemie, India	35
20.	Nitric acid	HNO_3	7697-37-2	Loba Chemie, India	69-72

Table 2.2. Summary on SAPO catalysts synthesis parameters.

Material	Molar Gel Composition					Crystallization Temp., Time	Structure Type
	SDA	Al_2O_3	SiO_2	P_2O_5	H_2O		
ZDCT	1.0[a]	1.0[c]	1.0[e]	1.0[g]	60.0	200°C, 0 days	Amorphous
2DCT	1.0[a]	1.0[c]	1.0[e]	1.0[g]	60.0	200°C, 2 days	AFI + CHA
4DCT	1.0[a]	1.0[c]	1.0[e]	1.0[g]	60.0	200°C, 4 days	Low crystalline CHA
7DCT / 1.0-SiO2-SAPO-44	1.0[a]	1.0[c]	1.0[e]	1.0[g]	60.0	200°C, 7 days	Pure CHA
0.8-SiO2-SAPO-44	0.8[a]	1.0[c]	1.0[e]	1.0[g]	60.0	200°C, 7 days	-
1.2-SiO2-SAPO-44	1.2[a]	1.0[c]	1.0[e]	1.0[g]	60.0	200°C, 7 days	-
1.4-SiO2-SAPO-44	1.4[a]	1.0[c]	1.0[e]	1.0[g]	60.0	200°C, 7 days	-
1.6-SiO2-SAPO-44	1.6[a]	1.0[c]	1.0[e]	1.0[g]	60.0	200°C, 7 days	-
ALPO-44	1.0[a]	1.0[c]	-	1.0[g]	60.0	200°C, 7 days	-
SP-44	1.0[a]	-	1.0[e]	1.0[g]	60.0	200°C, 7 days	-
SA-44	1.0[a]	1.0[c]	1.0[e]	-	60.0	200°C, 7 days	-
SAPO-5	0.15[a]	0.13[d]	0.5[f]	0.13[g]	13.0	200°C, 2.5 h	AFI
SAPO-11	1.0[b]	1.0[c]	0.1[f]	1.0[g]	40.0	200°C, 1 day	AEL
SAPO-46	4.0[b]	1.2[c]	0.6[e]	2.5[h]	100.0	200°C, 6 days	AFS

'SDA' stands for structure directing agent, ZDCT: Zero Day Crystallization Time, 2DCT: 2 Days Crystallization Time, 4DCT: 4 Days Crystallization Time, 7DCT: 7 Days Crystallization Time. [a]cyclohexylamine, [b]di-*n*-propyl amine, [c]pseudoboehmite, [d]aluminum iso-propoxide, [e]fumed silica, [f]40% silica sol, [g]orthophosphoric acid, [h]orthophosphoric acid + phosphorous acid.

2.2. Materials

The details on the chemicals purchased for the synthesis of various catalysts (silicoaluminophosphates and supported metal oxides) are summarized in Table 2.1. Analytical Reagent (AR) grade chemicals were used for the catalyst synthesis. All the chemicals were used as received without any further purification.

2.3. Structured Catalyst Synthesis

As discussed earlier in this chapter various structure solid acid catalysts were synthesized. The name 'structured' means the catalyst having definite channel structure, definite pore diameter etc. In this section, I will give details on the synthesis of various SAPO materials such as SAPO-44, SAPO-5, SAPO-11 and SAPO-46. Moreover, influence of crystallization time during synthesis of SAPO-44 material was also checked. Later, to understand the effect of precursors and silica concentration in SAPO-44 material synthesis, later those parameters were also varied during the synthesis of SAPO-44. All these materials are synthesized by hydrothermal methods and the molar gel composition for synthesis of materials are presented in Table 2.2.

2.3.1. Synthesis of SAPO-44

SAPO-44 material was synthesized using a molar gel composition of CHA: Al_2O_3: SiO_2: P_2O_5: H_2O = 1.0: 1.0: 1.0: 1.0: 60.0.[5,13] In a typical synthesis, 7.69 g orthophosphoric acid was mixed with 12.5 g of distilled water and to this mixture 4.6 g pseudoboehmite was added slowly at 30°C under vigorous stirring using overhead stirrer. This addition was completed in 2 h and the resulting mixture was termed as 'gel A'. In another container, 2.05 g of fumed silica was added slowly to 23.5 g of water at 30°C under stirring using magnetic stirrer followed by addition of 3.33 g cyclohyxylamine (CHA) dropwisely and the mixture was denoted as 'gel B'. Then 'gel B' was added to 'gel A' at 30°C and stirred vigorously for 6 h using overhead stirrer to form homogeneous gel. Now the gel was transferred to four Teflon lined steel autoclaves (250 mL) and subjected to aging (crystallization) for different time period (0 h, 48 h, 96 h and 176 h) under atmospheric pressure (at *RT*) at 200°C without stirring. After cooling down the autoclave, solid materials were separated from liquid part through filtration (Whatman 42, diameter = 90 mm, thickness = 200 μm, pore size = 2.5 μm), washed thoroughly with room

temperature distilled water (minimum 500 mL) and dried in oven at 60°C for 16 h. The materials were further dried at 150°C for 6 h under high vacuum (10^{-3} bar). Finally materials were calcined at 550°C at a heating rate of 1°C/min in tubular furnace for 6 h under air flow (10 mL/min). Material with crystallization time of 0 h was denoted as 'zero day crystallization time (ZDCT)', 48 h was symbolized as '2 days crystallization time (2DCT)', 96 h was denoted as '4 days crystallization time (4DCT)' and 176 h was termed as '7 days crystallization time (7DCT) / SAPO-44'. All the materials were stored in desiccator over activated silica gel. The details on the calcination program applied in the synthesis of SAPO-44 are shown in Fig. 2.1.

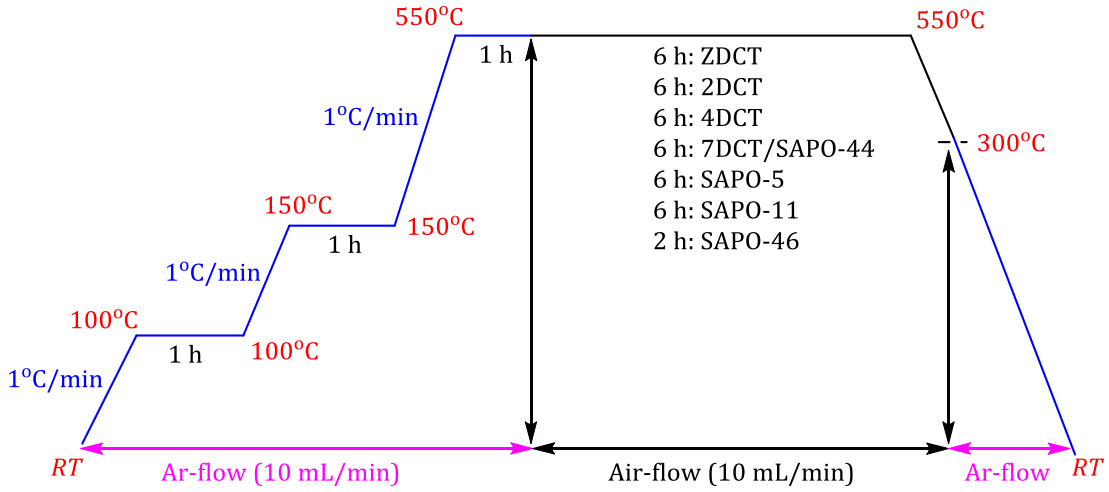

Fig. 2.1. Calcination program for ZDCT, 2DCT, 4DCT, 7DCT/SAPO-44, SAPO-5, SAPO-11 and SAPO-46 materials.

In addition to this, to check the influence of silica concentration in SAPO-44 material, various amount of silica (0.8-1.6 molar ratio) were used during synthesis of SAPO-44 materials (Table 2.2), keeping rest of the procedure same. The synthesized materials were termed as 0.8-SiO_2-SAPO-44, 1.0-SiO_2-SAPO-44, 1.2-SiO_2-SAPO-44, 1.4-SiO_2-SAPO-44 and 1.6-SiO_2-SAPO-44, respectively. Next, to understand the effects of composite materials (Si, Al, P) or precursors, synthesis of materials with varying elemental compositions was done. By varying the precursors (Si, Al and P) it is possible to prepare four different materials, *viz.* Si-Al (SA-44); made up of only silica and alumina precursors, Si-P (SP-44); made up of silica and phosphorus precursors, Al-P (ALPO-44); made up of only alumina and phosphorous precursors and Si-Al-P (SAPO-44); made up of silica, alumina and phosphorous precursors. All these materials were synthesized using similar procedure as described for synthesis of SAPO-44 material.

2.3.2. Synthesis of SAPO-5

SAPO-5 material was prepared using molar gel composition of CHA: Al_2O_3: SiO_2: P_2O_5: H_2O = 0.15: 0.13: 0.5: 0.13: 13.0.[13-15] Typical synthesis procedure for SAPO-5 is described here. 4.32 g of aluminium isopropoxide and 12 g of water were mixed together at 30°C and slurry was made. Now, in another beaker, diluted phosphoric acid was made by slow addition of 2.43 g H_3PO_4 in 3.60 g water. Diluted phosphoric acid solution was added drop by drop to previously made slurry at 30°C and mixed vigorously using magnetic stirrer for 1 h. Later, 1.26 g of CHA was added dropwisely to the resultant gel and stirred for another 1.5 h. After homogeneity was obtained in the system, 6.39 g silica sol was added slowly under stirring using magnetic stirrer and later, stirring was continued for another 0.25 h. Obtained solution was aged in an autoclave (10 mL) with Teflon liner for 2.5 h at 200°C (under static conditions). Then the autoclave was cooled to room temperature. The solid materials were separated from liquid part through filtration (Whatman 42, diameter = 90 mm, thickness = 200 μm, pore size = 2.5 μm), washed thoroughly with room temperature distilled water (minimum 500 mL) and dried in oven at 60°C for 16 h. The materials were further dried at 150°C for 6 h under high vacuum (10^{-3} bar). Final SAPO-5 material was obtained by calcining as-synthesized mass at 550°C at a heating rate of 1°C/min in tubular furnace for 6 h under the stream of air at 10 mL/min flow rate. Detail calcination program was shown in Fig. 2.1. White colour SAPO-5 was kept in a desiccator over activated silica gel.

2.3.3. Synthesis of SAPO-11

Synthesis of SAPO-11 material was done using molar gel composition of DPA: Al_2O_3: SiO_2: P_2O_5: H_2O = 1.0: 1.0: 0.1: 1.0: 40.0.[13,15] In a typical synthesis procedure of SAPO-11, 2.0 g pseudoboehmite was added slowly (within 2 h) to 4.71 g of water at 30°C and mixed thoroughly with vigorous stirring using magnetic stirrer. Later, addition of 3.17 g H_3PO_4 to previous mixture was done with constant stirring using magnetic stirrer. Then additional 4.70 g of water was added at 30°C and stirred for another 2 h to make it homogeneous. After that, 0.21 g silica sol (Ludox AS-40) was added dropwisely under vigorous stirring and finally addition of 1.4 g DPA was done with another 2 h continuous stirring afterwards. Obtained solution was aged in an autoclave (10 mL) with Teflon liner for 24 h at 200°C. After cooling down the autoclave, solid materials were separated

from liquid part through filtration (Whatman 42, diameter = 90 mm, thickness = 200 μm, pore size = 2.5 μm), washed thoroughly with room temperature distilled water (minimum 500 mL) and dried in oven at 60°C for 16 h. The materials were further dried at 150°C for 6 h under high vacuum (10^{-3} bar). White colored SAPO-11 material was obtained after calcination of as-synthesized material at 550°C at a heating rate of 1°C/min in tubular furnace for 6 h under the stream of air at 10 mL/min flow rate and stored in desiccator. Detail calcination program was shown in Fig. 2.1.

2.3.4. Synthesis of SAPO-46

Synthesis of SAPO-46 material was done using molar gel composition of DPA: Al_2O_3: SiO_2: H_3PO_3: H_3PO_4: H_2O = 4.0: 1.2: 0.6: 1.0: 1.5: 100.0.[6,13] In the synthesis of SAPO-46, 2.4 g of orthophosphoric acid was slowly mixed with phosphorus acid solution (1.2 g phosphorus acid + 10 g distilled water). This acid solution was added dropwise to 2.4 g of pseudoboehmite at 30°C with constant stirring using magnetic stirrer followed by 0.25 h continuation in stirring. Later, 10.0 g of distilled water was poured slowly to it and stirred for 0.5 h. To it 5.7 g of DPA was added drop by drop at 30°C and then the stirring was continued for 0.25 h. Water dispersed fumed silica (0.5 g fumed silica + 4.6 g distilled water) at 30°C was added slowly to the previous solution with stirring for 0.25 h. The gel obtained was taken in a Teflon lined stainless steel autoclave (150 mL) and kept for aging at 200°C for 144 h. Afterwards the autoclave was allowed to cool to room temperature. Solid mass was separated from liquid part by centrifugation and then washed thoroughly with room temperature distilled water and centrifugation (minimum 10 times; using 30 mL water each time). Material was first dried at 60°C for 16 h and then at 150°C for 6 h under high vacuum (10^{-3} bar). Final material was obtained after calcination of as-synthesized material at 550°C at a heating rate of 1°C/min in tubular furnace for 2 h under air flow (10 mL/min) and stored in desiccator. Detail calcination program was shown in Fig. 2.1.

2.4. Amorphous Catalyst Synthesis

As discussed earlier (section 2.1) in this chapter various amorphous supported metal oxide catalysts were synthesized. Here, the name 'amorphous' stands for the catalyst which doesn't have uniform pore structures. In this section, I will give details on the

synthesis of various supported metal oxide catalysts having 10 *wt*% metal loading using two different methods namely, wet-impregnation (WI) and sol-gel (SG). The detail procedures are discussed below.

2.4.1. Synthesis of ZrO_2 Support

In a typical synthesis procedure,[16] 5.0 g zirconyl nitrate hydrate was dissolved in 98.27 g distilled water. 5% diluted ammonia solution in distilled water was added to it drop by drop under vigorous stirring using magnetic stirrer until pH of solution becomes 9.1 and stirring was continued for 45 min at 30°C. Then the solid mass was aged for 12 h at 30°C without stirring. Finally the precipitation was separated from liquid by filtration using Whatman 41 filter paper, washed with distilled water till pH of filtrate become neutral. Material was first dried at 60°C for 16 h and then at 150°C for 6 h under high vacuum (10^{-3} bar). Calcination of the solid material was done at 500°C for 4 h in air stream (10 mL/min) which yields light brown zirconia. This synthesized zirconia was used as support in further synthesis. Detail calcination program is shown in Fig. 2.2.

Before use, all supports were activated at 150°C for 6 h under high vacuum (10^{-3} bar) and used for catalyst synthesis.

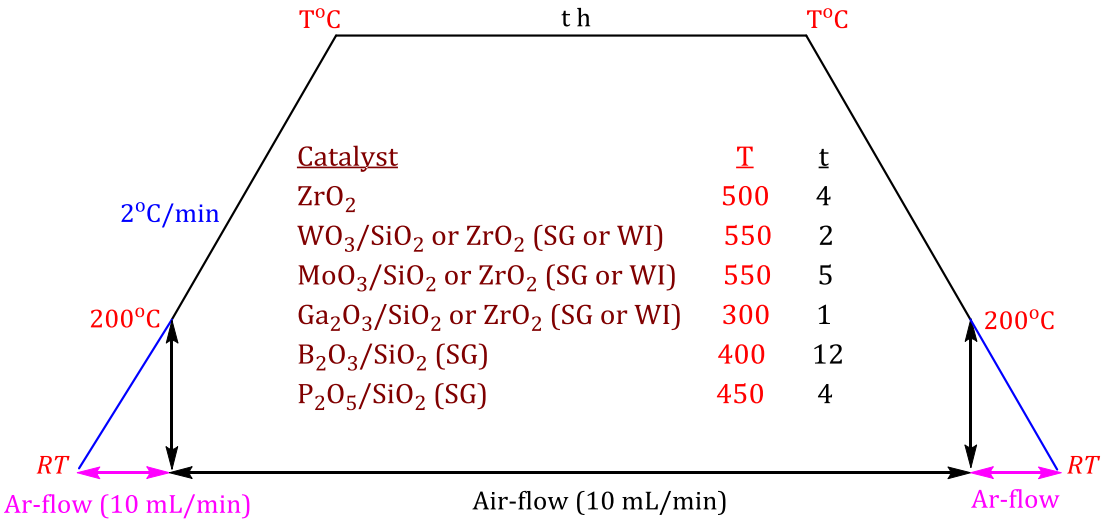

Fig. 2.2. Calcination program for ZrO_2 and supported metal oxide catalysts.

2.4.2. Synthesis of Wet-Impregnated (WI) Supported Metal Oxides

Two different supports *viz.* fumed silica and synthesized zirconia were used in the synthesis of supported metal oxide catalysts by WI method. For synthesis of all

catalysts, metal concentration was kept constant at 10 wt% based on support material. In a typical procedure,[16,17] 1.0 g of activated support was dispersed in 8 mL distilled water by stirring it using magnetic stirrer for 30 min at 30°C. Then 2 mL of metal salt solution was added dropwise to it at 30°C. For tungsten catalyst, 0.2238 g AMT; for molybdenum catalyst, 0.2065 g AHM; for gallium catalyst, 0.4076 g gallium nitrate hydrate was dissolved in 2 mL distilled water to prepare metal salt solution. Now the mixture was stirred for 16 h at 30°C. The water content in the prepared gel was removed using rotary evaporator. Solid material was dried at 60°C for 16 h followed by heating at 150°C for 6 h in high vacuum (10^{-3} bar). Calcination (for detail program see Fig. 2.2.) at required temperature and time (for tungsten: 550°C, 2 h; for molybdenum: 550°C, 5 h; for gallium: 300°C, 1 h) in presence of air produced final supported metal oxide catalyst which was stored in a desiccator.

2.4.3. Sol-Gel (SG) Synthesis for Supported Metal Oxides

In this section I will give details on the synthesis of various supported metal oxide catalysts using sol-gel method. In sol-gel synthesis, metals were incorporated in the support framework during synthesis. Using sol-gel method various supported metal oxide catalysts were prepared. For in-situ synthesis of silica support tetraethyl orthosilicate (TEOS) and for zirconia support zirconyl nitrate hydrate were used. All the procedure was carried out in round bottom (*RB*) flask.

2.4.3.1. WO_3/SiO_2

In a typical synthesis,[17,18] 10 mL of TEOS was added to 20 mL of distilled water and made it homogeneous by stirring using magnetic stirrer. Mixture was now hydrolyzed at 60°C by stirring for 14 h. Resulting ethanol was removed by rotary evaporator. During evaporation of ethanol water also removed from system and yields thick gel material. The silica gel formed was washed with distilled water (5 times; 30 mL water was used each time) and separated through centrifugation. Prepared silica gel was made acidic (pH = 1-1.5) with slow addition of 3.8 M HCl. In another beaker, 0.67 g AMT (calculated amount for 10 wt% W based on theoretical yield of silica) was dissolved in distilled water to obtain 6.5×10^{-3} M solution. pH of this solution was maintained at 1-1.5 by addition of 3.8 M HCl at 30°C and the solution was aged at static condition for 48 h at 30°C. Now, acidic tungstate gel was mixed slowly with acidic silica gel under vigorous

stirring for 1 h. Resulting solution was aged at 30°C under static condition for 12 h. Finally, water content in the prepared gel was removed using rotary evaporator. Solid material was dried at 60°C for 16 h followed by heating at 150°C for 6 h in high vacuum (10^{-3} bar). To get 10 wt% (metal basis) tungsten oxides on silica support materials, light yellow coloured solid dried material was calcined in air stream (10 mL/min) at 550°C for 2 h with heating rate of 2°C/min (Fig. 2.2).

2.4.3.2. MoO_3/SiO_2

In a typical method,[17,19] 0.64 g AHM (calculated amount for 10 wt% Mo based on theoretical yield of silica) was dissolved in 40 mL ethylene glycol and stirred for 0.5 h. Then 10 mL TEOS was added slowly to it under stirring using magnetic stirrer and the resulting solution was heated at 80°C for 5 h under vigorous stirring. The solution was then diluted with 20 mL of distilled water and acidified with 0.5 mL concentrated HNO_3. The solution was then kept at 80°C with stirring until it becomes a thick gel. Finally, the gel obtained was subjected to rotary evaporator for water removal. Solid material was dried at 60°C for 16 h followed by heating at 150°C for 6 h in high vacuum (10^{-3} bar). Finally, the as-synthesized material was calcined in air stream (10 mL/min) at 550°C for 5 h with heating rate of 2°C/min (Fig. 2.2) to obtain 10 wt% molybdenum oxide supported on silica catalyst.

2.4.3.3. Ga_2O_3/SiO_2

Typically,[17,20] 1.25 g gallium nitrate (calculated amount for 10 wt% Ga based on theoretical yield of silica) was solubilize in 21 mL ethanol. To the mixture, 10 mL of TEOS was added and stirred for 0.5 h using magnetic stirrer at 30°C. A thick gel was formed after the slow addition of ammonia solution to the previous mixture with constant stirring. The gel obtained was subjected to rotary evaporator for water removal. Solid material was dried at 60°C for 16 h followed by heating at 150°C for 6 h in high vacuum (10^{-3} bar). Finally, the as-synthesized material was calcined in air stream (10 mL/min) at 300°C for 1 h with heating rate of 2°C/min (Fig. 2.2) to obtained 10 wt% gallium oxide supported on silica catalyst.

2.4.3.4. B_2O3/SiO_2

In typical procedure,[21] 14.25 mL of 25% NH_4OH was mixed well with 90 mL of ethanol by stirring for 0.5 h using magnetic stirrer. To this mixture, 7.5 mL of TEOS was added at 30°C and the stirring was continued for another 0.5 h. In another container, 1.74 mL of tri-*n*-butyl borate (calculated amount for 10 wt% boron based on theoretical yield of silica) was dissolved in 10 mL ethanol and made homogeneous by stirring for 0.25 h. Now this metal salt solution was added drop by drop to TEOS solution at 30°C under vigorous stirring condition. The solution was then kept for aging at 30°C. After that, the liquid phase from the gel obtained was removed using rotary evaporator. Solid material was dried at 60°C for 16 h followed by heating at 150°C for 6 h in high vacuum (10^{-3} bar). To get 10 wt% (metal basis) boron oxides on silica support materials, as-synthesized solid dried material was calcined in air stream (10 mL/min) at 400°C for 12 h with heating rate of 2°C/min (Fig. 2.2).

2.4.3.5. P_2O_5/SiO_2

In a typical preparation,[22] TEOS (10.5 g), ethanol (11.8 g) and water (3.7 g) were mixed together in a molar ratio of 1:5:4 in 100 mL *RB* flask at 30°C under stirring using magnetic stirrer. The mixture was then kept for refluxing at 70°C for 0.25 h with vigorous stirring. Later, 0.7 mL orthophosphoric acid (calculated amount for 10 wt% phosphorous based on theoretical yield of silica) was added slowly to the previous solution with constant stirring. The mixture was then again stirred at 70°C for 12 h and slowly the gel formation occurs. After that, the liquid part in the gel obtained was removed using rotary evaporator. Solid material was dried at 60°C for 16 h followed by heating at 150°C for 6 h in high vacuum (10^{-3} bar). Finally, the as-synthesized material was calcined in air stream (10 mL/min) at 450°C for 4 h with heating rate of 2°C/min (Fig. 2.2) to obtained 10 wt% phosphorous oxide supported on silica catalyst.

2.4.3.6. WO_3/ZrO_2

In a typical synthesis,[17,23] 1.88 g zirconyl nitrate was dissolved in 30 mL distilled water by stirring it for some time. Then, pH of this solution was adjusted to 10 with drop by drop addition of 25% ammonia solution. In another container, 0.22 g AMT (calculated amount for 10 wt% tungsten based on theoretical yield of ZrO_2) + 7 mL distilled water

was prepared and made alkaline (pH = 10) with dropwise addition of 25% ammonia solution. Now zirconyl nitrate solution was added slowly to alkaline AMT solution drop by drop and a white gel was formed. The gel was aged at 30°C for 24 h under static condition. The gel obtained was washed with water (until neutral pH) and dried (first at 60°C for 16 h and then at 150°C for 6 h under evacuation, 10^{-3} bar). Finally, the as-synthesized material was calcined in air stream (10 mL/min) at 550°C for 2 h with heating rate of 2°C/min (Fig. 2.2) to obtained 10 wt% WO_3/ZrO_2 catalyst.

2.4.3.7. MoO_3/ZrO_2

In a typical synthesis of 1 g catalyst,[17,24] 1.88 g zirconyl nitrate was dissolved in 30 mL distilled water and made homogeneous by stirring for 0.25 h using magnetic stirrer. To it an aqueous solution (7 mL) of calculated amount AHM (0.21 g; to maintain 10 wt% Mo based on theoretical amount of ZrO_2) was added dropwisely at 30°C under vigorous stirring. 25% ammonia solution was then added to the mixture slowly under constant stirring until the solution pH was reached to 10. The gel formed was then aged at 30°C for 12 h under static condition. The gel made was washed with water (until neutral pH), dried (first at 60°C for 16 h and then at 150°C for 6 h under evacuation, 10^{-3} bar), and finally calcined at 550°C (heating rate = 2°C/min) for 5 h under air flow (10 mL/min) to obtained powdered MoO_3/ZrO_2 (Fig 2.2).

2.4.3.8. Ga_2O_3/ZrO_2

Typically for the synthesis of 1 g catalyst,[17,23] 1.88 g zirconyl nitrate was dissolved in 30 ml distilled water and pH of this solution was maintained at 10 with slow addition of 25% ammonia solution under vigorous stirring using magnetic stirrer. In another container, aqueous solution of gallium nitrate (0.41 g salt + 7 mL distilled water) was prepared and made alkaline (pH = 10) with dropwise addition of 25% ammonia under stirring. Now zirconyl nitrate solution was added slowly to alkaline salt solution at 30°C and formation of gel was observed. The gel was then aged at 30°C for 24 h under static condition. The gel made was washed with water (until neutral pH), dried (first at 60°C for 16 h and then at 150°C for 6 h under evacuation, 10^{-3} bar). Finally, the as-synthesized material was calcined in air stream (10 mL/min) at 300°C for 1 h with heating rate of 2°C/min (Fig. 2.2) to obtained 10 wt% Ga_2O_3/ZrO_2 catalyst.

2.5. Catalyst Characterizations

After synthesis of various catalysts, those were characterized using various physical (X-Ray Diffraction, Nuclear Magnetic Resonance, Infra-Red Spectroscopy, Raman Spectroscopy, X-Ray Photoelectron Spectroscopy, Ultra Violet – Visible Spectroscopy, Scanning Electron Microscopy, Transmission Electron Microscopy and Thermal Gravimetric Analysis) and chemical (Temperature Programmed Desorption of NH_3, N_2 sorption, Inductively Coupled Plasma-Optical Emission Spectroscopy) methods to understand several important properties of catalysts. The details on the instruments, sample preparation, analysis methods and analysis data are described below.

2.5.1. X-Ray Diffraction (XRD)

X-ray diffraction (XRD) analysis was undertaken to understand the phase purity in the material. For analysis, sample was prepared as a thin layer on a glass plate and analyzed by Rigaku Miniflex diffractometer (Netherland) using a Ni-filtered monochromatic Cu K_α radiation (λ = 1.5406 Å). The samples were scanned between a 2θ range of 5-80° at a scan rate of 2°/min. The sample analysis was carried out based on the analysis data of silicon (2θ = 28.45°) as a standard.

In case of SAPO's, the XRD patterns are presented in a 2θ value of 5-40° (Fig. 2.3) since after 2θ = 40° no peak is observed. All the structured SAPO catalysts showed highly crystalline phases in XRD patterns (Fig. 2.3). XRD patterns of SAPO's show that SAPO-44 has CHA morphology, SAPO-5 has AFI morphology, SAPO-11 has AEL morphology and SAPO-46 has AFS morphology. The characteristic peaks for CHA, AFI and AFS are indicated with asterisk (*) in Fig. 2.3. All the XRD patterns coincided well with those in the literature.[6,14,15,25] A detail discussion on influence of crystallization time is made in Chapter 3.

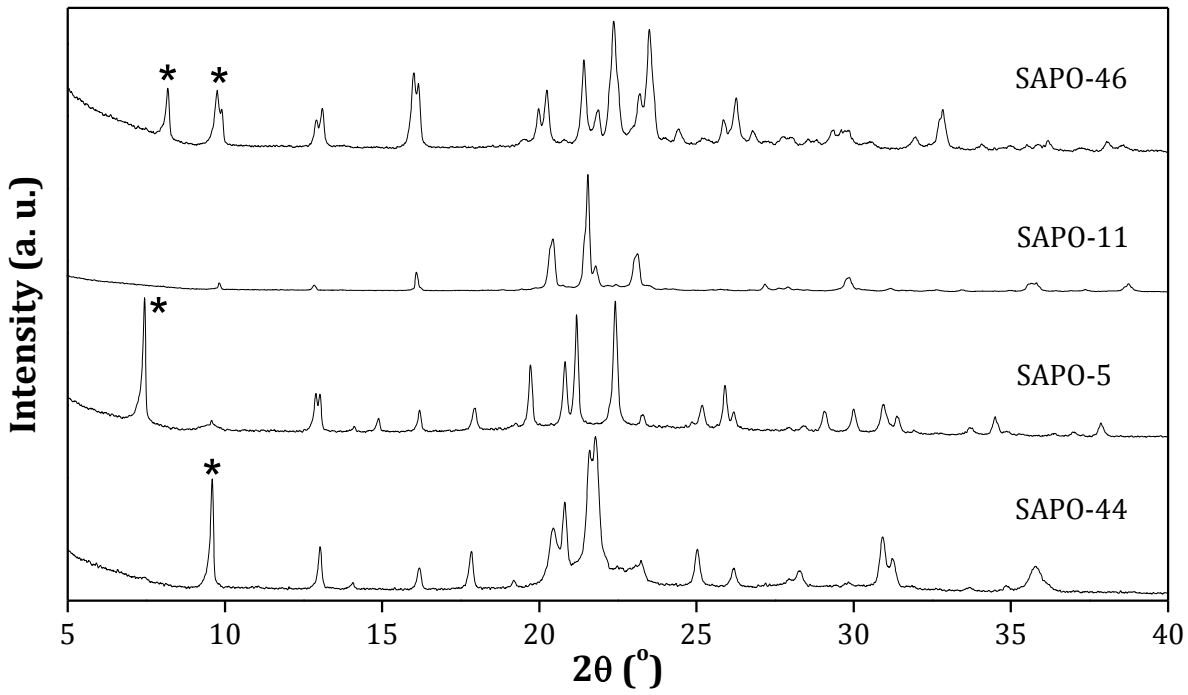

Fig. 2.3. XRD patterns for fresh SAPO's.

The catalysts synthesized using WI method shows crystalline phase for tungsten oxide and molybdenum oxide and amorphous phase for gallium oxide (Fig. 2.4). Presence of orthorhombic WO_3 crystals (JCPDS File No. 20-1324) and orthorhombic α-MoO_3 crystals (JCPDS File No. 76-1003) was confirmed with their crystalline phase in XRD patterns. The similar crystalline phase was also reported earlier.[18,26] But in the case of SiO_2 supported metal oxide catalysts synthesized by SG method (with similar metal loading as WI catalysts), peak only for amorphous phase is visible and that the peaks due to metal oxides are missing unlike observed in WI catalysts (Fig. 2.4). This indicates that the metal oxides are uniformly distributed in the silica framework when SG method is used for synthesis. Moreover, the shift visible in amorphous peak of SiO_2 shows that there is change in bonding characteristics in its structure.[27] Furthermore, absence of any separate metal oxide peaks in SG synthesized material is also indicative for the formation of smaller crystallite size metal oxide.[28]

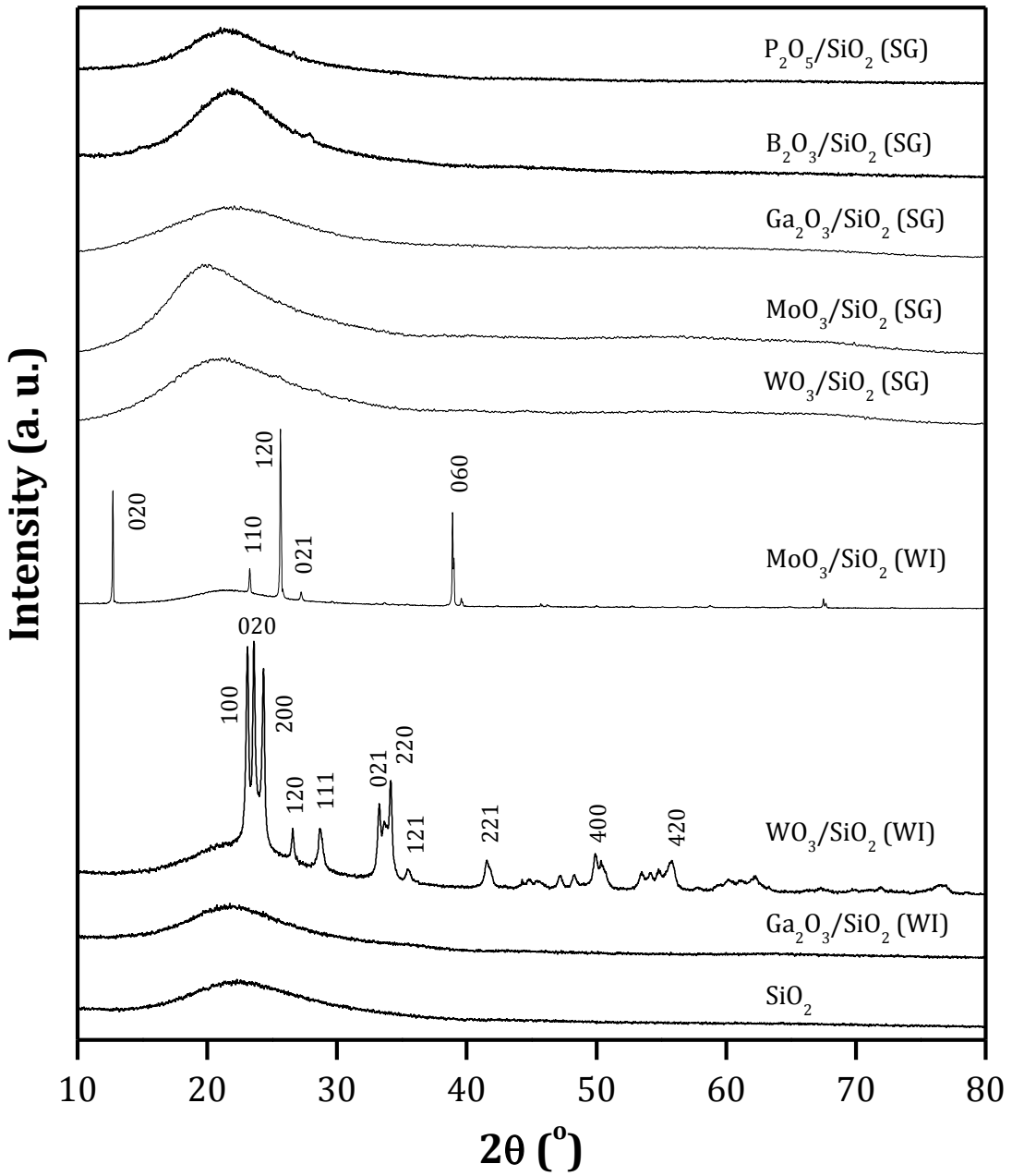

Fig. 2.4. XRD patterns of silica supported metal oxides synthesized by WI and SG method.

Fig. 2.5 shows the XRD patterns for bulk structures of pure ZrO_2 and ZrO_2 supported metal oxides synthesized by SG method. Pure ZrO_2 calcined at 500°C shows peaks for both the phases, monoclinic (JCPDS File No. 89-0943) and tetragonal (JCPDS File No. 81-1545). The similar observation is noted in the literature.[29] The incorporation of molybdenum in ZrO_2 shows characteristic peaks for orthorhombic MoO_3 species with change in the ZrO_2 peak pattern. The predominant presence of monoclinic phase of ZrO_2 in MoO_3/ZrO_2 catalyst is obvious since calcination at higher temperature (550°C)

modifies tetragonal phase into monoclinic phase in ZrO_2.[29] Moreover, it is also reported that peak due to $Zr(MoO_4)_2$ species can be observed around same 2θ value (30.2°) where peak due to tetragonal phase of ZrO_2 is observed. However, this possibility can be ruled out since only 10 wt% Mo was incorporated in catalysts and literature describe formation of $Zr(MoO_4)_2$ at very high Mo loading (37 wt%).[29] XRD pattern for WO_3/ZrO_2 catalyst shows typical peaks for orthorhombic WO_3 phase with tetragonal phase (major) in ZrO_2. The similar observation was reported in the literature for WO_3/ZrO_2.[30] Absence of metal oxide peaks in Ga_2O_3/ZrO_2 might be due to very high dispersion and ZrO_2 mostly remain in tetragonal phase since calcination was done at 300°C.[30]

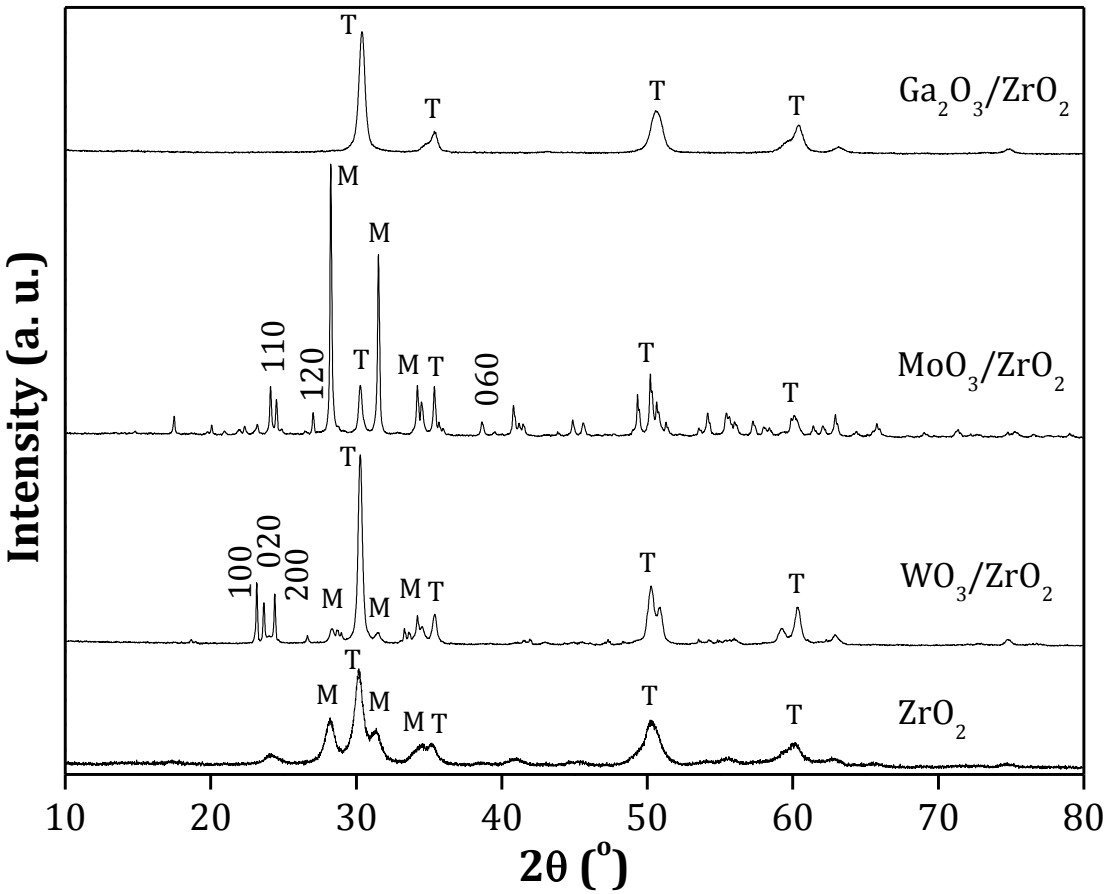

Fig. 2.5. XRD patterns of zirconia supported metal oxides synthesized by SG method. 'M' represents monoclinic ZrO_2 phase and 'T' represents tetragonal ZrO_2 phase.

2.5.2. Nuclear Magnetic Resonance (NMR)

Local environment around Si, Al and P nuclei in SAPO-44 was determined using solid state MAS (Magic Angle Spinning) NMR analysis. Solid state ^{29}Si, ^{31}P and ^{27}Al NMR spectra were recorded on a Bruker Avence-300 MHz spectrometer, operated at 7.06

tesla field. Fine powdered SAPO-44 was placed in a 4 mm zirconia rotor and spun at 10 kHz for all the nuclei.

In ^{29}Si MAS NMR spectra, SAPO-44 catalyst show multiple signals which suggests that Si is present in multiple environments (Fig. 2.6). Generally, in tetrahedral siliceous material, –OSi bond can be replaced by either –OAl or –OH bonds to form different silica environment and those are discussed below. Peak observed at -92.1 ppm is typically ascribed to [Si(4Al)] / Q^0 species since possibility of $Si(OH)_4$ species is difficult due to less stability. Moreover, quite higher intensity of Q^0 species confirmed that large amount of Si was incorporated in ALPO framework and hence, high acid amount can be expected in SAPO-44. Beside this peak, other moderate intense peaks were also observed; [Si(3Al)] / Q^1 (-96.2 ppm), [Si(2Al)] / Q^2 (-101.7 ppm) and [Si(1Al)] / Q^3 (-107.7 ppm). Presence of these peaks indicates that surface hydroxyl groups might be present in SAPO-44 to give rise to Brönsted acid sites. Another peak appearing at -112.8 ppm is the indicative of presence of Si[(0Al)] / Q^4 species. High intensity of Q^4 species indicate that some amount of silica was not incorporated in ALPO framework and forms additional SiO_2 species. This can also be evident from the XRD patterns of SAPO-44 which shows the presence of extra amorphous silica peak (2θ = 19-24°; Fig. 2.3) and ALPO peaks (2θ = 20.5°, 21.7°, 23.2°, 29.9° and 35.8°; Fig. 2.3). More detail discussion regarding this issue is made in section 3.2.1.5, chapter 3.

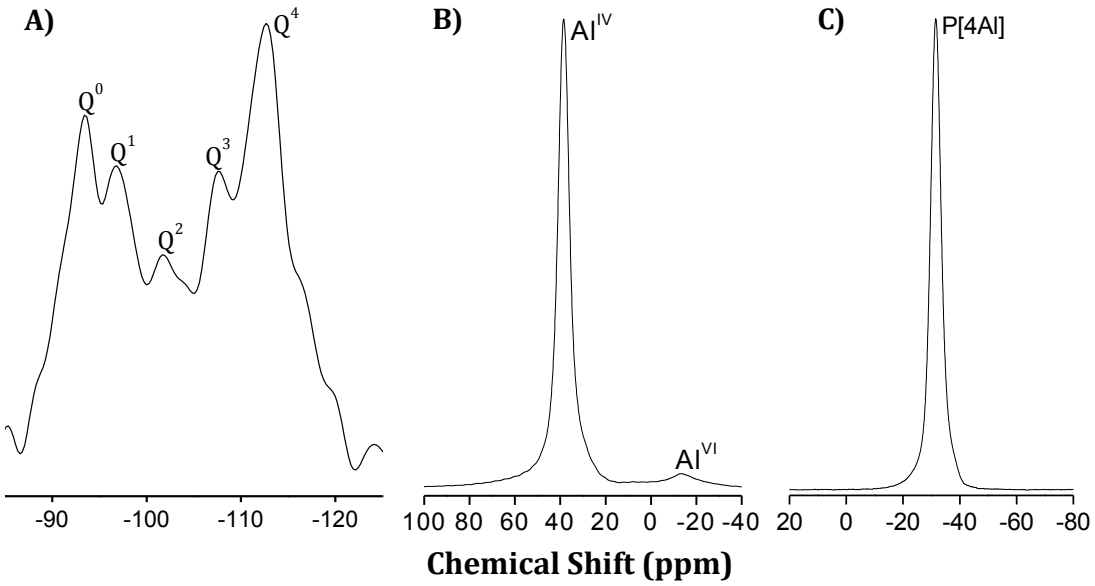

Fig. 2.6. Solid state NMR spectra of SAPO-44 catalyst; A) ^{29}Si, B) ^{27}Al and C) ^{31}P.

^{27}Al MAS NMR spectrum shows a major peak at 38.2 ppm which can be assigned to the presence of tetrahedrally coordinated aluminium (Al^{IV}) in the framework of SAPO-44 (Fig. 2.6). This suggests that aluminum is uniformly incorporated in the framework forming [$Al(OP/OSi)_4$] species. Additionally, a minor peak was observed at ca. -15.0 ppm for octahedral Al species (Al^{VI}) in SAPO-44. The presence of octahedral Al is not surprising since transition of Al^{IV} [$Al(OSi)_4$] to Al^{VI} [$Al(OSi)_3(H_2O)_3$] via coordination of water molecule is proven in literature in case of zeolite.[31]

^{31}P MAS NMR spectra suggests the presence of only tetrahedrally coordinated phosphorous, [P(4Al)] in SAPO-44 framework as single sharp peak was observed at -31.5 ppm (Fig. 2.6). It is notable that during the synthesis of SAPO-44, H_3PO_4 was used as phosphorous precursor and shifting of peak from δ = 0 ppm (for H_3PO_4)[32] to -31.5 ppm confirms the incorporation of phosphorous in framework forming [$P(OAl/OSi)_4$] species.

Finally, it can be said that NMR study gave a clear view on local environment around Si, Al and P elements in synthesized SAPO-44 catalyst. Furthermore, all the NMR patterns were compared with the literature reported data[5,25,33,34] and a good correlation was seen.

2.5.3. Infra-Red (IR) Spectroscopy

For determination of types of acid sites (Brönsted / Lewis) present in catalyst, sample was contacted with pyridine and NH_3 (probe molecule) and then IR spectra was recorded in Shimadzu FTIR-8201PC instrument. Before the injection of probe molecule, samples were activated at 300°C for 1 h under N_2 atmosphere (10 mL/min) to remove any adsorbed gases, water vapors and other impurities. The IR spectra of pyridine / NH_3 adsorbed on catalyst were recorded in the region of 1400-1650 cm^{-1} at 100°C after removal of physisorbed pyridine / NH_3 from catalyst surface.

Presence of both Brönsted acid (ν_{max}/cm^{-1} 1634 and 1542), Lewis acid (ν_{max}/cm^{-1} 1612 and 1452) and Brönsted + Lewis acid (ν_{max}/cm^{-1} 1490) sites in SAPO's was proved with pyridine IR analysis (Fig. 2.7). The Brönsted acid sites in SAPO materials are formed from substitution of P^{5+} by Si^{4+} in the aluminophosphate framework while Lewis acid sites are formed by three coordinated framework Al.[35] Others bands observed with

less intensity are corresponds to pyridine ring stretch and CH bend (ν_{max}/cm^{-1} 1593, 1576: C=C and C=N, ν_{max}/cm^{-1} 1510, 1430: C-C and C-N bonds).[36] It can be seen that the peaks for SAPO-44 arise at similar position as for other SAPO's with lower intensity. The lower intense peak in SAPO-44 catalyst may inform that the catalyst has less acid sites compared to other SAPO's. However, TPD-NH_3 studies (Table 2.3, section 2.5.6, chapter 2) present the contradictory results i.e. SAPO-44 has higher amount of acid sites (1.2 mmol/g) compared to other SAPO's (0.3-0.8 mmol/g). To realize the fact, kinetic diameter of pyridine and ammonia molecule was determined using earlier suggested equation[37] (for detail calculations please see below). The calculation shows that pyridine has kinetic diameter of 0.53 nm and ammonia has kinetic diameter of 0.32 nm. The similar kinetic diameter value (pyridine = 0.60 nm, ammonia = 0.26 nm) was also reported in literature.[13] The kinetic diameter values suggest that due to the smaller pore diameter (0.43 nm) in SAPO-44, it hinders the access of larger pyridine molecules but allows ammonia molecules to access acid sites present in SAPO-44 pores. The similar observation was also reported earlier.[38] To differentiate the acid sites present on SAPO-44 catalyst more clearly, NH_3 was used as a probe molecule for IR study (Fig. 2.7). Presence of both Brönsted acid site (ν_{max}/cm^{-1} 1457) and Lewis acid site (ν_{max}/cm^{-1} 1623) were confirmed SAPO-44. Beside these two peaks, some more peaks were observed in the spectrum. To identify those peaks, IR spectra for pure NH_3 (gas) was recorded and it was confirmed that all other peaks were due to NH_3 IR vibrations. The same observation is also reported in National Institute of Standards and Technology (NIST) Chemistry WebBook.[39]

Calculation of kinetic diameter

Kinetic diameters of pyridine and ammonia molecules are calculated using the earlier suggested equation[37] which correlates the kinetic diameter with weight of a molecule.

$$\text{Kinetic diameter } (\sigma) = 1.234 \times (Mw)^{1/3} \qquad \text{..... (Equation 2.1)}$$

Where, Mw is molecular weight of molecule in g/mol. This calculation assumes molecule as spherical and hence, the critical mass is correlated to the size of the sphere.

Molecular weight of pyridine molecule is 79,

So Kinetic diameter (σ) of pyridine = $1.234 \times (79)^{1/3}$ = 5.29 Å = 0.53 nm.

Molecular weight of ammonia is 17,

So Kinetic diameter (σ) of ammonia = $1.234 \times (17)^{1/3}$ = 3.17 Å = 0.32 nm.

The pyridine-IR spectra for WO_3/SiO_2, MoO_3/SiO_2 and Ga_2O_3/SiO_2 catalysts synthesized by SG method confirms the presence of Lewis acid sites only in all three catalysts since the peaks at ν_{max}/cm^{-1} 1440-1455, 1480-1490 and 1590-1600 were observed (Fig. 2.7). Although, the peak position at 1480-1490 can be assigned as presence of Lewis + Brönsted acid sites, but in this case absence of Brönsted acid sites confirms it as only Lewis acid sites.

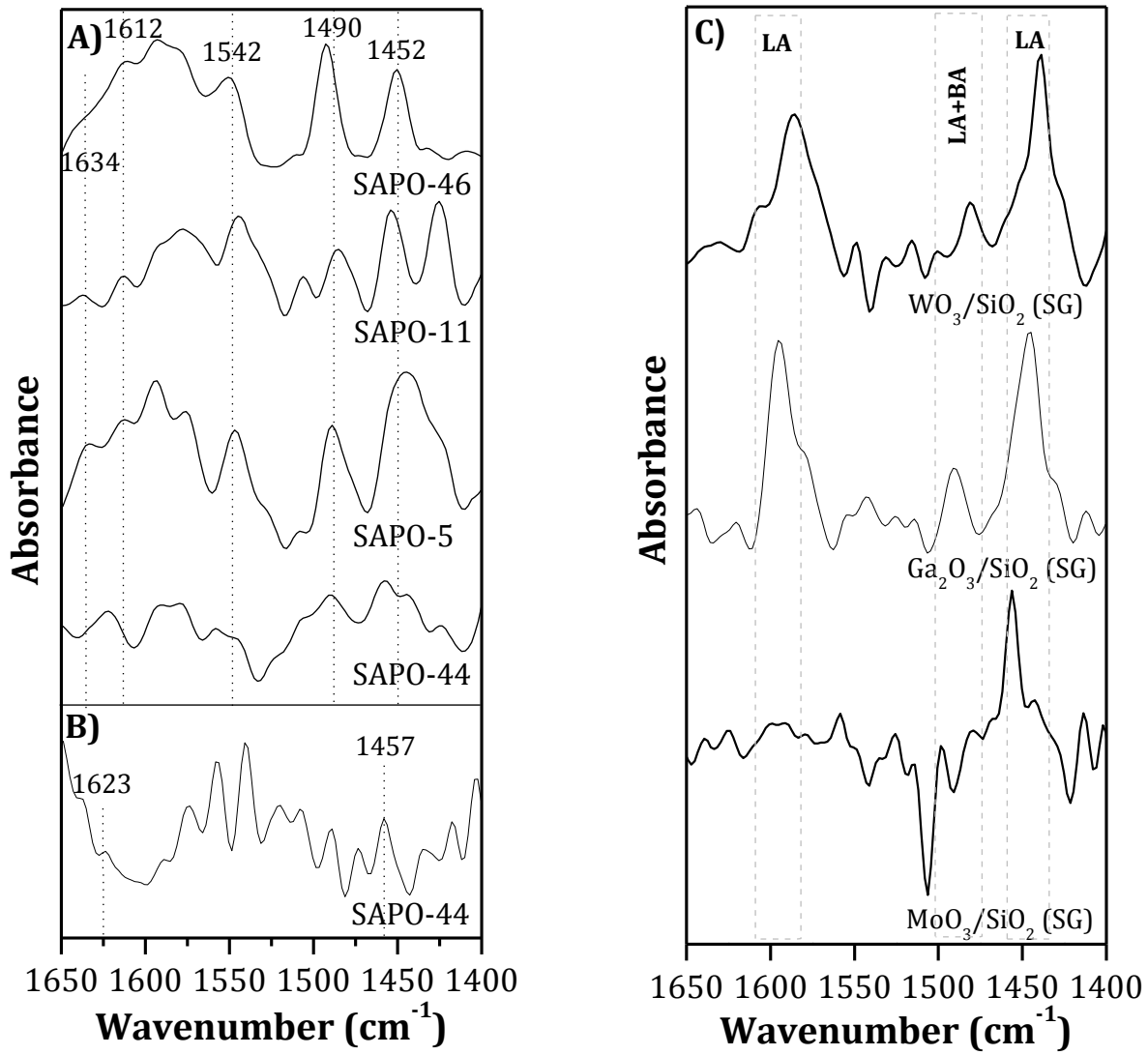

Fig. 2.7. Pyridine / NH_3-IR analysis of synthesized catalysts. 'BA' stands for Brönsted acid sites and 'LA' stands for Lewis acid sites; A) Pyridine-IR spectra of SAPO's, B) NH_3-IR spectra of SAPO-44, C) Pyridine-IR spectra of SG synthesized supported metal oxides.

Furthermore, the functional groups present on supported metal oxides were determined using solid state IR analysis. Fourier Transform Infra-red (FT-IR) spectra of supported metal oxide catalysts were recorded in Bruker Optics ALPHA-E spectrometer with a universal Zn-Se ATR (attenuated total reflection) accessory in the wavelength region of 600-4000 cm^{-1} at a scan rate of 4°/min. For collection of IR spectra directly powdered sample was taken.

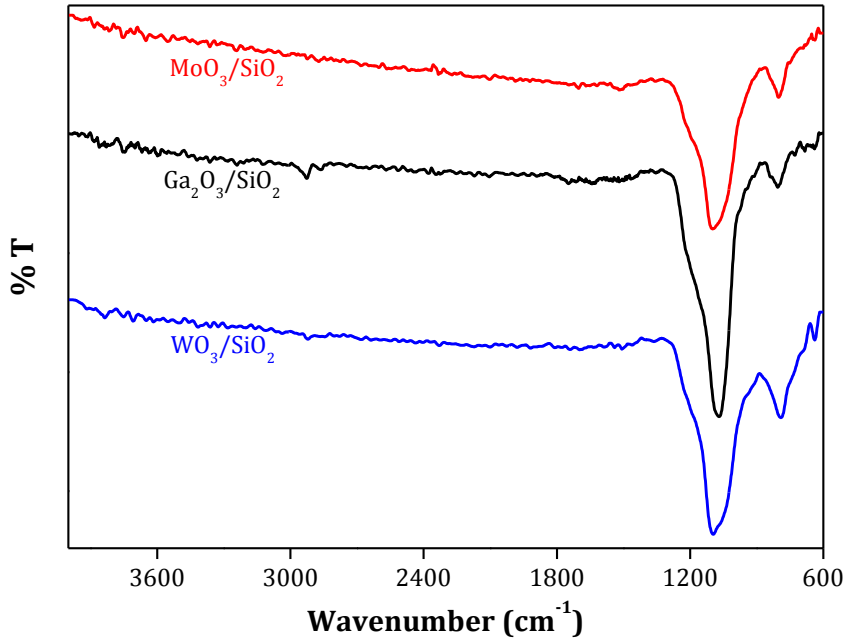

Fig. 2.8. Solid phase IR spectra of supported metal oxides synthesized by SG method.

Silica supported tungsten, molybdenum and gallium oxide catalysts synthesized by SG method were subjected for solid state IR analysis to elucidate their structure. Fig. 2.8 presents two clear bands for WO_3/SiO_2, MoO_3/SiO_2 and Ga_2O_3/SiO_2 catalysts in IR spectra. The band at ν_{max}/cm^{-1} 1100-890 represents the terminal M=O stretching vibrations and another band at ν_{max}/cm^{-1} 850-750 represents M-O-M and/or O-M-O stretching vibrations.[40] The presence of M=O and M-O-M species in supported metal oxides were also confirmed in earlier study.[41] Additionally, a small hump can be seen at ν_{max}/cm^{-1} 1270-1150 in case of all three catalysts which corresponds to the presence of M-O bending vibration.[42] The absence of broad peak in a region of ν_{max}/cm^{-1} 1050-400 ruled out the possibility of presence of bulk metal oxide phase in support.[40] In addition to this, the vibration band at ν_{max}/cm^{-1} 850-750 is also due to the presence of Si-O-Si and/or O-Si-O ring stretching as silica tend to form 3-4 membered rings.[43] It can be

predicted that calcination of catalyst at high temperature may lose catalyst surface -OH groups and therefore surface hydroxyl groups were not detected under the analysis environment.[43]

2.5.4. Raman Spectroscopy

The Raman spectroscopy of supported metal oxides identifies the type of metallic species and metal-support interaction present in the sample. All synthesized supported metal oxide catalysts were subjected for Raman analysis using LabRAM HR Evolution instrument (HORIBA Scientific). Before analysis all the samples were activated at 150°C for 6 h under evacuation (10^{-3} bar). For Raman analysis finely powdered form of sample was used.

The Raman spectra for all the supported metal oxides along with fumed silica and synthesized zirconia are shown in Fig. 2.9. In case of tungsten catalysts, absence of peak at 960 cm^{-1} and a broad peak at 600-720 cm^{-1} ruled out the presence of hydrated tungsten species in the sample.[18] The intense line at 718 and 809 cm^{-1} in WO_3/SiO_2 (WI) and WO_3/ZrO_2 (SG) catalysts confirmed the presence of bulk WO_3 species in samples [Fig. 2.9. c), e)].[18] However, WO_3/SiO_2 synthesized by SG method exhibits different peak patterns compared to others two catalysts. Three distinct broad lines at 927, 560 and 200-430 cm^{-1} spectral range [Fig. 2.9. d)] confirmed the presence of polymeric oxotungstate entity interacting with silica support i.e. silicotungstic species in WO_3/SiO_2 (SG) catalyst.[18] In addition to tungsten oxide peaks, some other peaks due to ZrO_2 support were also observed in WO_3/ZrO_2 (SG) catalyst (marked with asterisk). The characteristic sharp bands at 818 and 996 cm^{-1} were observed in MoO_3 supported on silica synthesized by WI and SG methods [Fig. 2.9. f), g)] indicated the presence of α-MoO_3 species.[44] In case of MoO_3/ZrO_2 (SG) catalyst broad peaks at similar position were observed [Fig. 2.9. h)]. Peaks for presence of ZrO_2 were also dominant in MoO_3/ZrO_2 (SG) catalyst (marked with asterisk). Furthermore, when gallium oxide catalysts were investigated, only peaks for silica and zirconia were observed without any additional peak for gallium oxide [Fig. 2.9. i), j), k)].

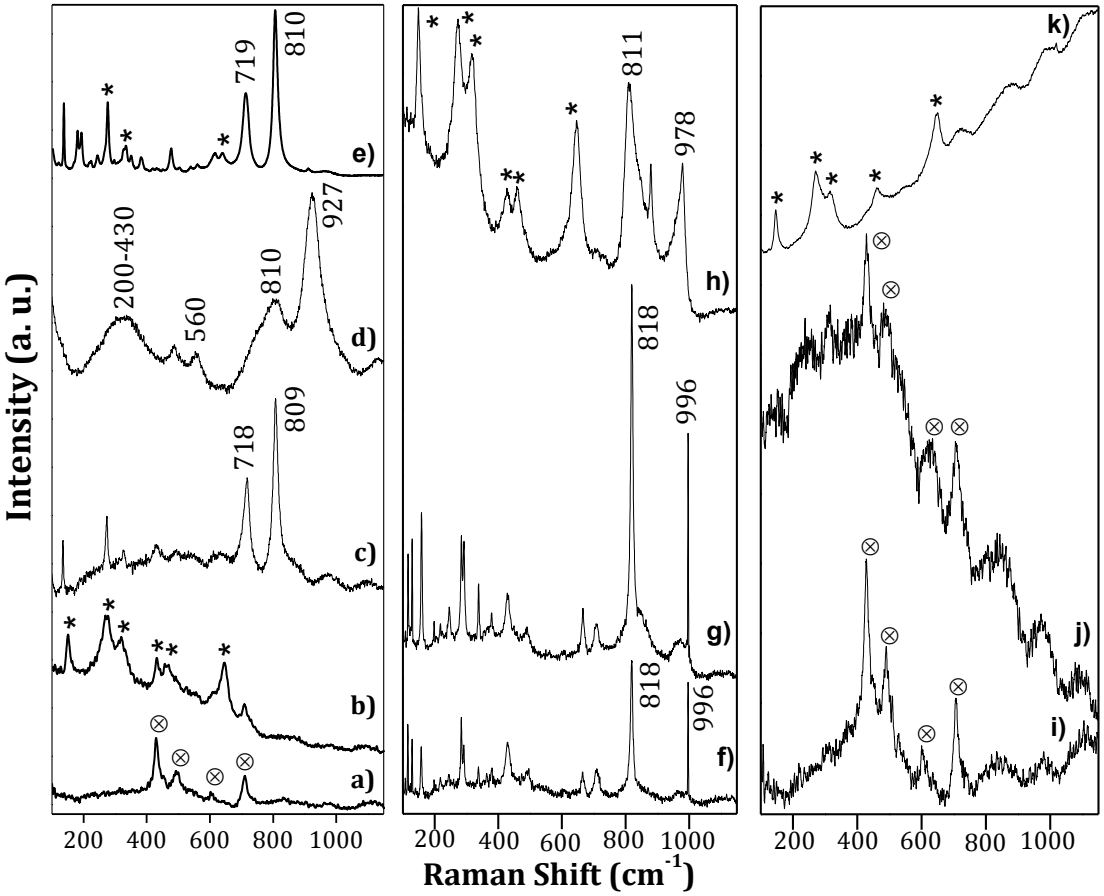

Fig. 2.9. Raman spectra for supported metal oxides. a) fumed silica, b) synthesized ZrO_2, c) WO_3/SiO_2 (WI), d) WO_3/SiO_2 (SG), e) WO_3/ZrO_2 (SG), f) MoO_3/SiO_2 (WI), g) MoO_3/SiO_2 (SG), h) MoO_3/ZrO_2 (SG), i) Ga_2O_3/SiO_2 (WI), j) Ga_2O_3/SiO_2 (SG), k) Ga_2O_3/ZrO_2 (SG). ['*' indicates the peaks for ZrO_2 and '⊗' indicates the peaks for SiO_2].

2.5.5. X-Ray Photoelectron Spectroscopy (XPS)

For better understanding of metal oxidation state in supported metal oxides further, XPS spectra were collected. Silica supported tungsten, molybdenum and gallium oxides synthesized by SG method were used for this study. XPS was recorded using an ESCA-3000 instrument (VG Scientific LTD, England) with a 9 channeltron CLAM4 analyzer under a vacuum > 10^{-8} Torr, using Al-Kα (1486.6 eV) and constant pass energy of 50 eV.

The binding energy value was charge-corrected to the C-1s signal (284.6 eV). The binding energies of O 1s (532.7 eV) and Si 2p (103.3 eV) levels for all the catalysts are agreed with the standard value. XPS spectra of all three catalysts are shown in Fig. 2.10. W 4f XPS spectra of tungsten catalyst showed doublet peaks characteristic due to presence of only W^{6+} species in oxidic surroundings in catalyst.[18] Absence of any peak in

the binding energy range of 31-33 eV precluded the possibility of presence of lower oxidation state (0 and 4) in tungsten. Furthermore, the well-defined peaks at 35.8 eV ($4f_{7/2}$) and 37.4 eV ($4f_{5/2}$) position are the characteristics of tungsten trioxide (WO_3) in the catalyst.[18,45] In case of Mo 3d spectrum of the catalyst, two broad peaks were observed which after de-convolution divided into four distinct peaks. The two peaks at binding energy of 231.0 eV ($3d_{5/2}$) and 234.1 eV ($3d_{3/2}$) are due to the presence of MoO_2 species.[45] Another two peaks correspond to binding energy of 232.6 eV ($3d_{5/2}$), 235.7 eV ($3d_{3/2}$) are due to the presence of MoO_3 species.[45] Again absence of any peak in binding energy range of 227-229 eV confirms the absence of Mo(0) oxidation state.[45,46] Additionally, presence of Ga $2p_{3/2}$ singlet at binding energy of 1117.9 eV confirms the only presence of Ga^{3+} species as Ga_2O_3 in catalyst.[45,47] Although, the gallium metal peak overlap in the similar region as that of Ga^{3+} however, the broad spectrum nature confirmed the presence of only Ga^{3+} species and this is expected since in catalyst gallium is covered by heteroatom oxygen.

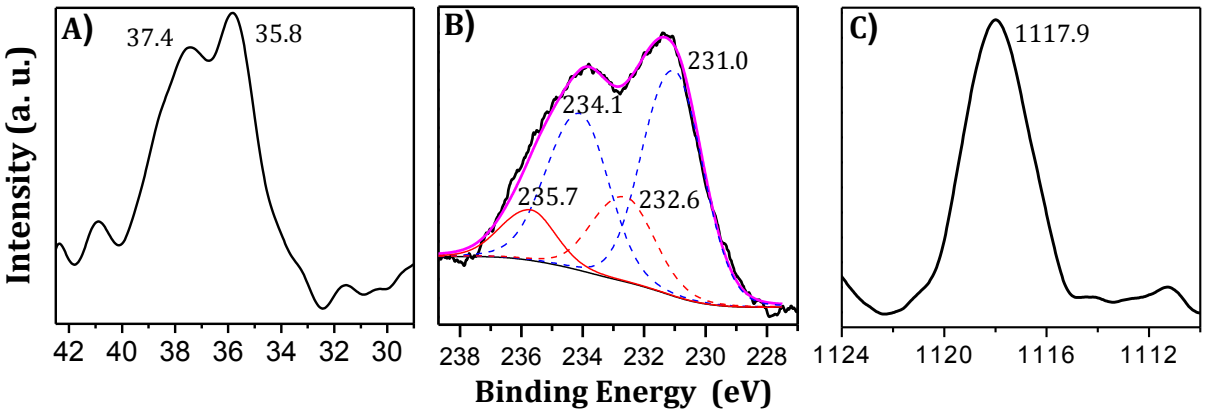

Fig. 2.10. XPS spectra of supported metal oxides; A) WO_3/SiO_2 (SG), B) MoO_3/SiO_2 (SG) and C) Ga_2O_3/SiO_2 (SG).

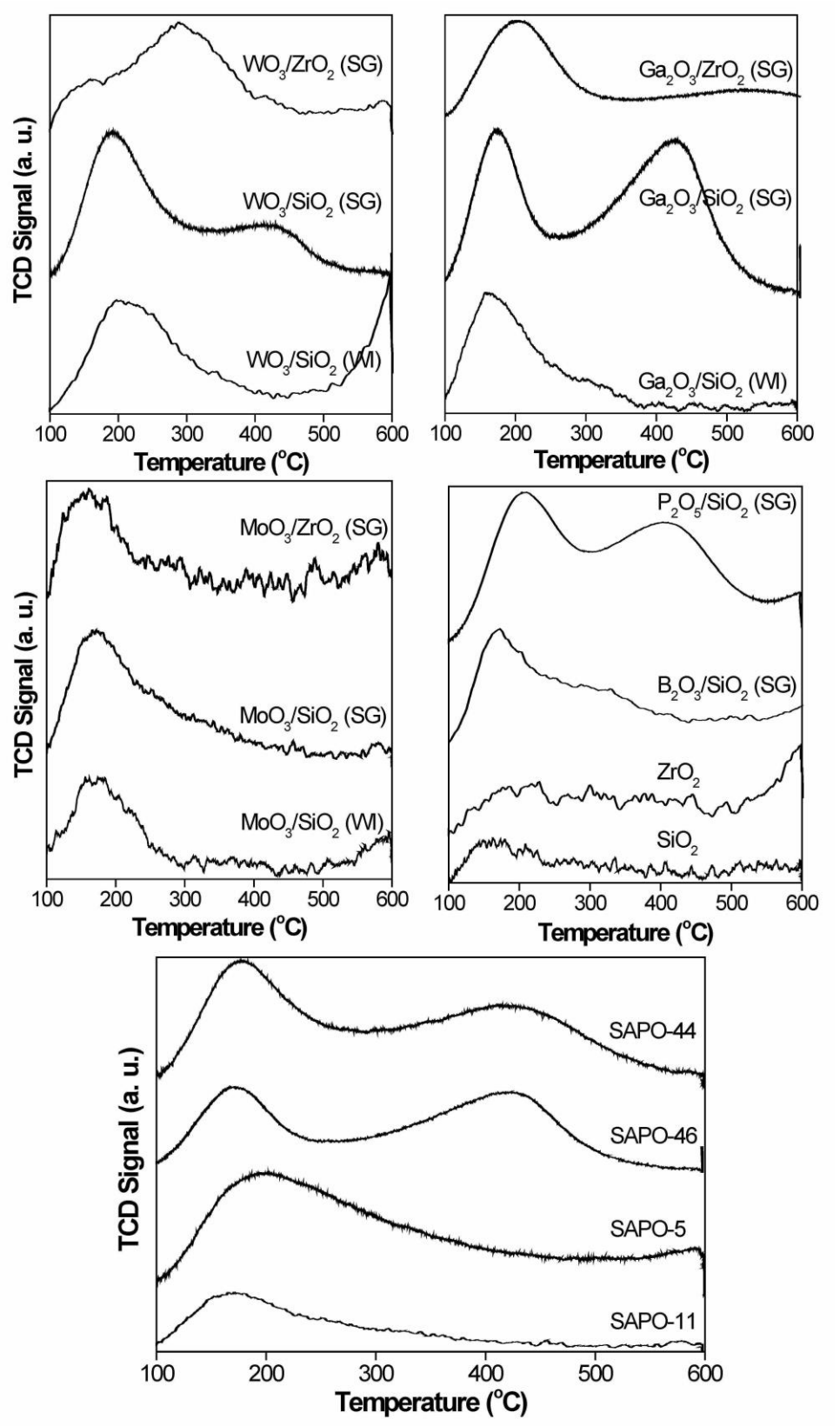

Fig. 2.11. TPD-NH_3 profile for synthesized catalysts.

2.5.6. Temperature Programmed Desorption of NH_3 (TPD-NH_3)

The total acid amount and acid amount distribution (weak and strong) in synthesized catalysts was measured with the help of TPD-NH_3 study. For this analysis, finely powdered sample was placed in a sample holder ('U' shaped) in Micromeritics AutoChem-2920 instrument, equipped with TCD. Typically, catalyst was activated at 600°C (4°C/min) in helium flow (30 mL/min) for 1 h. The temperature was decreased to 50°C and NH_3 was adsorbed by exposing the samples to 10% NH_3 in helium for 1 h. It was then flushed with helium for another 1 h at 100°C to remove all the physisorbed NH_3. Desorption of NH_3 was carried out in helium flow (30 mL/min) by increasing the temperature from 100 to 600°C at the rate of 10°C/min. The quantification of acid amount (NH_3 desorbed) was carried out with the help of standard calibration. The TPD-NH_3 profiles for all the synthesized catalysts are shown in Fig. 2.11. The TPD-NH_3 peak in temperature range of 100-250°C is assigned as weak acid sites and 350-500°C assigned as strong acid sites.

The analyzed data is shown in Table 2.3. In all catalysts, acid amount as well as acid amount distribution was found to be varied. Precisely, among SAPO's, SAPO-44 has the highest total acid amount with highest amount of strong acid sites. Strong acid sites were also present in SAPO-46 catalyst however; SAPO-5 and SAPO-11 have only weak acid sites. The total acid amount in SAPO's was decreased in the following order, SAPO-44 > SAPO-46 = SAPO-5 > SAPO-11. Based on the total acid amount and presence of strong acid sites, it can be expected that SAPO-44 might show better catalytic activity compared to other SAPO's. Furthermore, the total acid amount with acid amount distribution values for zeolite catalysts are provided in the Table 2.3 for comparison purpose.

The increased acid amount for supported metal oxide catalysts compared with only SiO_2 and only ZrO_2, specifies the presence of metals along with support. Absence of strong acid sites and presence of lower total acid amount in silica supported WI synthesized catalyst in comparison to SG synthesized catalyst indicates that SG method distribute metal centers in silica framework in better way and creates superior acid sites. Again, when zirconia was used as support material, it can be seen that lower acid amount with less strong acid sites were present in the material. Hence, it can be

concluded that silica is a better support material for synthesis of supported metal oxide catalysts compared to zirconia.

Table 2.3. TPD-NH_3 and N_2 sorption analysis of synthesized catalysts.

Catalyst	Weak acid amount (100-250°C) (mmol/g)[a]	Strong acid amount (350-500°C) (mmol/g)[a]	Total acid amount (mmol/g)[a]	Surface area (m^2/g)[b]
SAPO-44	0.7	0.5	1.2	369
SAPO-5	0.8	0	0.8	309
SAPO-11	0.3	0	0.3	42
SAPO-46	0.4	0.4	0.8	132
HUSY (Si/Al=15)	0.1	0.5	0.6	780[48]
HMOR (Si/Al=10)	0.5	0.7	1.2	500[48]
Hβ (Si/Al=19)	0.2	0.7	0.9	710[48]
SiO_2	0.05	0.00	0.05	395
WO_3/SiO_2 (WI)	0.09	0.00	0.09	155
MoO_3/SiO_2 (WI)	0.06	0.00	0.06	63
Ga_2O_3/SiO_2 (WI)	0.18	0.00	0.18	210
WO_3/SiO_2 (SG)	0.09	0.05	0.14	278
MoO_3/SiO_2 (SG)	0.09	0.00	0.09	148
Ga_2O_3/SiO_2 (SG)	0.32	0.28	0.60	299
B_2O_3/SiO_2 (SG)	0.16	0.00	0.16	n.d
P_2O_5/SiO_2 (SG)	0.33	0.18	0.51	n.d
ZrO_2	0.02	0.00	0.02	82
WO_3/ZrO_2 (SG)	0.06	0.00	0.06	45
MoO_3/ZrO_2 (SG)	0.05	0.02	0.07	34
Ga_2O_3/ZrO_2 (SG)	0.06	0.05	0.11	64

[a]TPD-NH_3 analysis, [b]N_2 sorption analysis.

2.5.7. N_2-Sorption Study

The specific surface areas of catalysts were calculated using a Nova 1200 and Autosorb 1C Quanta Chrome instruments, USA. Before analysis all the samples were dried under evacuation (10^{-6} bar) at 300°C for 2 h. The surface area values were documented in

Table 2.3. From the data it can be seen that surface area of SAPO catalysts varied in a range of 42-369 m^2/g. Moreover, higher surface area (369 m^2/g) of SAPO-44 catalyst compared to other SAPO's may suggest that it might show better catalytic activity than others. Incorporation of metals in support was confirmed from the lower surface area value for metal oxide catalyst compared to only support material. Due to uniform metal dispersion in support framework while SG method was used for synthesis those material showed higher surface area compared to WI method. It can be expected that due to higher surface area silica supported catalyst might show better catalytic activity compared to zirconia supported one.

2.5.8. Inductively Coupled Plasma-Optical Emission Spectroscopy (ICP-OES)

The elemental composition in SAPO's and the metal loadings in supported metal oxides were analyzed with ICP-OES method. ICP-OES analysis was done on a Spectro Acros FHS12 instrument equipped with winlab software. Standard solutions were used for calibration of particular elements. For materials with silica component (SAPO's and silica supported metal oxides), to 0.025 g of solid material in polypropylene (PP) bottle, few drops of hydrofluoric acid (HF), 0.3 mL of water was added and heated at 80°C up to dryness. Then, 0.2 mL of H_2SO_4 and 0.5 mL of water were added to it and again evaporated to dryness. Upon addition of HF, it reacts with silica in sample to form silicon tetrafluoride (SiF_4) and fluorosilicic acid (H_2SiF_6). Strong acid H_2SO_4 was added to fasten the reaction between HF and silica. Now, while heating the mixture at 80°C, H_2SiF_6 decomposes to SIF_4 and HF which has a very low BP (–86°C and 19.5°C, respectively) and hence it evaporates easily from the mixture. This process removes silica completely and thereby prevents interference in ICP analysis.

$$SiO_2 + 4HF \longrightarrow SiF_4\,(g)\uparrow + 2H_2O$$

$$SiO_2 + 6HF \longrightarrow H_2SiF_6 + 2H_2O$$

$$H_2SiF_6 \longrightarrow SiF_4\,(g)\uparrow + 2HF$$

Afterwards, the mass remained in PP bottle was washed with water and transferred to 25 mL volumetric flask and finally volume was made-up and analyzed using an ICP-OES instrument. For zirconia supported catalyst, 0.025 g of catalyst was digested in a beaker with 0.5 mL of aqua regia (conc. HNO_3 + conc. HCl = 1:3; molar ratio) and then evaporated to dryness at 80°C. Then, 0.2 mL of H_2SO_4 and 0.5 mL of water were added

to it and again evaporated to dryness. Now, the mass was carefully washed with water and transferred to 25 mL volumetric flask and finally volume was made-up and analyzed using an ICP-OES instrument.

Table 2.4 summarizes the amount of elements present in synthesized SAPO's. Careful view of the data presented in Table 2.4 informs that the amount of Al and P present in all the material were almost similar to the expected value as per theoretical calculations. For better understanding theoretical calculations for SAPO-44 is described below.

Table 2.4. ICP-OES analysis of SAPO's.

Material	Amount of Al present (ppm)		Amount of P present (ppm)	
	Theoretical†	ICP-OES	Theoretical†	ICP-OES
SAPO-44	22.8	22.5	26.0	24.6
SAPO-5	19.1	19.8	20.3	19.4
SAPO-11	22.9	22.1	26.7	25.5
SAPO-46	21.6	21.2	26.5	26.1

†Theoretical calculations for SAPO-44

For synthesis of SAPO-44, precursors were taken in the molar gel composition of 1.0 CHA: 1.0 Al_2O_3: 1.0 SiO_2: 1.0 P_2O_5: 60.0 H_2O

Pseudoboehmite (70% Al_2O_3) taken = 4.6 g

So Al_2O_3 amount = (4.6 × 70)/100 = 3.22 g

i.e. Al present = (3.22 × 54)/102 = 1.70 g [$A.Wt_{Al}$=27 and $M.Wt_{Al2O3}$=102]

H_3PO_4 (85%) taken = 7.28 g

So H_3PO_4 amount = (7.28 × 85)/100 = 6.19 g

i.e. P present = (6.19 × 31)/98 = 1.96 g [$A.Wt_P$=31 and $M.Wt_{H3PO4}$=98]

Weight of final calcined material = 10.51 g

Now for ICP-OES analysis 0.0035 g SAPO-44 material was taken in 25 mL water.

So the solution prepared for ICP-OES contains,

Amount of Al = (1.70 × 0.0035 × 1000)/10.51 = 0.57 mg in 25 mL water

Amount of P = (1.96 × 0.0035 × 1000)/10.51 = 0.65 mg in 25 mL water

Therefore, theoretical calculation will be

Amount of Al = 22.8 ppm

Amount of P = 26.0 ppm

The theoretical and actual metal loadings after synthesis of metal oxides were calculated and are represented in Table 2.5. It can be seen that after synthesis of silica supported catalysts, almost similar amount of metal was present as used theoretically (10 wt%) however, zirconia support accommodate very less amount of metal in its structure. This might be due to less surface area available in zirconia (82 m^2/g; Table 2.3) to accommodate metals in comparison to silica surface area (395 m^2/g; Table 2.3). Since zirconia supported catalysts have lower metal loading, those are expected to show less acid amount compared to silica in which higher metal loading was seen.

Table 2.5. ICP-OES analysis of supported metal oxides.

Synthesis method	Material	Metal loading (wt%)	
		Theoretical	Actual (ICP-OES)
Wet-impregnation (WI)	WO_3/SiO_2	10	9.8
	MoO_3/SiO_2	10	8.7
	Ga_2O_3/SiO_2	10	9.2
Sol-gel (SG)	WO_3/SiO_2	10	9.9
	MoO_3/SiO_2	10	9.0
	Ga_2O_3/SiO_2	10	9.4
	B_2O_3/SiO_2	10	8.2
	P_2O_5/SiO_2	10	8.6
	WO_3/ZrO_2	10	2.9
	MoO_3/ZrO_2	10	3.4
	Ga_2O_3/ZrO_2	10	4.7

2.5.9. Ultra Violet-Visible (UV-Vis) Spectroscopy

Subsequently, to confirm the incorporation of tungsten, molybdenum and gallium in silica framework synthesized by SG method, solid state UV-Vis analysis was undertaken. All the UV-Vis spectra of samples were recorded on Jesco V-570 spectrophotometer in the wavelength range of 200-800 nm. Before analysis all the finely powdered samples were activated at 150°C for 6 h and directly used for analysis. Actually, from this analysis I tried to understand the state of metal center (i.e. presence of silicotungstic or silicomolybdic or galosilicate type species) and particle size of metal oxide (i.e. bulk form or smaller particle form) in the catalyst as described in earlier report[28] but

unfortunately I was not succeeded. However, from Fig. 2.12 it can be concluded that metal oxides were incorporated in silica framework as a broad UV-Vis absorption was seen in case of supported metal oxides whereas only silica didn't show any UV-Vis absorption.

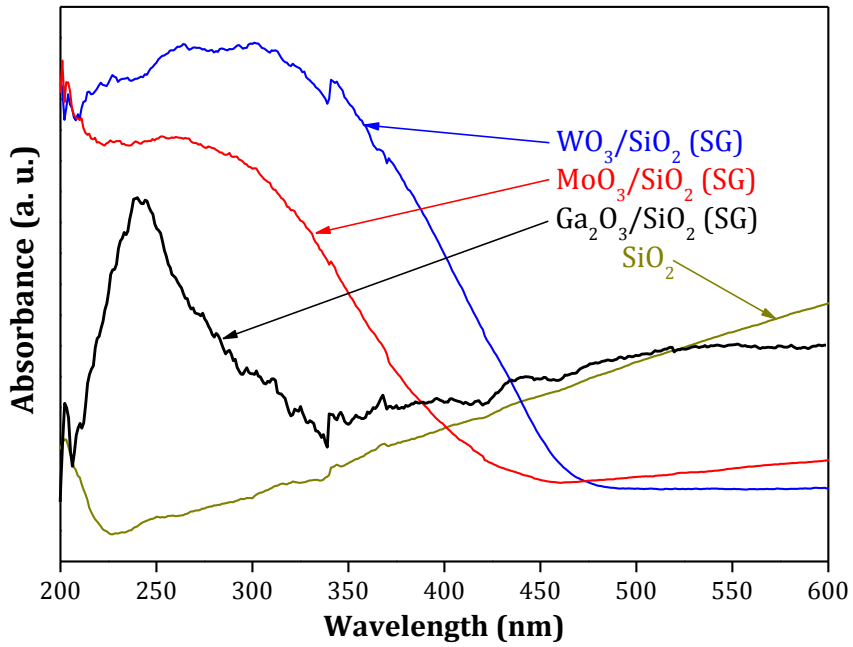

Fig. 2.12. UV-Vis absorption of SG synthesized silica supported metal oxides.

2.5.10. Scanning Electron Microscopy (SEM)

To know the external morphology and chemical composition of SAPO's, SEM analysis was undertaken. The SEM micrographs of the samples were obtained on a Leo Leica Cambridge UK Model Stereoscan 440 scanning electron microscope. The samples were loaded on stubs and sputtered with thin gold film to prevent surface charging and also to protect from thermal damage due to electron beam. For quantitative analysis of elemental composition of sample, SEM instrument was coupled with Energy Dispersive X-ray spectroscopic (EDX) method.

Fig. 2.13 represents that SAPO-44, SAPO-5, SAPO-11 and SAPO-46 crystallized with cubic, spherical, spherical and prismic morphology respectively. Cubic edge length in SAPO-44 was ca. 2.8 μm, spherical diameter of SAPO-5 and SAPO-11 were 15.5 and 7.5 μm respectively. Furthermore, based on EDX analysis SAPO-44 composition (atom %) was determined as Si = 22.9, Al = 37.9 and P = 39.2. Based on the elemental analysis

data, framework composition of SAPO-44 was calculated as $(Si_{0.24}Al_{0.40}P_{0.36})O_2$ which is almost similar as described in earlier report.[5]

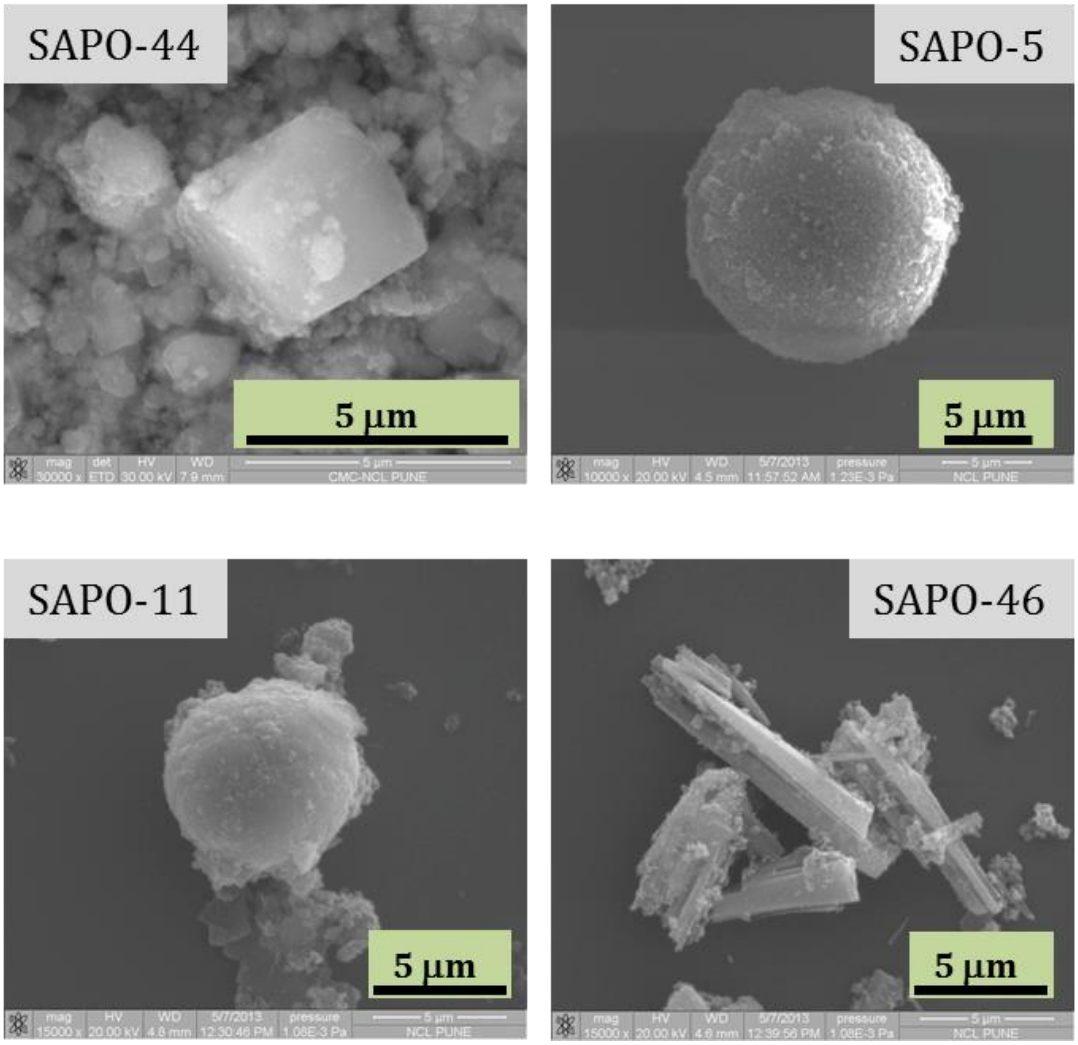

Fig. 2.13. SEM images of SAPO's.

Correlation between the data obtained with SEM-EDX analysis and ICP-OES analysis of SAPO-44 catalyst

SEM-EDX analysis of SAPO-44 catalyst showed elemental composition in wt% as

Al = 19.75, Si = 11.62, P = 22.75 and O = 45.89

As mentioned earlier (section 2.5.8), for ICP-OES analysis 0.0035 g = 3.5 mg SAPO-44 catalyst was used.

So, 3.5 mg SAPO-44 contains,

Al = [(19.75 / 100) × 3.5] mg = 0.6913 mg

Si = [(11.62 / 100) × 3.5] mg = 0.4067 mg

P = [(22.75 / 100) × 3.5] mg = 0.7963 mg

Since, 3.5 mg of SAPO-44 catalyst was dissolved in 25 ml water for ICP-OES sample preparation (section 2.5.8) so; the above calculated amount of elements is present in 25 mL water.

Therefore, the concentration of elements will be,

Al = [(0.6913 / 25) × 1000] ppm = 27.6 ppm

Si = [(0.4067 / 25) × 1000] ppm = 16.3 ppm

P = [(0.7963 / 25) × 1000] ppm = 31.8 ppm

The calculated values for elemental composition in SAPO-44 from the data obtained with SEM-EDX analysis (Al = 27.6 ppm, P = 31.8 ppm) are almost matching with the data obtained with ICP-OES analysis (Al = 22.5 ppm, P = 24.6 ppm; section 2.5.8).

2.5.11. Transmission Electron Microscopy (TEM)

TEM photographs of silica supported tungsten, molybdenum and gallium oxides synthesized by WI and SG method were taken with FEI TECNAI T20 Model instrument operated at an accelerating voltage of 200 kV. Samples were prepared by placing droplets of homogeneously dispersed sample in *iso*-propanol on a polymeric carbon coated Cu grid.

TEM images of silica supported tungsten, molybdenum and gallium oxides synthesized by WI and SG method are shown in Fig. 2.14. In all the images, amorphous nature of silica support can be visible. The TEM images obtained for SG catalysts show smaller particles, which are uniformly distributed in silica support. An average particle size of 3-4 nm for WO_3/SiO_2 (SG), ca. 5 nm for MoO_3/SiO_2 (SG) and <2 nm for Ga_2O_3/SiO_2 (SG) was obtained through SG synthesis method. However, the catalysts synthesized by

WI method produces bigger metal particle for WO_3/SiO_2 (25-50 nm) and MoO_3/SiO_2 (30-50 nm). For Ga_2O_3/SiO_2 (WI) catalyst metal particle are not clearly visible. This further suggests that WI synthesis method is not a good technique for better dispersion of metal particle on silica support.

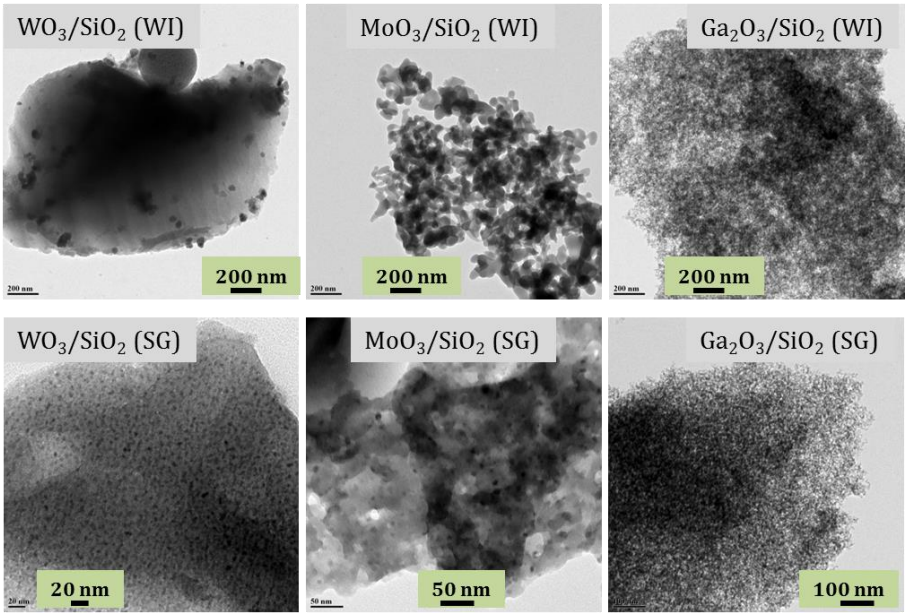

Fig. 2.14. TEM images of SG synthesized silica supported metal oxides.

2.5.12. Thermal Gravimetric Analysis (TGA)

Thermal stability of synthesized catalyst was analyzed with the help of TGA study. For TGA analysis only SAPO-44, WO_3/SiO_2 (SG) and Ga_2O_3/SiO_2 (SG) were used. This is because, as it will be discussed in proceeding chapters that these three catalysts are better active than others and hence, the stability of other catalysts was not checked. TGA of finely powdered samples was carried out using Mettler Toledo TGA/SDTA 851 series, USA instrument under air atmosphere with a heating rate of 10°C/min in a range of 25-1000°C.

TGA profile (Fig. 2.15) of SAPO-44 shows 7.9% mass loss at 92.7°C, which corresponds to loss of water. Further loss of 0.8% at 400°C is due to decomposition of remaining structure directing agent (SDA) from SAPO-44. No subsequent loss even after heating up the sample to 1000°C implies that SAPO-44 material is thermally stable.

The TGA profiles for supported metal oxides were shown in Fig. 2.15. At lower temperature, mass loss of 4.5% and 10.4% in WO_3/SiO_2 (SG) and Ga_2O_3/SiO_2 (SG), respectively was observed typically due to the release of adsorbed water in the catalyst.

However, further increase in temperature up to 1000°C, did not show any mass loss, which indicates that both the catalysts are stable. Although, some noise in the TGA profile was observed for WO_3/SiO_2 (SG) above 750°C but those can be neglected since the losses were very low (0.2%, 0.2% and 0.4%).

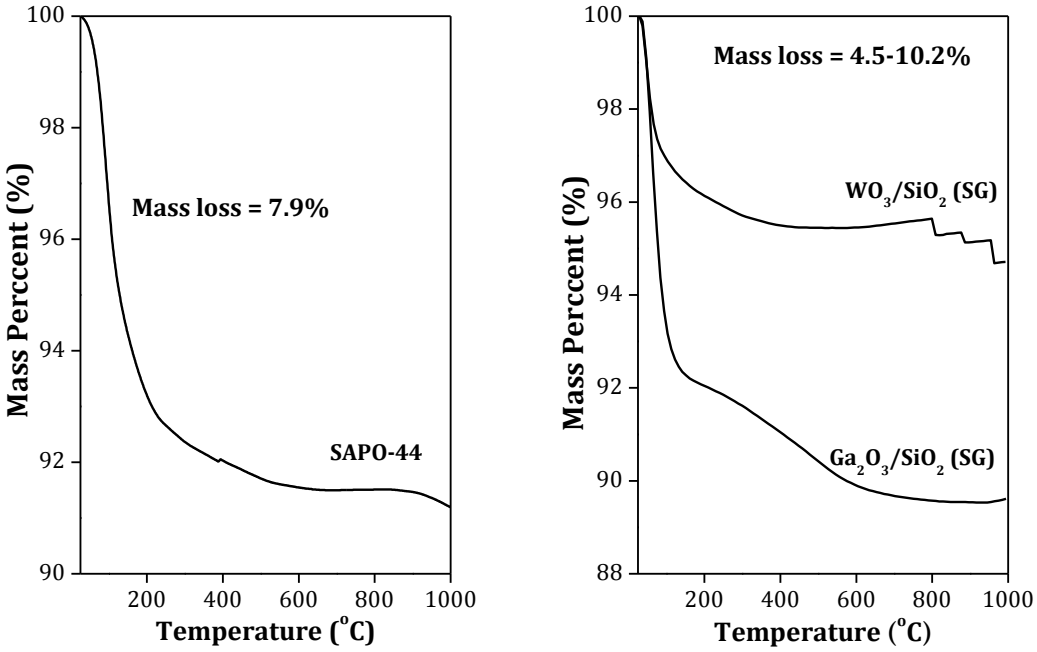

Fig. 2.15. TGA profile for synthesized catalysts.

2.6. Crop Waste Characterization Methods

As discussed in earlier chapter, due to profuse availability of crop wastes (raw biomass) those can be used for value-added chemical synthesis in this work. Seven different crop wastes *viz.* bagasse (I), bagasse (II), bagasse (III), rice husk (I), rice husk (II), rice husk (III) and wheat straw were collected from several regions of India (Fig. 2.16).

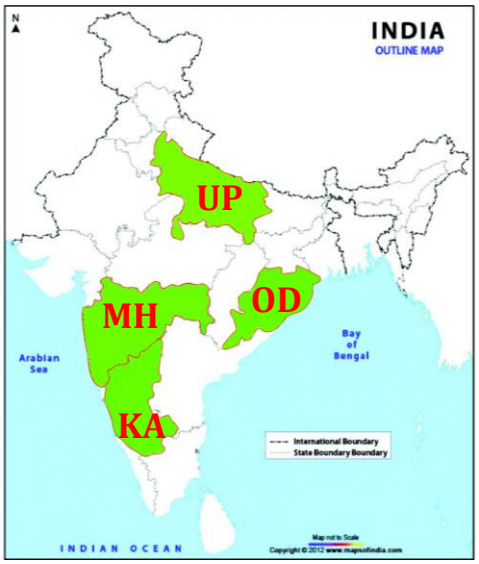

Crop Waste	Collected From
Bagasse (I)	Maharashtra
Bagasse (II)	Maharashtra
Bagasse (III)	Uttar Pradesh
Rice Husk (I)	Odisha
Rice Husk (II)	Karnataka
Rice Husk (III)	Uttar Pradesh
Wheat Straw	Uttar Pradesh

Fig. 2.16. Sources of crop wastes (raw biomass).

Before subjecting these substrates to catalytic reactions, it was essential to determine their compositions and so that accurate quantification of products would be possible. Dryness, ash, cellulose, pentosan and lignin concentrations were analyzed by TAPPI (Technical Association of the Pulp and Paper Industry) method, nutrients concentrations were determined by ICP-OES and thermal stability of substrates were checked by TGA analysis.[49] The detail analysis procedures are described below.

2.6.1. Dryness Analysis

Typically, in a procedure 0.5 g of biomass sample was dried in an oven at 100°C for 12 h under evacuation (10^{-3} bar). Based on the dryness in sample, calculation of oven dried (OD) weight was done for each sample (Equation 2.2).

Dryness (%) = [100 – {(weight before drying – weight after drying) / weight before drying} × 100 …….. (Equation 2.2)

2.6.2. Analysis of Ash

In a typical method, 2 g biomass sample was taken in a quartz boat and kept in preheated muffle furnace at 620°C for 2 h in presence of air. While cooling, when the temperature of furnace was reduced to 200°C, immediately the boat was transferred to a desiccator to prevent moisture adsorption in leftover mass. After cooling, weight of boat with remaining residue (ash) was taken. OD weight of sample was calculated based on dryness analysis of biomass. Ash content was calculated using Equation 2.3.

Ash (%) = [{final weight of (boat + ash) – weight of empty boat} / OD weight of sample] × 100 …….. (Equation 2.3)

2.6.3. Analysis of Pentosan

In a typical method, 4-5 g of biomass sample and 300 mL of 13.5 M HCl were added in a 500 mL *RB* flask and the mixture was heated at 100°C in a mantle heater as shown in Fig. 2.17. During boiling, reaction vapour passes through the condenser and finally distillate was collected in a 250 mL volumetric flask. Simultaneously, the reaction solution volume was reduced and to maintain it, additional HCl solution (13.5 M) was added continuously drop by drop from the top (as shown in Fig. 2.17). The heating was

continued for a time period until 250 mL distillate was collected. After proper dilution (approximate 200 times) of distillate, its UV-Vis absorbance was determined at a wavelength of 280 nm. Alongside, to carry out blank measurement 13.5 M HCl solution was used. Pentosan content in crop wastes was calculated using Equation 2.4.

Pentosan (%) = [(Absorbance of distillate × dilution factor × 1.563) / (151 × OD weight of sample)] × 100 …….. (Equation 2.4)

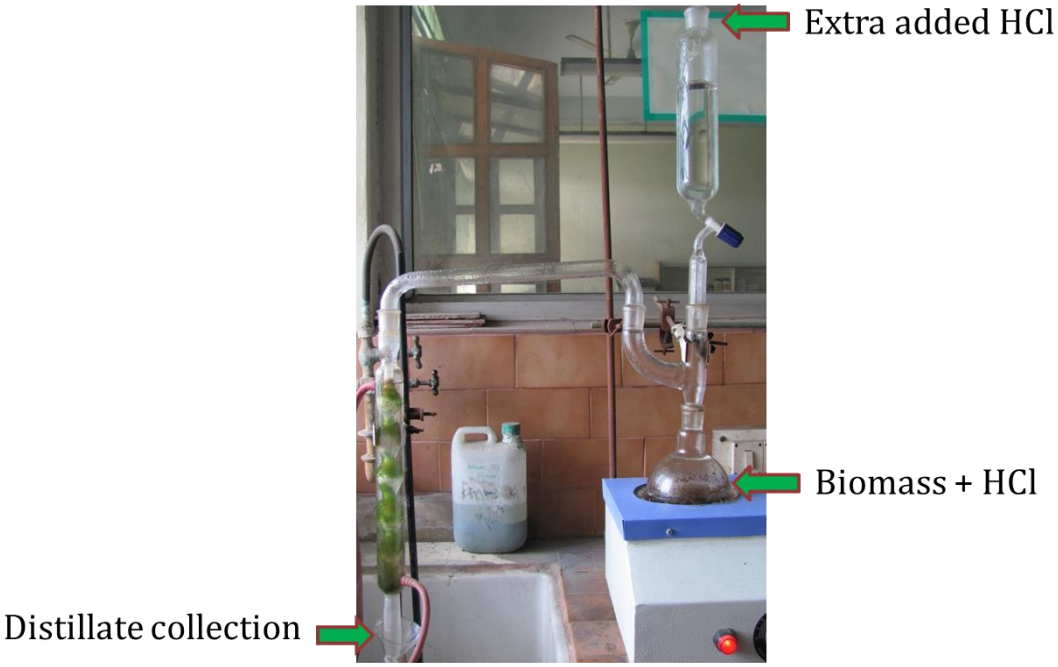

Fig. 2.17. Pentosan analysis set-up.

2.6.4. Analysis of Lignin

For the analysis of lignin concentration, 1 g biomass sample was taken in a 100 mL *RB* flask and to it 15 mL 72% H_2SO_4 was added slowly. Then the mixture was stirred vigorously at 30°C for 2 h. Next, in another 1000 mL *RB*, 150 mL of water was taken and to it H_2SO_4 digested mass was slowly added (exothermic reaction). Later, the leftover H_2SO_4 digested mass in 100 mL *RB* was washed thoroughly with 195 mL water and the washing solution was transferred into 1000 mL same *RB* (current H_2SO_4 concentration = 3%). Then 1000 mL *RB* flask was placed in preheated oil bath at 100°C and heated for 4 h with continuous stirring. Later, the *RB* was kept at room temperature (30°C) for overnight (16 h) to settle down the solid. After settling down, the solid mass was filtered through G2 crucible and then the solid was thoroughly washed with room temperature water. The solid collected in crucible was dried at 60°C for 16 h and then at 110°C for 1

h. This solid mass was called as 'uncorrected lignin'. Later, the uncorrected lignin mass was transferred carefully to a quartz boat and subsequently, it was heated at 620°C for 2 h in presence of air for ash correction (as described in section 2.6.2) in uncorrected lignin. Lignin content in crop wastes was calculated using Equation 2.5 and 2.6.

Weight of uncorrected lignin (g) = [weight of (crucible + solid) – weight of empty crucible] …….. (Equation 2.5)

Ash corrected lignin (%) = [(weight of uncorrected lignin – weight of ash) / OD weight of biomass] × 100 …….. (Equation 2.6)

2.6.5. Analysis of Holocellulose and α-, β- and γ-Cellulose

Basically, holocellulose is described as a mixture of cellulose and hemicellulose in lignocelluloses. In a procedure, de-lignification of biomass was carried out to obtain white powdered holocellulose which is composed of cellulose (α- and β-form) and hemicellulose (termed as γ-cellulose). De-lignification process of biomass sample to obtain holocellulose is described here. In a typical method, 2.5 g biomass sample and 80 mL water were taken in a 250 mL conical flask. Next, the mixture was heated at 70°C in a water bath for 1 h by covering the mouth of conical flask with another small conical flask inversely (Fig. 2.18). While heating, to the mixture, 0.75 g $NaClO_2$ + 0.25 mL acetic acid were added 3-4 times at a certain interval and the mass was mixed manually. Then, the content in conical flask was cooled down and filtered through G2 crucible. Subsequently, the solid mass collected in crucible was washed with excess of room temperature water and finally with small amount of acetone (to remove residual lignin, if any). Next, the solid collected in crucible was dried at 60°C for 16 h and then at 110°C for 1 h (holocellulose: Equation 2.7, 2.8). Now, the dried solid was divided into three parts; part-I: used for α-, β- and γ-cellulose analysis, part-II: used for lignin analysis as described in section 2.6.4, part-III: used for ash analysis as described in section 2.6.2.

Weight of uncorrected holocellulose (g) = [weight of (crucible + solid) – weight of empty crucible] …….. (Equation 2.7)

Corrected holocellulose (%) = [(weight of uncorrected holocelluose – weight of ash – weight of lignin) / OD weight of biomass] × 100 …….. (Equation 2.8)

Fig. 2.18. Set-up for de-lignification process.

The analysis procedure for α-, β- and γ-cellulose from part-I of holocellulose is discussed here. In a typical method, 100 mL of 5.2 N NaOH was added slowly to 1.5 g of holocellulose taken in a *RB* flask and stirred at room temperature (30°C) for 0.5 h. Next, 100 mL water was added to the mixture and stirring was continued for another 0.5 h at room temperature. The mass was then filtered through G2 crucible and the solid left (contains ash, residual lignin and α-cellulose) in crucible was discarded. The collected filtrate was then used for the quantification of α-, β- and γ-cellulose as the procedure described below.

For the quantification of α-cellulose, 5 mL of filtrate was taken in a 250 mL conical flask and to it 10 mL of 0.5 N $K_2Cr_2O_7$ solution and 50 mL conc. H_2SO_4 were added slowly. After that the solution was mixed manually. While mixing, the solution got heated and hence, the conical flask was kept in an ice water bath to cool the solution at room temperature. After cooled down, 3-4 drops of ferroin indicator was added to the solution and titrated against 0.1 N ferrous ammonium sulfate (FAS) solutions. The end point of titration was marked with orange colour. Simultaneously, for blank titration, 5 mL (5.2/2) N NaOH solution was used instead of 5 mL filtrate, using rest of the procedure same. Later, to standardization of FAS, 5 mL of 0.1 N $K_2Cr_2O_7$ solution and 50 mL conc. H_2SO_4 were taken in a 250 mL conical flask and heated at 105°C for 0.25 h. Then, the mixture was cooled to room temperature using ice water bath and additional 50 mL water was added. Finally, the solution was titrated against 0.1 (N) ferrous ammonium sulfate solutions (FAS) after addition of 3-4 drops of ferroin indicator. Amount of α-cellulose was calculated using Equation 2.9.

α-cellulose (%) = [100 – {6.85 × (blank reading – sample reading) × FAS strength ×20} / (5 × OD weight of sample)] × 100 …….. (Equation 2.9)

For quantification of β- and γ-cellulose, 50 mL of filtrate (from NaOH digestion of holocellulose) was taken in a 100 mL volumetric flask and to it 50 mL of 3 N H_2SO_4 was added. After proper mixing, the solution was heated at 80°C for 0.5 h in water bath. Then, the solid in solution was kept for 16 h settling. Next, 5 mL of supernatant solution was taken in 250 mL conical flask. To it 10 mL of 0.5 N $K_2Cr_2O_7$ solution and 90 mL H_2SO_4 were added slowly. The solution was mixed manually and then cooled to room temperature using ice water bath. Next, the solution was titrated against 0.1 N ferrous ammonium sulfate solutions (FAS) after addition of 3-4 drops of ferroin indicator and the end point of titration was marked with orange colour. The amount of γ-cellulose and β-cellulose were calculated using Equation 2.10 and 2.11, respectively.

γ-cellulose (%) = {6.85 × (blank reading – sample reading) × FAS strength ×20} / (2.5 × OD weight of sample) …….. (Equation 2.10)

β-cellulose (%) = [% of holocellulose – (% of α-cellulose + % of γ-cellulose)] % …….. (Equation 2.11)

For better understanding, here I am summarizing the complete procedure of holocellulose, α-cellulose, β-cellulose and γ-cellulose analysis in Fig. 2.19.

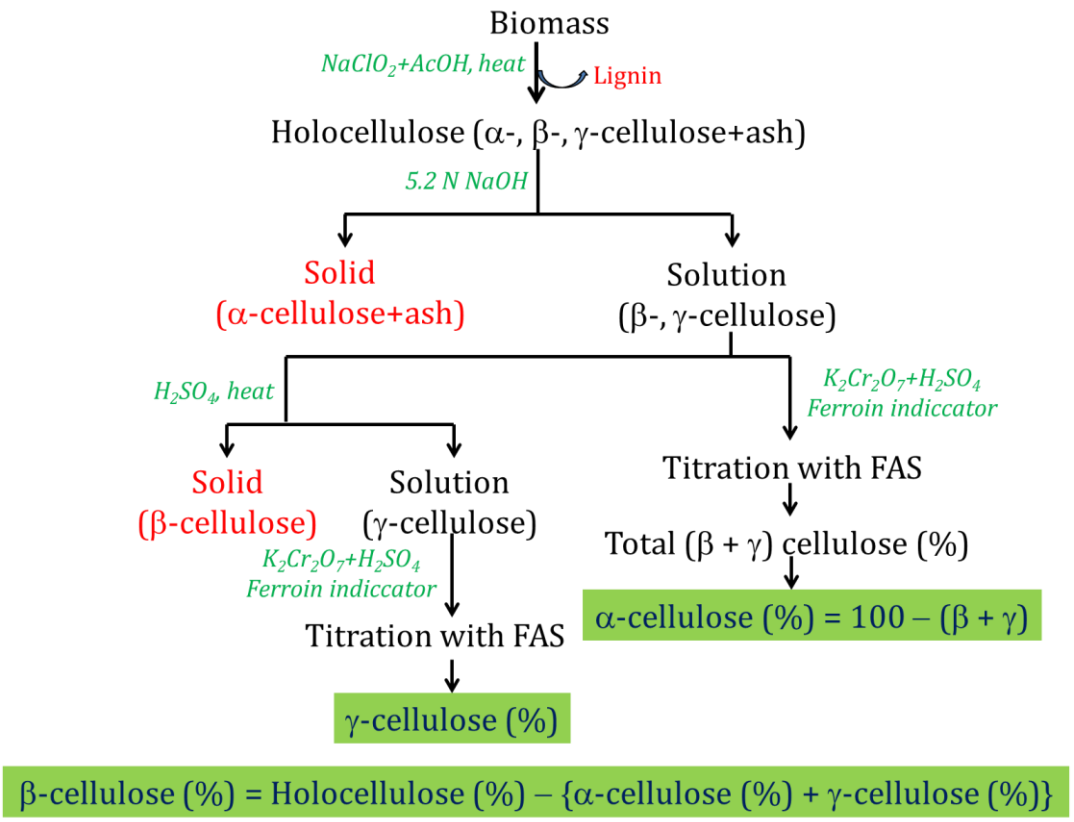

Fig. 2.19. Schematic for analysis procedure of holocellulose and α-, β-, γ-cellulose.

2.6.6. Nutrient Composition by ICP-OES

For analysis of nutrients (metal components), ash of biomass sample was taken in a beaker and digested with 5 mL concentrated HCl at 80°C. Later, the mass was filtered through Whatman 41 filter paper (diameter 90 mm, thickness 220 μm, pore size 20-25 μm). Filtrate was then analyzed with ICP-OES to know the actual concentration of metal components and the data is presented in Table 2.6. From the data it was clear that the metal concentrations in these seven types of raw biomass are very less and thereby it might be expected that poisoning of catalyst acid sites due to presence of metals in these substrate might be negligible.

2.6.7. Thermal Stability by TGA Analysis

Thermal degradability of all the biomass samples were analyzed with the help of TGA analysis in both nitrogen and air atmosphere. Heating under nitrogen atmosphere only removes volatile matter (VM) from biomass in addition to water however, heating in presence of excess oxygen (air atmosphere) completely burnt off carbon from biomass leaving only unburnt mass (ash and metals). The data represented in Table 2.6 indicates the mass left over after heating of sample under different atmosphere. The remaining residue after heating under air can be assigned as ash (inorganic) component however, some excess amount of residue was left after heating of biomass in nitrogen which can be assigned as mixture of ash and carbonized material. The data presented in Table 2.6 shows that the leftover mass after heating of biomass in air are similar to the value of ash component analysis which further approves the expected fact.

Based on the above described procedures, all the seven crop wastes (bagasse: collected from three places, rice husk: collected from three places and wheat straw: collected from one place of India) were characterized. All the experiments were repeated 3 times and the error in the results was ±2% (based on the actual value). The quantified data for all the crop wastes are presented in Table 2.6.

Table 2.6. Characterization data for crop wastes (raw biomass).

Parameters	Substrate[a]						
	BG (I)	BG (II)	BG (III)	RH (I)	RH (II)	RH (III)	WS
Dryness (%)	98.2	97.4	95.5	97.9	97.5	98.5	96.8
Inorganic & organic composition in % (by TAPPI method)							
Ash	2.1	2.8	3.3	15.7	17.0	18.6	12.4
Pentosan	30.0	24.1	21.6	15.9	11.2	12.4	21.4
Lignin	15.2	20.4	21.6	24.1	21.7	22.7	17.8
Holocellulose	63.2	71.1	68.3	60.5	52.4	52.6	63.2
α-cellulose	38.5	41.2	39.9	37.1	28.5	34.3	36.7
β-cellulose	12.9	15.2	15.3	9.9	11.7	6.8	17.1
γ-cellulose	11.8	14.7	13.1	13.5	12.2	11.5	9.4
Nutrients composition in mmol/g of biomass (by ICP-OES analysis)							
Na	0.0	0.0	0.0	0.0	0.0	0.0	0.0
K	0.04	0.03	0.02	0.07	0.05	0.07	0.12
Ca	0.03	0.03	0.07	0.02	0.01	0.03	0.03
Mg	0.03	0.02	0.03	0.01	0.04	0.04	0.02
Al	0.01	0.01	0.02	0.01	0.01	0.02	0.02
P	0.02	0.01	0.01	0.01	0.05	0.05	0.01
Left over residue in % after heating (by TGA analysis)							
In N_2	n.d.	20.8	10.2	n.d.	29.3	31.8	n.d.
In air	1.9	3.0	n.d.	16.2	n.d.	20.7	12.7

[a] BG (I): bagasse (I), BG (II): bagasse (II), BG (III): bagasse (III), RH (I): rice husk (I), RH (II): rice husk (II), RH (III): rice husk (III), WS: wheat straw. n.d. stands for not done.

2.7. Catalytic Methods

2.7.1. Furfural Synthesis

2.7.1.1. Materials

Xylan (isolated hemicellulose) from oat spelt (softwood; Aldrich, USA, Product No X0627: xylose ≥70%, glucose ≤15%, arabinose ≤10%), beechwood (hardwood; TCI, USA, Product No X0064: xylose ≥80%) and birchwood (hardwood; Aldrich, USA,

Product No X0502: xylose ≥90%), xylose (Loba Chemie, India, 99.5%), arabinose (s. d. fine, India, 99.99%), glucose (s. d. fine, India, 99.99%), fructose (Loba Chemie, India, 99.5%), furfural (Loba Chemie, India, 98%), 5-hydroxymethyl furfural (HMF) (Aldrich, USA 99%), toluene (Loba Chemie, India, 99.5%), methyl iso-butyl ketone / MIBK (Loba Chemie, India, 99%), *p*-xylene (Loba Chemie, India, 99%) were purchased and were used as received. All the crop wastes (bagasse, rice husk and wheat straw) were collected directly from field / farmers from various parts of India and used in the reaction without any chemical pre-treatment. The crop wastes were crushed and made into average size of 1 mm.

2.7.1.2. Experimental Set-up

General schematic for furfural synthesis reaction method is shown in Fig. 2.20.

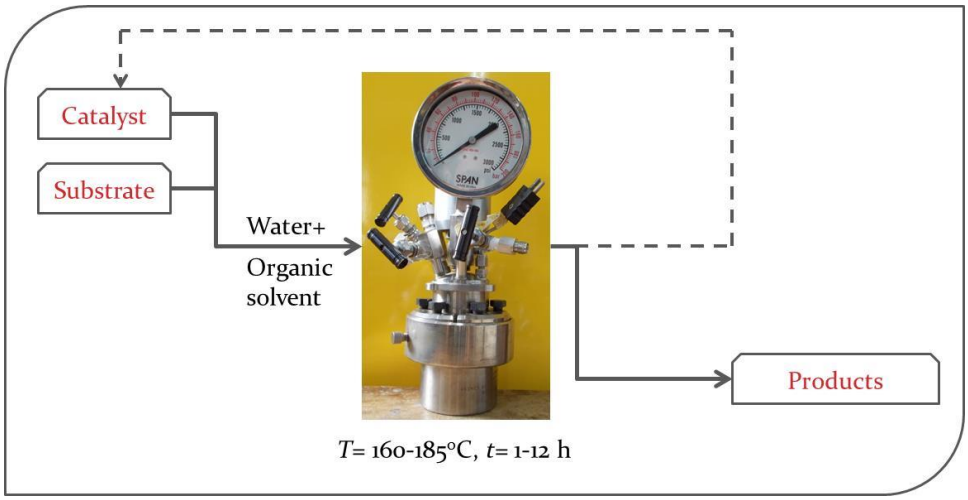

Fig. 2.20. General schematic of experimental set-up.

For isolated hemicellulose reaction, oat spelt xylan or beechwood xylan or birch wood xylan were used as substrate. In a typical reaction, isolated hemicellulose and solid acid catalyst were mixed with 60 mL of water + organic solvent (in various *v/v* ratios) in a Parr autoclave. Autoclave was flushed with N_2 gas for three times to ensure complete inert environment inside the autoclave. Finally, N_2 gas was filled in the autoclave in a range of 1-20 bar. Autoclave was heated at desired temperature under initial slow stirring (100 rpm). When temperature of reactor was reached just 5°C below the desired temperature, stirring was increased to 800 rpm and this time was considered as a start time of reaction. Now the reaction was allowed to continue for desired time period (1-12 h. After completion of reaction, autoclave was cooled to room

temperature. Next, the solid was separated from the reaction mixture by centrifugation and subsequently, the aqueous and organic layers were separated from each other using separating funnel.

For real substrate reaction, crop waste (bagasse or rice husk or wheat straw) and SAPO-44 or WO_3/SiO_2 (SG) or Ga_2O_3/SiO_2 (SG) were mixed with 60 mL water + toluene (1:1 or 1:2 *v/v*) in a Parr autoclave and reaction was carried out as per the procedure described for isolated hemicellulose reaction.

2.7.1.3. Recycle Experiment

In catalyst recycle study (for isolated hemicellulose), after each run, catalyst was separated from reaction mixture as mentioned in section 2.7.1.2 and washed thoroughly with distilled water to remove any adsorbed water soluble products. The catalyst (wet, without drying) thus obtained was used directly in the next reaction.

For crop wastes, catalyst + unreacted biomass was separated from the reaction mixture and washed with distilled water properly. First solid was dried (Lab oven: 60°C, 16 h; vacuum oven: 150°C, 6 h, 10^{-3} bar) and further it was subjected to calcination at 550°C for 12 h in presence of air (flow rate = 10 mL/min) to remove all the unreacted part of biomass. Finally this calcined catalyst was used in recycle runs.

2.7.1.4. Analysis Procedure

After separation of solvent layers as described in section 2.7.1.2, aqueous layer sample was centrifuged (1.5 mL tube) and then filtered through 0.22 μm syringe filter prior to analysis. Aqueous layer containing water soluble products (oligomers, sugars, furfural) was analyzed using High Performance Liquid Chromatography (HPLC, Agilent, 1200 Infinity Series), equipped with Pb^{2+} column (300 mm × 7.8 mm, 80°C) and refractive index detector (Agilent, 1200 Infinity Series, cell temperature of 40°C). Millipore water was used as a mobile phase with 0.6 mL/min flow rate. For HPLC analysis each time 10 μL sample was injected.

Organic layer samples were filtered through 0.22 μm syringe filter and then analyzed on a Varian gas chromatograph (CP3800), equipped with HP-5 column (50 m × 0.22 μm *ID*) and flame ionization detector (FID). For analysis injector temperature was

kept at 200°C and detector temperature at 250°C. During analysis column was heated step wisely; initial temperature: 70°C, hold time: 1 min, temperature increase up to 200°C with a ramp rate of 7°C/min. Each time 1 μL sample was injected in GC.

2.7.1.5. Calculations

Calculation for isolated hemicellulose reaction:

$$\underset{M.\ wt.\ =\ 132}{\text{Hemicellulose}} \rightarrow \underbrace{\underset{M.\ wt.\ =\ 150}{\text{Xylose}} + \underset{}{\text{Arabinose}}}_{C_5\text{-Sugar}} + \underbrace{\underset{M.\ wt.\ =\ 180}{\text{Glucose}} + \underset{}{\text{Fructose}}}_{C_6\text{-Sugar}} \rightarrow \underset{M.\ wt.\ =\ 96}{\text{Furfural}} + \underset{M.\ wt.\ =\ 126}{\text{HMF}}$$

Hemicellulose contains negligible amount of C_6-sugars with a large percentage of C_5-sugars. So for simplicity in calculation of molecular weight of hemicellulose, it was considered as a homo-polymer of C_5-sugars. Hemicellulose molecular weight was taken as 132 considering loss of 18 (due to water removal) from xylose / arabinose (molecular weight of 150) during polymerization to form hemicellulose.

So, 132 g hemicellulose will form 150 g C_5 sugars (xylose + arabinose) (considering 100% conversion and selectivity).

% Yield of C_5 sugars = [weight of C_5 sugars (HPLC) / weight of C_5 sugars (theoretical)] × 100 …….. (Equation 2.12)

% Yield of C_6 sugars (glucose / fructose) = [weight of C_6 sugars (HPLC) / weight of C_6 sugars (theoretical)] × 100

Molecular weight of furfural is 96. So, 96 g furfural yield is possible from 150 g C_5 sugars (considering 100% yield and selectivity).

% Yield of furfural = [weight of furfural (GC [org] + HPLC [water]) / weight of furfural (theoretical)] × 100 …….. (Equation 2.13)

Molecular weight of HMF is 126. So, 126 g HMF yield is possible from 180 g C_6-sugars (considering 100% yield and selectivity).

% Yield of HMF = [weight of HMF (GC [org] + HPLC [water]) / weight of HMF (theoretical)] × 100 …….. (Equation 2.14)

For the quantification of oligomers, xylan (hemicellulose) reactions were done only in water at 110°C for 2 h in the absence of catalyst. Subsequently, reaction mixture was centrifuged to separate out unreacted xylan from reaction mixture. Then, the solid obtained was dried and weighed to know the conversion of xylan. Moreover, the water phase was analyzed using HPLC (under similar conditions as described in section 2.7.1.4) to confirm that the xylan was converted into only oligomers. Furthermore, the water phase comprising soluble oligomers was subjected to rotary evaporator to remove water and then, the solids got were dried at (60°C for 16 h in oven, 150°C for 6 h in vacuum; 10^{-3} bar). Next, the known amount dried oligomers were dissolved in known amount of water to prepare standard solutions of oligomers. Later, these standard solutions were injected on HPLC and calibration curve was drawn. This calibration curve was used for the quantification of oligomers formed in all reactions.

Xylan (hemicellulose) conversion was calculated based on solid charged and recovered (weight basis).

% Xylan conversion = [(total solid charged in the reaction – solid recovered after reaction) / (weight of initial xylan charged in the reactor)] × 100 ……. (Equation 2.15)

Calculations for crop waste reaction:

Product yields were calculated based on the pentosan present in the respective crop waste (bagasse or rice husk or wheat straw). For example when the reactions were carried out with 0.67 g bagasse (I) which contains 30% pentosan i.e. 0.201 g pentosan is present in the system. So the product yield calculations are done using 0.201 g hemicellulose.

2.7.2. HMF Synthesis

2.7.2.1. Materials

Fructose (Loba Chemie, India, 99.5%), glucose (s. d. fine, India, 99.9%), maltose monohydrate (s. d. fine, India), cellobiose (s. d. fine, India), potato starch (Loba Chemie, India), HMF (Aldrich, USA, 99%), MIBK (Loba Chemie, India, 99%) and ethanol (Chanshu Yangyuan Chemicals, China, 99.9%) were procured and used as obtained.

2.7.2.2. Experimental Set-up

Schematic for HMF synthesis reaction is shown in Fig. 2.20.

Various substrates *viz.* fructose, glucose, maltose, cellobiose and starch were used for HMF synthesis. To carry out reaction, 0.5 g of substrate (fructose or glucose or maltose or cellobiose or starch, 10% *wt*/*wt* with respect to water charge) and 0.143 g catalyst were added to water + organic solvent = 5 mL + 25 mL or 30 mL water / organic solvent in 100 mL Parr autoclave. Next, the autoclave was heated at desired temperature under initial slow stirring (100 rpm). Later, the stirring speed was increased to 800 rpm when temperature of autoclave was reached just 5°C below the desired temperature and this time was considered as a start time of reaction. After carrying out the reaction for desired time, the autoclave was cooled down to room temperature. Next, the solid was separated from the reaction mixture by centrifugation and subsequently, the aqueous and organic layers were separated from each other using separating funnel.

2.7.2.3. Recycle Experiment

For recycle study, separated catalyst from reaction mixture (as described in section 2.7.2.2) was washed thoroughly with water, dried in oven (Lab oven: 60°C, 16 h; vacuum oven: 150°C, 6 h, 10^{-3} bar vacuum) and finally calcined in presence of air (flow rate = 10 mL/min) at 550°C for 6 h. The calcined catalyst was used for the recycle reaction.

2.7.2.4. Analysis Procedure

After separation of solvent phase (as described in section 2.7.2.2), aqueous layer sample was centrifuged (1.5 mL tube) and then filtered through 0.22 μm syringe filter prior to analysis. Aqueous layer containing water soluble products (oligomers, sugars, furfural) were analyzed by High Performance Liquid Chromatography (HPLC, Agilent, 1200 Infinity Series), equipped with Pb^{2+} column (300 mm × 7.8 mm, 80°C) and refractive index detector (Agilent, 1200 Infinity Series, cell temperature of 40°C). Millipore water was used as a mobile phase with 0.6 mL/min flow rate. For HPLC analysis each time 10 μL sample was injected.

Organic layer samples were filtered through 0.22 μm syringe filter and then analyzed on a Varian gas chromatograph (CP3800), equipped with BPX-5 column (50 m × 0.22 μm *ID*) and flame ionization detector (FID). For analysis injector temperature was kept at 200°C and detector temperature at 250°C. During analysis column was heated step wisely; initial temperature: 70°C, hold time: 1 min, temperature increase up to 200°C at a ramp rate of 7°C/min. Each time 1 μL sample was injected in GC.

2.7.2.5. Calculations

All the yields and conversions were calculated based on GC and HPLC results. Details on the calculations are mentioned below,

% Yield = [weight of product formed (GC [org] + HPLC [water]) / weight of product possible (theoretical)] × 100 …….. (Equation 2.16)

% Conversion = [{initial weight of substrate – unconverted weight of substrate (HPLC)} / initial weight of substrate] × 100 …….. (Equation 2.17)

However, in case of starch reaction, conversion was calculated based on solid charged and recovered (weight basis).

% Conversion = [(total solid charged in the reaction – solid recovered after reaction) / (weight of initial starch charged in the reactor)] × 100 …….. (Equation 2.18)

2.8. Conclusions

In summary, considering the issue of catalyst instability under reaction conditions, I tried to synthesize catalysts having higher stability. It was thought that structured SAPO catalysts having higher hydrothermal stability might remain unchanged under reaction conditions. Moreover, amorphous supported metal oxides were synthesized with anticipation that catalyst structure cannot change since those don't have definite pore structure. Moreover, various methods such as hydrothermal, wet-impregnation, sol-gel were used to synthesize SAPO's and supported metal oxide catalysts. All the synthesis processes are discussed thoroughly in this chapter. After synthesis of these catalysts, to understand their physical and chemical properties next, various techniques such as XRD, NMR, IR, Raman, XPS, UV-Vis, SEM, TEM, TGA, TPD-NH_3, N_2 sorption and ICP-OES

were used. All the details on instrumentation, sample preparation and analysis data are summarized.

XRD analysis suggests that all the SAPO catalysts were synthesized with their respective phase (SAPO-44: CHA, SAPO-5: AFI, SAPO-11: AEL, SAPO-46: AFS). The phase purity in SAPO's is also confirmed from the crystallite morphology of SAPO's as recorded using SEM instrument. XRD patterns for silica supported metal oxide catalysts inform that SG method uniformly disperses the metal center on support material and hence only amorphous peak for silica was observed. However, in case of WI synthesized silica supported catalysts, in addition to amorphous silica peak, crystalline phase for metal oxide was visible. Moreover, XRD patterns suggest that silica is better support material compared to zirconia for the uniform dispersion of metals. Later, from the solid state NMR analysis, it is understood that the elements are present in different local environment in SAPO-44. Both Al and P are present mainly in tetrahedral environment with small fraction of octahedral environment. However, Si is present in various environment *viz.* [Si(4Al/P)], [Si(3Al/P)(1Si)], [Si(2Al/P)(2Si)], [Si(1Al/P)(3Si)] and [Si(4Si)]. The presence of some amount of siliceous environment i.e. [Si(4Si)] was also observed from the XRD patterns of SAPO-44. The IR analysis of supported metal oxides confirms the presence of terminal M=O, M-O-M and O-M-O bonds in catalysts. Supported metal oxide catalyst synthesized by SG method produces smaller particles of metal oxide but WI method forms bulk form of metal oxide as can be seen from Raman analysis. Presence of metal nanoparticles in silica supported metal oxide catalysts synthesized by SG method is also confirmed using solid state UV-Vis analysis. Later, TEM images also confirm the presence of smaller particles in case of catalyst synthesized by SG method compared to WI method. Moreover, Raman analysis confirms the presence of silicotungstic species only in case of WO_3/SiO_2 catalyst synthesized by SG method. Due to this phenomenon more acid sites are seen in WO_3/SiO_2 (SG) catalyst compared to other supported metal oxide catalysts as quantified using TPD-NH_3 technique. XPS spectra informs the presence of W^{6+}, Mo^{6+}, Mo^{4+} and Ga^{3+} species in silica supported metal oxide catalysts synthesized by SG methods. ICP-OES analysis data illustrates that use of SG synthesis method and silica support accommodate more amount of metals (active phase) in catalysts compared to use of WI method or zirconia support. The elemental composition in SAPO's is also analyzed using ICP-OES method

and the data suggests that almost similar concentrations of elements are incorporated in material as used during synthesis. For SAPO catalysts also TPD-NH_3 analysis was carried out and the data shows that SAPO-44 has highest amount of acid sites as well as highest amount of strong acid sites than other SAPO's. The pyridine-IR spectra taken for SAPO's and supported metal oxide catalysts informs that SAPO catalysts have both Brönsted and Lewis acid sites but metal oxides mainly consists of Lewis acid sites. N_2 sorption analysis shows that SAPO-44 has highest surface area compared to other SAPO's. In case of supported metal oxide catalysts, silica supported catalysts shows higher surface area than zirconia supported catalysts. Moreover, SG synthesis provides better surface area compared to WI synthesis. Later, to understand the thermal stability of catalysts, those are subjected for TGA analysis and the data suggests that the catalysts are highly stable.

From the above discussed physico-chemical characterization data, it can be anticipated that since SAPO-44 has higher surface area, acid amount, strong acid sites and thermal stability compared to other SAPO's, it may act as a better catalyst for biomass conversion into chemicals. In supported metal oxide catalysts also, WO_3/SiO_2 (SG) catalyst has highest surface area, acid amount, strong acid sites and stability than others. Moreover, WO_3/SiO_2 (SG) catalyst shows the presence of silicotungstic species. Hence, WO_3/SiO_2 (SG) catalyst can be expected to show better activity compared to others. Further discussions on catalytic activity are mentioned in next chapters.

Additionally, the crop waste (bagasse, rice husk and wheat straw) used in this work is thoroughly characterized with the help of TAPPI method, ICP-OES analysis and TGA analysis. The detail characterization methods and analysis data is presented in this chapter. Bagasse and wheat straw consists of higher amount of pentosan concentration (21.4-30%) compared to rice husk (11.2-15.9%). However, the ash content found in rice husk and wheat straw (12.4-18.6%) is more compared to bagasse and wheat straw (2.1-3.3%). These data are used in quantification of various products obtained from conversion of crop wastes.

Furthermore, all the materials used, catalytic reaction details, analysis of reaction products and calculations are thoroughly described in this chapter.

2.9. References

(1) Lok, B. M.; Messina, C. A.; Patton, R. L.; Gajek, R. T.; Cannan, T. R.; Flanigen, E. M. *J. Am. Chem. Soc.* **1984**, *106*, 6092.
(2) Chakrabarty, D. K.; Viswanathan, B. *Heterogeneous Catalysis*; New Age International (P) Limited, 2009.
(3) Kozhevnikov, I. V. *Chem. Rev.* **1998**, *98*, 171.
(4) Mul, G.; Moulijn, J. A. In *Supported Metals in Catalysis*; Anderson, J. A., Garcia, M. F., Eds.; World Scientific: 2005; Vol. 5, p 1.
(5) Prakash, A. M.; Unnikrishnan, S.; Rao, K. V. *Appl. Catal. A: Gen.* **1994**, *110*, 1.
(6) Kong, W.; Dai, W.; Li, N.; Guan, N.; Xiang, S. *J. Mol. Catal. A: Chem.* **2009**, *308*, 127.
(7) Sinha, A. K.; Sainkar, S.; Sivasanker, S. *Micro. Meso. Mater.* **1999**, *31*, 321.
(8) Lopez, C. M.; Rodri-guez, K.; Mendez, B.; Montes, A.; Machado, F. J. *Appl. Catal. A: Gen.* **2000**, *197*, 131.
(9) Nieminen, V.; Kumar, N.; Heikkila, T.; Laine, E.; Villegas, J.; Salmi, T.; Murzin, D. Y. *Appl. Catal. A: Gen.* **2004**, *259*, 227.
(10) Barton, D.; Soled, S.; Iglesia, E. *Top. Catal.* **1998**, *6*, 87.
(11) Chary, K. V. R.; Reddy, K. R.; Kishan, G.; Niemantsverdriet, J. W.; Mestl, G. *J. Catal.* **2004**, *226*, 283.
(12) Saito, M.; Watanabe, S.; Takahara, I.; Inaba, M.; Murata, K. *Catal. Lett.* **2003**, *89*, 213.
(13) Bhaumik, P.; Dhepe, P. L. *ACS Catal.* **2013**, *3*, 2299.
(14) Young, D.; Davis, M. E. *Zeolites* **1991**, *11*, 277.
(15) Das, J.; Lohokare, S. P.; Chakrabarty, D. K. *Ind. J. Chem.* **1992**, *31A*, 742.
(16) Sahu, R., University of Pune, 2011.
(17) Bhaumik, P.; Kane, T.; Dhepe, P. L. *Catal. Sci. Technol.* **2014**, *4*, 2904.
(18) Colque, S.; Payen, E.; Grange, P. *J. Mater. Chem.* **1994**, *4*, 1343.
(19) Suzuki, K.; Hayakawa, T.; Shimizu, M.; Takehira, K. *Catal. Lett.* **1994**, *30*, 159.
(20) Delgado, M. R.; Arean, C. O. *J. Mater. Sci. Lett.* **2003**, *22*, 783.
(21) Jubb, N. J.; Bowen, H. K. *J. Mater. Sci.* **1987**, *22*, 1963.
(22) Manriquez, M. E.; Lopez, T.; Gomez, R.; Picquart, M.; Hernandez-Cortez, J. G. *J. Non-Cryst. Solid* **2004**, *345-346*, 643.
(23) Cortes-Jacome, M.; Angeles-Chavez, C.; Bokhimi, X.; Toledo-Antonio, J. A. *J. Solid State Chem.* **2006**, *179*, 2663.
(24) Li, L.; Yoshinaga, Y.; Okuhara, T. *Phy. Chem. Chem. Phy.* **1999**, *1*, 4913.
(25) Ashtekar, S.; Chilukuri, S. V. V.; Chakrabarty, D. K. *J. Phy. Chem.* **1994**, *98*, 4878.
(26) Kido, A.; Iwamoto, H.; Azuma, N.; Ueno, A. *Catal. Sur. Asia* **2002**, *6*, 45.
(27) Martinez, J. R.; Palomares-Sanchez, S.; Ortega-Zarzosa, G.; Ruiz, F.; Chumakov, Y. *Mater. Lett.* **2006**, *60*, 3526.
(28) Liu, G.; Wang, X.; Wang, X.; Han, H.; Li, C. *J. Catal.* **2012**, *293*, 61.
(29) Xie, S.; Chen, K.; Bell, A. T.; Iglesia, E. *J. Phy. Chem. B* **2000**, *104*, 10059.
(30) Sohn, J. R.; Park, M. Y. *J. Ind. Eng. Chem.* **1998**, *4*, 84.
(31) Bourgeat-Lami, E.; Massiani, P.; Di Renzo, F.; Espiau, P.; Fajula, F.; Des Courieres, T. *Appl. Catal.* **1991**, *72*, 139.
(32) http://chem.ch.huji.ac.il/nmr/techniques/1d/row3/p.html and http://www.chem.uni-potsdam.de/tools/e_31p.html.

(33) Akolekar, D.; Bhargava, S.; Gorman, J.; Paterson, P. *Colloid Surf. A: Physicochem. Eng. Aspect* **1999**, *146*, 375.
(34) Huang, Y.; Machado, D.; Kirby, C. W. *J. Phy. Chem. B* **2004**, *108*, 1855.
(35) Qiu, S.; Tian, W.; Pang, W.; Sun, T.; Jiang, D. *Zeolites* **1991**, *11*, 371.
(36) Zhuravlev, K. K.; Traikov, K.; Dong, Z.; Xie, S.; Song, Y.; Liu, Z. *Phy. Rev. B* **2010**, *82*, 064116.
(37) Wang, H.; Frenklach, M. *Combust. Flame* **1994**, *96*, 163.
(38) Borade, R. B.; Clearfield, A. *J. Mol. Catal.* **1994**, *88*, 249.
(39) National Institute of Standards and Technology: Chemistry WebBook; http://webbook.nist.gov/cgi/cbook.cgi?ID=C7664417&Type=IR-SPEC&Index=1.
(40) Maity, S. K.; Rana, M. S.; Srinivas, B. N.; Bej, S. K.; Murali Dhar, G.; Prasada Rao, T. S. R. *J. Mol. Catal. A: Chem.* **2000**, *153*, 121.
(41) Smith, M. R.; Ozkan, U. S. *J. Catal.* **1993**, *141*, 124.
(42) Rougier, A.; Portemer, F.; Quede, A.; El Marssi, M. *Appl. Surf. Sci.* **1999**, *153*, 1.
(43) Asomoza, M.; Dominguez, M. P.; Solis, S.; Lara, V. H.; Bosch, P.; Lopez, T. *Mater. Lett.* **1998**, *36*, 249.
(44) Thielemann, J. P.; Ressler, T.; Walter, A.; Tzolova-Muller, G.; Hess, C. *Appl. Catal. A: Gen.* **2011**, *399*, 28.
(45) National Institute of Standards and Technology: XPS Database; http://srdata.nist.gov/xps/Default.aspx.
(46) Damyanova, S.; Petrov, L.; Centeno, M. A.; Grange, P. *Appl. Catal. A: Gen.* **2002**, *224*, 271.
(47) Serykh, A. I.; Amiridis, M. D. *Surf. Sci.* **2010**, *604*, 1002.
(48) http://www.zeolyst.com/our-products.aspx.
(49) Bhaumik, P.; Dhepe, P. L. *RSC Adv.* **2014**, *4*, 26215.

CHAPTER-3

STRUCTURED CATALYSTS: STABLE, RECYCLABLE SAPO's FOR THE EFFICIENT SYNTHESIS OF C_5 SUGARS & FURFURAL FROM CROP WASTES

3.1. Introduction

In chapter 1, a discussion is made for the available heterogeneous catalyzed processes in the literature for the furfural synthesis (an important value-added chemical).[1-5] Based on the discussions, it can be said that there are few drawbacks in the available processes and those are summarized below.

- Use of edible sugar, xylose as substrate
- Un-stability of structured catalysts
- Non-recyclability of catalysts
- Low and non-selective furfural yield
- Difficulty in recovering furfural in pure form from reaction mixture containing high boiling solvent

Hence, in this work, it was decided to try to resolve these problems. In this chapter, detailed discussions on the catalytic results for the synthesis of value-added furan derivative, furfural and C_5 sugars from biomass (Scheme 3.1) using various structured solid acid catalysts are made. Structured silicoaluminophosphate (SAPO's) catalysts were used for biomass conversion with the anticipation that those might have better stability compared to zeolite due to incorporation of shorter P-O bonds (higher force constant) in aluminosilicate (zeolite) framework (more detail discussion was mentioned in section 1.8, chapter 1).[6] Beside SAPO catalysts, some other solid acid catalysts *viz.* zeolite, resins and niobium pentoxide were also evaluated for the synthesis of furfural from isolated hemicellulose.[7] In this Work, as a biomass feedstock, various substrates were used such as isolated hemicellulose (xylan) derived from softwood and hardwood, untreated crop waste (raw biomass) (bagasse: collected from 3 places, rice husk: collected from 3 places and wheat straw: collected from 1 place).[7,8] Furthermore, reaction conditions were optimized thoroughly with a catalyst, which showed better activity compared to other catalysts evaluated to obtain highest possible yields for furfural. To confirm the catalyst stability a through catalyst characterization studies were undertaken.

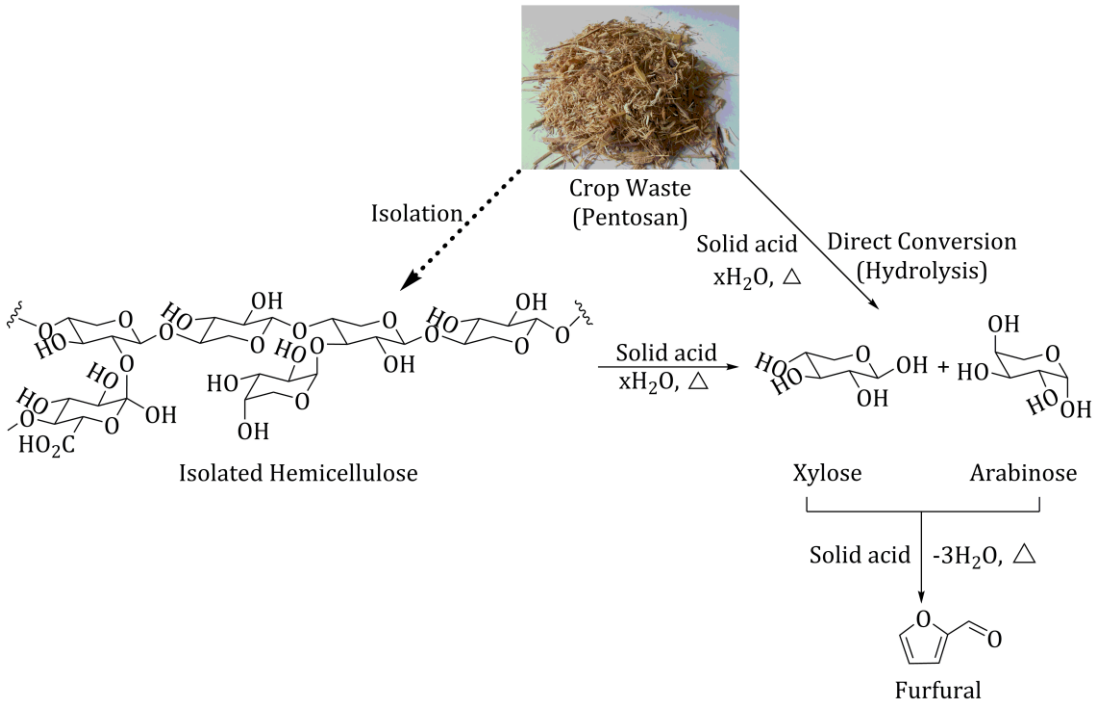

Scheme 3.1. Pathway for the synthesis of C_5 sugars (xylose, arabinose) and furfural from biomass. The dotted arrow shown in this scheme is not my work.

3.2. Results and Discussions

3.2.1. Use of Isolated Hemicellulose

In this work, several types of hemicelluloses (softwood: oat spelt xylan, hardwood: beechwood xylan and birch wood xylan)[7,8] were used however, at first the results obtained with oat spelt xylan will be presented. All the optimization of reaction parameters were done with oat spelt xylan (xylose ≥70%, glucose ≤15%, arabinose ≤10%) and later under the final optimized reaction conditions all other hemicelluloses were used as substrate. Moreover, from the earlier studies on hemicellulose conversion into furfural using zeolite catalysts [HUSY (Si/Al = 15), HMOR (Si/Al = 10), Hβ (Si/Al = 19)] it is understood that use of biphasic solvent system (water + toluene in 1:1 *v/v* ratio) yields the best amount of furfural at 170°C.[9] Hence, in this work, it was decided to check the activity of catalyst under the similar conditions those were used in earlier work.

3.2.1.1. Comparison of Activity and Stability of SAPO's and Zeolites

In chapter 1, it is hypotheses that SAPO catalysts may have better stability compared to zeolites due to their higher structural stability and hence, those may show better

catalytic activity. Hence, first I decided to compare the results of SAPO's with zeolites under the known conditions [170°C, 8 h, water + toluene (1:1 *v/v*)].[9] The catalytic activities of SAPO's and zeolite catalysts in the conversion of oat spelt xylan are presented in Fig. 3.1. It can be seen that all the SAPO catalysts are active and among them, SAPO-44 catalyst showed the best results with 63% yield (68% selectivity) for furfural along with 7% oligomers and 6% C_5 sugars (xylose + arabinose) in one-pot method. Moreover, ca. 15% glucose present in oat spelt xylan converted into 5% fructose and 2% 5-hydroxymethylfurfural (HMF) with unconverted glucose of 5% under reaction conditions. This is because SAPO catalysts have both Lewis and Brönsted acid sites and in literature, it is discussed that isomerization of glucose to fructose over Lewis acid sites and further dehydration of fructose into HMF over Brönsted acid site is possible (for more details please refer section 2.5.3, chapter 2).[10,11] Basically, by combining the entire products yields, a total of 88% carbon balance is observed with 92% conversion of hemicellulose using SAPO-44 as a catalyst. In contrast, when zeolite catalysts such as Hβ (Si/Al = 19), HUSY (Si/Al = 15), HMOR (Si/Al = 10) were used, a moderate yields (44-56%) for furfural were possible (Fig. 3.1).

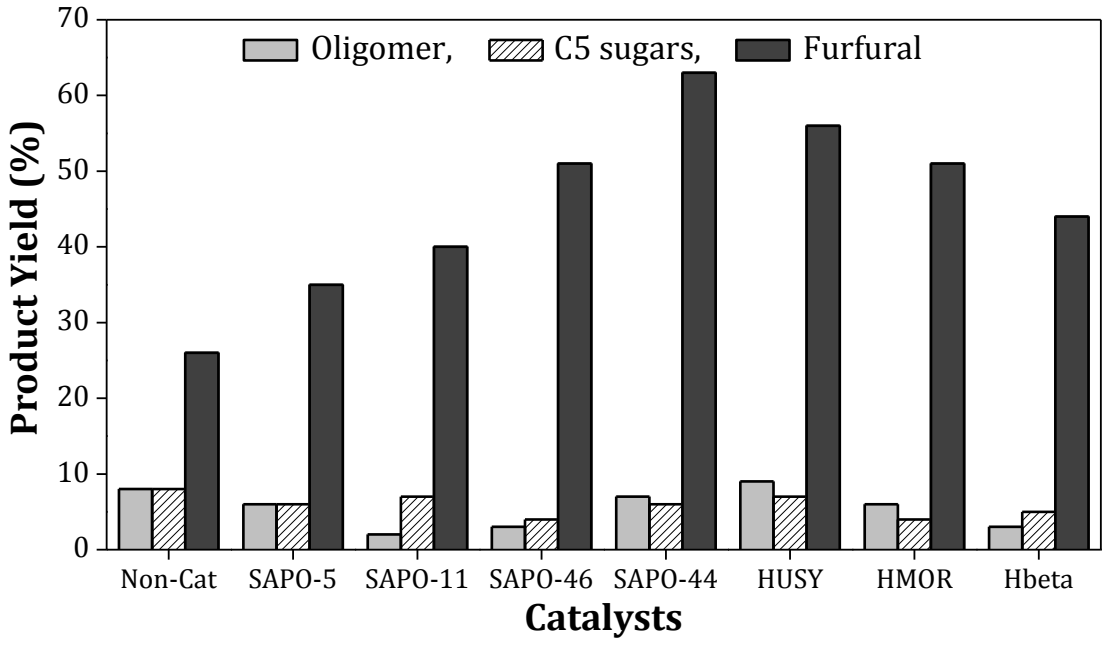

Fig. 3.1. Comparison of catalytic activity of SAPO's and zeolite catalysts in the conversion of oat spelt xylan in one-pot method. Reaction conditions: xylan (0.3 g), catalyst (0.075 g), water + toluene = 60 mL (1:1 *v/v*), 2 bar N_2 at *RT* (~9 bar N_2 at 170°C), 170°C, 8 h.

Under the similar conditions, when a reaction is carried out without catalyst only 26% furfural yield with 53% carbon balance was obtained (Fig. 3.1). Non-catalytic activity in reaction can be attributed to the thermal processes which is because of increasing dissociation of water at higher temperatures (pK_w value of water = 13.99 at 25°C and 11.64 at 150°C).[12] From these data it can be commented that the catalyst plays a major role in diverting reaction to desired products (sugars and furfural) due to their acid sites. Other SAPO series catalysts such as SAPO-5, SAPO-11 and SAPO-46 were also evaluated for the reaction but the furfural yield remained in the lower range of 30-51% (Fig 3.1). The lower catalytic activity in SAPO-5 and SAPO-11 could be attributed to the presence of very less total acid amount and absence of strong acid sites [SAPO-5: 0.8 mmol/g, weak, (100-250°C) and SAPO-11: 0.3 mmol/g, weak, (100-250°C)] in these catalysts (Table 2.3; chapter 2). In case of SAPO-46 due to lack of sufficient amount of strong acid amount (0.4 mmol/g) as well as total acid amount (0.8 mmol/g) in catalyst compared to SAPO-44 (strong: 0.5 mmol/g, total: 1.2 mmol/g), it yields lower amount of furfural (51%).

From the above discussed data it can be seen that zeolite; HMOR and HUSY can produce comparable yields for furfural (51 and 56%, respectively) as like SAPO-46 and SAPO-44 catalyst (51 and 63%, respectively) under similar reaction conditions. However, in the earlier study it was shown that zeolite catalysts are not stable under reaction conditions as confirmed by various characterization techniques (XRD, TPD-NH_3, NMR, ICP etc.).[9] Hence, it is important to know whether SAPO catalysts which show better activity than zeolites are stable under reaction conditions or not. To understand this, in the next step, catalyst recycle study was performed with SAPO-44, SAPO-46, HMOR and HUSY catalysts. The data presented in Fig. 3.2 confirms that both SAPO-44 and SAPO-46 catalysts are stable since those offered similar furfural yields in minimum 4 recycle runs however; all the zeolites lose their catalytic activity in each consecutive run. This emphasizes the fact that SAPO catalysts are stable under the reaction conditions.

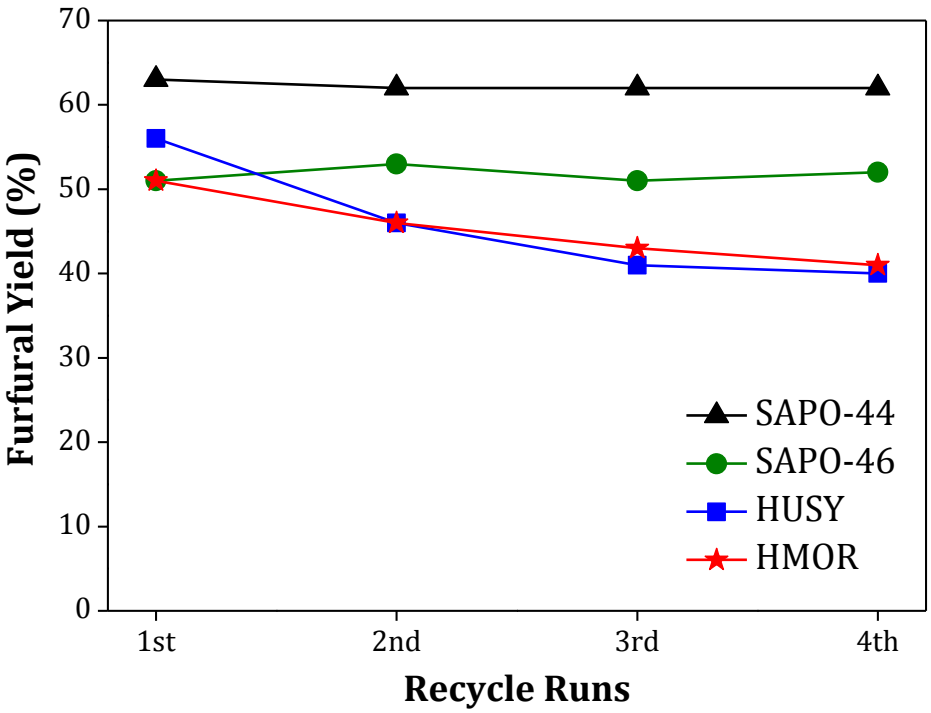

Fig. 3.2. Recycle activity of SAPO's and zeolite catalysts in the conversion of oat spelt xylan into furfural. Reaction conditions: xylan (0.3 g), catalyst (ca. 0.075 g), water + toluene = 60 mL (1:1 *v/v*), 2 bar N_2 at *RT*, 170°C, 8 h.

Although, SAPO-44 catalysts showed recyclable activity, it was important to know whether the catalyst is structurally stable or not. To further confirm structural stability of catalysts, XRD patterns of both fresh and spent SAPO-44 and HMOR were recorded. Fig. 3.3 confirms that the XRD patterns of spent SAPO-44 catalyst remain preserved as like fresh SAPO-44 catalyst. Whereas, the peak patterns of spent HMOR catalyst has lower peak intensity compared with fresh catalyst (Fig. 3.3). This in turn informs that morphological changes in HMOR catalyst under the reaction conditions are happening. It is also discussed in the literature that under hydrothermal conditions, zeolite framework Al ions reacts with water and H^+ ions to the release of Al from zeolite as aluminum cation or aluminum hydroxide.[13] Similar morphological modification was also reported when HZSM-5 zeolite is heated under hydrothermal conditions in presence of acid (H_3PO_4).[14] Under such condition, the Si–O–Al bonds in HZSM-5 were found to break as proven with the help of solid state MAS NMR technique. It is interesting to know that although; in SAPO catalyst similar type of bonding (Si–O–Al) is

present however, due to presence of phosphorous, the catalyst framework becomes stable.

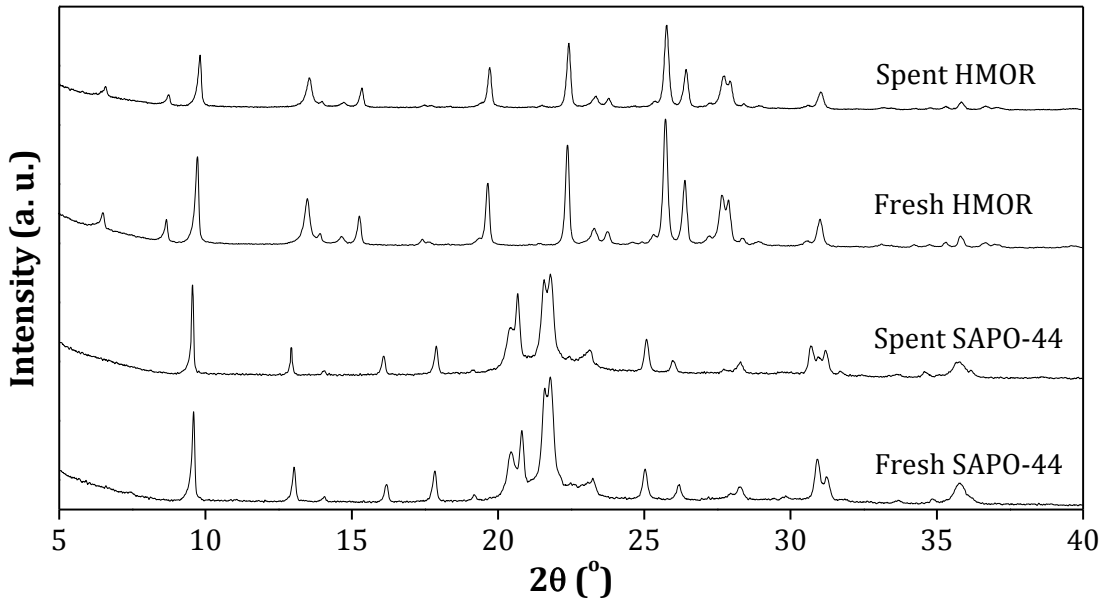

Fig. 3.3. XRD patterns of fresh and spent SAPO-44 and HMOR.

From the above discussed data it is now suggested that SAPO catalysts were stable under the processing conditions of oat spelt hemicellulose into C_5 sugars and furfural. Also, it was shown that SAPO-44 catalyst is the best active catalyst compared to other SAPO catalysts. Though, SAPO-44 catalyst showed better activity than zeolite, it was essential to compare its activity with very well-known solid acid catalysts like ion-exchanged resins (Amberlyst-15 and Nafion SAC-13) and metal oxide (niobium pentoxide; Nb_2O_5). The details on this are presented in next section.

3.2.1.2. Evaluation of Other Solid Acid Catalyst Activities

To evaluate the catalytic activity of Amberlyst-15, Nafion SAC-13 and Nb_2O_5 catalysts in oat spelt xylan conversion, I decided to employ similar reaction conditions [170°C, 8 h, water + toluene (1:1 *v/v*)] used to compare activities of SAPO's and zeolites (Fig. 3.1) A promising amount of furfural yield of 61%, 52% and 55% was possible with Amberlyst-15, Nafion SAC-13 and Nb_2O_5 catalyst, respectively. However, as shown earlier, under the similar reaction conditions 63% furfural formation was evident using SAPO-44 catalyst. Beside furfural formation, minor amount of oligomers (2%, 6%, 2%, respectively) and C_5 sugar (16%, 10%, 8%, respectively) formation was also observed

with Amberlyst-15, Nafion SAC-13 and niobium pentoxide catalyst. Since these catalysts were also active in yielding furfural in higher concentration, it was decided to check their activity in recycle runs. When these catalysts were recycled after simple washing with water showed decrease in the activity [Amberlyst-15: 1st run = 61%, 2nd run = 51%, Nafion SAC-13: 1st run = 52%, 2nd run = 49%, niobium pentoxide: 1st run = 56%, 2nd run = 46%]. The decrease with Amberlyst-15 catalyst is obvious since it has very low hydrothermal stability (<120°C).[15] Moreover, it was proposed that in case of Nafion catalyst due to presence of sulfonic acid groups (Fig. 1.8, chapter 1); those got solvated (poisoned) by reaction water and thereby, reduce catalytic activity in recycle runs.[16] Considering these results, it is suggested that amongst all the solid acid catalysts, SAPO-44 shows better activity and stability.

3.2.1.3. Influence of Hydrophilicity-Hydrophobicity of Catalysts

It is important to note here that the total acid amount in SAPO-44 and HMOR were same (1.2 mmol/g, Table 2.3; chapter 2), yet as seen from Fig. 3.1, HMOR gave lower yield of furfural (51%) than the SAPO-44 (63%). This indicates that not only acid amount but other factors are also playing important role in achieving higher activity with SAPO-44. From literature it is understood that one of the main reasons behind lower furfural yield is due to condensation reaction between unconverted sugars and formed furfural in presence of acidic catalyst to form humins.[17-19] So, it can be expected that separation of furfural from solid acid catalysts may suppress the side reactions. This can be possible if the catalyst has higher hydrophilic properties. It was anticipated that if the catalyst is hydrophilic in nature then eventually it will prefer to remain in water phase where substrates (oligomers, sugars) are present and thus, will give better catalytic activity to yield furfural. In the same time, the formed furfural will separate out from catalyst since it has been extracted immediately in toluene phase in case of water + toluene biphasic system. In SAPO catalyst due to presence of more electronegative phosphorous element (E.N. = 2.2; Pauling scale) compared to zeolite ($E.N._{Al}$ = 1.6; Pauling scale, $E.N._{Si}$ = 1.9; Pauling scale), phosphorous may attract water more towards its surface and it can be expected that SAPO catalyst will have higher hydrophilicity compared to zeolite.[20] To understand the catalyst property further, a comparative study on the hydrophilicity-hydrophobicity property of zeolite, HMOR and SAPO's was undertaken. Basically, here

two methods were adopted to understand the hydrophilicity-hydrophobicity property of catalyst,

1. water-organic solvent distribution of catalyst

2. TGA study

1. Water-Organic Solvent Distribution of Catalyst:

In this process of determination of hydrophilicity-hydrophobicity property of catalyst, first water + toluene solvent system was chosen since; the same solvent system was used for the reaction. In two identical test tubes equal amounts (~0.1 g) of HMOR and SAPO-44 were taken and to it 5 mL water was added. Then to these test tubes toluene (d = 0.86 g/mL at 25°C) was added by maintaining 1:1 *v/v* ratio. It was interesting to observe that immediately after shaking the test tubes to disperse catalyst in both solvent layers, SAPO-44 went to aqueous layer giving clear organic phase (Fig. 3.4). However, HMOR was almost equally distributed in both the layers (Fig. 3.4). This study indicates that SAPO-44 has higher hydrophilic character as compared to HMOR. Although, in water + toluene solvent system, it is presented that SAPO-44 has higher hydrophilicity however, it is possible that due to heaviness of SAPO-44, it may remain in lower layer (water). To check this effect next, I moved to a system wherein water has lower density compared to organic solvent. The similar experiment was carried out with carbon tetrachloride (CCl_4) solvent having higher density (1.58 g/mL at 25°C) than water (0.997 g/mL at 25°C). In this case also SAPO-44 immediately transferred into upper water layer however, HMOR remained almost equally distributed in both the layers (Fig. 3.4). Further, I checked the density of SAPO-44 and HMOR catalysts and found out that SAPO-44 catalyst is heavier (d = 0.61 g/mL) than HMOR (d = 0.35 g/mL). Interestingly, although SAPO-44 is heavier still when CCl4 is used, it preferably remains in upper water layer. These results clearly suggest that SAPO-44 is more hydrophilic than HMOR.

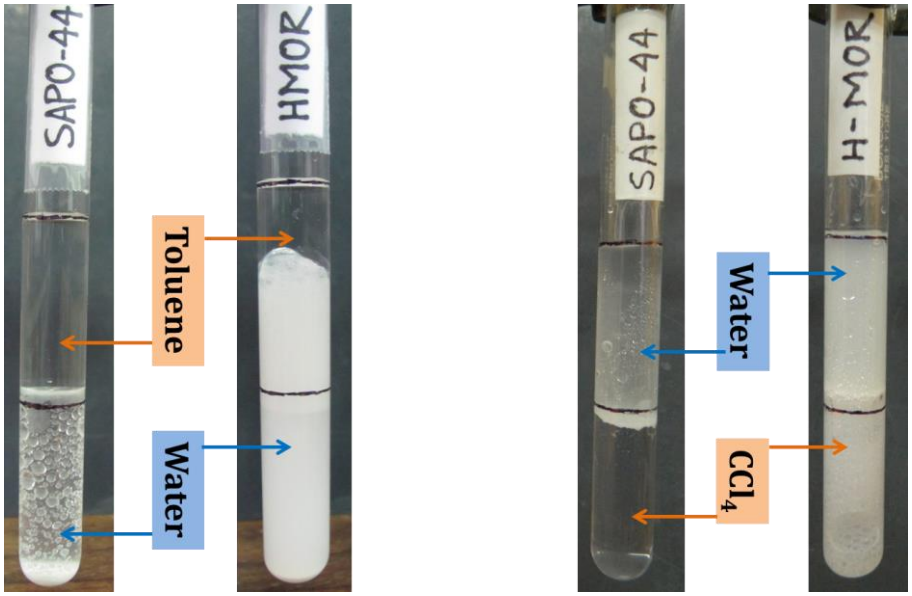

Fig. 3.4. Comparison of hydrophilicity-hydrophobicity properties of SAPO-44 and HMOR catalysts by water-organic solvent distribution method.

2. TGA Study:

Though, earlier method summarized that SAPO-44 is more hydrophilic than HMOR however, to quantify this property, TGA study was undertaken. In this method, first, fresh SAPO-44 and fresh HMOR catalysts without any treatment were subjected to TGA analysis under air atmosphere after activation at 150°C for 6 h (Fig. 3.5). A more detailed discussion on TGA profile was made in section 2.5.12, chapter 2. The results shown in Fig. 3.5 inform that with both the catalysts I didn't observe any major difference in the weight loss (7.9-8.4%) below 300°C (water loss). Next, it was planned to carry out the same experiment (TGA) after exposing both the catalysts to water since; reactions are undertaken in water. Experimentally, both the samples were kept in a closed desiccator containing water for 48 h at 30°C (Fig. 3.6). Under such condition, due to vapour pressure of water (4.2 kPa at 30°C) it distributed in closed desiccator and this water vapor was adsorbed on both the sample. The process is illustrated in Fig. 3.6. Just before TGA analysis, water vapor exposed samples were taken out from desiccator. Basically, the amount of extra adsorbed water vapor in both the samples will give the quantitative affinity of catalyst for water i.e. hydrophilicity-hydrophobicity.

The profile for activated and water exposed SAPO-44 and HMOR catalysts are displayed in Fig. 3.5. It can be seen that an excess of 9.3% water was adsorbed on SAPO-

44 catalyst whereas only 4.1% water was adsorbed on HMOR catalyst. This data gave a clear quantitative idea of higher hydrophility in SAPO-44 higher hydrophilicity as compared to HMOR.

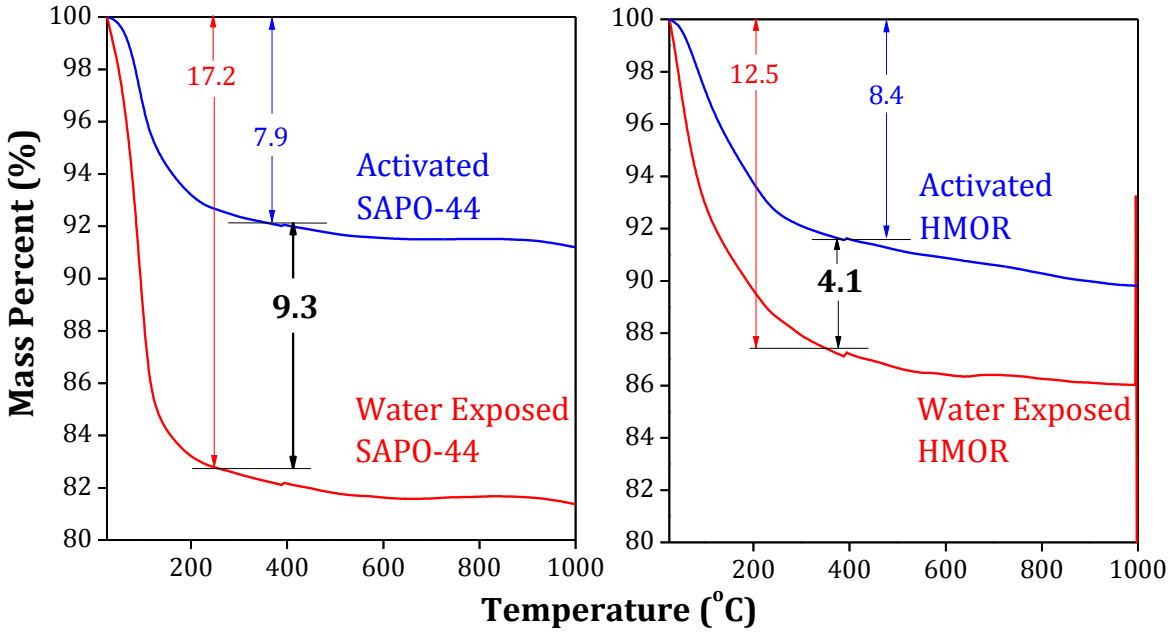

Fig. 3.5. Comparison for hydrophilicity-hydrophobicity properties of SAPO-44 and HMOR catalysts by TGA analysis.

Because of higher hydrophilicity in SAPO-44 catalyst, it preferred to remain in water phase and thus was completely available for hydrolysis and dehydration reactions and at the same time it remained separated from the produced furfural since it was extracted in organic solvent layer. This phenomenon might suppress the degradation reactions of furfural. On the contrary, HMOR catalyst is present in both the layers and hence, less amount of catalyst might be present in water phase to carry out hydrolysis-dehydration reaction and also presence of catalyst in toluene layer increases the chances of degradation reactions (contact between furfural and HMOR). Therefore, it is safe to say that higher hydrophilic SAPO-44 catalyst is better catalyst compared to less hydrophilic zeolite.

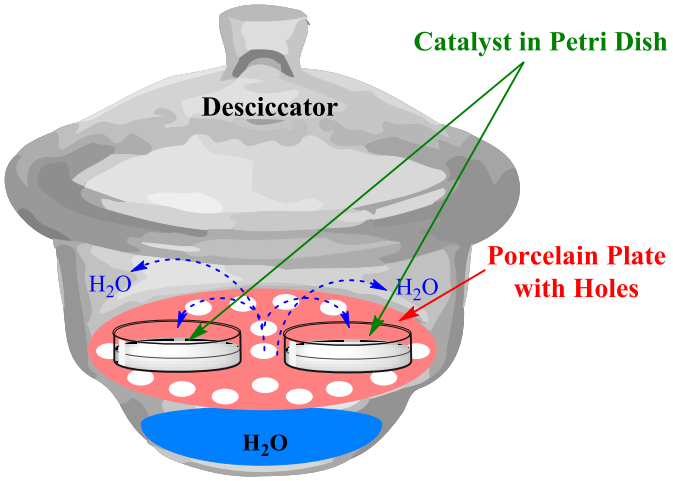

Fig. 3.6. Illustration for water adsorption method on SAPO-44 and HMOR catalysts.

Since SAPO-44 showed higher hydrophilicity than HMOR, later the hydrophilicity-hydrophobicity property of other SAPO catalysts *viz.* SAPO-46, SAPO-5 and SAPO-11 was checked with the help of distribution of catalyst in water-toluene solvent layers (1:1 *v/v*). The method used was similar as described for SAPO-44 and HMOR catalysts. From Fig. 3.7 it is clear that other SAPO catalysts (SAPO-46, SAPO-5 and SAPO-11) are also highly hydrophilic.

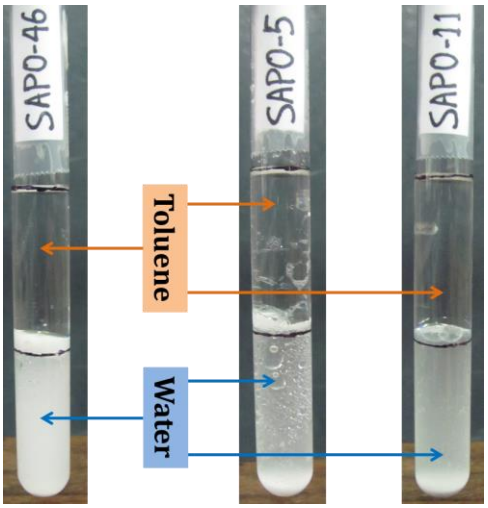

Fig. 3.7. Comparison of hydrophilicity-hydrophobicity property of SAPO-46, SAPO-5 and SAPO-11 catalysts by water-toluene distribution method.

3.2.1.4. Hammett Acidity Correlation for Catalyst Activity

The strength of acid centers reflects how effectively an acid site on catalyst can interact with substrate molecule via either proton donation or acceptance of electron pairs. For

the determination of the acid strength in solid catalysts, Hammett function (H_0) analysis technique was chosen.[21,22] The purpose of this study was to draw a correlation between catalytic activity among SAPO's and zeolite, HMOR with their acid strength.

Determination of Hammett acidity was carried out with the use of a basic indicator, *p*-nitro aniline (*p*-NA).[23] It is known that with the increase in acid strength in sample, the absorbance of the un-protonated form of basic indicator decreased, whereas the protonated form of indicator could not be observed because of its small molar absorptivity. In a typical procedure, 0.0027 g of catalyst was added to 10 mL standard aqueous solution of *p*-NA (10 ppm, pK_a = 0.99), stirred for 0.5 h and filtered the solution through 0.22 µm syringe filter. Absorbance of filtrate was checked with Jesco V-570 spectrophotometer in the range of 200-800 nm. A maximum absorbance for all the samples was observed at 380 nm. Hammett acidity (H_0) of samples was calculated according to the following equation (Equation 3.1).

$$H_0 = pK(I)_{aq} + \log_{10} ([I] / [IH^+]) \quad \text{…….. (Equation 3.1)}$$

In this equation, $pK(I)_{aq}$ stands for the pK_a value of standard indicator in aqueous solution, [I] stands for percentage of un-protonated indicator and $[IH^+]$ stands for percentage for protonated indicator. Calculations of H_0 are shown in Table 3.1.

Table 3.1. Determination of Hammett acidity in solid acid catalysts

Catalyst	A_{max}	[I]%	$[IH^+]$%	H_0
Blank (only indicator solution)	1.155	100	0	-
Fresh SAPO-5	1.135	98.3	1.7	2.75
Spent SAPO-5	1.134	98.2	1.8	2.73
Fresh SAPO-11	1.132	98.0	2.0	2.68
Spent SAPO-11	1.133	98.1	1.9	2.70
Fresh SAPO-46	1.110	96.1	3.9	2.38
Spent SAPO-46	1.112	96.3	3.7	2.41
Fresh SAPO-44	1.136	98.4	1.6	2.78
Spent SAPO-44	1.138	98.5	1.5	2.81
Fresh HMOR	0.992	85.9	14.1	1.77
Spent HMOR	1.151	99.7	0.3	3.51

After calculation of H_0 value for different catalysts, I decided to check the correlation between this value and catalyst activity. As shown in Fig. 3.8, all the catalysts showed a good correlation between the catalytic activity (in term of furfural yield) and H_0 except SAPO-44 catalyst. It has a high H_0 value (2.78), than other catalysts might be due to the restricted access of larger indicator chemical [*p*-NA; kinetic diameter = 0.64 nm calculated using earlier suggested equation {kinetic diameter = $1.234(Mw)^{1/3}$; Mw = molecular weight in g/mol}].[24] to the acid sites present on smaller pore (0.45 nm) of SAPO-44. The careful observation suggests that although SAPO-46 has high H_0 value (2.38) (i.e. lower acid strength) than HMOR (1.77) it shows almost similar catalytic activity. It is interesting to note here that in case of all the SAPO catalysts H_0 remains similar in both fresh and spent catalysts while in case of HMOR, H_0 value was increased from 1.77 to 3.51. This increase in H_0 value is basically due to morphological modification in HMOR under reaction conditions (Fig. 3.3). Furthermore, this increased H_0 value i.e. decreased acid strength can be correlated with the decrease in HMOR catalytic activity during recycle runs (Fig. 3.2). Considering all the above discussions now it is safe to say that SAPO catalysts particularly, SAPO-44 is the best catalyst among all the catalyst evaluated.

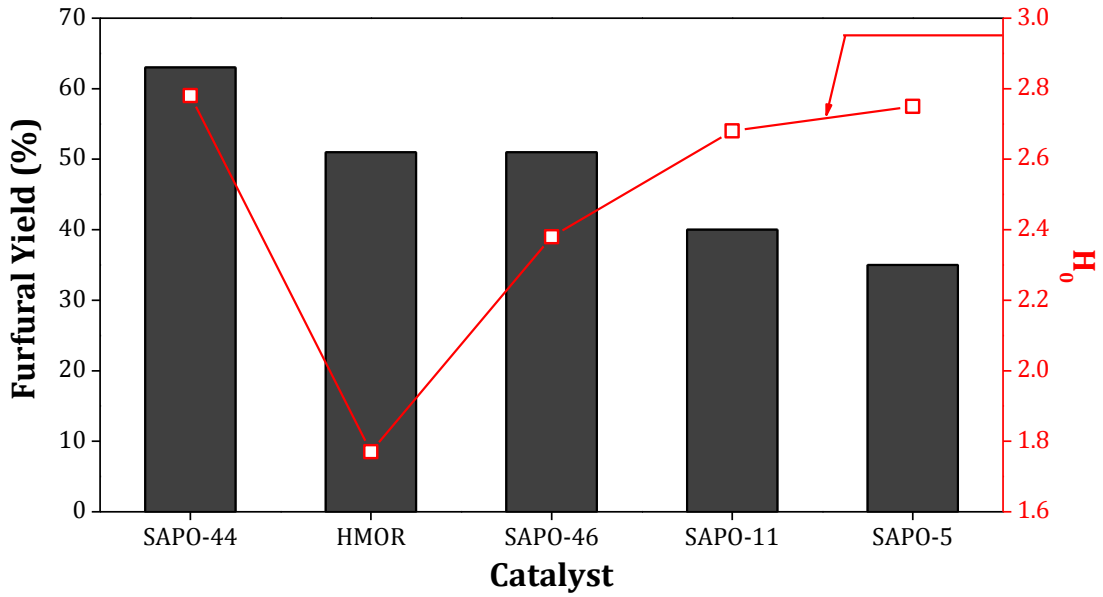

Fig. 3.8. Comparison of acid strength with solid acid catalyst activity in oat spelt xylan conversion into furfural. Reaction conditions: xylan (0.3 g), catalyst (0.075 g), water + toluene = 60 mL (1:1 *v/v*), 2 bar N_2 at *RT*, 170°C, 8 h.

Now, it is important to identify whether any of the synthesis parameter was influencing the catalytic activity as well as phase purity in SAPO-44. Basically, from this study optimization for SAPO-44 synthesis was investigated to obtain best catalytic activity.

3.2.1.5. Investigation on Chabazite (CHA) Phase Formation in SAPO-44

In the synthesis of SAPO-44, pseudoboehmite, fumed silica and orthophosphoric acid are used as precursors (please refer section 2.3.1; chapter 2). To understand the individual contribution from oxides of Si and Al in the synthesis of SAPO-44, I did XRD analysis of fumed silica and psuedoboehmite. Fig. 3.9 shows that the XRD peaks due to fumed silica and pseudoboehmite (un-calcined form) are not matching with the SAPO-44 sample. Furthermore, up on calcination of pseudoboehmite (carried out at 550°C for 6 h; identical condition for SAPO-44 material calcinations, please refer section 2.3.1, chapter 2) formation of γ-Al_2O_3 phase is observed [JCPDS file No. 10-0425]. Similar observation is made in the earlier works where during the calcinations of boehmite formation of γ-Al_2O_3 is observed.[25] Comparison of XRD patterns of calcined pseudoboehmite with SAPO-44 material also confirm that the phases present in SAPO-44 are different from calcined SAPO-44. From this study it is substantiated that SAPO-44 does not have contribution from individual precursor phases (Al_2O_3). These results suggest that in the preparation of SAPO-44, all the three components are involved in the framework and finally form chabazite (CHA) morphology. Moreover, it can be seen that a low intense broad peak at 2θ = 19-24° due to presence of amorphous SiO_2 is exist in addition to SAPO-44 peak which further suggest that not all SiO_2 is incorporated in ALPO framework to give SAPO framework.

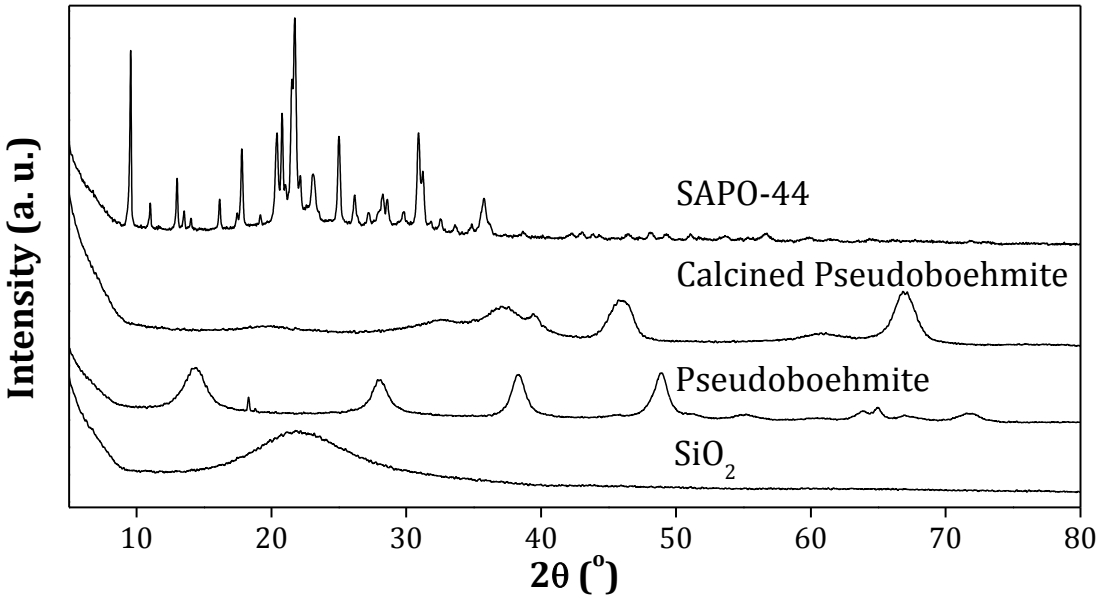

Fig. 3.9. XRD patterns of SAPO-44 and its individual precursors.

Further to understand the effects of composite materials (Si, Al, P) on the catalysis, I have carried out a study on the synthesis of materials with varying elemental compositions. With the involvement of three elements (Si, Al, P), it is possible to prepare four different materials, *viz.* Si-Al (SA-44), made up of only silica and alumina precursors; Si-P (SP-44), made up of silica and phosphorus precursors; Al-P (ALPO-44), made up of only alumina and phosphorous precursors and Si-Al-P (SAPO-44), made up of silica, alumina and phosphorous precursors. All the materials were synthesized using similar procedure as described for synthesis of SAPO-44 material (section 2.3.1, chapter 2) taking only the particular precursors.

XRD patterns for SP-44, SA-44, ALPO-44 and SAPO-44 are shown in Fig. 3.10. XRD of SP-44 shows peak for amorphous material, which indicates that the phosphoric acid does not form crystalline P_2O_5 (JCPDS No. 85-1120). In case of SA-44 material, peaks for two separate entities namely; silica (SiO_2) and γ-Al_2O_3 arising from fumed silica and pseudoboehmite, respectively are observed (Fig. 3.10). It is known from the literature that in the synthesis of aluminosilicate type materials alkaline or acidic mediums are helpful for hydrolyzing the precursors.[26] It is important to note here that, during synthesis of SA-44, absence of phosphoric acid, disallow hydrolysis process of Al_2O_3 (pseudoboehmite) and hence, mixing up of precursors under synthesis conditions cannot form any composite (zeolite type) structure. SAPO based materials are generally

synthesized by the incorporation of Si in the ALPO framework through various mechanism (substitution of Si with only P or only Al or both P and Al).[27] Consequently, there remains a chance of retaining some of the ALPO phase in SAPO material. The same observation can be seen in SAPO-44 material while comparing XRD patterns of ALPO-44 and SAPO-44 (Fig. 3.10). This is obvious since use of only 1.0 mole of SiO_2 with 1.0 mole of Al_2O_3 and 1.0 mole of H_3PO_4 in the preparation of SAPO-44 incidentally can only partially replace Al or P and hence, some amount of Al-O-P bonding may remain. Moreover, due to partial replacement of Al and P by Si, some additional amorphous SiO_2 peak (2θ = 19-24°) is also evident in SAPO-44 XRD patterns.

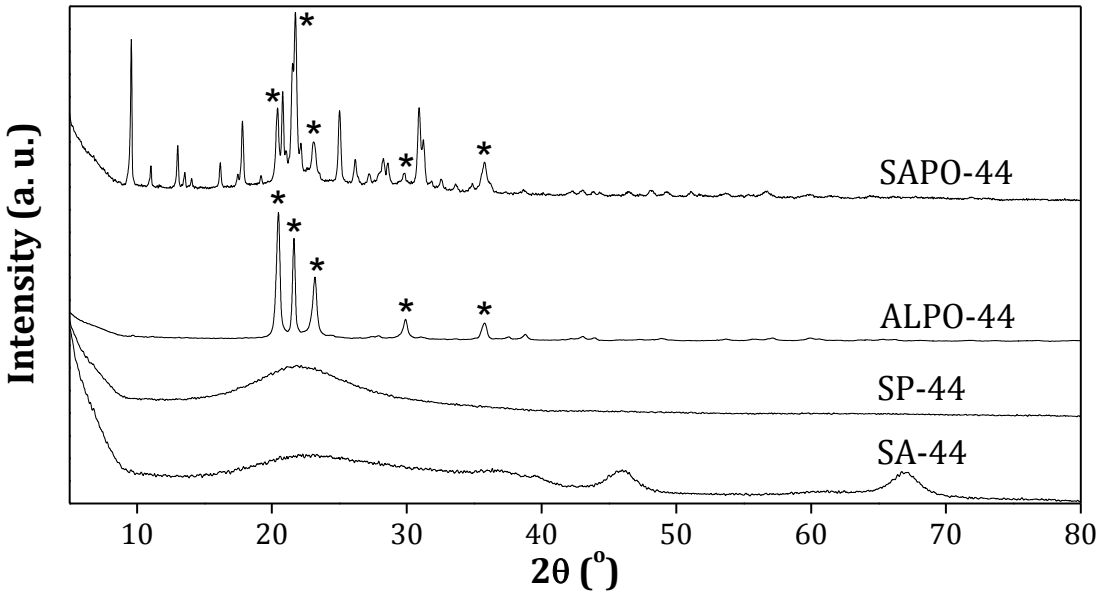

Fig. 3.10. XRD patterns comparison for SAPO-44 along with its analogues synthesized from other combinations of precursors. Asterisk (*) indicate the presence of ALPO-44 phase in SAPO-44.

After synthesis of these materials, it was decided to check the acidic sites by pyridine IR and TPD-NH_3 analysis. The type of acid sites in materials was determined by pyridine IR analysis. The detail procedure for the analysis is described in section 2.5.3, chapter 2. In brief, samples were exposed to pyridine first and next, physisorbed pyridine was removed from catalyst surface by heating at 100°C under nitrogen gas flow. Subsequently, IR spectra were recorded for these pyridine exposed samples. The acid amount in samples were measured with the help of TPD technique using NH_3 as probe molecule (for details please see chapter 2, section 2.5.6).

Fig. 3.11 showed that SP-44 material has only Brönsted acidic (BA) sites because of the presence of phosphorous whereas, SA-44 consists of only Lewis acid (LA) sites due to individual presence of SiO_2 and γ-Al_2O_3 phases as evidenced by XRD study. IR spectrum recorded for ALPO-44, did not show any peaks for BA and LA sites (Fig. 3.11). However, TPD-NH_3 study informs that ALPO-44 material has fewer amount of acidity (weak; 0.3 mmol/g). These contradictory observations (IR and TPD) can be explained on the basis of size of probe molecules. In case of IR study, pyridine is used as a probe molecule which has a kinetic diameter of 0.53 nm (for detail calculation please see section 2.5.3, chapter 2), and hence it is difficult for this molecule to penetrate inside the small pore openings of ALPO-44 (0.41 nm). On the contrary, in case of TPD study, ammonia having very small size (kinetic diameter, 0.32 nm; for detail calculation please see section 2.5.3, chapter 2) can penetrate inside the pores and can access acidic sites and thus show some acidity. The similar explanation can also be extended in case of SAPO-44 catalyst (pore diameter = 0.45 nm) where with NH_3-TPD study, 1.2 mmol/g of acidity is observed but in IR spectra very low intensity peaks were visible (Fig. 3.11). The absence of IR peaks in ALPO-44 and observance of low intensity peaks in SAPO-44 material (even having similar pore diameter) is due to difference in total acidity of materials. Taking into account both XRD and pyridine IR analysis for SAPO-44 and its composites now, it can be said that by proper mixing of its precursors and subsequent hydrothermal treatment SAPO-44 was synthesized with CHA morphology.

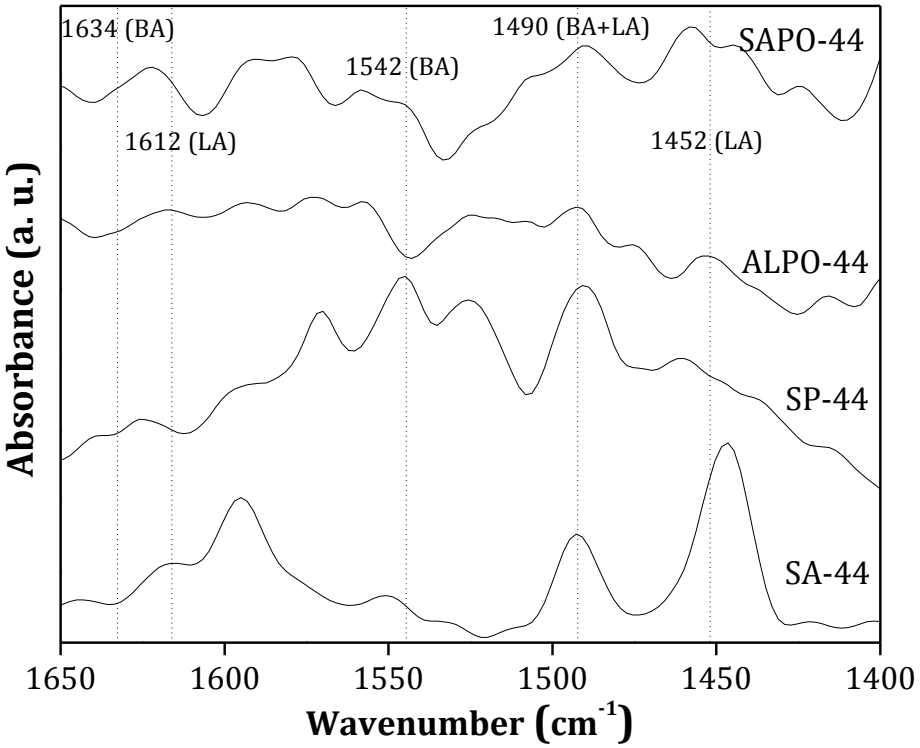

Fig. 3.11. Pyridine IR analysis of SAPO-44 and its composites.

Further all these materials were checked for their catalytic activity in oat spelt xylan conversion reaction at 170°C for 8 h. SA-44 having only weak acid sites (0.4 mmol/g) produced 40% furfural from oat spelt xylan. Slightly higher yield obtained with SA-44 compared to non-catalytic reaction (26% yields) is due to the acidity of γ-Al_2O_3 phase (0.4 mmol/g). To compare the results obtained with SA-44, oat spelt xylan reactions with only SiO_2 and γ-Al_2O_3 were carried out under similar reaction conditions (170°C, 8 h) and furfural yields of 28% and 35%, respectively are obtained. The activity observed with only SiO_2 catalyst is comparable to the non-catalytic reaction. However, slightly enhanced activity observed with SA-44 and γ-Al_2O_3 suggests that even weak acid sites are capable of converting oat spelt xylan into furfural (via xylose formation). When SP-44 catalyst having total acidity of 0.6 mmol/g was used in the reaction, 54% yield for furfural is observed. The slight increase in activity however is due to the leaching of phosphorous in the aqueous phase. To confirm the catalytic activity due to leaching of phosphorous later, recycle activity was checked with SP-44 catalyst. When spent SP-44 catalyst was used in the next run (2^{nd} run) lower yield of furfural (27%) is seen. This result is similar to the SiO_2 catalyzed reaction where 28% of furfural is observed. These results confirm that during the reaction, phosphorous is leached out in the solution. Oat

spelt xylan conversions carried out using ALPO-44 catalyst produced lower amount of furfural (41%) compared SAPO-44 catalyst (63% furfural). This is due to the presence of lower acidity in ALPO-44 materials than SAPO-44. Based on the catalytic results obtained in xylan reaction, it is clear that the combination of Si, Al and P in the material is essential to obtain best yields among all other combinations (Si-P, Si-Al, Al-P).

It is surprising to note here that pyridine molecules (kinetic diameter = 0.53 nm) are unable to access the acid sites present inside the smaller pore (0.45 nm) of SAPO-44 catalyst however, from the results it can be seen that SAPO-44 catalyzes the reaction with bigger xylan molecule. To understand this phenomenon, pH of the various solid acid catalysts (SAPO-44, HUSY, HZSM-5, Ambrlyst-15, and SO_4^{2-}/ZrO_2) dispersed in water is measured. For pH measurement, ~0.5 g of solid acid catalyst was well-dispersed in 10 mL water taken in 15 mL test-tube by stirring for 5 min. pH of solid acid catalyst dispersed water was measured immediately using a pH electrode (make: Endress + Hauser Conducta Inc., India; model: SOTA). Next, the solid catalyst was allowed to settle at the bottom of a test tube for 4 h after closing the mouth of test tube to avoid CO_2 intake by water. Then again pH of upper water layer was measured using the same electrode. Later, the solid catalyst is removed from water by centrifugation followed by filtration through 0.22 μm syringe filter. Subsequently, the pH of filtered solution was measured using the same pH electrode. Before all pH measurement, the electrode was calibrated using standard buffer solution (pH = 4.01, 6.86 and 9.19). Moreover, to confirm the value, all the pH measurements were repeated twice and the variation in results was ±0.05. All the pH data are presented in Table 3.2.

Table 3.2. pH measurement of various solid acid catalysts dispersed in water

Catalyst	pH		
	After dispersion	Solution (after settling of solid catalysts)	Solution (after removal of solid catalysts)
Water	6.65	-	-
SAPO-44	3.38	3.51	3.51
HUSY (Si/Al=15)	3.82	3.96	3.86
HZSM-5 (Si/Al=11.5)	5.23	5.80	5.75
Amberlyst-15	2.12	2.24	2.26
SO_4^{2-}/ZrO_2	4.36	4.50	4.48

From the data presented in Table 3.2, it is clear that the dispersion of solid acid catalysts in water provides acidity to water (pH = 2.12-5.23) even after removal of catalysts from solution. In case of solid acid catalysts, protons (H^+) are present in the vicinity of a catalyst surface and hence it can be expected that the pH should remain neutral. But, lower pH values of water solution suggests that some of the protons (H^+) present on the solid acid catalyst are labile and hence, those are floating around in water in the form of hydronium ions (H_3O^+). The similar phenomenon of partial proton transfer to water from Brönsted acid sites of zeolite to form hydronium ion is also proven earlier with the support of infra-red spectroscopy and quantum chemical ab initio studies.[28,29] However, due to very rapid transfer of H^+ from one water molecule to another may ultimately remove the labile protons from catalyst surface into the bulk water where bigger xylan molecules are present. These protons will then interact with the xylan glycosidic bonds to give hydrolysis reaction to form sugars. The possible pathway of this phenomenon is demonstrated in Fig. 3.12.

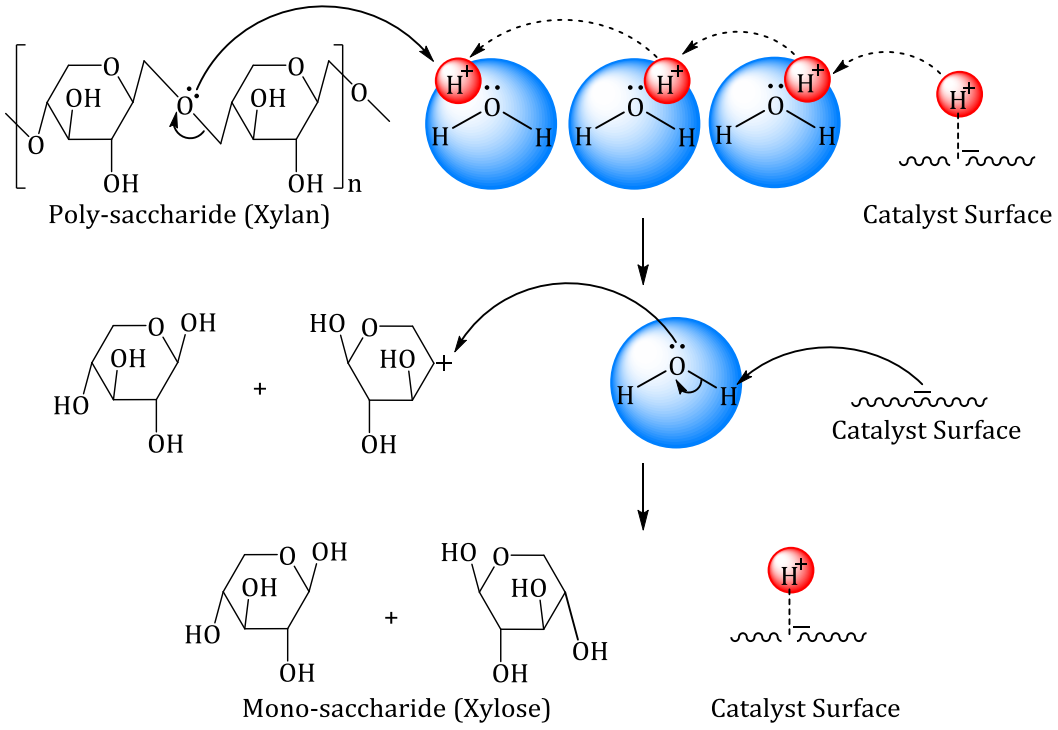

Fig. 3.12. Possible pathway for xylan hydrolysis to C_5 sugars by proton transfer from catalyst surface to the reaction center via water molecule.

Now, after hydrolysis reaction, smaller C_5 sugars (xylose and arabinose; kinetic diameter = 0.66 nm; for calculation see below) were produced. It is reported in the literature that the kinetic diameter of sugar molecules calculated using this equation may vary based on its structure (cyclic-acyclic form and orientation of hydroxyl groups).[24] Hence, although, the kinetic diameter calculated was bigger compared to pore diameter of SAPO-44 (0.45 nm) however, good catalytic activity data (furfural formation in high yields) may suggests that in the reaction system, sugar molecules have smaller kinetic diameter to access the acid sites of SAPO-44 to give dehydration reaction.

Calculation of kinetic diameter of C_5 sugars

Kinetic diameters of C_5 sugar molecules are calculated using the earlier suggested equation (Equation 3.2) which correlates the kinetic diameter with weight of molecule.[24]

$$\text{Kinetic diameter } (\sigma) = 1.234 \times (Mw)^{1/3} \quad \text{..... (Equation 3.2)}$$

Where, Mw is molecular weight of molecule in g/mol. This calculation assumes molecule as spherical and hence, the critical mass is correlated to the size of the sphere.

Molecular weight of C_5 sugars (xylose, arabinose) molecule is 150,

So Kinetic diameter (σ) of C_5 sugars = $1.234 \times (150)^{1/3}$ = 6.56 Å = 0.66 nm.

3.2.1.6. Effect of Crystallization Time in SAPO-44 Synthesis

It is understood from chapter 2 (section 2.5.1) that for the synthesis of SAPO-44 catalyst with pure CHA morphology, the material needs to be hydrothermally treated for 7 days during synthesis. So, to know whether catalyst activity is structure dependent or not further, I decided to check the effect of crystallization time during its synthesis with catalytic activity. Also, it was anticipated that materials having lower crystallinity (or mixed phases) may not have a proper structure but if these materials show good catalytic activity then those materials can be used as preferred catalysts since those

require less time to synthesize. In view of this, I have studied the influence of crystallization time on the phase formation in SAPO-44 material using XRD technique. The detail synthesis procedure is described in section 2.3.1, chapter 2.

Fig. 3.13 shows that first, amorphous gel (ZDCT, zero day crystallization time) is obtained after mixing all the precursors. This gel obtained after 2-day crystallization time (2DCT) shows presence of two phases, AFI and CHA. The characteristic peaks for both AFI (2θ = 7.5°) and CHA (2θ = 9.6°, 20.4°, 20.8°) were present in 2DCT sample with lower intensities. The observance of AFI phase is natural because, synthesis of SAPO-44 proceeds via formation of another material SAPO-5 having AFI morphology.[30] Hence, it can be said that 2DCT sample has a morphology which is a transition state between AFI to CHA phase. In line with this, increase in crystallization time to 4 days (4DCT) improved the intensity of the peak due to CHA morphology (Fig. 3.13). Finally, SAPO-44 (7DCT) with perfect CHA morphology is obtained after 176 h (7 days 8 h) of crystallization time. After synthesis of materials (ZDCT, 2DCT, 4DCT and SAPO-44), those were characterized by N_2 sorption technique. It was found that the surface area gradually increased with the increase in crystallization time (ZDCT: 106 m^2/g → 2DCT: 113 m^2/g → 4DCT: 144 m^2/g → SAPO-44: 369 m^2/g). Nevertheless, critical view on the surface area data suggests that up to 4 days crystallization time, improvement in surface area value is less (106-144 m^2/g) but after 7 days crystallization time surface area improved to 369 m^2/g. This might be due to improvement of phase purity in material as discussed in XRD analysis results (section 2.5.1, chapter 2). Furthermore, with increase in crystallization time, average pore size and pore volume was found to be decreased [average pore size: ZDCT: (13 nm) → 2DCT (5.8 nm) → 4DCT (1.3 nm) → SAPO-44: (0.45 nm), pore volume: ZDCT (0.676 cc/g) → 2DCT (0.319 cc/g) → 4DCT (0.298 cc/g) → SAPO-44: (0.112 cc/g)]. These data emphasizes that with increase in crystallization time phase purity in material is possible.

Furthermore, the acid amount of all these materials were quantified using TPD-NH_3 technique and it is found that with increase in crystallization period, acidity in material is also improved. Both ZDCT and 2DCT materials shows presence of only weak acid sites (0.3 mmol/g and 0.4 mmol/g, respectively) however, 4DCT material shows presence of both weak (0.6 mmol/g; 100-250°C) and strong (0.3 mmol/g; 350-500°C)

acid sites. In SAPO-44 with pure CHA phase, highest amount of both weak (0.7 mmol/g; 100-250°C) and strong (0.5 mmol/g; 350-500°C) acid sites are observed.

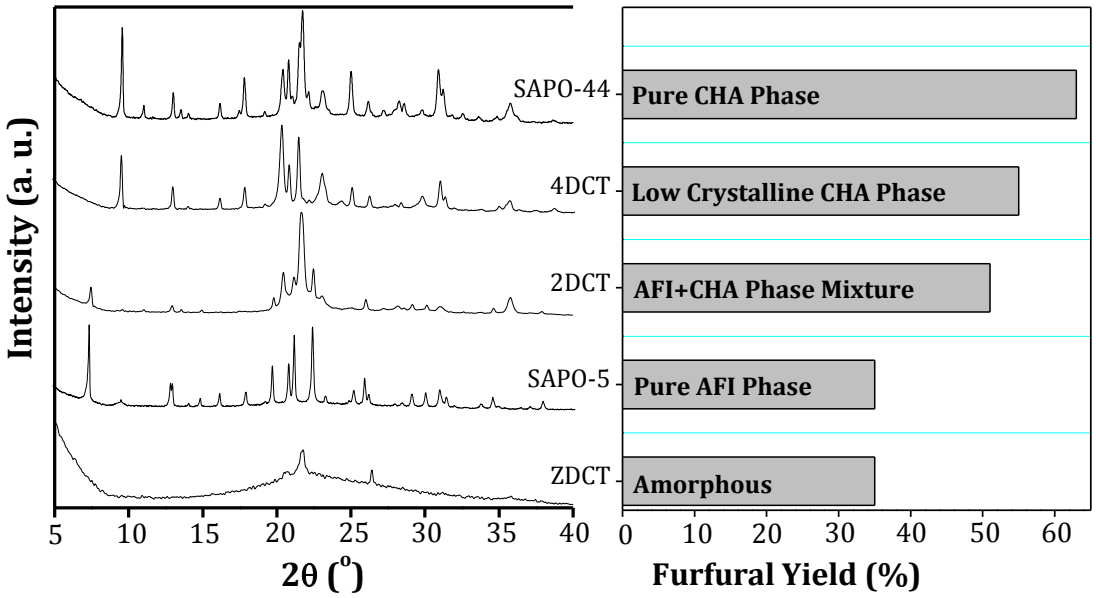

Fig. 3.13. Correlation between SAPO-44 phase purity and catalytic activity for furfural synthesis from oat spelt xylan. Reaction conditions: xylan (0.3 g), catalyst (0.075 g), water + toluene = 60 mL (1:1 *v/v*), 2 bar N_2, 170°C, 8 h.

Moreover, the variation in catalytic activity with all these materials was studied in oat spelt xylan conversion into furfural reaction (Fig. 3.13). ZDCT catalyst shows very low furfural yield (35%) which is similar to the activity of γ-Al_2O_3 (35%) catalyzed reaction. Furfural yield is improved with increase in crystallization time of material (2DCT: 51%, 4DCT: 55%, 7DCT: 63%). It is important to note here that even with lower acid amount present in 4DCT catalyst (0.9 mmol/g) compared to SAPO-44 catalyst (1.2 mmol/g), the activity per acid site is seen to be higher with 4DCT catalyst (TON = 18.5) than SAPO-44 (TON = 15.9). Similarly, in case of 2DCT catalyst also higher TON (38.6) is observed since 2DCT has only 0.4 mmol/g of acidity. Considering this, I have carried out reaction by charging higher amount 4DCT catalyst (0.1 g) to achieve similar acid amount (0.09 mmol) in reaction system as like SAPO-44 catalyst (0.075 g contains 0.09 mmol acid amount). But a furfural yield of only 57% is achieved. This reflects to the fact that to attain higher catalytic activity, CHA morphology and presence of strong acid sites is necessary.

3.2.1.7. Effect of SiO_2 Concentration in SAPO-44

It is evident from the earlier results obtained in this study that presence of silica in SAPO-44 framework is the main reason for achieving higher acidity in the material. The similar observations were also reported in earlier works.[20] Since conversion of hemicellulose into furfural requires acidic catalysts it was thought that if Si concentration is varied in the SAPO-44 catalyst, it may possible to achieve higher furfural yields. Considering this, during the synthesis of SAPO-44 material, I have varied concentration (0.8-1.6 mole) of Si and rest of the synthesis procedure was kept similar (for detail synthesis procedure of SAPO-44 please refer section 2.3.1, chapter 2). The XRD patterns of all the materials are shown in Fig. 3.14 and it is clear from this pattern that with the increase in silica molar ratio from 0.8 to 1.0, improvement in the crystallinity of the material is achieved. It is notable that due to presence of excess amount of silica in 1.6-SiO_2-SAPO-44, XRD pattern of the material shows very low crystallinity with visible presence of amorphous peak due to SiO_2 (2θ = 19-24°). This also confirms that higher concentration of silica, does not necessarily replace framework Al and/or P and silica may just be present along with SAPO-44 material. Further, by studying the XRD patterns of 1.6-SiO_2-SAPO-44 and γ-Al_2O_3 materials, it is suggested that since peaks in these two spectra does not match indicate that Al_2O_3 does not form separate (individual) phase when higher silica is used to prepare the catalyst.

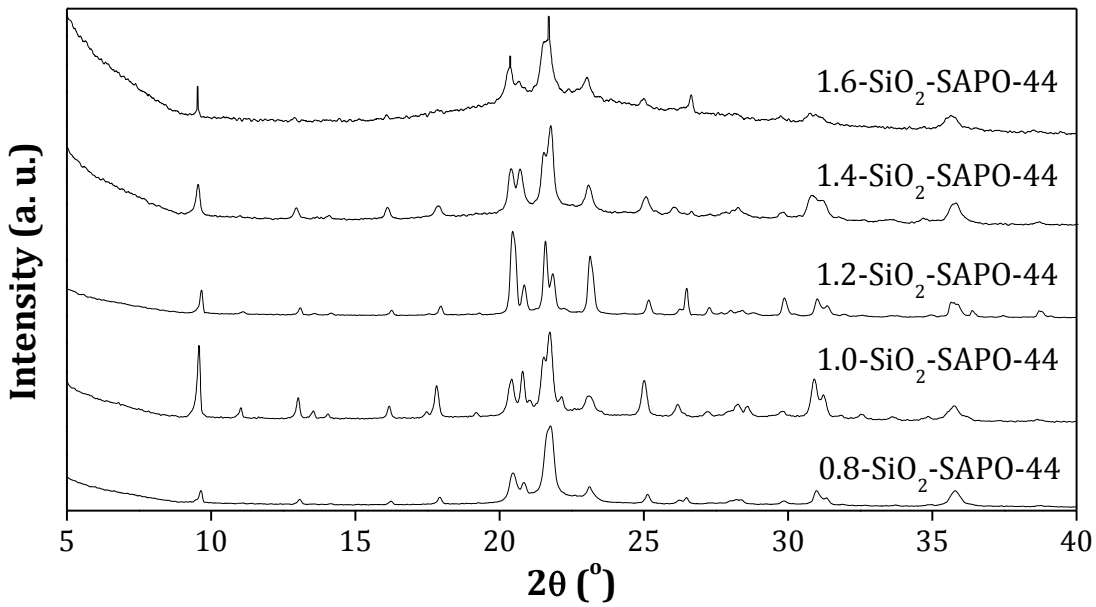

Fig. 3.14. XRD patterns comparison for SAPO-44 with variation in silica molar ratio.

To check whether actual concentration of elements present in prepared materials matches with the theoretical concentration of elements used during the synthesis of materials, SEM equipped with EDX technique was used. Table 3.3 describes the atom% of Si, Al and P in all the catalysts. The data shows increase in the Si atom percentage for SAPO-44 catalyst with increasing silica molar ratio of 0.8-1.6, respectively. This in turn, endorses the excess silica added during synthesis is present in SAPO-44 material. Based on the elemental analysis data, the compositions of all the materials are calculated and the data is represented in Table 3.3. It can be seen that 1.0-SiO_2-SAPO-44 catalyst framework composition $(Si_{0.24}Al_{0.40}P_{0.36})O_2$ matches well with the literature report.[31]

Table 3.3. Elemental microanalysis of materials using SEM-EDX technique

Material	Elemental composition (atom%)			Framework composition
	Si	Al	P	
0.8-SiO_2-SAPO-44	17.1	40.9	42.0	$(Si_{0.18}Al_{0.44}P_{0.38})O_2$
1.0-SiO_2-SAPO-44	22.9	37.9	39.2	$(Si_{0.24}Al_{0.40}P_{0.36})O_2$
1.2-SiO_2-SAPO-44	23.3	37.6	39.1	$(Si_{0.24}Al_{0.40}P_{0.36})O_2$
1.4-SiO_2-SAPO-44	25.0	37.1	37.9	$(Si_{0.26}Al_{0.39}P_{0.35})O_2$
1.6-SiO_2-SAPO-44	27.2	35.7	37.1	$(Si_{0.28}Al_{0.38}P_{0.34})O_2$

Acid amount distribution for all SAPO-44 with various silica molar ratios was evaluated with TPD-NH_3 technique and the values are listed in Fig. 3.15. Based on the TPD studies, the samples can be arranged in the order of increasing total acidity as,

1.6-SiO_2-SAPO-44 (0.8 mmol/g) < 0.8-SiO_2-SAPO-44 (0.9 mmol/g) < 1.4-SiO_2-SAPO-44 (1.0 mmol/g) < 1.2-SiO_2-SAPO-44 (1.2 mmol/g) = 1.0-SiO_2-SAPO-44 (1.2 mmol/g)

Later, the effect of silica concentration in SAPO-44 on the hemicellulose conversion to furfural was evaluated at 170°C within 8 h reaction time in presence of water + toluene (1:1 *v/v*) (Fig. 3.15). Results show that, SAPO-44 with silica mole ratio of 1.0 gives the highest (63%) furfural yield. 0.8 mole silica SAPO-44 yields lower (50%) furfural and this might be due to presence of less acid amount (0.9 mmol/g) in the

material compared to 1.0 mole silica SAPO-44 (1.2 mmol/g). However, increase in silica concentration in SAPO-44 shows marginal effect on catalysis.

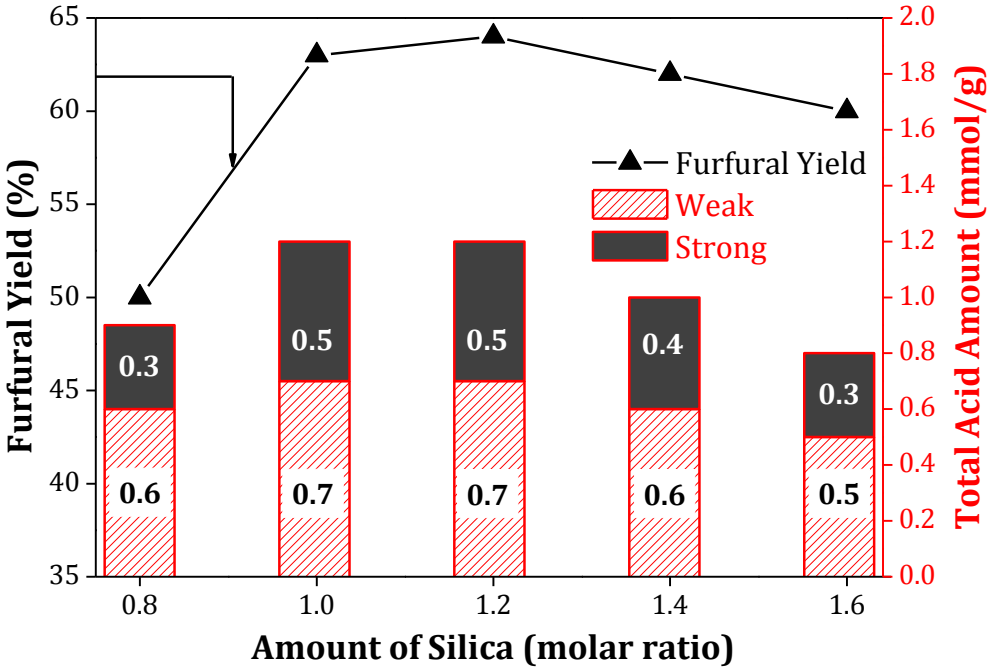

Fig. 3.15. Effect of silica concentration on generation of acid sites in SAPO-44 and its catalytic activity in the synthesis of furfural from oat spelt xylan. Reaction conditions: xylan (0.3 g), catalyst (0.075 g), water + toluene = 60 mL (1:1 *v/v*), 2 bar N_2 at *RT*, 170°C, 8 h.

Finally, after optimization of synthesis parameters in SAPO-44 preparation it can be concluded that 1.0 silica molar gel composition SAPO-44 crystallized after 176 h with perfect CHA morphology is the better active catalyst. Now, as discussed earlier, another objective of my work is to improve furfural yield and selectivity. Hence, next, improvement of furfural yield and selectivity was done by optimization of reaction parameters in presence of SAPO-44 catalyst with silica molar ratio of 1.0.

3.2.1.8. Influence of Temperature, Time and Pressure

Optimization of reaction temperature was investigated by carrying out reactions in a range of 160-180°C. Fig. 3.16 demonstrated that with change in reaction temperature, the product distribution varies. Reaction carried out at lower temperature (160°C) mainly converted xylan (poly-saccharide) into oligomers (25%) and C_5 sugars (42%) with less amount of furfural (31%). With increase in reaction temperature to 170°C

favored the conversion of more oligomers into C_5 sugars and further conversion of C_5 sugars into furfural. Hence, 63% furfural yield was achieved with lower yield of oligomers (7%) and C_5 sugars (6%). Further increase in reaction temperature to 180°C didn't affect much to the product distribution (furfural = 63%, C_5 sugars = 5%, oligomers = 5%) as compared to 170°C reaction. This suggests that to yield enhanced amount of furfural, reactions should be preferably done at 170°C. To check the stability of furfural, reactions with furfural as a substrate were carried out with or without catalyst under similar reaction conditions as like hemicellulose conversion however, no measurable conversions were observed indicating that furfural does not undergo any conversion under reaction condition.

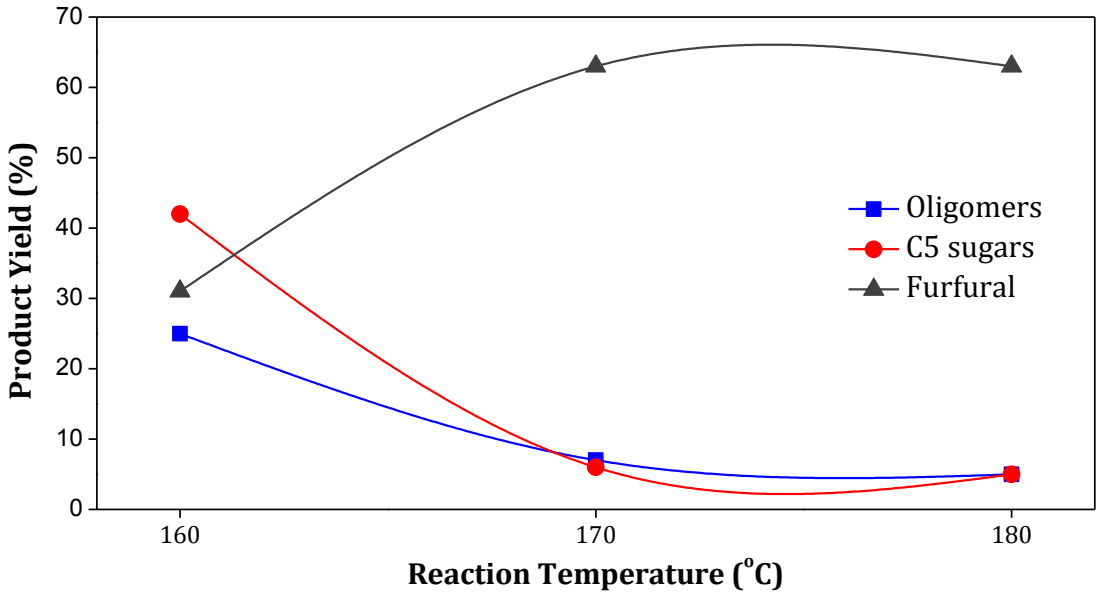

Fig. 3.16. Influence of reaction temperature on deciding product distribution from oat spelt xylan conversion. Reaction conditions: xylan (0.3 g), catalyst (0.075 g), water + toluene = 60 mL (1:1 *v/v*), 2 bar N_2 at *RT*, 8 h.

To understand the influence of reaction time, further reactions were carried out at different time period (Fig. 3.17). The reaction carried out with SAPO-44 catalyst and water + toluene (1:1 *v/v*) solvent system revealed the formation of oligomers in high concentrations (75%) at the initial time of reaction (1 h). A critical view on Fig. 3.17 reveals that up to 4 h reaction time, the formation of enhanced amount C_5 sugars and furfural was possible due to conversion of oligomer. At 6 h reaction time 53% furfural yield was observed which increased to 63% after 8 h. Further increase in time (10 h)

gave 71% furfural yield. However, furfural yield remained constant even after conducting reaction for 12 h (72%).

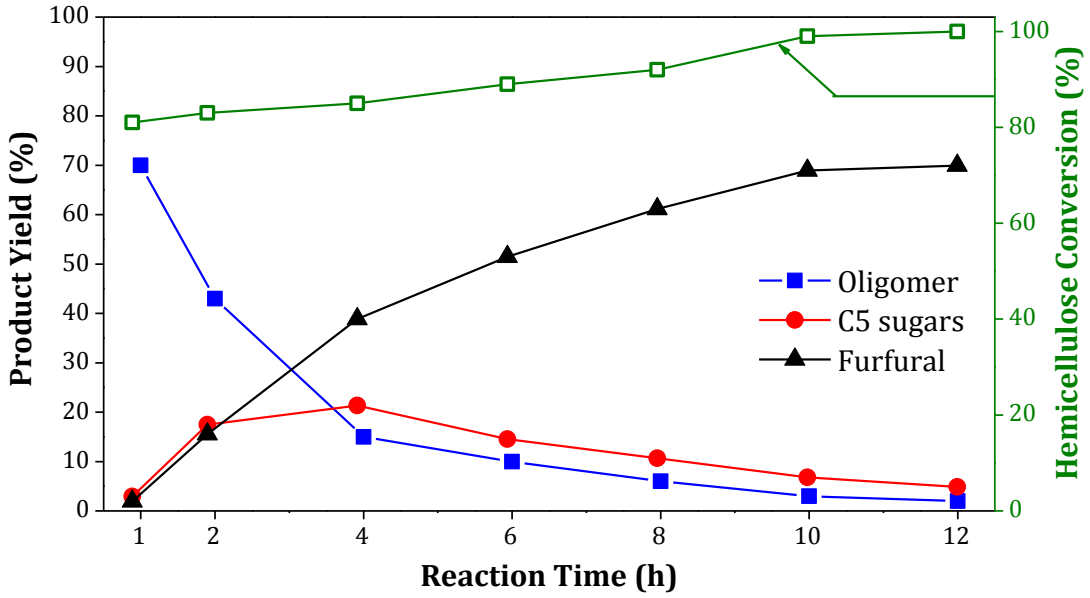

Fig. 3.17. Influence of reaction time on product distribution from oat spelt xylan conversion. Reaction conditions: xylan (0.3 g), catalyst (0.075 g), water + toluene = 60 mL (1:1 *v/v*), 2 bar N_2 at *RT*, 170°C.

From the above data it can be concluded that, first hemicellulose is converted to oligomers and then to monomers (xylose + arabinose) and subsequently into furfural. The optimum furfural yield (71%) was possible after reaction was carried out for 10 h at 170°C using SAPO-44 catalyst.

To enable a process compatible for industry, it is desired to use lowest pressures, if possible close to ambient pressures due to several safety restrictions. Here, I tried to identify the lowest possible pressure for the reaction (Table 3.4). Basically, oat spelt xylan conversion was carried out in presence of inert gas (nitrogen) to minimize any possible undesired product formation due to oxidation reaction of substrate and product in presence of air. Studies showed that in presence of SAPO-44 catalyst at 170°C even 2 bar nitrogen pressure (at 30°C) is well enough for yielding similar amount of furfural (62%) as observed with 10 bar (at 30°C) and 20 bar (at 30°C) pressures (63%). Unfortunately, further decrease in nitrogen pressure to 1 bar, showed slight decrease in the furfural yield (54%). At low pressure, the number of contact / collisions

between substrates and catalysts might be less and hence shows less furfural yields. Moreover, it was suggested in literature that with increase in N_2 gas pressure in reaction system, solubility of N_2 in water increases (solubility of N_2 in water at 170°C, under 1 bar pressure: 1.1089×10^{-4}, under 5 bar pressure: 5.8×10^{-4}, under 50 bar pressure: 38.9484×10^{-3}).[9] Hence, it can be expected that increase in N_2 gas pressure in reactor decreases the hydrogen bonds between water molecules and substrate. This in turn may breakdown the xylan structure to form oligomers and monomers. The similar phenomenon was also seen in this reaction system when N_2 gas pressure is increased from 1 bar to 2 bar. However, further increase in N_2 gas pressure has not influences in the reaction.

Table 3.4. Studies on reaction operating pressure for oat spelt xylan conversion

Pressure (bar)	Conversion (%)	Products Yield (%)		
		Oligomers	C_5 Sugars	Furfural
20	92	7	6	63
10	91	6	8	63
2	91	7	7	62
1	87	10	8	54

Reaction conditions: xylan (0.3 g), SAPO-44 (0.075 g), water + toluene = 60 mL (1:1 *v/v*), 2 bar N_2 at *RT*, 170°C, 8 h.

3.2.1.9. Effect of Catalyst and Substrate Concentrations

The use of large quantity of catalyst may not allow the process to be efficient in terms of cost. Therefore, optimization of catalyst concentration in reaction is important to study. Experiments were conducted with varying catalyst amount to check whether at higher S/C ratio better results could be achieved. The reaction carried out with low catalyst concentration (0.0375 g; S/C = 8, *wt/wt*) yielded only 57% furfural and 11% C_5 sugars. Later, catalyst concentration was increased to 0.075 g to maintain S/C = 4 (*wt/wt*) in reaction system keeping all other reaction parameters same. With this system, the furfural yield was improved to 63% by further conversion of C_5 sugars and hence, fewer amounts of C_5 sugars were available in reaction mixture (6%). This data claims that when lower catalyst concentration (0.0375 g) was used due to absence of sufficient

amount of acid sites in the reaction system dehydration reaction of C_5 sugars into furfural get suppressed and eventually, low furfural yield was obtained. Hence, in the next reaction, catalyst amount was further increased from 0.075 g to 0.15 g and 0.3 g, i.e. S/C = 4 to 2 to 1 (*wt/wt*), keeping all other reaction parameters constant. Surprisingly, a similar furfural yield of 63±2% was evident with the entire S/C ratio at 170°C. This suggests that use of 0.075 g SAPO-44 catalyst (S/C = 4) is well-enough to carry out the reaction. This also confirms that no further increase in catalyst amount is required. Hence, it is safe to say that S/C ratio of 4 is optimum to achieve these results.

From the industry point of view, it is desirable to use maximum possible substrate concentration; so that from a single processing maximum amount of desired product will be available. Ultimately, use of concentrated substrate solution will make the process energy and cost efficient. To study this, optimization of hemicellulose concentration (change of water to substrate ratio, keeping S/C ratio same) were done. When reactions were carried out at 170°C for 8 h with 1 wt% oat spelt xylan solution (0.3 g in 30 mL water), 7% oligomers, 6% C_5 sugars and 63% furfural yield was observed. The catalytic activity was almost constant (Oligomers = 8%, C_5 sugars = 6%, furfural = 61%) when reactions were conducted using 5 wt% hemicellulose solutions (1.5 g in 30 mL water). Further increase in hemicellulose concentration to 10 wt% (3 g in 30 mL water) leads to lower yields of furfural (42%) although, almost similar yields for oligomers (8%) and C_5 sugars (7%) were obtained. It clearly suggests that use of very high concentration of substrate is not favorable. If very high concentration of oat spelt xylan is present, under the reaction conditions it will give high concentration solutions of C_5 sugars and furfural and hence, those might interact in presence of acid sites to give rise to undesired products (humin). This phenomenon was further confirmed from the dark colour of reaction solution.

3.2.1.10. Effect of Solvent System and Biphasic Media Ratio

It is a well-known fact that solvent system has an important influence in deciding the product distribution as well as desired product selectivity for xylose dehydration into furfural reaction. So here, further studies were undertaken for oat spelt xylan conversion in various solvent systems with SAPO-44 catalyst. Purposefully, the study

with HMOR (zeolite) catalyst was also carried out to show that with a change in solvent system still SAPO-44 remains the best catalyst for furfural synthesis. With water only solvent system, 41% furfural yield along with 4% oligomers and 14% monomers (xylose, arabinose and glucose) were observed over SAPO-44 catalyst at 170°C within 8 h. Although, 86% hemicellulose conversion was detected but the total mass balance remains in the lower range (59%). This might be due to the formation of undesired side products in the water only system as evident in xylose dehydration reactions.[32-34] In comparison, HMOR catalyst in water yields only 36% furfural with 87% hemicellulose conversion and 52% mass balance.

Later, water + organic solvent system were used to improve the furfural yields. Here, basically the purpose of organic solvent was to extract the formed product, furfural from the water phase where actually catalyst is residing and thereby protecting furfural from catalyst contact and suppressing the side reactions. Moreover, it can be expected that furfural might have varying extent of solubility in different organic solvents and hence, variation of organic solvent may change furfural yields. Hence, three different solvent systems namely, water + toluene, water + methyl *iso*-butyl ketone (MIBK) and water + *p*-xylene in 1:1 (*v/v*) ratio were tested in this reaction. Under the reaction conditions, using SAPO-44 catalyst, water + toluene system showed the best yield of furfural (63%) compared to water + MIBK system (53%) and water + *p*-xylene system (55%). To understand the varying efficiency of organic solvent in furfural synthesis, further calculation of partition co-efficient of furfural in organic/water phase was carried out.

In a typical study, toluene, MIBK and *p*-xylene solvents were used in addition to water for the calculation of partition co-efficient of furfural at 30°C. Experimentally, ~0.2180 g furfural (maximum possible yield of furfural from 0.3 g oat spelt xylan conversion) was taken in 30 mL water and mixed properly. Later, 30 mL of organic solvent (toluene or MIBK or *p*-xylene) was added and the mixture was stirred vigorously in Paar autoclave (same autoclave used for reaction) at 30°C for 0.5 h. After that, both the layers were separated from each other using separating funnel. Amount of furfural in water and organic medium were analyzed using HPLC and GC. Partition co-

efficient was calculated according to the following equation (Equation 3.3) and data is summarized in Table 3.5.

Partition co-efficient, $(\log P)_{organic/water} = \log_{10}([furfural]_{organic} / [furfural]_{water})$

…….. (Equation 3.3)

Table 3.5. Partition co-efficient of furfural in water/organic solvent system

Solvent System	Distribution of Furfural		Partition Co-efficient
	Organic Phase (g)	Aqueous Phase (g)	
Water/toluene	0.18	0.034	0.72
Water/MIBK	0.19	0.024	0.89
Water/*p*-xylene	0.17	0.045	0.58

The partition co-efficient values for toluene and *p*-xylene were in good correlation with the experimental results for furfural formation from oat spelt xylan but discrepancy was observed in case of MIBK solvent. Even if MIBK has a higher partition co-efficient value than other two solvents, lower furfural yield (53%) was seen with water + MIBK system. This can be explained in terms of mutual miscibility of solvents. Since MIBK has a higher miscibility with water (19.1 g/L at 20°C) compared to toluene in water (0.47 g/L at 20°C) and p-xylene in water (0.18 g/L at 20°C), phase separation of MIBK and water was not clear. This may allow greater interactions between C_5 sugars and furfural in presence of catalyst to give rise to undesired products. Moreover, in greener aspect toluene can be chosen as preferred solvent, since Life Cycle Assessment (LCA) value for toluene is 2 as compared to MIBK and *p*-xylene (LCA = 9 and 3, respectively).[35]

Now, it is clear from the partition co-efficient study that after extraction of furfural in organic layer, yields of furfural have enhanced. Hence, one can anticipate that increase in organic solvent volume may upsurge the furfural yields since more preferably it will be extracted. Therefore, a study with alteration in water to toluene ratio from 1:1 to 1:2 to 1:4 (*v/v*) keeping total solvent volume same (60 mL) was undertaken. During this process substrate/water and substrate/SAPO-44 ratio were kept constant. As expected, an improved yield of furfural (75%) was achieved by using

1:2 (*v/v*) ratio compared to 1:1 (*v/v*) ratio (63%) when reactions were done at 170°C for 8 h. However, use of 1:4 ratio showed lower furfural yields (49%).

It was proved earlier (section 3.2.1.8) that with increase in reaction time improves the furfural yield. The same understanding was applied with the best solvent ratio of 1:2 (*v/v*). Successfully, an extraordinarily high furfural yield (82%) was achieved after conducting the reaction for 10 h instead of 8 h (75%) at 170°C. Further increase in time (12 h) under similar reaction condition yields a slightly higher amount of furfural (85%). However, when reactions were carried out for longer time (13 and 14 h) furfural yields remains similar (85% and 83%, respectively).

3.2.1.11. Recycle Study

Earlier in this chapter (section 3.2.1.1), it is already proven that SAPO-44 catalyst shows stable catalytic activity in several recycle runs. However, the purpose of present study was to understand whether SAPO-44 catalyst can show similar activity under the final optimized reaction conditions or not. The final optimum reaction conditions determined to obtain best catalytic yields for furfural (82%) from oat spelt xylan are: xylan concentration of 5 *wt*% (with respect to water), SAPO-44 catalyst with S/C (*wt*/*wt*) ratio of 4, water + toluene = 1:2 (*v/v*), 2 bar N_2 pressure at *RT*, 170°C and 10 h. Hence in catalyst recycle study, these conditions were adopted. Catalyst recycle study was carried out with the recovered SAPO-44 catalyst from the earlier reaction (10 h, 82% yield). The catalyst was washed with distilled water (100 mL) and then the wet catalyst was subjected to the next reaction without any treatment. Fig. 3.18 showed that upon 8 recycle experiments SAPO-44 catalyst was offering similar activity with similar product yields (furfural = 83±1, oligomers = 2-3%, total monomer sugars = 14-16% and HMF = 2-3%). This data set revealed that a very high carbon balance of 100±2% was achieved from 100% conversion of softwood hemicellulose in all the reactions.

To understand the catalyst handling loss during processing, after 8th run SAPO-44 was recovered from the reaction mixture by centrifugation, washed with distilled water, dried first at 60°C in oven for 16 h and then in vacuum oven (10^{-3} bar) at 110°C for 6 h. Later, the dried mass was calcined at 550°C for 12 h in air using tubular furnace to obtain only catalyst. The heating rate was fixed at 1°C/min and the air flow provided

was at a rate of 10 mL/min. Now the catalyst weight loss was calculated by weight difference between initially charged catalyst (1st reaction) and catalyst recovered after 8th run (calcined). It was found that negligible amount of catalyst is lost (ca. 9%) during this processing.

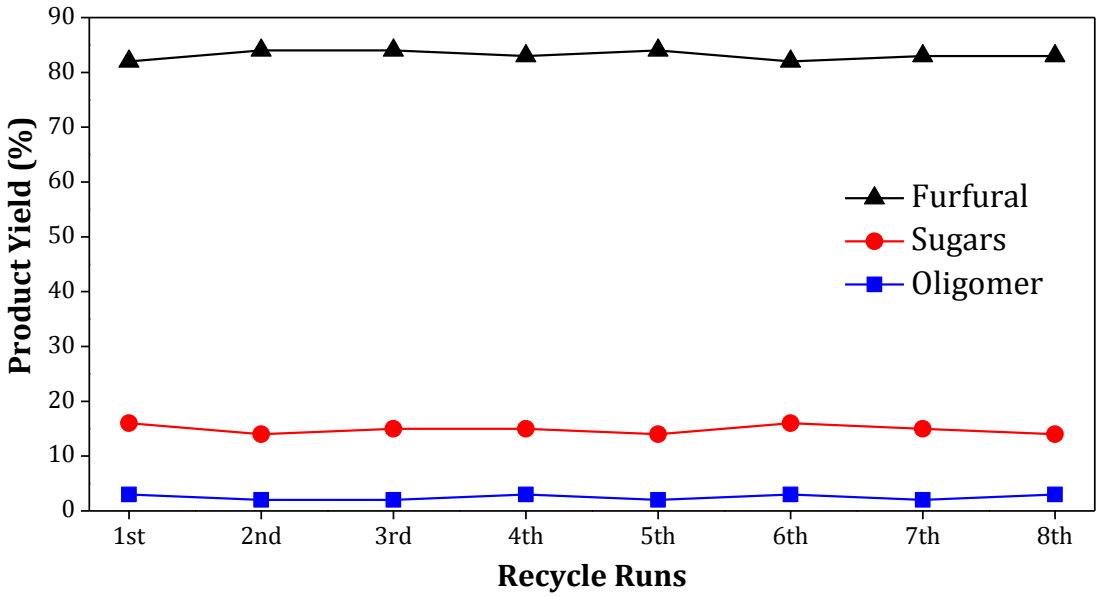

Fig. 3.18. Recycle study using SAPO-44 catalyst for oat spelt xylan conversion under optimized reaction conditions. Reaction conditions: xylan (1.0 g), catalyst (0.25 g), water + toluene = 60 mL (1:2 *v/v*), 2 bar N_2 at *RT*, 170°C, 10 h.

3.2.1.12. Processing of Variety of Hemicellulose Sources

As discussed earlier in the introduction of this chapter, several types of hemicelluloses / xylans derived from variety of sources such as oat spelt (softwood; xylose ≥70%, glucose ≤15%, arabinose ≤10%), beechwood (hardwood; xylose ≥80%) and birch wood (hardwood; xylose ≥90%) were collected. Hence, successful processing of all types of hemicelluloses under optimum conditions might provide a uniform methodology for furfural synthesis. When birch wood xylan was processed in water + toluene (1:2, *v/v*) solvent system at 170°C for 10 h (optimum conditions), 69% furfural with 4% oligomers, and 13% C_5 sugars (xylose + arabinose) yields were obtained (total carbon recovery = 86%). Under similar reaction conditions, the processing of both oat spelt derived hemicellulose and beechwood derived hemicellulose showed comparable activity (furfural yield = 82-83% with ca. 100±2% carbon balance) over SAPO-44 catalyst.

3.2.2. Use of Crop Waste (Raw Biomass)

As discussed earlier (section 2.6, chapter 2), seven different crop wastes (raw biomass) *viz.* bagasse (collected from 3 places), rice husk (collected from 3 places) and wheat straw (collected from 1 place) were collected and without any physical or chemical pre-treatment those were used directly for the synthesis of C_5 sugars and furfural. Before subjecting crop wastes as substrate in reaction, those compositions were quantified with the help of TAPPI method (for detail characterization methods and data please refer to section 2.6, chapter 2). From Table 2.6 (chapter 2), it can be seen that the pentosan content in crop wastes follows the below order,

Rice Husk (II) (11.2%) < Rice Husk (III) (12.4%) < Rice Husk (I) (15.9%) < Wheat Straw (21.4%) < Bagasse (III) (21.6%) < Bagasse (II) (24.1%) < Bagasse (I) (30.0%)

SAPO-44 was used as catalyst for the conversion crop wastes into C_5 sugars and furfural since it was proven as the best catalyst in various isolated hemicellulose conversion. In this study, first reaction conditions were optimized taking bagasse (I) as feedstock and later on all other feedstocks were screened.

3.2.2.1. Influence of Feedstock Concentrations, Reaction Time and Solvent System

For optimization of reaction parameters, bagasse (I) with 30% pentosan content was considered as feedstock for furfural synthesis. From the knowledge of isolated hemicellulose processing, the reaction temperature was set at 170°C in presence of SAPO-44 for bagasse conversion. 0.3 g bagasse (1 wt% with respect to water; same substrate concentration as isolated hemicellulose reaction) was charged to reactor along with 0.075 g SAPO-44 catalyst, water + toluene (60 mL, 1:1 *v/v*) and 2 bar N_2 pressure (at *RT*) and reaction was carried out at 170°C for 8 h. Result showed the possibility of conversion of pentosan part from bagasse to produce 79% furfural with 14% oligomers and 12% C_5 sugars (xylose + arabinose). In comparison, when bagasse reaction under similar conditions was carried out in absence of catalyst, a lower furfural yield (36%) was achieved. Later, the bagasse concentration was increased (3.33 wt% with respect to water) in the reaction system to maintain the pentosan concentration of 1 wt% (with respect to water) in reaction system keeping all other parameters same. The similar catalytic activity was observed (furfural = 82%, oligomer = 11%, xylose +

arabinose = 10%). Further increase in bagasse concentration to 5 wt% also yield similar amount of furfural (80%). However, bagasse has very high water absorption tendency and hence, when 5 wt% bagasse was used, it absorbs reaction water completely leaving semi-solid type mass which is very difficult to stir. So afterwards, crop waste concentration was taken as 3.33 wt%.

Studies on influence of reaction time in desired product formation from bagasse conversion were carried out at 170°C in presence of SAPO-44 catalyst in water + toluene (60 mL, 1:1 *v/v*) solvent and the results are shown in Fig. 3.19. A maximum furfural yield (82%) can be attained at 8 h reaction. Reaction carried out for lesser time (4 h and 6 h) yields lower amount of furfural (52% and 71%, respectively) while, longer reaction time (10 h) doesn't affect furfural yields (83%).

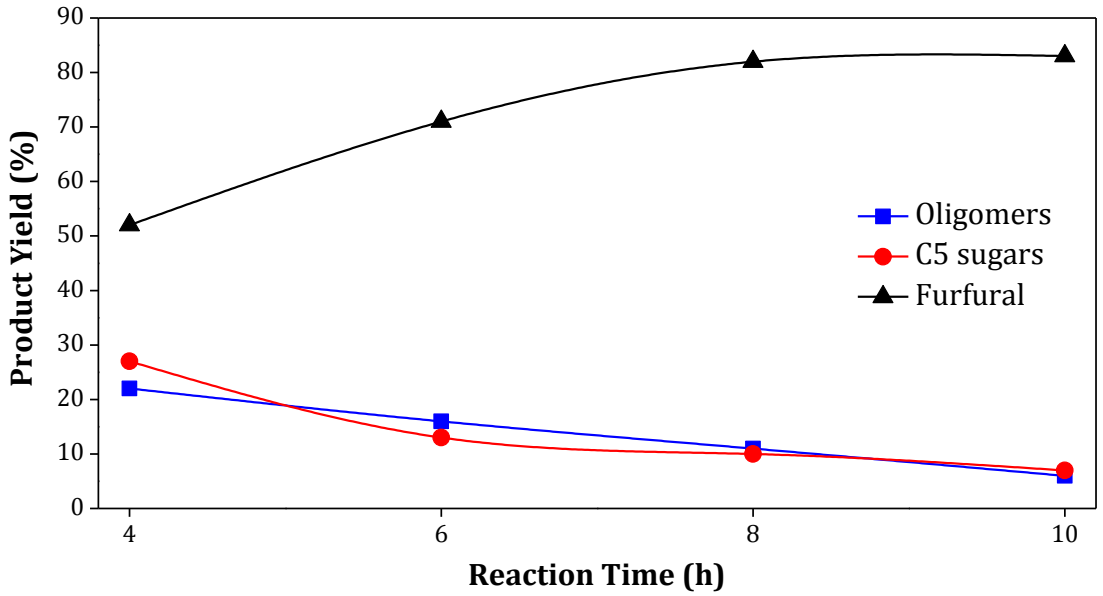

Fig. 3.19. Influence of reaction time on product distribution from bagasse conversion. Reaction conditions: bagasse (I) (1 g; 3.33 wt%), SAPO-44 (0.075 g), water + toluene = 60 mL (1:1 *v/v*), 2 bar N_2 at *RT*, 170°C.

From the earlier study with isolated hemicellulose (section 3.2.1.10, chapter 3), it is understood that use of higher proportion of toluene (best extracting solvent) improves furfural yield. So, in this study also the same concept was adopted. Reactions were carried out with 3.33 wt% bagasse (with respect to water) in water + toluene (60 mL, 1:2 *v/v*) in presence of SAPO-44 catalyst at 170°C, 8 h. An extraordinarily high furfural yield (93%) was achieved with 6% oligomer and 5% xylose + arabinose.

3.2.2.2. Concept of Selective Pentosan Conversion from Bagasse

When bagasse was treated under the optimum reaction conditions, it was found that minimal amount of C_6 derived products *viz.* glucose (7%), fructose (11%) and HMF (2%) were also formed along with oligomers, C_5 sugars and furfural. The origin of these compounds can be attributed to the conversion of some cellulose part of bagasse under the reaction conditions. To confirm this, separately, reaction was carried out with isolated cellulose (microcrystalline) under reaction conditions and the results showed 20% cellulose conversion with total product yield of 18%. The conversion of cellulose was further confirmed with the XRD analysis of fresh and recovered bagasse (along with catalyst) after reaction. Basically, the XRD showed the amorphous (2θ = 15.8°) and crystalline (2θ = 22.1°) peaks for cellulose. The assigned peaks in XRD patterns (Fig. 3.20) were for the presence of SAPO-44 catalyst in recovered bagasse. The decrease in intensity for cellulose crystalline peak (2θ = 22.1°) from 660 unit (fresh bagasse) to 547 unit (recovered bagasse) was observed in XRD pattern (Fig. 3.20) which confirmed that some part of cellulose is converted under reaction conditions. For calculation of peak intensity of recovered bagasse the dilution of cellulose peak intensity due to presence of catalyst in recovered bagasse was neglected since minute amount of catalyst was present compared to cellulose amount. Also it is evident that the maximum part (amorphous and crystalline) of cellulose was not converted. This in turn allowed commenting that the reaction conditions employed can selectively convert pentosan part of bagasse leaving other component intact.

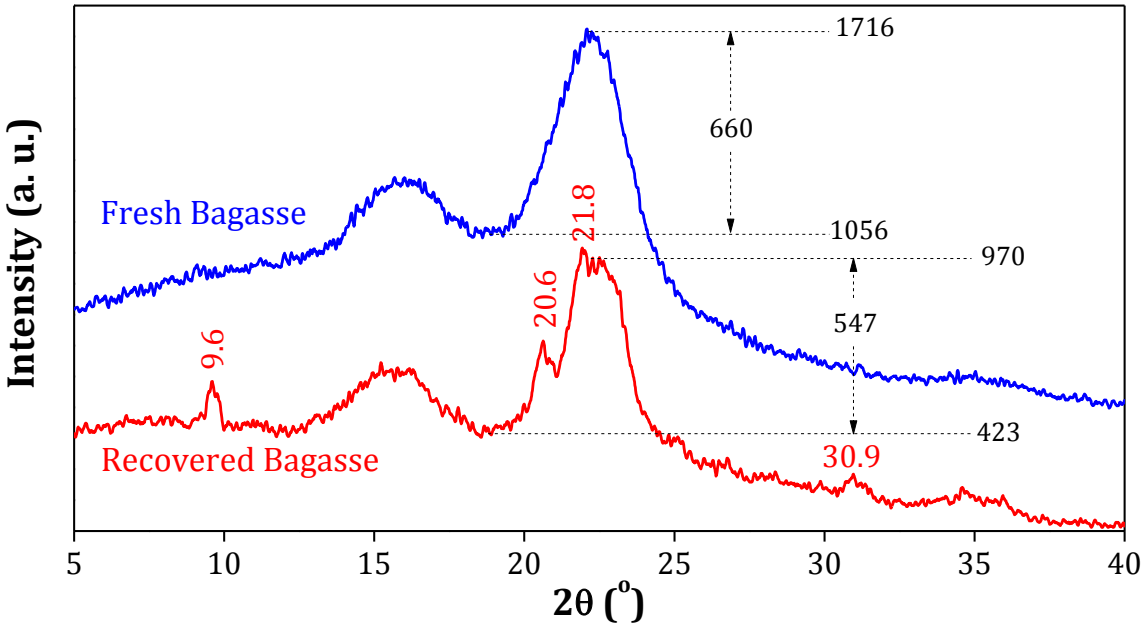

Fig. 3.20. XRD patterns for fresh and recovered bagasse (along with SAPO-44 catalyst). The assigned peaks are corresponds to SAPO-44 catalyst phase remained with recovered bagasse after reaction.

3.2.2.3. Various Crop Waste Conversions Using SAPO-44 Catalyst

The optimized reaction conditions [substrate concentration (3.33 wt% with respect to water), SAPO-44 (0.05 g), water + toluene (60 mL, 1:2 *v/v*), 2 bar N_2 pressure at *RT*, 170°C, 8 h] acquired from the bagasse (I) reactions was then employed for the processing of other crop wastes. Under the reaction conditions, all the substrates converted to furfural (86-93±1%) selectively (Fig. 3.21). The results demonstrated the capability of SAPO-44 catalyst to process un-purified (non-isolated) pentosan (hemicellulose) from raw biomass to furfural in high yields and selectivity.

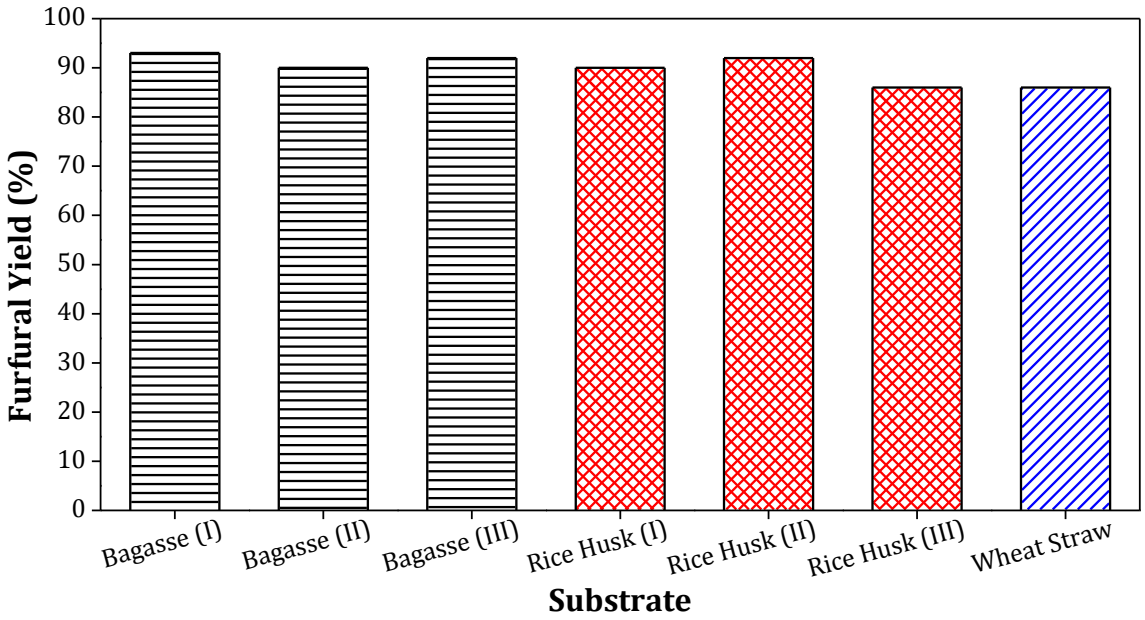

Fig. 3.21. Utilization of pentosan part from un-treated crop wastes. Reaction conditions: substrate (0.67 g; 3.33 wt%), SAPO-44 (0.05 g), water + toluene = 60 mL (1:2 *v/v*), 2 bar N_2 at *RT*, 170°C, 8 h.

3.2.2.4. Recycle Study of SAPO-44 Catalyst

To check SAPO-44 stability and activity while using real substrates, recycle study was undertaken. For this study, SAPO-44 from earlier reaction was recovered and used in the next run after calcination at 550°C for 12 h (for details see section 2.7.1.3 in chapter 2). Briefly, the recovered catalyst + unreacted solid was separated from the reaction mixture, washed with distilled water and dried (Lab oven: 60°C, 16 h; vacuum oven: 150°C, 6 h, 10^{-3} bar). Later the dried mass was subjected to calcination at 550°C for 12 h in presence of air (flow rate = 10 mL/min) to remove all the unreacted biomass part. Finally this calcined catalyst was used in recycle runs. As a representative, bagasse (I), rice husk (I) and wheat straw were evaluated as substrates for recycle runs. It is apparent from Fig. 3.22 that the SAPO-44 catalyst showed more or less matching activity at least in 8 cycles even with different crop wastes. This clearly emphasizes the fact that SAPO-44 catalyst is very robust and stable under the reaction conditions.

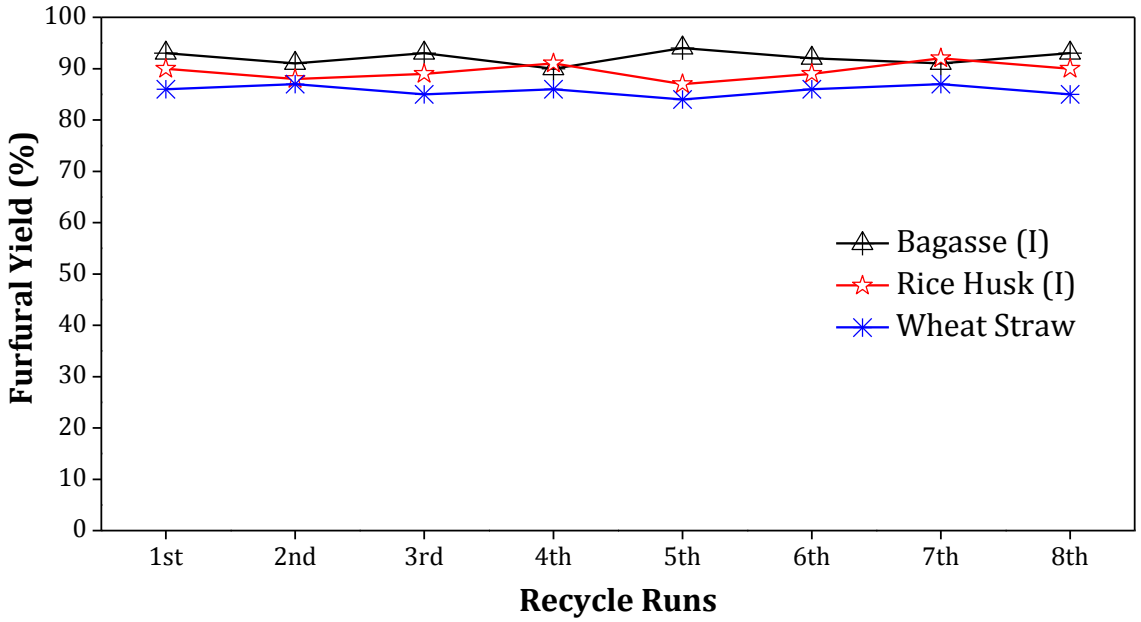

Fig. 3.22. Recycle study of SAPO-44 catalyst used in crop waste reaction. Reaction conditions: substrate (0.67 g), SAPO-44 (recycle quantity, approx. 0.05g), water + toluene = 60 mL (1:2 *v/v*), 2 bar N_2 at *RT*, 170°C, 8 h.

3.2.2.5. Isolation of Furfural

It was shown that in presence of SAPO-44 catalyst under the reaction conditions a very high furfural yield was possible from variety of substrates. Now, it is important to develop an isolation process for furfural from reaction mixture in pure form. To isolate furfural from reaction mixture the following methodology was used.

First toluene layer containing furfural was separated from reaction mixture (water + toluene) using separating funnel. Due to lower boiling temperature (b. p. = 110.6°C) of toluene compared to furfural (b. p. = 161.7°C), toluene was easily evaporated from reaction solution (toluene phase) using rotary evaporator leaving semi-solid material. Now, the semi-solid obtained was characterized with ^{1}H and ^{13}C NMR spectroscopy. The NMR data presented in Fig. 3.23 confirms the formation of furfural in pure form. Later, the isolated yield of furfural was calculated as 79% with an error of ±2% (in repeated attempts) considering total furfural yield in the reaction as 100%.

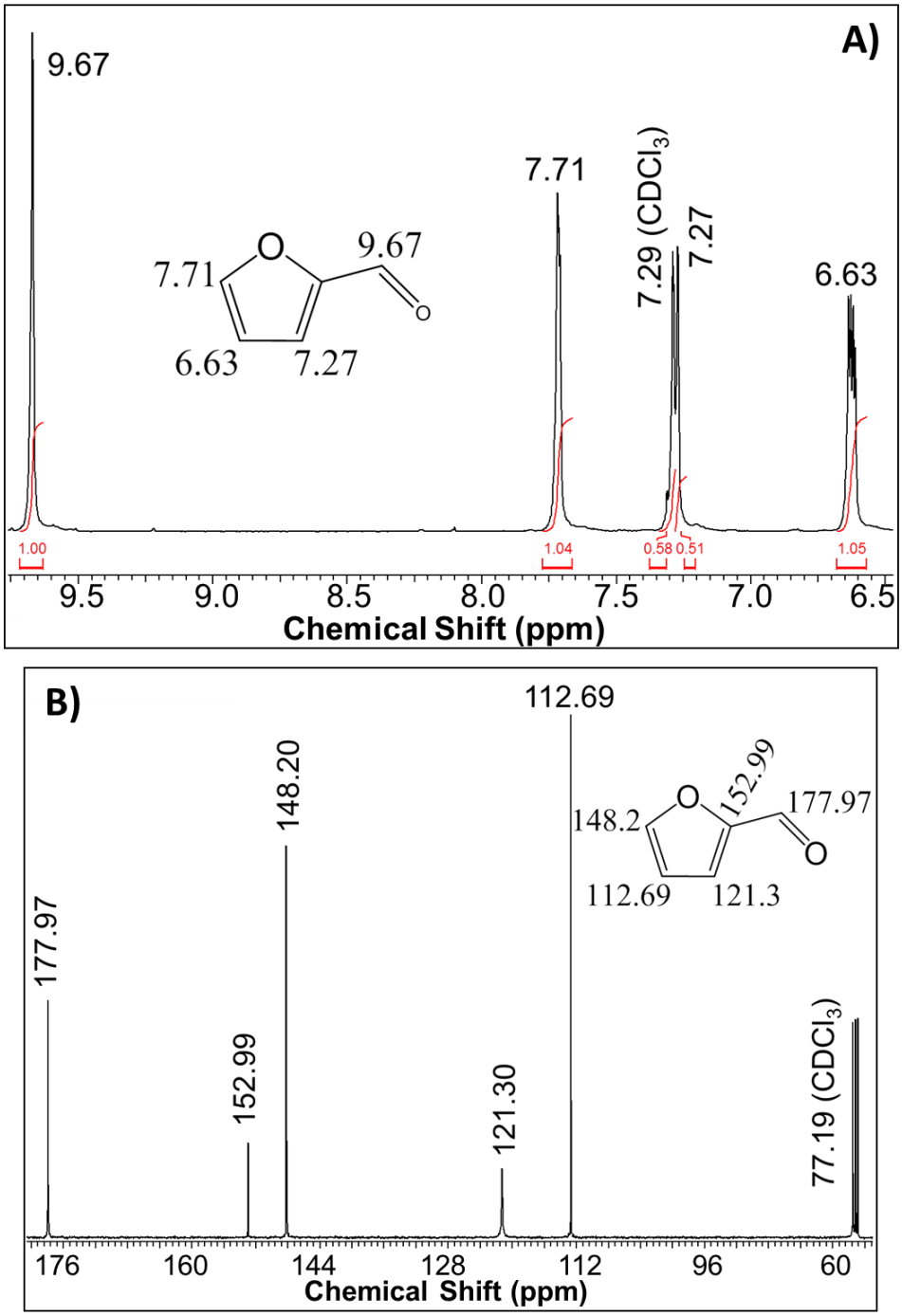

Fig. 3.23. NMR spectra for isolated furfural from reaction mixture. A) ^{1}H NMR, B) ^{13}C NMR.

3.3. Catalyst Characterizations: Fresh and Spent SAPO-44

From the recycle study of SAPO-44 catalyst, it was now confirmed that SAPO-44 was capable of providing similar activity in several runs with all types of substrates *viz.*

isolated hemicellulose and various crop wastes. To support further the stability of SAPO-44 catalyst, various characterization methods were used to check the state of spent (recovered) SAPO-44 catalyst.

3.3.1. XRD Analysis

XRD patterns for spent SAPO-44 catalysts recovered from the isolated hemicellulose reactions indicated the presence of all the peaks corresponding to CHA morphology as were seen in fresh SAPO-44 catalyst[6] and that the intensity of peaks were almost same (Fig. 3.24). This data confirmed the structural stability of SAPO-44 on bulk level. Further, XRD patterns were collected for spent SAPO-44 catalyst used in raw biomass reactions (Fig. 3.24). Before analysis all spent SAPO-44 catalyst used in raw biomass reactions were calcined at 550°C for 12 h in air flow (10 mL/min) to remove unreacted part of biomass. CHNS analysis data confirmed the absence of carbon residue in spent catalyst after calcination. This suggests that all the unreacted biomass part is burnt off during calcination in air atmosphere. It was observed that bagasse doesn't affect much on the crystallinity of SAPO-44 however, due to the presence of high SiO_2 content (ash, 12.4-18.6%) in rice husk and wheat straw (Table 2.6, chapter 2) a slight hump (amorphous silica peak) between 2θ = 19-24° was observed. This data further approved the stability of SAPO-44.

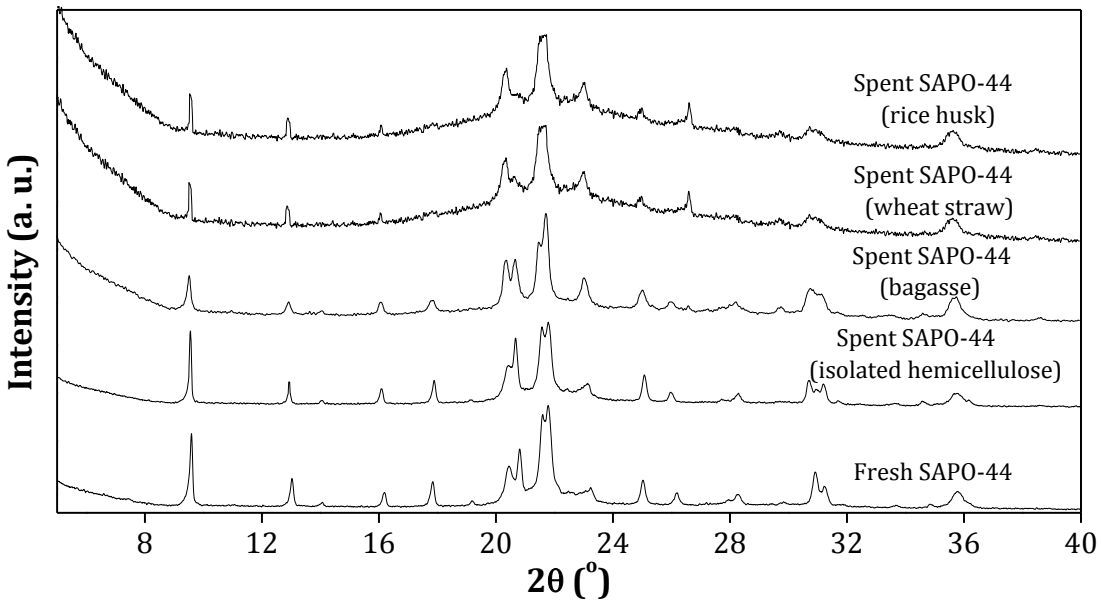

Fig. 3.24. XRD patterns of fresh and spent SAPO-44 used in presence of various substrates.

3.3.2. Solid State NMR Analysis

Solid state ^{29}Si, ^{27}Al and ^{31}P MAS NMR spectra further corroborate the structural stability of SAPO-44 [Fig. 3.25. A), B), C)]. In ^{29}Si NMR, both fresh and spent SAPO-44 (used in isolated hemicellulose reaction) showed the peaks corresponding to Q^0 [Si(4Al)], Q^1 [Si(3Al)], Q^2 [Si(2Al)], Q^3 [Si(1Al)] and Q^4 [Si(0Al)] species at –92.4, –96.2, –101.7, –107.7 and –112.8 ppm, respectively with comparable intensity. All the peak patterns matches well with the literature.[31] The more detail discussions on ^{29}Si NMR spectral patterns of fresh SAPO-44 is made in section 2.5.2, chapter 2. The presence of only a sharp single peak with similar intensity at 38.2 ppm in ^{27}Al NMR is the indicative for the tetrahedral Al environment in both fresh and spent SAPO-44 (isolated hemicellulose reaction). Beside this sharp peak, another small peak at -15 ppm due to the presence of octahedral Al is observed in both fresh and spent catalysts. Similar ^{27}Al NMR spectral pattern was also reported earlier in literature.[31] ^{31}P NMR spectra also approves the SAPO-44 structural stability as only tetrahedral environment for P is observed in both fresh and spent catalyst (used in isolated hemicellulose reaction). The peak corresponding to -31.5 ppm is due to the existence of P[4Al] environment in SAPO-44 framework. The ^{27}Al NMR spectral pattern also matches well with literature report.[31] Presence of additional SiO_2 (ash; Table 2.6, chapter 2) in raw biomass affects the solid state NMR spectra of spent catalyst so it was difficult to confirm the structural stability of SAPO-44 in these reactions by using NMR technique.

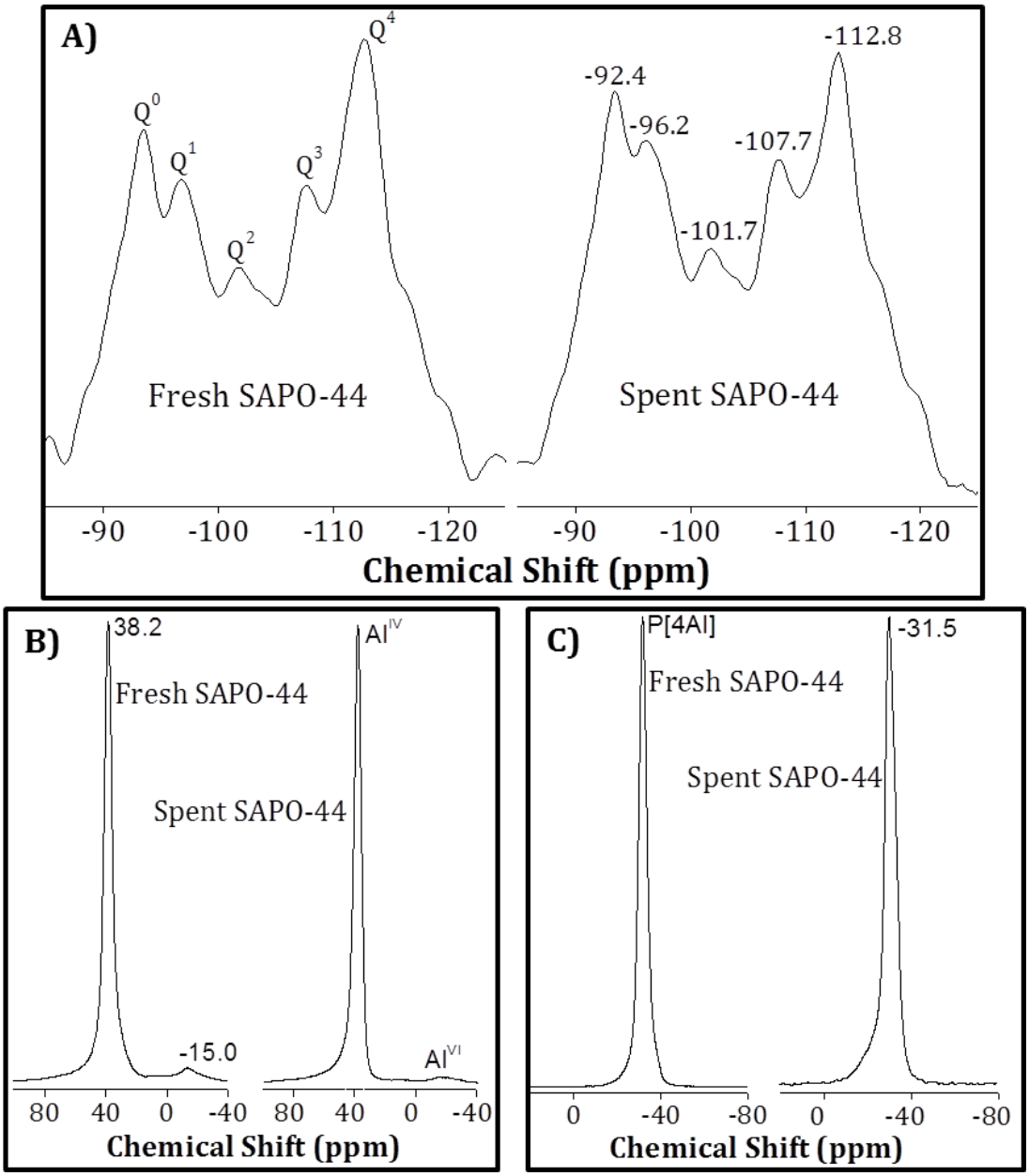

Fig. 3.25. Solid state MAS NMR spectra of fresh and spent SAPO-44 used in isolated hemicellulose reaction. A) ^{29}Si NMR, B) ^{27}Al NMR, C) ^{31}P NMR.

3.3.3. TPD-NH_3 and N_2 Sorption Analysis

Before these analysis spent SAPO-44 was subjected for calcination at 550°C for 12 h in presence of air flow (10 mL/min) to remove the unreacted part of biomass. The acid amount value and acid amount distribution of fresh and spent SAPO-44 catalyst used with all crop waste samples is shown in Table 3.6. It can be seen that the total acid amount (1.2 mmol/g) present in fresh SAPO-44 catalyst remains almost preserved (1.1-

1.2 mmol/g) in all spent SAPO-44 catalysts. Furthermore, the weak and strong acid sites are distributed similarly in fresh and spent SAPO-44 catalysts. It is important to note here that crop waste contains silica (ash) material and hence for the calculation of acid amount in spent SAPO-44 catalysts used in crop waste reactions, silica correction† was done.

---

†Silica correction calculation in TPD-NH_3 analysis of spent SAPO-44 catalyst used with rice husk (I):

Rice husk (I) contains 15.7% of silica (ash) as shown in chapter 2, Table 2.6.

For reaction 0.67 g rice husk is used; it consists (0.67 × 0.157) = 0.1052 g silica.

SAPO-44 used in reaction = 0.05 g

So total weight of recovered SAPO-44 + silica (after calcination at 550°C) = 0.1552 g

Now, the TPD-NH_3 analysis results obtained with recovered solid (0.1552 g) was.

Weak acid amount = 0.034 mmol and strong acid amount = 0.022 mmol

Hence, the final silica corrected acid amount calculation will be

Weak acid amount = (0.034/0.05) = 0.68 mmol/g of catalyst ≈ 0.7 mmol/g

Strong acid amount = (0.022/0.05) = 0.44 mmol/g of catalyst ≈ 0.4 mmol/g

Total acid amount = 1.1 mmol/g

Table 3.6. TPD-NH_3 and N_2 sorption analysis data for fresh and spent SAPO-44 catalysts used in reaction with various substrates.

Catalyst	Acid amount (mmol/g)			Surface area (m^2/g)	Pore size (nm)
	Weak (100-250°C)	Strong (350-500°C)	Total		
Fresh SAPO-44	0.7	0.5	1.2	369	0.45
Spent SAPO-44 (isolated hemicellulose)	0.6	0.5	1.1	359	0.48
Spent SAPO-44 (bagasse)	0.6	0.6	1.2	351	0.46
Spent SAPO-44 (rice husk)	0.7	0.4	1.1	n.d.	n.d.
Spent SAPO-44 (wheat straw)	0.6	0.5	1.1	n.d.	n.d.

n.d. stands for analysis not done.

N_2-sorption study confirmed that the surface area of SAPO-44 was approximately same even after use in either isolated hemicellulose or real biomass reactions (Table 3.6). Consequently, almost similar pore size for SAPO-44 was also observed in all the cases (Table 3.6). This data further proved that the SAPO-44 is a very stable catalyst under the reaction conditions.

3.3.4. ICP-OES and SEM-EDX Analysis

In most of the cases reported earlier, the catalyst undergoes deactivation under reaction condition due to leaching of its active species. Therefore, the possibility of Al and/or P leaching out in the solution during the reaction was examined by subjecting fresh and spent SAPO-44 catalyst and reaction solution to ICP-OES analysis (for detail procedure please refer section 2.5.8, chapter 2). Here, the spent SAPO-44 recovered from raw biomass reactions were not analyzed since presence of silica and nutrients might influence the analysis to show complicated results. Data presented in the Table 3.7 confirmed that the composition of spent SAPO was not altered from fresh samples. Further to reconfirm this result, ICP-OES characterization of reaction solution was carried out however, the presence of Al or P was not detected (Table 3.7). This again augmented the claim that catalysts are stable under reaction conditions.

Table 3.7. Elemental analysis of fresh and spent SAPO-44 catalyst used in isolated hemicellulose reaction.

Catalyst	ICP-OES analysis (ppm)		SEM-EDX analysis (atom%)		
	Al	P	Si	Al	P
Fresh SAPO-44	22.5 (22.8)†	24.6 (26.0)†	22.9	37.9	39.2
Spent SAPO-44	24.7	25.1	24.6	36.9	38.5
Reaction mixture	0	0	n.d.	n.d.	n.d.

† The data given in bracket indicate theoretical value (for detail calculation please see chapter 2, section 2.5.8). n.d. stands for analysis not done.

To claim further stability of catalyst, SEM images of both fresh and spent SAPO-44 catalysts were taken. Fig. 3.26 showed the similar cubic morphology for spent SAPO-44 catalyst used in isolated hemicellulose reaction as like fresh SAPO-44 catalyst. The cube edge measured for fresh (3.13 μm) and spent (3.16 μm) SAPO-44 catalyst were

also similar. SEM characterization coupled with EDX microanalysis was carried out for fresh and spent SAPO-44 and it was found that similar atomic weight percentage of Si, Al and P were present in both the fresh and spent SAPO-44 (Table 3.7). Based on this elemental composition data, framework composition was calculated as, $(Si_{0.24}Al_{0.40}P_{0.36})O_2$ in fresh SAPO-44 and $(Si_{0.25}Al_{0.39}P_{0.36})O_2$ in spent SAPO-44. These analyses gave unambiguous evidence that SAPO-44 catalyst is highly stable catalysts. Earlier report also showed that similar framework composition of SAPO-44 catalyst as $(Si_{0.27}Al_{0.38}P_{0.35})O_2$.[31] Furthermore, SEM images of spent SAPO-44 used in raw biomass reactions were checked (Fig. 3.26). SEM image of SAPO-44 used in bagasse reaction showed the similar cubic morphology with edge length of 3.02 μm however, that of rice husk and wheat straw reaction showed cubic morphology (edge length = 2.89-3.21 μm) with a lot of amorphous silica which basically contributed from raw biomass.

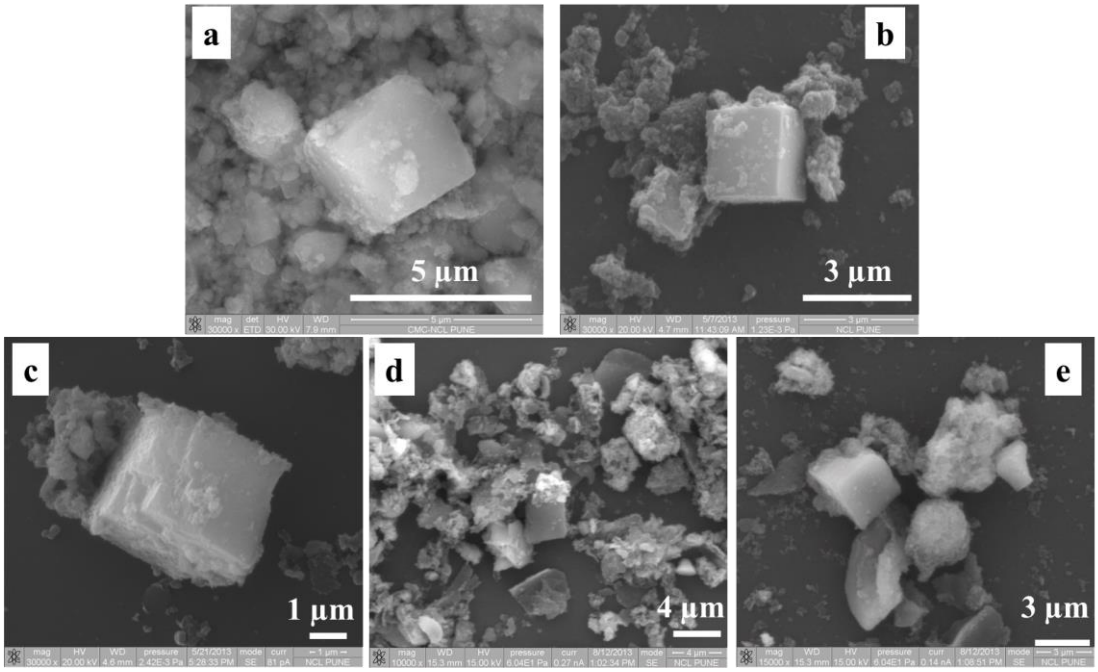

Fig. 3.26. SEM images of fresh and spent SAPO-44 catalysts used with various substrates. a. fresh SAPO-44, b. spent SAPO-44 (isolated hemicellulose), c. spent SAPO-44 (bagasse), d. spent SAPO-44 (rice husk), e. spent SAPO-44 (wheat straw).

3.4. Conclusions

In summary, abundant and inexpensive non-edible isolated hemicelluloses derived from softwood and hardwood was shown to be converted using several solid acid catalysts.

Presence of the best active catalyst, SAPO-44 and biphasic system (water + toluene) with 1:2 *v/v* ratio works well to give a maximum of 85% furfural yield in a one-pot method at 170°C. It was demonstrated that due to higher hydrophilicity of SAPO catalysts compared to zeolites, SAPO exhibit better catalytic activity by minimizing side reactions. Also it was proven that presence of strong acid sites in catalyst boost up the furfural formation. Several synthesis parameters for SAPO-44 were optimized to obtain a better active catalyst for furfural synthesis. Furthermore, a highly efficient one-pot pathway is shown to process the non-isolated hemicellulose (pentosan) part of raw biomass (bagasse, rice husk & wheat straw) directly to furfural with an extraordinarily high yield of 86-93%. The direct processing of raw biomass without any additional treatment into a very high yield of furfural was thus nullified the need to isolate hemicellulose from raw biomass in a separate process and also obtaining xylose in another reactor from hemicellulose. Stability of SAPO-44 was checked in presence of all the substrates by carrying out recycle reactions and it was found that similar furfural yield was possible in minimum eight recycle runs. Additionally, it is substantiated that SAPO-44 catalyst was highly stable under reaction conditions by subjecting the same to various physico-chemical characterizations. A methodology is shown to recover formed furfural from reaction mixture and further its purity was confirmed with the help of NMR spectroscopy.

Here, I wish to comment further on the issue raised at the introduction in this chapter regarding problems with the current literature reports for synthesis of C_5 sugars and furfural and how far I have succeeded to resolve them.

- One-pot processing of various non-edible hemicelluloses and direct crop wastes (raw biomass) was shown for furfural synthesis. This developed process will overcome the problem with use of edible sugars.

- In this work, SAPO-44 catalyst was proven as a robust catalyst with the help of several physico-chemical characterizations although it is structured.

- Well recyclability of SAPO-44 catalyst minimum up to 8 runs was shown in presence of either isolated hemicellulose or un-treated crop wastes.

- An extraordinarily high and selective furfural yield was demonstrated directly from various non-edible feedstocks.
- A suitable and easy recovery process was shown for furfural and the process assured the isolation of furfural in purest form.

Finally, now it is safe to say that by developing the process for furfural synthesis using SAPO-44 catalyst I have tried to overcome almost all the problems associated with earlier systems.

3.5. References

(1) Kobayashi, H.; Fukuoka, A. *Green Chem.* **2013**, *15*, 1740.
(2) Dutta, S.; De, S.; Saha, B.; Alam, M. I. *Catal. Sci. Technol.* **2012**, *2*, 2025.
(3) Gallezot, P. *Chem. Soc. Rev.* **2012**, *41*, 1538.
(4) Hu, L.; Zhao, G.; Hao, W.; Tang, X.; Sun, Y.; Lin, L.; Liu, S. *RSC Adv.* **2012**, *2*, 11184.
(5) Dutta, S. *RSC Adv.* **2012**, *2*, 12575.
(6) Ashtekar, S.; Chilukuri, S. V. V.; Chakrabarty, D. K. *J. Phy. Chem.* **1994**, *98*, 4878.
(7) Bhaumik, P.; Dhepe, P. L. *ACS Catal.* **2013**, *3*, 2299.
(8) Bhaumik, P.; Dhepe, P. L. *RSC Adv.* **2014**, *4*, 26215.
(9) Sahu, R.; Dhepe, P. L. *ChemSusChem* **2012**, *5*, 751.
(10) Nikolla, E.; Leshkov, Y. R.; Moliner, M.; Davis, M. E. *ACS Catal.* **2011**, *1*, 408.
(11) Bhaumik, P.; Dhepe, P. L. *RSC Adv.* **2013**, *3*, 17156.
(12) Bandura, A. V.; Lvov, S. N. *J. Phy. Chem. Ref. Data* **2006**, *35*, 15.
(13) Okuhara, T. *Chem. Rev.* **2002**, *102*, 3641.
(14) Zhuang, J.; Ma, D.; Yang, G.; Yan, Z.; Liu, X.; Liu, X.; Han, X.; Bao, X.; Xie, P.; Liu, Z. *J. Catal.* **2004**, *228*, 234.
(15) Dow Water & Process Solutions, Dow Chemical Company; http://www.dowwaterandprocess.com/en/products/a/amberlyst_15wet.
(16) Liu, Y.; Lotero, E.; Goodwin Jr, J. G. *J. Catal.* **2006**, *242*, 278.
(17) van Zandvoort, I.; Wang, Y.; Rasrendra, C. B.; van Eck, E. R. H.; Bruijnincx, P. C. A.; Heeres, H. J.; Weckhuysen, B. M. *ChemSusChem* **2013**, *6*, 1745.
(18) Patil, S. K. R.; Lund, C. R. F. *Energy Fuels* **2011**, *25*, 4745.
(19) Girisuta, B.; Janssen, L. P. B. M.; Heeres, H. J. *Green Chem.* **2006**, *8*, 701.
(20) Lok, B. M.; Messina, C. A.; Patton, R. L.; Gajek, R. T.; Cannan, T. R.; Flanigen, E. M. *J. Am. Chem. Soc.* **1984**, *106*, 6092.
(21) Corma, A. *Chem. Rev.* **1995**, *95*, 559.
(22) Alemdaroglu, T. *Commun. Fac. Sci. Univ. Ank. Series B* **2001**, *47*, 27.
(23) Wang, Y.; Gong, X.; Wang, Z.; Dai, L. *J. Mol. Cat. A: Chem.* **2010**, *322*, 7.
(24) Wang, H.; Frenklach, M. *Combust. Flame* **1994**, *96*, 163.
(25) Boumaza, A.; Favaro, L.; Ledion, J.; Sattonnay, G.; Brubach, J. B.; Berthet, P.; Huntz, A. M.; Roy, P.; Tetot, R. *J. Solid State Chem.* **2009**, *182*, 1171.
(26) Meng, X.; Xiao, F. S. *Chem. Rev.* **2014**, *114*, 1521.

(27) Martens, J. A.; Mertens, M.; Grobet, P. J.; Jacobs, P. A. In *Studies in Surface Science and Catalysis*; Grobet, P. J., Mortier, W. J., Vansant, E. F., Schulz-Ekloff, G., Eds.; Elsevier: 1988; Vol. 37, p 97.
(28) Sauer, J.; Horn, H.; Haser, M.; Ahlrichs, R. *Chem. Phy. Lett.* **1990**, *173*, 26.
(29) *Theoretical Aspects of Heterogeneous Catalysis*; Nascimento, M. A. C., Ed.; Kluwer Academic, Springer: The Netherlands, 2002; Vol. 8.
(30) Young, D.; Davis, M. E. *Zeolites* **1991**, *11*, 277.
(31) Prakash, A. M.; Unnikrishnan, S.; Rao, K. V. *Appl. Catal. A: Gen.* **1994**, *110*, 1.
(32) Karinen, R.; Vilonen, K.; Niemela, M. *ChemSusChem* **2011**, *4*, 1002.
(33) Agirrezabal-Telleria, I.; Requies, J.; Guemez, M. B.; Arias, P. L. *Green Chem.* **2012**, *14*, 3132.
(34) O'Neill, R.; Ahmad, M. N.; Vanoye, L.; Aiouache, F. *Ind. Eng. Chem. Res.* **2009**, *48*, 4300.
(35) Hargreaves, C. R.; Zeneca, A.; Manley, J. B. *Collaboration to deliver a solvent selection guide for the pharmaceutical industry, ACS GCI phermaceutical roundtable*, American Chemical Society, USA, 2008.

CHAPTER-4

AMORPHOUS CATALYSTS: SiO_2 & ZrO_2 SUPPORTED METAL OXIDES IN THE CONVERSION OF CROP WASTES TO C_5 SUGARS & FURFURAL

4.1. Introduction

In this chapter I will discuss about the development of amorphous solid acid catalysts without having definite structure (channel structure, pore diameter), so that the problem associated with the structured catalysts (definite channel structure, definite pore diameter) as reported earlier[1] can be avoided. Although, in earlier chapter (chapter 3), it is shown that the structured catalysts, SAPO's can be successfully used in the hemicellulose and crop waste conversion reaction[2,3] but, at the beginning of the work my objectives were set to develop stable structured and amorphous catalysts. A range of supported metal oxide catalysts having acidic property were synthesized by wet-impregnation (WI) and sol-gel (SG) method (details on synthesis procedure and characterizations data are provided in section 2.4 and 2.5, chapter 2). Two support materials *viz.* silica (SiO_2) and zirconia (ZrO_2) were used for the synthesis of catalysts. Various metals are used such as tungsten, molybdenum, gallium, boron and phosphorous for synthesis of 10 *wt*% WO_3/SiO_2, MoO_3/SiO_2, Ga_2O_3/SiO_2, WO_3/ZrO_2, MoO_3/ZrO_2, Ga_2O_3/ZrO_2, B_2O_3/SiO_2 and P_2O_5/SiO_2 catalyst either by WI method or by SG method. For easy identification of catalysts preparation method, in this chapter, I have used nomenclature as WO_3/SiO_2 (WI) for 10 wt% tungsten oxide supported on silica using wet-impregnation method, WO_3/SiO_2 (SG) for 10 wt% tungsten oxide supported on silica using sol-gel method and so on.

Further, those catalysts were screened for furfural synthesis from various substrates *viz.* xylose, isolated hemicelluloses and crop wastes (bagasse: collected from 3 places, rice husk: collected from 3 places and wheat straw: collected from 1 place; section 2.6, chapter 2).[4] The reaction pathway of synthesis of C_5 sugars (xylose + arabinose) and furfural from various substrates is shown in Scheme 4.1. Moreover, a thorough optimization of reaction conditions is presented to obtain the highest possible amount of furfural. Furthermore, effort is given to understand the properties of supported metal oxide catalysts which are playing a major role in deciding the product distribution. Additionally, to realize the state of catalyst after reaction, detailed characterizations were undertaken.

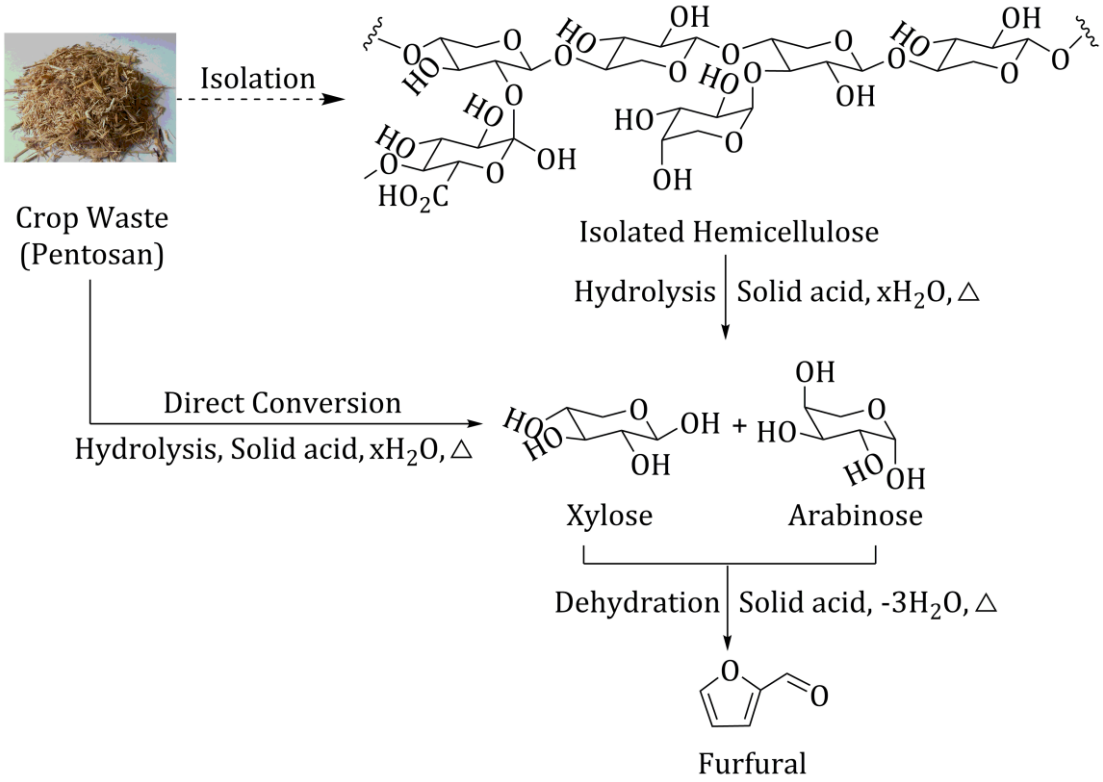

Scheme 4.1. Pathway for the synthesis of furfural from various substrates. The work indicated by dotted arrow is not done by me.

4.2. Results and Discussions

Initial screening of supported metal oxide catalysts synthesized by WI and SG method was carried out with the use of C_5 sugar, xylose as substrate. Later, all other substrates (isolated hemicelluloses and crop wastes) were utilized.

4.2.1. Xylose to Furfural: All Synthesized Catalysts

It is well-known that xylose is a simplest substrate for furfural synthesis through dehydrocyclization reaction ($-3H_2O$).[5-10] Hence, in this work, xylose was used as a substrate in presence of all the synthesized supported metal oxides. Although, xylose is an edible sugar but the purpose of using it as a substrate was to identify the active catalyst among all catalysts. All the catalysts *viz.* WO_3/SiO_2 (WI, SG), MoO_3/SiO_2 (WI, SG), Ga_2O_3/SiO_2 (WI, SG), WO_3/ZrO_2 (SG), MoO_3/ZrO_2 (SG), Ga_2O_3/ZrO_2 (SG), SiO_2 and ZrO_2 were screened for xylose to furfural reaction.

Fig. 4.1 summarizes the catalytic results of all the synthesized catalysts for the production of furfural from xylose at 170°C, 8 h in water + toluene (1:1 *v/v*). The solvent system, water + toluene is used directly in this work, since in chapter 3 (section 3.2.1.10) it was shown that toluene has a better tendency (partition coefficient, miscibility, LCA value) to extract furfural from water phase where acid catalysts are present and hence, suppression of side reactions is possible. It was evident that all the silica supported metal oxides synthesized by SG method showed good catalytic activity for furfural formation (yield = 50-59%) compared to WI method (furfural yield = 35-39%). Besides furfural, 5±2% oligomers (condensation products) and 4±3% arabinose formation was also observed with silica supported SG catalysts (WO_3/SiO_2, MoO_3/SiO_2 and Ga_2O_3/SiO_2) and this leads to a total of ca. 72% product yield with 70-75% xylose conversion.

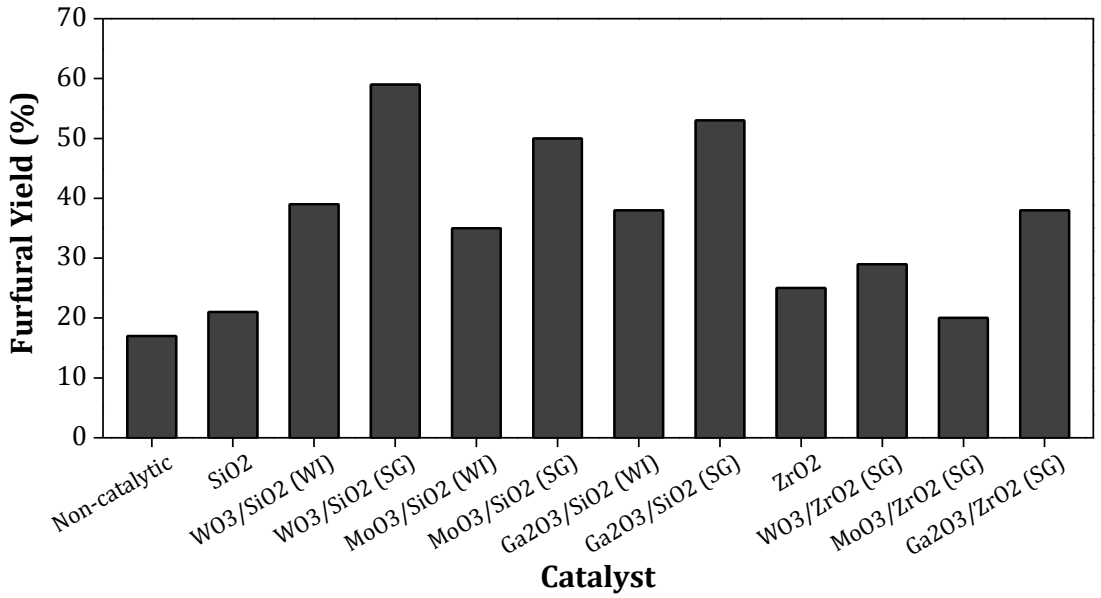

Fig. 4.1. Xylose conversion to furfural in presence of supported metal oxide catalysts. Reaction condition: xylose (0.3 g), catalyst (0.075 g), water + toluene = 60 mL (1:1 *v/v*), 2 bar N_2 at *RT* (~9 bar N_2 at 170°C), 170°C, 8 h.

In literature, it is discussed that the presence of Lewis acid centers in Sn-beta (zeolite) catalyst promotes xylose isomerization reaction into xylulose (xylo-ketose) and next, presence of Brönsted or Lewis acid sites can catalyze xylulose dehydration into furfural (Scheme 4.2).[11,12] But in this reaction system xylulose was not detected although, metal oxide catalysts have mainly Lewis acid sites proved by pyridine probed

IR characterizations (Fig. 2.7, section, 2.5.3, chapter 2). This might be because of quick conversion of xylulose into furfural under the reaction conditions since in literature it is shown that xylulose to furfural dehydration reaction occurs with faster rate (Ea = 23.1 kcal/mol) compared to xylose conversion reaction (Ea ≈ 30-32 kcal/mol).[12] However, another possibility is that there might be some fraction of xylulose was present in reaction system but unfortunately I was unable to detect those since xylulose standard was not available with me. Yet, I have not observed any extra peak in HPLC analysis. Compared to this, non-catalytic and only SiO_2 catalyzed reactions yield lower amount of furfural (17% and 21% respectively) due to absence of significant amount of acid sites in reaction system as like catalytic system. However, under these systems, reactions are mainly driven by thermal pathway due to increase in dissociation of water at higher temperatures (pK_w value of water = 13.99 at 25°C and 11.64 at 150°C).[1,13]

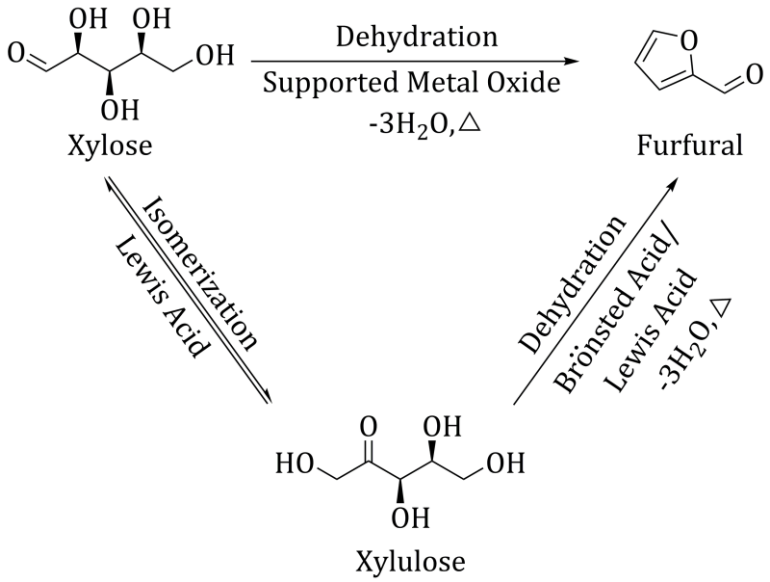

Scheme 4.2. Lewis + Brönsted acid catalyzed xylose conversion into furfural.

Formation of Lower concentration of furfural (20-38%) was evident with ZrO_2 supported SG catalysts due to the presence of less acid amount and absence of strong acid sites (Table 2.3, chapter 2). All the silica supported catalysts synthesized by WI method were also assessed for their catalytic activity, but those yield lower amount of furfural (35-39%) along with 7-9% oligomers (condensation products) and 2-3% arabinose formation (Fig. 4.1). The lower activity of silica supported WI catalysts can be explained in terms of presence of less acid amount and absence of strong acid sites in

WI synthesized catalysts compared to silica supported SG synthesized catalysts (Table 2.3, chapter 2). Moreover, XRD study shows that SG synthesis method distributes metals into the framework of silica uniformly and hence, only amorphous silica peak is visible from XRD patterns unlike characteristic metal oxide peaks in case of WI catalysts (Fig. 2.4, chapter 2). However, leaching of metal was the major issue with the WI synthesized catalyst under the reaction conditions (confirmed with ICP analysis). For WI synthesized catalyst decrease in metal loading (*wt*%) was observed after use (WO_3/SiO_2: 9.79 to 5.32, MoO_3/SiO_2: 8.74 to 4.11 and Ga_2O_3/SiO_2: 9.22 to 6.89). However, when those metals are incorporated in silica framework via SG method, the metal loadings (*wt%*) remains similar after use (WO_3/SiO_2: 9.95 to 9.93, MoO_3/SiO_2: 9.01 to 9.03 and Ga_2O_3/SiO_2: 9.36 to 9.30). Literature suggests that tungsten and molybdenum metals are generally leached out in solution as octahedral polyoxometalate (VI) species ($W_{12}O_{40}$, $Mo_{12}O_{40}$).[14,15] Due to these problems, the WI synthesized catalysts were not examined further. Under the reaction conditions, WO_3/SiO_2 (SG) catalyst showed the best activity (Fig. 4.1) and produced 5% oligomers (condensation products), 7% arabinose and 59% furfural yield from 72% xylose conversion. To reconfirm the superiority of biphasic solvent system later, reaction was carried out in only water as a solvent under the similar reaction conditions (170°C, 8 h). The results showed a lower furfural yield of 42% along with 3% oligomers and 10% arabinose from xylose (67% conversion) in presence of WO_3/SiO_2 (SG) catalyst. Finally, the catalytic activity (in terms of furfural formation) of all the catalyst can be arranged in the following order.

MoO_3/ZrO_2 (SG) (20%) ≈ SiO_2 (21%) < ZrO_2 (25%) < WO_3/ZrO_2 (SG) (29%) < MoO_3/SiO_2 (WI) (35%) < Ga_2O_3/ZrO_2 (SG) (38%) ≈ Ga_2O_3/SiO_2 (WI) (38%) ≈ WO_3/SiO_2 (WI) (39%) < MoO_3/SiO_2 (SG) (50%) < Ga_2O_3/SiO_2 (SG) (53%) < WO_3/SiO_2 (SG) (59%)

4.2.2. Use of Isolated Hemicelluloses

Since, all the SG synthesized supported metal oxides were active for furfural synthesis from xylose next, those were evaluated with isolated hemicelluloses as substrate. It was shown in previous study (section 4.2.1) that WI synthesized catalysts were not stable under the reaction conditions (leaching of metal in solution) and hence, those were not

studied further. First, oat spelt xylan (hemicellulose derived from softwood) was used as a substrate for screening of catalysts and optimization of reaction conditions and later, all other types of isolated hemicelluloses (beechwood xylan: hardwood and birch wood xylan: hardwood) were studied in presence of best catalyst and optimized reaction conditions. In chapter 3, it was shown that solid acid catalyst (SAPO-44) can carry out xylan conversion reaction into C_5 sugars and furfural at 170°C for 8 h in water + toluene (1:1 *v/v*) solvent system. The similar reaction conditions were chosen to screen various supported metal oxide catalyst in oat spelt xylan conversion reaction in this chapter.

4.2.2.1. Evaluation of Sol-Gel (SG) Synthesized Supported Metal Oxides

Various supported metal oxide catalysts synthesized by SG technique such as; WO_3/SiO_2, MoO_3/SiO_2, Ga_2O_3/SiO_2, B_2O_3/SiO_2, P_2O_5/SiO_2, ZrO_2, WO_3/ZrO_2, MoO_3/ZrO_2 and Ga_2O_3/ZrO_2 were evaluated in the conversion of oat spelt xylan. Typically, in all the reactions, xylan concentration was used as 1 *wt*% (with respect to water) and S/C ratio was taken as 4 (*wt*/*wt*). One-pot conversion of oat spelt xylan to C_5 sugars and furfural was studied in water + toluene (1:1 *v/v*) solvent at 170°C for 8 h using all the catalysts (SG) and the results are presented in Fig. 4.2.

The data elucidated that, amongst all the catalysts, WO_3/SiO_2 (SG) and Ga_2O_3/SiO_2 (SG) showed better activity for furfural formation (51-53%) directly from xylan. Total products yield of 84±3% (oligomer = 8±1%, C_5 sugars = 7±1%, furfural = 52±2%, C_6 sugars = 12±2%, 5-hydroxymethylfurfural (HMF) = 2%) is possible with 88±2% hemicellulose conversion. The formation of C_5 sugars in these reactions is obvious since hemicellulose is first hydrolyzed to C_5 sugars (xylose and arabinose) and then it converts into furfural. The formation of C_6 sugars, glucose (ca. 7%) and fructose (ca. 6%) in the reaction solution is possible as oat spelt xylan contains 15% glucose.[16] It is shown in the literature that presence of Lewis acid sites in a catalyst can catalyze isomerization reaction of glucose into fructose via 1,2 hydride transfer mechanism (section 1.7.2, chapter 1).[17-20] Moreover, presence of glucose and fructose in reaction solution further produced HMF via dehydration reaction in presence of solid acid catalyst.[17]

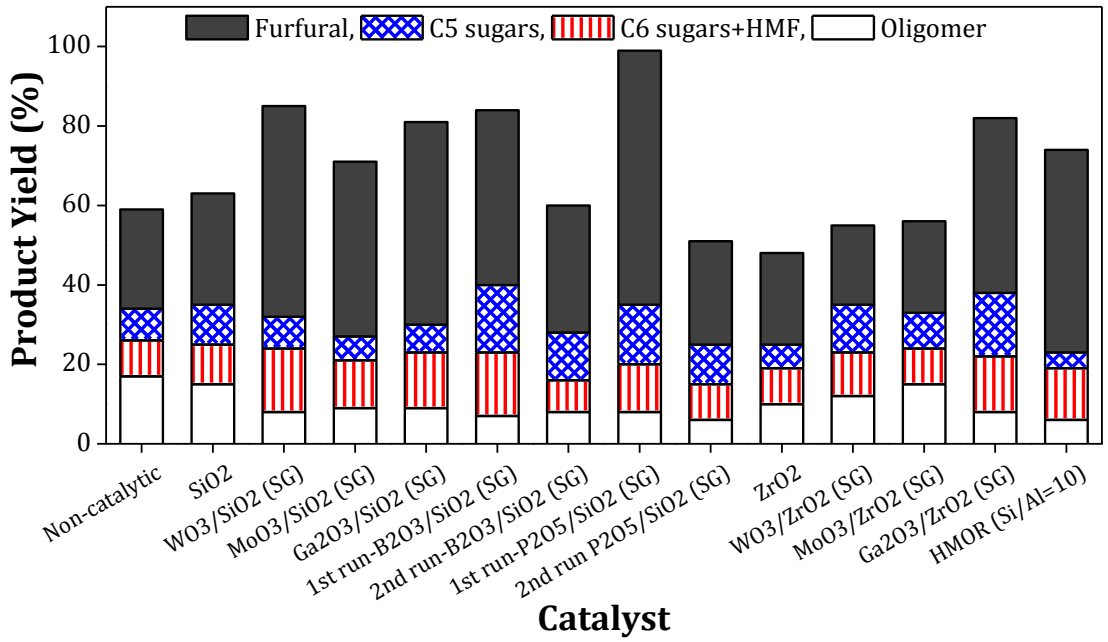

Fig. 4.2. Solid acid catalyzed one-pot conversion of oat spelt xylan. Reaction condition: xylan (0.3 g), catalyst (0.075 g), water + toluene = 60 mL (1:1 *v/v*), 2 bar N_2 at *RT*, 170°C, 8 h.

From Fig. 4.2 it can be seen that P_2O_5/SiO_2 catalyst showed the highest catalytic activity (64% furfural yield) among all the catalysts. However, with this catalyst the possibility of active species (may be in the form of acids of phosphorous) leaching out in solution might be a problem. To confirm this, pH of reaction solution before and after reaction was checked and it was found to alter from 6.9 to 1.2, which assured the leaching of phosphorous species. Further to reconfirm this, reaction was carried out with the recovered catalyst after thorough washing with water and drying. The results confirmed that the recovered P_2O_5/SiO_2 (SG) catalyst was not active (Fig. 4.2) which in turn indicates that under the reaction conditions phosphorous species were leached out in solution giving a homogeneous catalytic system. The same observation was evident in case of B_2O_3/SiO_2 (SG) catalyst. Catalytic results obtained with SiO_2 only system (28% furfural yield) proves that the incorporation of metal in SiO_2 is responsible for the generation of active sites, those could carry out hemicellulose conversion to C_5 sugars and furfural. ZrO_2 supported tungsten and molybdenum oxide catalysts were almost not active for furfural synthesis under the reaction conditions since these catalysts have very less acid amount (chapter 2, Table 2.3). Although, total products yield of 81±2% was observed with Ga_2O_3/ZrO_2 (SG) catalyst but it was less active for dehydration

reaction to yield furfural (44%). For the comparison of data obtained in this work with the earlier reported HMOR (Si/Al = 10) catalyst[1]; in this work, reactions were done at 170°C for 8 h using water + toluene solvent. Though, HMOR catalyst also showed better result for furfural (51%) formation, the catalyst lost its crystallinity which is evident from the XRD data (Fig. 4.3). Furthermore, recycle study carried out with HMOR catalyst shows that the catalytic activity of HMOR decreases continuously in each run (for more detail please see Fig. 3.2, section 3.2.1.1, chapter 3). Also, a more detailed discussion on the HMOR morphological changes is already discussed in the literature based on several characterizations.[1]

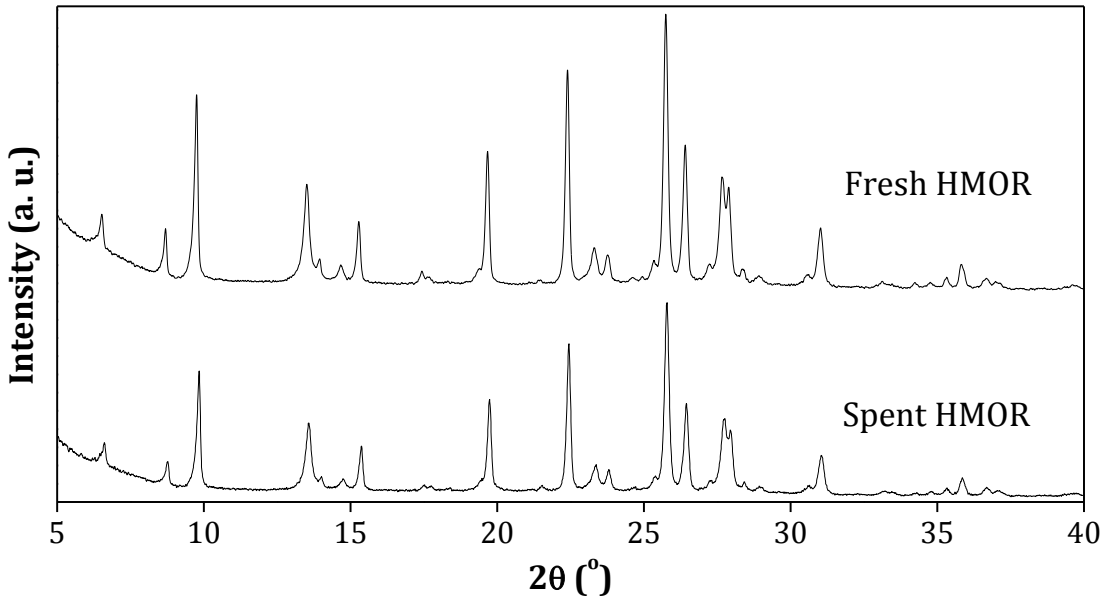

Fig. 4.3. XRD patterns for fresh and spent HMOR used in oat spelt xylan reaction.

Now, it was found that both WO_3/SiO_2 (SG) and Ga_2O_3/SiO_2 (SG) catalysts are showing better activity for isolated hemicellulose conversion into furfural. Hence, further optimization of reaction parameters were carried out in presence of both these catalysts.

4.2.2.2. Effect of Temperature and Time

First, influence of reaction temperature on product distribution was studied. All the reactions were carried out with oat spelt xylan concentration of 1 *wt*% (with respect to water), catalyst = 0.075 g, water + toluene = 60 mL (1:1 *v/v*), 8 h. The data plotted in Fig. 4.4 suggests that, 170°C is the optimum temperature to carry out xylan conversion to

yield furfural in the presence of both WO_3/SiO_2 (SG) and Ga_2O_3/SiO_2 (SG) catalysts. Under the reaction conditions C_5 sugars (xylose + arabinose) yield was less (7-8%) with both the catalysts. However, at lower temperature (150 and 160°C) formation of oligomers and C_5 sugars was found to be in major amount (150°C: oligomers = 51-53%, C_5 sugars = 5-6% and 160°C: oligomers = 32-39%, C_5 sugars = 13-18%) and this suggests that hydrolysis requires lower temperature compared to dehydration reaction. With increase in temperature to 180°C, both C_5 sugars and furfural yield was seen to be decreased as compared to the yields obtained at 170°C in presence of both the catalysts. This suggests that at higher temperature secondary reactions might favor at the expense of C_5 sugars and furfural in presence of acid catalyst.[21-23] Moreover, after reaction it was seen that insoluble brown colour solids were left in reactor.

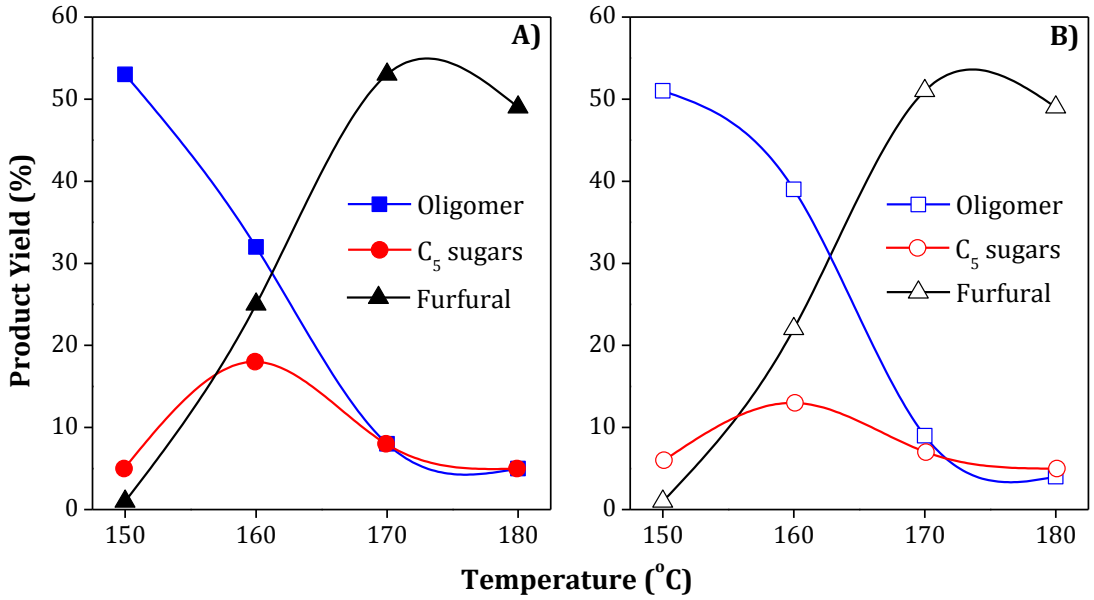

Fig. 4.4. Optimization of reaction temperature for one-pot oat spelt xylan conversion in presence of sol-gel (SG) synthesized catalysts. A) WO_3/SiO_2, B) Ga_2O_3/SiO_2. Reaction conditions: xylan (0.3 g), catalyst (0.075 g), water + toluene = 60 mL (1:1 *v/v*), 2 bar N_2 at *RT*, 8 h.

The time profile data (Fig. 4.5) obtained using WO_3/SiO_2 (SG) and Ga_2O_3/SiO_2 (SG) catalyst at 170°C clearly implies that first, hemicellulose undergoes hydrolysis reaction to yield oligomers and then C_5 sugars formation starts. Under the reaction conditions, a maximum of 26-28% C_5 sugars formation was evident when the reaction was carried out for 4 h in presence of both the catalysts. Later on, these sugars undergo

dehydration reaction to yield furfural. It can be seen from the data that both the catalysts give maximum amount of furfural (55-61%) at a reaction time of 10 h and beyond this time due to secondary (condensation) reactions (detail study is discussed in section 5.3, chapter 5) becoming prominent concentration of furfural starts decreasing.

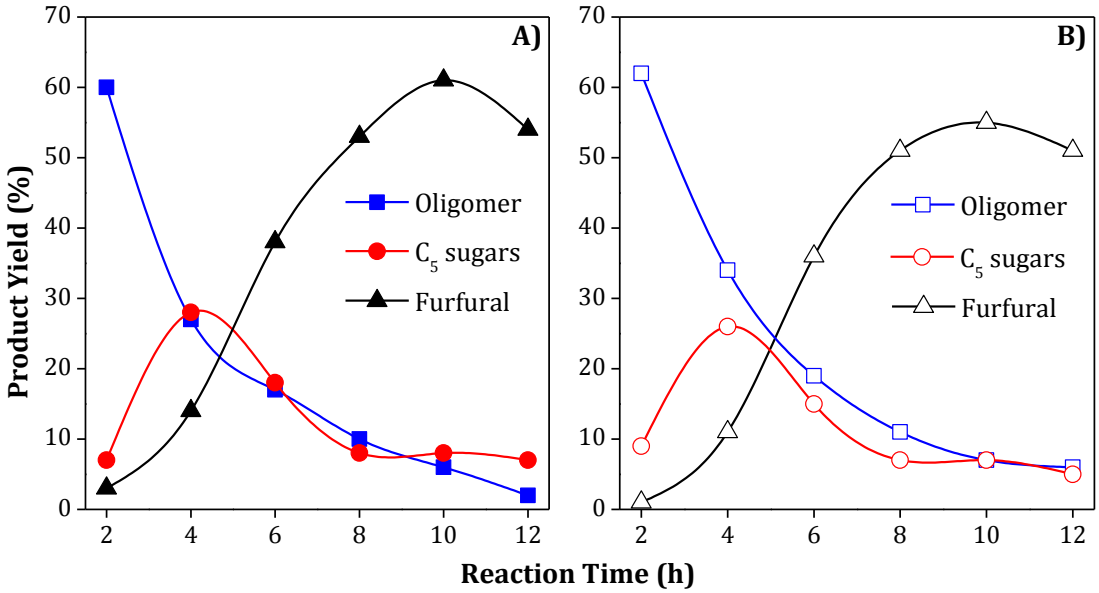

Fig. 4.5. Optimization of reaction time for one-pot oat spelt xylan conversion in presence of SG synthesized catalysts. A) WO_3/SiO_2, B) Ga_2O_3/SiO_2. Reaction conditions: xylan (0.3 g), catalyst (0.075 g), water + toluene = 60 mL (1:1 *v/v*), 170°C, 2 bar N_2 at *RT*.

4.2.2.3. Effect of Catalyst and Substrate Concentration

Use of less amount of catalyst can boost its applicability quotient. Consequently, a study with both WO_3/SiO_2 (SG) and Ga_2O_3/SiO_2 (SG) was undertaken at 170°C by altering the S/C ratio (*wt*/*wt*) from 1 to 8 by keeping substrate amount constant (1 *wt*%). Similar yield of furfural (55-61%) after 10 h reaction was detected with the S/C ratio maintained in the range of 1-4, but with the increase in ratio to 8, decrease in the yield (ca. 47%) with lower hemicellulose conversion (86%) was seen. This was quite obvious as insufficient amount of acid sites were present in the system to catalyze reactions. It can be noted that the use of higher catalyst amount (S/C = 1) also yields similar amount of products as like S/C = 4 system. This suggests that use of better extracting solvent (toluene) immediately separates furfural from the catalyst contact and hence formation of secondary products are minimized even if, higher catalyst concentration is used.

From this data it is understood that S/C ratio of 1-4 is in the allowable range to favor better furfural formation. Hence, in next reactions, S/C ratio of 4 was fixed.

Besides, lowering the catalyst quantity it is also beneficial if higher substrate amount can be used and hence reactions were conducted using 1, 5 and 10 *wt*% hemicellulose concentration (with respect to water). The results indicate that, with 1 and 5 *wt*% substrate concentrations, similar furfural yields (WO_3/SiO_2 (SG) = 61±2%, Ga_2O_3/SiO_2 (SG) = 56±1%) can be achieved. However, with the increase in concentration to 10 *wt*%, lower furfural yields (WO_3/SiO_2 (SG) = 45%, Ga_2O_3/SiO_2 (SG) = 40%) were obtained. The lower yield of furfural with 10 *wt*% substrate can be due to the occurrence of side reactions since concentrated solution of furfural and xylose is present.

4.2.2.4. Effect of Biphasic Ratio

In earlier chapter it was proven that in the presence of SAPO-44 catalyst with change in biphasic solvent (water + toluene) ratio furfural yields were altered. The same possibility was also checked for supported metal oxide catalyst. In all the studies, S/C and substrate/water ratio was kept constant. Use of higher water + toluene ratio of 1:2 (*v/v*), produced better amount of furfural (WO_3/SiO_2 = 71%, Ga_2O_3/SiO_2 = 60%) compared to 1:1 (*v/v*) ratio (WO_3/SiO_2 = 61%, Ga_2O_3/SiO_2 = 55%) at 170°C, 10 h. However, further increase in toluene amount (1:4 *v/v*) lowers furfural yields (WO_3/SiO_2 = 51%, Ga_2O_3/SiO_2 = 49%). It was expected that with an increase in toluene amount in reaction system, it might improve furfural yield since better extraction of furfural from water phase is possible. However, surprisingly, use of water + toluene in 1:4 *v/v* ratio reduces the furfural yield.

4.2.2.5. Recycle Study

To verify the robustness of these catalysts, reusability study of catalyst was undertaken under the optimum reaction conditions; oat spelt xylan (5 *wt*%), S/C=4, water + toluene (1:2 *v/v*), 2 bar N_2 at *RT*, 170°C, 10 h. The recovered catalyst from previous run after centrifugation was simply washed with water and without any further treatment was reused directly in the subsequent run. Fig. 4.6 showed the extraordinarily constant

activity for both the catalysts [WO_3/SiO_2 (SG): 71±1% and Ga_2O_3/SiO_2 (SG): 61±1%] in furfural formation from isolated hemicellulose in at least 8 runs. Along with furfural, formation of oligomers (5±1%), C_5 sugars (6±1%), C_6 sugars (8±2%) and HMF (ca. 5%) was also observed when >99% of conversion was achieved with both the catalysts. Later, the formed furfural was isolated from reaction mixture by following the procedure described in chapter 3 (section 3.2.2.5) and from NMR study its purity was confirmed.

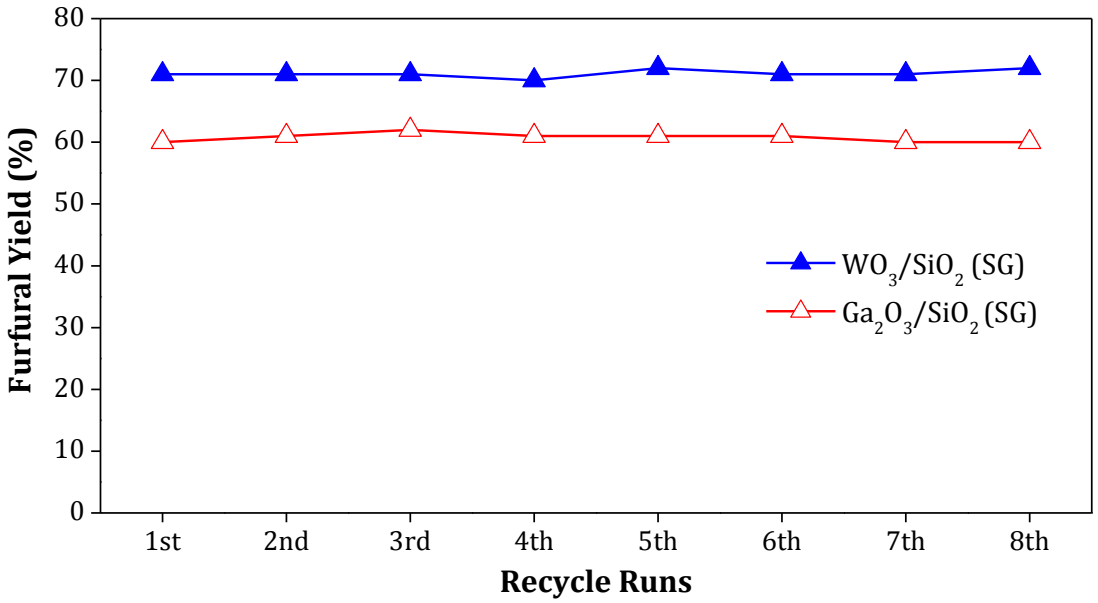

Fig. 4.6. Recycle runs for WO_3/SiO_2 (SG) and Ga_2O_3/SiO_2 (SG) catalyst. Reaction condition: oat spelt xylan (1.0 g), catalyst (0.25g), water + toluene = 60 mL (1:2 *v/v*), 2 bar N_2 at *RT*, 170°C, 10 h.

The steady activity of both the catalysts can be explained in terms of their thermal stability checked with TGA analysis. It can be seen from Fig. 2.15 (chapter 2) that both the catalysts showed stability up to 1000°C excluding the loss of water (4.5-10.2%) at lower temperature (<150°C). The similar observation for stability of both the catalysts was also reported earlier.[24-26] This property of catalyst allows it to remain stable under reaction conditions.

Further, to check the carbon deposition on spent catalyst surface, CHNS analysis was undertaken and the results ruled out the possibility of carbon presence on spent catalyst surface. Moreover, the catalysts were recovered from the reaction mixture after

8th run, washed thoroughly, dried and calcined at 550°C (WO_3/SiO_2) and 300°C (Ga_2O_3/SiO_2) for 12 h to understand loss in catalyst handling. The calculation depicts that a slight loss (ca. 6%) was evident during catalyst recycling for both the catalysts.

4.2.2.6. Hammett Acidity Correlation for Catalytic Activity

From all the previously discussed data, it can be seen that WO_3/SiO_2 (SG) catalyst shows better activity compared to Ga_2O_3/SiO_2 (SG) catalyst although, WO_3/SiO_2 (SG) catalyst has a lower total acid amount (0.14 mmol/g) compared to Ga_2O_3/SiO_2 (SG) catalyst (0.6 mmol/g). To understand this issue, supported metal oxide catalysts [WO_3/SiO_2 (SG), MoO_3/SiO_2 (SG) and MoO_3/SiO_2 (SG)] acid strength analysis was carried out through Hammett acidity function (H_0) calculation (Table 4.1).[27,28] The detail analysis procedure was described in section 3.2.1.4, chapter 3. Briefly, for analysis of Hammett acidity, *p*-nitro aniline (*p*-NA) was used as a basic indicator.[28] Typically, ~ 0.0027 g of catalyst was added to 10 mL standard *p*-NA solution in water having concentration of 10 ppm (pK_a = 0.99), stirred for 0.5 h and filtered the solution through 0.22 µm syringe filter. Absorbance of filtrate was checked with Jesco V-570 spectrophotometer in the range of 200-800 nm. At 380 nm maximum absorbance was observed. Hammett acidity (H_0) of samples was calculated according to the following equation (Equation 4.1).

$$H_0 = pK(I)_{aq} + \log_{10} ([I] / [IH^+]) \quad \text{..... (Equation 4.1)}$$

In this equation, $pK(I)_{aq}$ indicates the pK_a value of standard indicator in aqueous solution. [I] indicates percentage of un-protonated indicator and [IH^+] indicates percentage for protonated indicator. The lower H_0 value indicates the higher acid strength of catalysts.

Table 4.1. Determination of Hammett acidity in supported metal oxide catalysts.

Catalyst	A_{max}	[I]%	[IH^+]%	H_0
Blank (only indicator solution)	1.105	100	0	-
Fresh WO_3/SiO_2 (SG)	0.918	83.1	16.9	1.68
Spent WO_3/SiO_2 (SG)	0.911	82.4	17.6	1.66
Fresh MoO_3/SiO_2 (SG)	1.027	92.9	7.1	2.11
Spent MoO_3/SiO_2 (SG)	1.033	93.5	6.5	2.15
Fresh Ga_2O_3/SiO_2 (SG)	0.990	89.6	10.4	1.92
Spent Ga_2O_3/SiO_2 (SG)	0.995	90.0	10.0	1.95

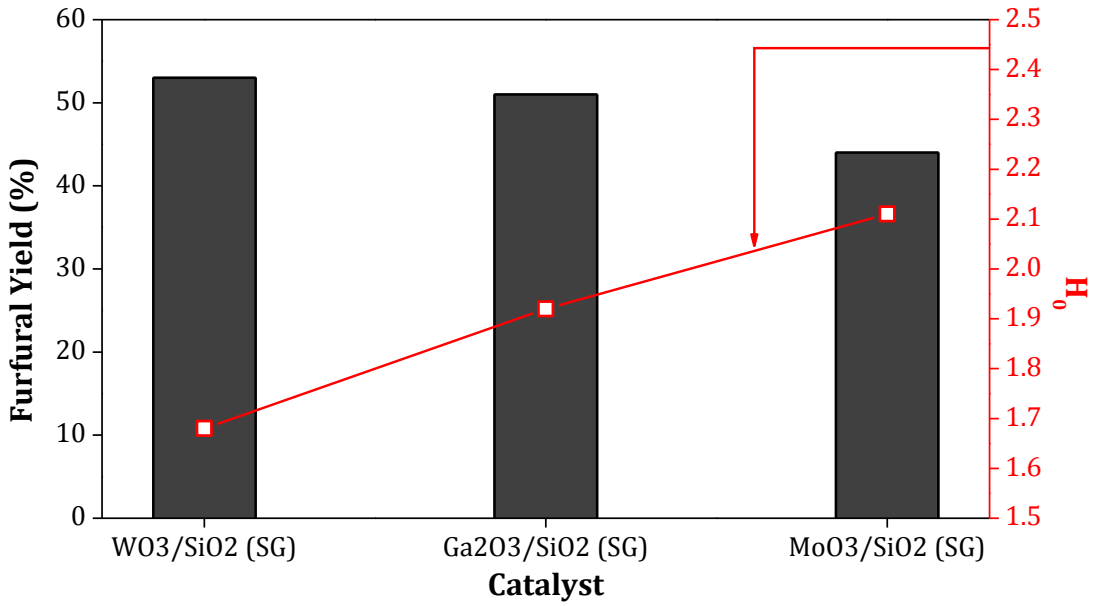

Fig. 4.7. Correlation of Hammett acidity with catalytic activity. Reaction condition: oat spelt xylan (0.3 g), catalyst (0.075 g), water + toluene = 60 mL (1:1 *v/v*), 2 bar N_2 at *RT*, 170°C, 8 h.

Fig. 4.7 displayed a good correlation between catalytic activity and catalyst acid strength (H_0). This data ratifies the fact that the incorporation of tungsten in silica framework generates more strong acid sites compared to gallium. Furthermore, Raman study also supports this data. The Raman spectral profile discussed in section 2.5.4, chapter 2 suggest that in case of WO_3/SiO_2 (SG) catalyst existence of three distinct broad lines at 927, 560 and 200-430 cm^{-1} confirmed the presence of polymeric tungsten-silica species i.e. silicotungstic species.[29] However, this type of species were not present in case of molybdenum and gallium catalysts (section 2.5.4, chapter 2). Hence, it can be suggested that due to presence of silicotungstic species, WO_3/SiO_2 (SG) catalyst shows stronger acid sites as evident from lower H_0 value. All the spent catalysts also showed similar H_0 value as compared to fresh catalysts (Table 4.1) which further confirms the catalyst stability. Although, H_0 value is calculated for supported metal oxide catalysts but several literature reports argued about this techniques suitability.[27,30,31] Basically, Hammett function is appropriate for homogeneous acid catalytic system.[27] It is suggested that the basic indicator molecule can adsorb on heterogeneous acid catalyst surface (physisorption) and hence may lead to misinterpretation of result.[27] However, several other researchers are using this analysis

method to comment on acid strength of solid acid catalysts.[28,32] It is also suggested in the literature that Hammett acidity can also be measured for Lewis acid catalyst.[27,31] Hence, in this analysis method, it is suggested that the interaction between Lewis acid center in catalyst and Lewis base center (–NH_2 group) in indicator molecule might be happening.

4.2.2.7. Processing of Variety of Hemicellulose Sources

After successful transformation of oat spelt xylan (softwood) into C_5 sugars and furfural later, all other types of isolated hemicelluloses *viz.* beechwood xylan (hardwood) and birch wood xylan (hardwood) were subjected as substrate under the optimum reaction conditions [xylan (5 *wt*%), S/C = 4 (*wt/wt*), water + toluene (1:2 *v/v*), 2 bar N_2 at *RT*, 170°C, 10 h]. Processing of beechwood xylan in presence of WO_3/SiO_2 (SG) catalyst produces almost similar furfural yields (73%) as like oat spelt xylan (71%). Beside furfural, formation of 3% oligomers and 8% C_5 sugars was also evident. Under similar reaction conditions, birch wood xylan was also converted into 56% furfural, 16% C_5 sugars and 7% oligomers in presence of WO_3/SiO_2 (SG) catalyst. These results permit to comment that supported metal oxide catalysts were capable of producing furfural selectively from various types of isolated hemicelluloses.

4.2.3. Use of Crop Wastes (Raw Biomass)

All the seven crop wastes (raw biomass) collected from various regions of India were used as substrate for converting their pentosan part directly into C_5 sugars and furfural. Both WO_3/SiO_2 (SG) and Ga_2O_3/SiO_2 (SG) catalysts were screened. The optimized reaction conditions for isolated hemicellulose conversion reactions obtained with SAPO-44 catalyst (chapter 3) and supported metal oxide catalysts (chapter 4) were same. Hence, conversion of crop wastes were carried out under the already optimized reaction conditions determined using SAPO-44 catalyst in section 3.2.2.1, chapter 3 [substrate concentration (3.33 wt% with respect to water), catalyst (0.05 g), water + toluene (60 mL, 1:2 *v/v*), 2 bar N_2 at *RT*, 170°C, 8 h].

4.2.3.1. Various Crop Wastes Conversions

Table 4.2 shows the results for direct conversion of various un-treated crop wastes into furfural selectively. In all cases, furfural yields were calculated based on the pentosan content in crop waste. An extraordinarily high yield of furfural (72-87%) was detected with both the catalysts using crop wastes. Beside furfural yields, some amount of oligomer (ca. 6%), C_5-sugar (ca. 9%), C_6-sugar (ca. 14) and HMF (ca. 4%) was evident under reaction conditions. This assures good capability of supported metal oxides for synthesis of furfural directly from abundant and inexpensive real feedstock.

Table 4.2. Synthesis of furfural from one-pot conversion of crop wastes using supported metal oxide catalysts.

Entry No.	Substrate	Furfural Yield (%)	
		WO_3/SiO_2 (SG)	Ga_2O_3/SiO_2 (SG)
1	Bagasse (I)	87	83
2	Bagasse (II)	84	81
3	Bagasse (III)	86	81
4	Rice husk (I)	76	72
5	Rice husk (II)	81	78
6	Rice husk (III)	79	75
7	Wheat Straw	78	76

Reaction conditions: crop waste (3.33 *wt*% with respect to water), catalyst = 0.05 g, water + toluene = 60 mL (1:2 *v/v*), 2 bar N_2 at *RT*, 170°C, 8 h.

4.2.3.2. Recycle Study

Further, to express stability of both the catalysts, catalyst reutilization study with real substrates was performed. Before reuse, the catalyst was recovered from reaction mixture via centrifugation, washed thoroughly with water, dried (Lab oven: 60°C, 16 h; vacuum oven: 150°C, 6 h, 10^{-3} bar) and calcined at 550°C for 12 h in air (flow rate = 10 mL/min). Only three substrates were considered *viz.* bagasse (I), rice husk (I) and wheat straw (I) for the analysis to avoid complications. The data presented in Fig. 4.8 showed that both the catalysts were recyclable minimum up to 8th run without losing their activity. This approves the robustness of amorphous supported metal oxides.

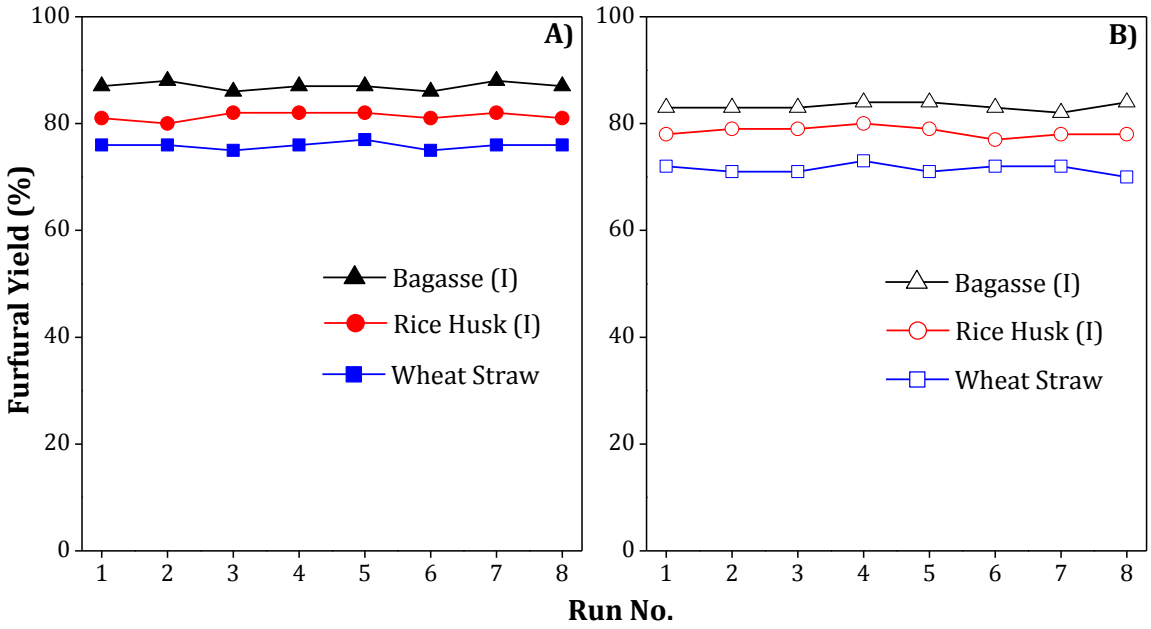

Fig. 4.8. Recycle study for furfural synthesis from crop wastes using supported metal oxide catalysts. A) WO_3/SiO_2 (SG), B) Ga_2O_3/SiO_2 (SG). Reaction conditions: crop waste (3.33 *wt*% with respect to water), catalyst (approx. 0.05 g), water + toluene = 60 mL (1:2 *v/v*), 2 bar N_2 at *RT*, 170°C, 8 h.

4.3. Proposed Reaction Mechanism

Based on the above discussed results, it can be said that in presence of Lewis acid catalysts xylose first isomerizes into xylulose (xylo-ketose) via 1, 2-hydride shifting. Next, xylulose undergoes cyclization and dehydration reaction to form furfural in presence of Lewis acid catalysts. The possible mechanism is shown below in Fig. 4.9.

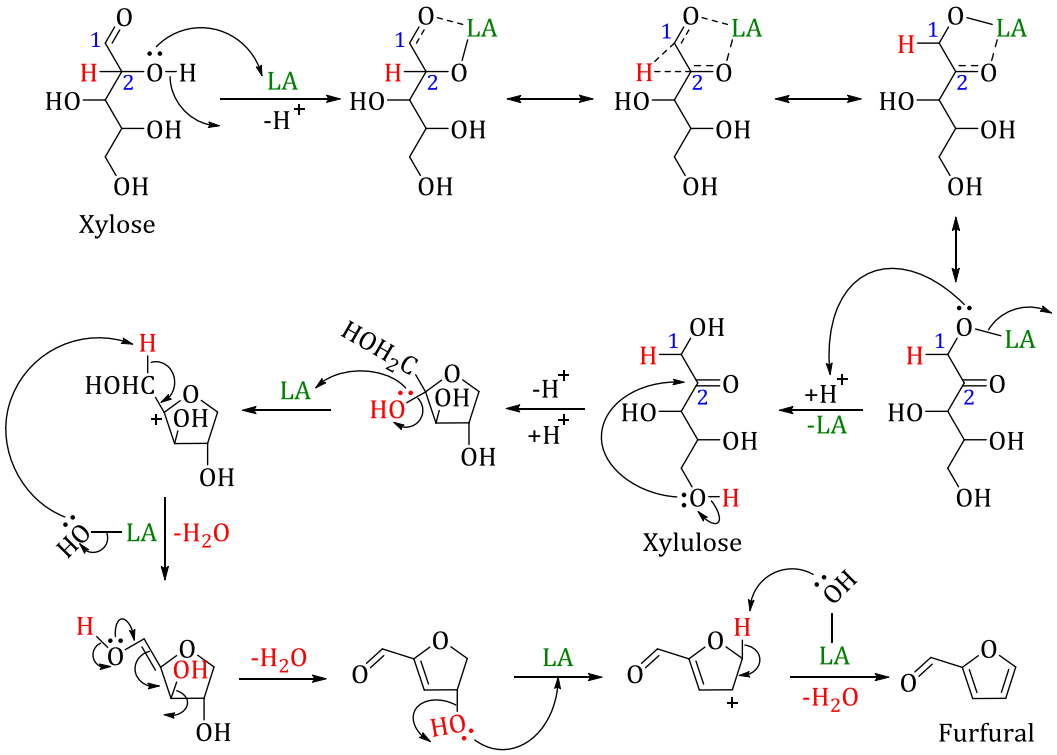

Fig. 4.9. Possible mechanism for furfural formation from xylose via xylulose formation in presence of Lewis acid catalysts. 'LA' stands for Lewis acid catalysts.

4.4. Catalyst Characterizations: Fresh and Spent Catalyst

The discussed data in this chapter suggests that both WO_3/SiO_2 (SG) and Ga_2O_3/SiO_2 (SG) were better active catalysts for furfural synthesis from various feedstock as well as those were stable under reaction conditions. To support further the stability of both the catalysts, the fresh and spent catalysts were subjected to various characterizations. Before all the characterizations the recovered catalysts were calcined at respective temperatures as used during synthesis of catalysts (WO_3/SiO_2: 550°C, Ga_2O_3/SiO_2: 300°C) for 12 h to remove unconverted part of crop wastes (cellulose, lignin, unconverted pentosan).

4.4.1. XRD Analysis

The detail discussions made in section 2.5.1, chapter 2 confirms that SG synthesis disperses metals (W, Ga) uniformly in silica framework and therefore XRD analysis couldn't detect any separate metal oxide peak, showing only amorphous silica peak. Fig. 4.10 shows the amorphous nature of fresh WO_3/SiO_2 (SG) and Ga_2O_3/SiO_2 (SG)

catalysts. Later, the XRD patterns for spent catalysts used in either isolated hemicellulose reaction or crop wastes reaction were recorded. Before analysis all spent catalysts used in crop waste reactions were calcined to remove unreacted part of biomass. The XRD patterns for spent catalysts used in either isolated hemicellulose or crop wastes show the similar amorphous nature as like fresh catalyst (Fig. 4.10). Additionally, after reaction, absence of any peaks due to metal oxides was indicative of the fact that metal oxides were still highly dispersed in silica framework, otherwise peaks due to metal oxides would have been visible as observed in WI catalysts[29] (Fig. 2.4, chapter 2). This data highlights the fact that the catalysts are stable under reaction conditions and hence reproducible catalytic activity in recycle runs was observed.

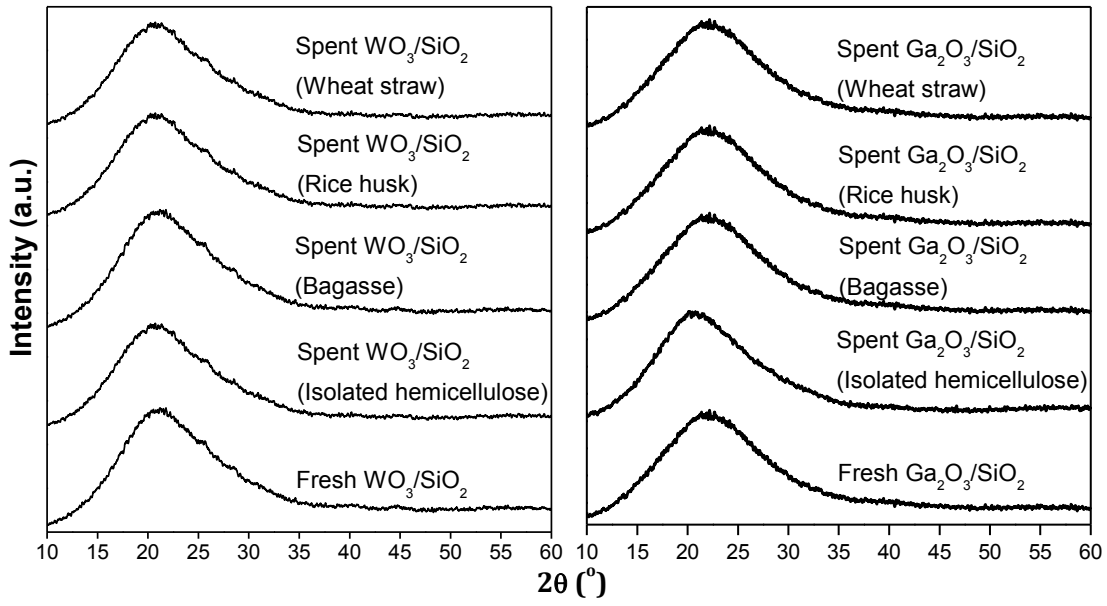

Fig. 4.10. XRD patters for fresh and spent catalysts used with all the substrates.

4.4.2. TPD-NH_3 and N_2 Sorption Analysis

Table 4.3 presents the data for total acid amount, acid amount distribution and surface area of fresh and spent WO_3/SiO_2 (SG) and Ga_2O_3/SiO_2 (SG) catalysts used with both isolated hemicellulose and raw biomass. For the calculation of acid amount in spent catalyst used with raw biomass, silica correction was done since raw biomass consists of silica material. For more details on calculation of silica correction please refer section 3.3.3 in chapter 3. The values for acid amount and surface area in spent catalysts were well matching with that of fresh catalysts. The TPD-NH_3 profile for all the catalysts are

shown in Fig. 4.11. This further approves the stable catalytic activity of supported metal oxides synthesized by SG method.

Table 4.3. TPD-NH_3 and N_2 sorption analysis data for fresh and spent catalysts used in reaction with various substrates.

Catalyst	Acid Amount (mmol/g)[a]			Surface Area
	Weak	Strong	Total	(m^2/g)[b]
Fresh WO_3/SiO_2 (SG)	0.09	0.05	0.14	278
Spent WO_3/SiO_2 (SG) (isolated hemicellulose)	0.10	0.06	0.16	267
Spent WO_3/SiO_2 (SG) (bagasse)	0.08	0.05	0.13	291
Spent WO_3/SiO_2 (SG) (rice husk)	0.08	0.05	0.13	n.d.
Spent WO_3/SiO_2 (SG) (wheat straw)	0.08	0.06	0.14	n.d.
Fresh Ga_2O_3/SiO_2 (SG)	0.32	0.28	0.60	299
Spent Ga_2O_3/SiO_2 (SG) (isolated hemicellulose)	0.30	0.28	0.58	295
Spent Ga_2O_3/SiO_2 (SG) (bagasse)	0.28	0.31	0.59	317

[a]TPD-NH_3 analysis for details please refer section 2.5.6 in chapter 2, [b]N_2 sorption analysis for details please refer section 2.5.7 in chapter 2.

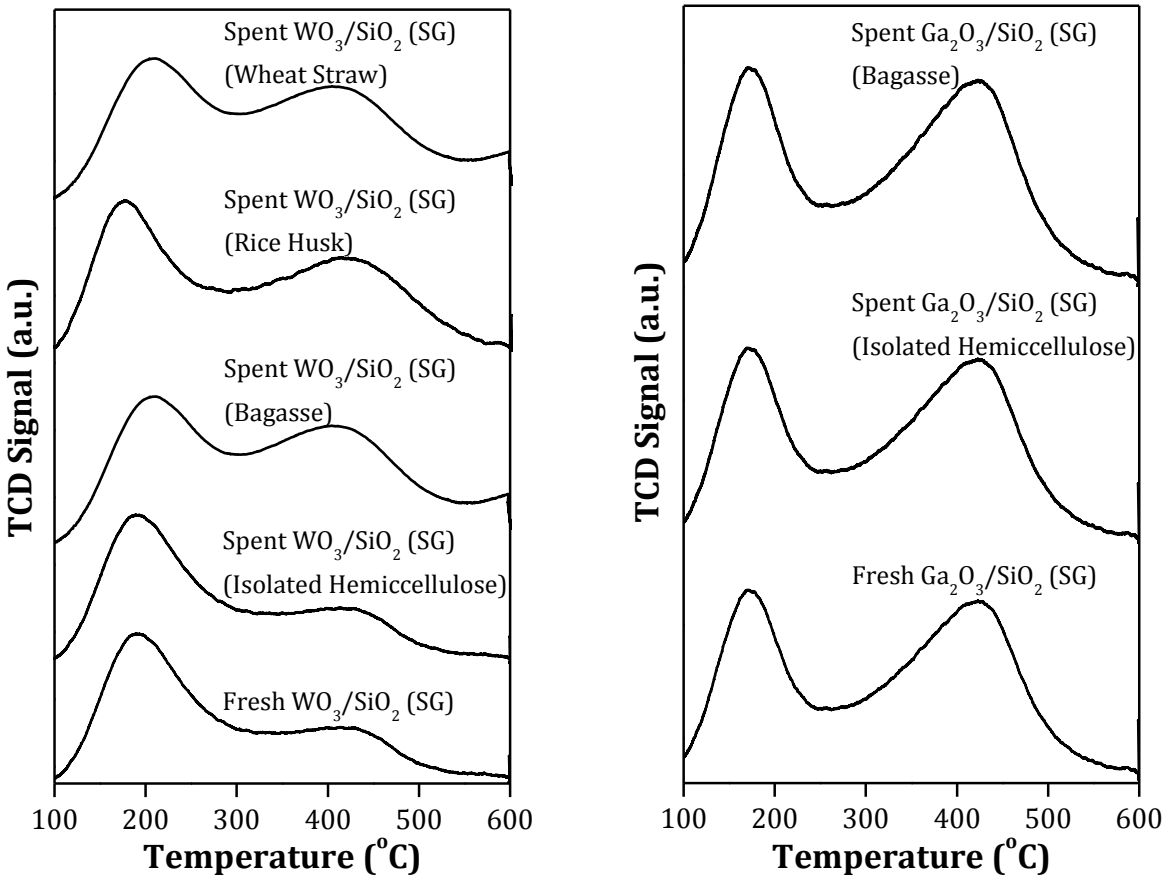

Fig. 4.11. TPD-NH_3 profile for fresh and spent supported metal oxide catalysts.

4.4.3. TEM Analysis

TEM images for fresh and spent WO_3/SiO_2 (SG) and Ga_2O_3/SiO_2 (SG) catalyst used in isolated hemicellulose reaction are shown in Fig. 4.12. In all the images, amorphous nature of silica support was visible. Images confirmed that smaller metal particles were uniformly distributed over silica. An average particle size of 3-4 nm for fresh and spent WO_3/SiO_2 (SG) and <2 nm for fresh and spent Ga_2O_3/SiO_2 (SG) was observed. It is interesting to note here that although, metal oxide particles are visible in TEM images but the XRD patterns couldn't detect them showing only amorphous silica peak. The similar observation was also reported earlier in case of tungsten oxide and gallium oxide catalyst supported on silica.[33,34] This further approves the highly dispersed metal particles over silica support. The preservation of particle size and uniformity in distribution in spent catalyst further confirms the catalyst stability and hence a stable catalytic activity was evident in recycle runs.

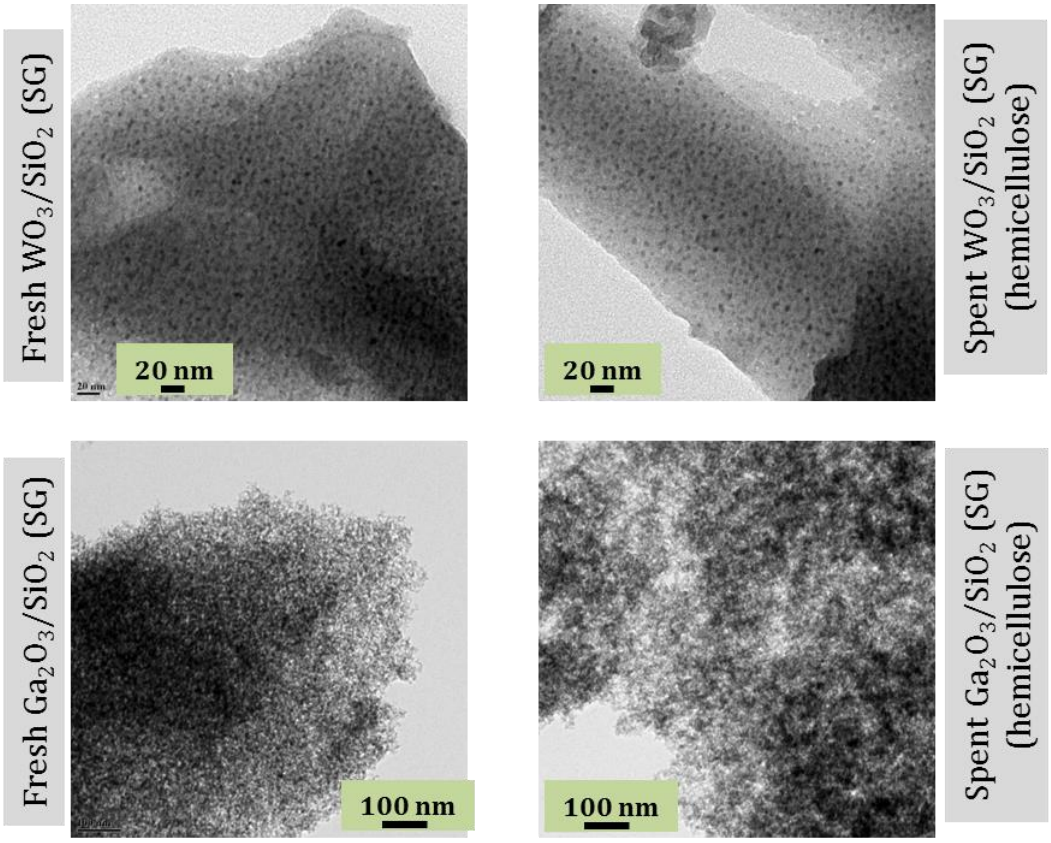

Fig. 4.12. TEM images of fresh and spent catalysts used in isolated hemicellulose reaction.

4.5. Conclusions

In summary, amorphous supported metal oxide catalysts having mainly Lewis acidity (as proven by pyridine-IR analysis) were shown as an effective catalyst for synthesis of C_5 sugars and furfural from various substrates *viz.* xylose, isolated hemicelluloses and crop wastes. Silica and zirconia were used for supporting tungsten, molybdenum, gallium, boron and phosphorous metals. Moreover, the influence of synthesis technique (wet-impregnation and sol-gel) was investigated. After systematic evaluation of all the catalysts it was affirmed that WO_3/SiO_2 and Ga_2O_3/SiO_2 catalyst synthesized by SG method were very active for selective synthesis of furfural. Under optimized reaction conditions, a very high yield of furfural was possible from isolated hemicelluloses in presence of WO_3/SiO_2 (SG) (yield = 72%) and Ga_2O_3/SiO_2 (SG) (yield = 60%). Later, the reaction was extended with the direct use of crop wastes as substrate. An extraordinary yield of 76-86% [with WO_3/SiO_2 (SG)] and 72-81% [Ga_2O_3/SiO_2 (SG)] for furfural was

achieved from the conversion of seven crop wastes. Additionally, both the catalysts were shown to be stable and recyclable minimum up to 8 runs using either isolated hemicellulose or crop wastes. Based on the catalytic results, mechanism of xylose conversion into furfural via xylulose formation was proposed. Later, several physico-chemical characterizations (XRD, TPD-NH_3, N_2-sorption and TEM) were undertaken with fresh and spent catalysts which further enlighten the catalyst stability. These characterization data suggests that both the catalysts were stable under the reaction conditions.

The purpose of this study was to develop a stable catalyst in terms of amorphous nature i.e. no uniform channel structure since earlier it was shown that structured catalysts are prone to alter its morphology.[1] Finally, it is now safe to say that the problem has successfully overcome by developing amorphous supported metal oxide catalysts which are highly active as well as stable under reaction conditions.

4.5. References

(1) Sahu, R.; Dhepe, P. L. *ChemSusChem* **2012**, *5*, 751.
(2) Bhaumik, P.; Dhepe, P. L. *ACS Catal.* **2013**, *3*, 2299.
(3) Bhaumik, P.; Dhepe, P. L. *RSC Adv.* **2014**, *4*, 26215.
(4) Bhaumik, P.; Kane, T.; Dhepe, P. L. *Catal. Sci. Technol.* **2014**.
(5) Kobayashi, H.; Fukuoka, A. *Green Chem.* **2013**, *15*, 1740.
(6) Dutta, S.; De, S.; Saha, B.; Alam, M. I. *Catal. Sci. Technol.* **2012**, *2*, 2025.
(7) Gallezot, P. *Chem. Soc. Rev.* **2012**, *41*, 1538.
(8) Dutta, S. *RSC Adv.* **2012**, *2*, 12575.
(9) Hu, L.; Zhao, G.; Hao, W.; Tang, X.; Sun, Y.; Lin, L.; Liu, S. *RSC Adv.* **2012**, *2*, 11184.
(10) Climent, M. J.; Corma, A.; Iborra, S. *Green Chem.* **2011**, *13*, 520.
(11) Choudhary, V.; Pinar, A. B.; Sandler, S. I.; Vlachos, D. G.; Lobo, R. F. *ACS Catal.* **2011**, *1*, 1724.
(12) Choudhary, V.; Sandler, S. I.; Vlachos, D. G. *ACS Catal.* **2012**, *2*, 2022.
(13) Bandura, A. V.; Lvov, S. N. *J. Phy. Chem. Ref. Data* **2006**, *35*, 15.
(14) Miao, S.; Liu, L.; Lian, Y.; Zhu, X.; Zhou, S.; Wang, Y.; Bao, X. *Catal. Lett.* **2004**, *97*, 209.
(15) Okuhara, T. *Chem. Rev.* **2002**, *102*, 3641.
(16) Sigma-Aldrich; http://www.sigmaaldrich.com/catalog/product/sigma/x0627?lang=en&region=IN.
(17) Bhaumik, P.; Dhepe, P. L. *RSC Adv.* **2013**, *3*, 17156.
(18) Moliner, M.; Roman-Leshkov, Y.; Davis, M. E. *Proc. Nat. Acad. Sci.* **2010**, *107*, 6164.
(19) Roman-Leshkov, Y.; Moliner, M.; Labinger, J. A.; Davis, M. E. *Angew. Chem. Int. Ed.* **2010**, *49*, 8954.

(20) Choudhary, V.; Pinar, A. B.; Lobo, R. F.; Vlachos, D. G.; Sandler, S. I. *ChemSusChem* **2013**, *6*, 2369.
(21) Girisuta, B.; Janssen, L. P. B. M.; Heeres, H. J. *Green Chem.* **2006**, *8*, 701.
(22) Patil, S. K. R.; Lund, C. R. F. *Energy Fuels* **2011**, *25*, 4745.
(23) van Zandvoort, I.; Wang, Y.; Rasrendra, C. B.; van Eck, E. R. H.; Bruijnincx, P. C. A.; Heeres, H. J.; Weckhuysen, B. M. *ChemSusChem* **2013**, *6*, 1745.
(24) Hu, B.; Liu, H.; Tao, K.; Xiong, C.; Zhou, S. *J. Phy. Chem. C* **2013**, *117*, 26385.
(25) Newman, A. D.; Brown, D. R.; Siril, P.; Lee, A. F.; Wilson, K. *Phy. Chem. Chem. Phy.* **2006**, *8*, 2893.
(26) Saito, M.; Watanabe, S.; Takahara, I.; Inaba, M.; Murata, K. *Catal. Lett.* **2003**, *89*, 213.
(27) Corma, A. *Chem. Rev.* **1995**, *95*, 559.
(28) Wang, Y.; Gong, X.; Wang, Z.; Dai, L. *J. Mol. Catal. A: Chem.* **2010**, *322*, 7.
(29) Colque, S.; Payen, E.; Grange, P. *J. Mater. Chem.* **1994**, *4*, 1343.
(30) Benesi, H. A. *J. Am. Chem. Soc.* **1956**, *78*, 5490.
(31) Alemdaroglu, T. *Commun. Fac. Sci. Univ. Ank. Series B* **2001**, *47*, 27.
(32) Okayasu, T.; Saito, K.; Nishide, H.; Hearn, M. T. W. *Green Chem.* **2010**, *12*, 1981.
(33) Bohstrom, Z.; Rico-Lattes, I.; Holmberg, K. *Green Chem.* **2010**, *12*, 1861.
(34) Yang, Y.; Tran, C.; Leppert, V.; Risbud, S. H. *Mater. Lett.* **2000**, *43*, 240.

CHAPTER-5

ONE-POT SYNTHESIS OF 5-HYDROXYMETHYLFURFURAL FROM BIOMASS DERIVED C_6 CARBOHYDRATES

5.1. Introduction

In this chapter discussions on the synthesis of industrially important chemical 5-hydroxymethylfurfural (HMF)[1,2] from various feedstocks using solid acid catalysts are made. In the introduction chapter of this thesis, detailed discussions on the available heterogeneous catalyzed process for the synthesis of HMF are documented. From the discussion, it is understood that most of the available heterogeneous catalyzed processes for HMF synthesis have several drawbacks such as low and non-selective yields of HMF, difficulty in HMF recovery due to use of high boiling solvent (DMSO, DMF etc.), use of edible sugar (fructose) etc. Later, researchers have shown that inexpensive and abundant C_6 sugar, glucose can be used as a substrate for HMF synthesis using solid acid catalyst. However, very few reports are available using solid acid catalysts since processing of glucose into HMF in one-pot method is complex. For the synthesis of HMF from glucose, first it has to undergo isomerization reaction to yield fructose, which is typically catalyzed by base catalyst and later, in presence of acid catalysts fructose undergoes dehydration reaction to form HMF.[3,4] One of the strategy to convert glucose into HMF in one-pot fashion is to use two separate catalysts having basic and acidic properties. However, combined use of base + acid in a single-pot may neutralize catalytic system and hence lower activity might be observed. To avoid this problem, lot of efforts is shown by the researchers and finally, it is proposed that the use of Lewis acid catalysts can carry out isomerization reaction of glucose into fructose and next, dehydration of fructose into HMF is possible in presence of Brönsted acid catalysts. In short, acid catalysts consist of both Lewis and Brönsted acid sites can convert glucose into HMF in one-pot. Furthermore, it is obvious that direct use of non-edible C_6 sugar polymers for the synthesis of HMF using solid acid catalysts is preferable since those poly-saccharides are abundantly available in nature. However, most of the available reports fail to contribute a recyclable catalyst, which is a most important criterion for a catalyst to be industrially applicable.

Considering the issues of catalyst structural instability with the available reports, synthesis of structured solid acid catalyst silicoaluminophosphates (SAPO's) were undertaken and used in HMF synthesis reaction.[5,6] Due to higher hydrothermal and thermal stability of SAPO's determined through TGA analysis,[7-9] it is expected that those

can serve as stable catalysts under reaction conditions. By using several types of SAPO's with difference in properties, it is tried to correlate the catalyst structure-activity relations. SAPO catalysts were evaluated for the synthesis of HMF from variety of substrates such as mono-saccharides (fructose and glucose), di-saccharides (maltose and cellobiose) and poly-saccharide (starch).[5] Furthermore, various physico-chemical characterization techniques were used to understand the catalyst morphology and finally efforts are taken to draw catalyst structure-activity correlation.

5.2. Results and Discussions

5.2.1. Conversion of Fructose into HMF

From literature, it is understood that fructose (C_6 sugar) is the most commonly used substrate for HMF synthesis through acid catalyzed dehydration reaction (Scheme 5.1). Hence, at first fructose was taken as a substrate to know the best solid acid catalyst among others and next, this catalysts was used to optimize the reaction conditions to achieve maximum possible HMF yield. Moreover, literature shows that the use of water + methyl *iso*-butyl ketone (MIBK) in 1:5 (*v/v*) ratio yields the better amount of HMF from fructose compared to water or organic only solvent system.[2,10-17] Hence, in this study the same solvent system (water + MIBK; 1:5 *v/v*) was used to carry out fructose to HMF reaction. The further optimization processes are discussed below.

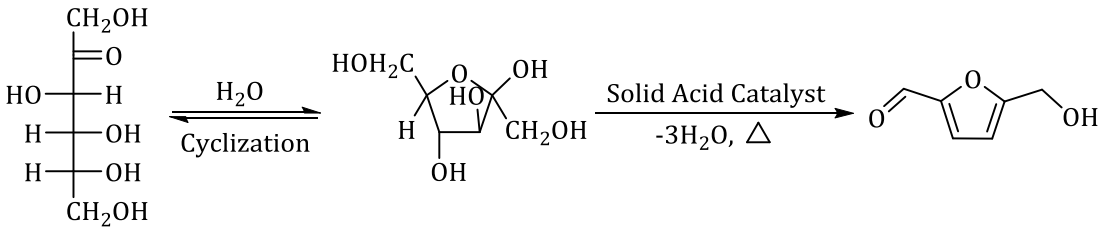

Scheme 5.1. Acid catalyzed dehydration of fructose into HMF.

5.2.1.1. Use of Various Solid Acid Catalysts

Zeolite, HMOR (Si/Al = 10) was considered as a benchmark catalyst since it was shown as the best catalyst among other zeolites (HZSM-5, Hβ).[11,12] Various solid acid catalysts[5] such as SAPO-44, SAPO-46, SAPO-5, SAPO-11 and HMOR (Si/Al = 10) were evaluated for the conversion of fructose in water + MIBK (30 mL, 1:5 *v/v*) at 175°C for 1 h and the

results are shown in Fig. 5.1. As observed, amongst all the catalysts, SAPO-44 catalyst showed the best activity of 78% HMF yield with 88% selectivity (89% conversion).[5] In addition to HMF formation, 6% yield of glucose was also observed. Combining the entire product yields, a total of 94% carbon balance was observed implying that carbon loss due to degradation reactions is negligible. Furthermore, the elemental analysis data confirmed presence of ca. 4% carbon deposition deposited carbon on the spent catalyst surface. Under similar reaction conditions, HMOR yields lower amount of HMF (63%) with inferior selectivity (72%) compared to SAPO-44 since, fructose conversion is high (88%). Moreover, with HMOR catalyst, 6% glucose yield along with HMF formation (63%) displays lower carbon balance (79%). Reaction carried out without catalyst performed under similar reaction conditions presented 29% HMF yield with 74% fructose conversion. It is shown in chapter 2 that with the variation in crystallization time during synthesis of SAPO-44, different materials are synthesized *viz.* zero day crystallization time (ZDCT), 2 days crystallization time (2DCT), 4 days crystallization time (4DCT) and 7 days crystallization time (7DCT/SAPO-44). Further, influence of crystallization time during synthesis of SAPO-44 catalyst on the catalytic activity of material for HMF synthesis from fructose was also investigated (Fig. 5.1). It was found that with increase in crystallization time (ZDCT → 2DCT → 4DCT → SAPO-44) yields of HMF also increases (43% → 60% → 67% → 78% respectively) with improvement in HMF selectivity (55% → 74% → 79% → 88% respectively). It is presented in earlier chapter (section 3.2.1.5, chapter 3) that with increase in crystallization time the CHA phase purity in the material is improved from amorphous phase (ZDCT) to AFI + CHA phase (2DCT) to low crystalline CHA phase (4DCT) to pure CHA phase (SAPO-44). The results also were seen to be improved in the similar line of CHA phase purity in material. The SAPO-46 catalyst was also seen to be active for fructose conversion (79%) into HMF (61%) with better selectivity (77%) compared to HMOR under similar reaction conditions. Other SAPO's *viz.* SAPO-5 and SAPO-11 were less active for fructose conversion and under reaction conditions yielded only 32% and 28% HMF, respectively. This activity difference might be because of lower acid amount and absence of strong acid sites in SAPO-5 (0.8 mmol/g, only weak acid sites) and SAPO-11 (0.3 mmol/g, only weak acid sites). Moreover, it can be seen that though the total acid amount is same (0.8 mmol/g) in both SAPO-5 and SAPO-46 yet, due to absence of strong acid sites, SAPO-5

exerts lower catalytic activity (HMF yield = 32%) compared to SAPO-46 (HMF yield = 61%). This further suggests that presence of strong acid sites in catalyst influences its activity.

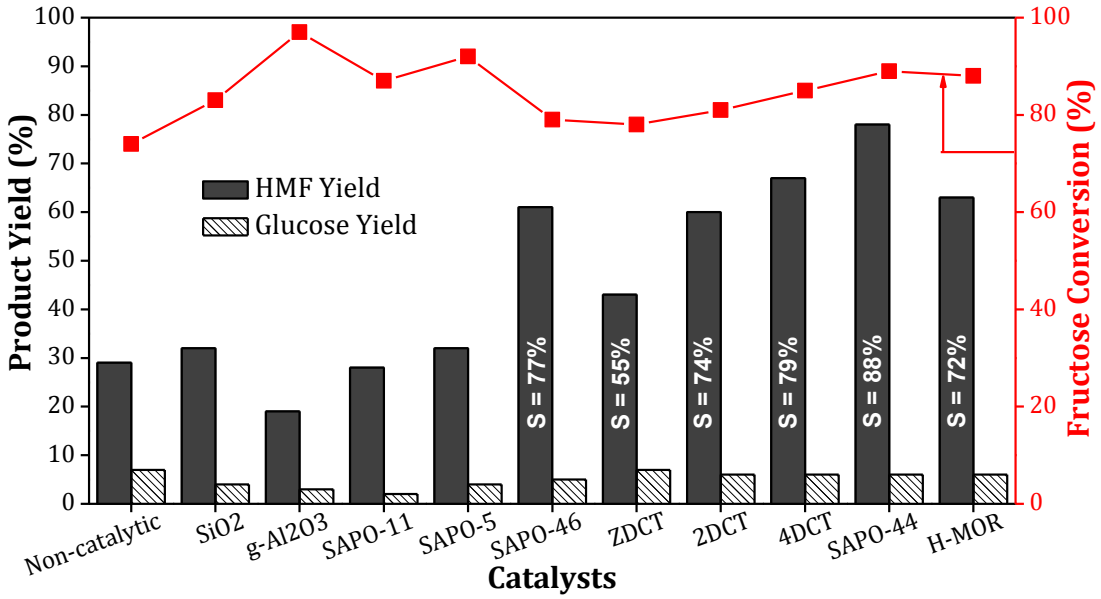

Fig. 5.1. Evaluation of various solid acid catalysts for the conversion of fructose. Reaction conditions: fructose (10 wt% with respect to water), catalyst (0.143 g), water + MIBK = 30 mL (1:5 *v/v*), 175°C, 1 h.

Since SAPO's are made of Si, Al, P elements and HMOR is made of Si, Al elements further, reactions were carried out with individual SiO_2 and γ-Al_2O_3 to understand the effect of those. However, poor yields of HMF were observed with these catalysts due to very less acid amount (SiO_2: weak = 0.1 mmol/g and γ-Al_2O_3: weak = 0.1 mmol/g, moderate = 0.3 mmol/g). Another important factor observed was the formation of humins in these reactions which can be visibly evident from dark black colour of reaction mixture. The similar phenomenon was also evident in earlier literature reports.[18,19] After discussion of all the results it can suggested that addition of Si, Al and P precursors in proper proportions followed by optimized hydrothermal treatment lead to formation of SAPO-44 catalyst which shows better catalytic activity compared to other catalysts.

5.2.1.2. Influence of Reaction Temperature and Atmosphere

Optimization of reaction parameters may play an important role to yield HMF in major amount. Hence, influence of various reaction parameters such as temperature, time and reaction atmosphere were studied for fructose conversion into HMF. SAPO-44 catalyst

showed the best activity among other catalysts for HMF formation from fructose and hence in next studies only SAPO-44 catalyst was used.

Fig. 5.2 represents the influence of reaction temperature and time on fructose conversion into HMF in presence of SAPO-44 catalyst. When the reaction was carried out at lower temperature (165°C) for 1 h, a lesser HMF yield of 43% (77% selectivity) was observed with lower fructose conversion (56%). Now, it was expected that at 165°C by increasing the reaction time to 2 h, yield of HMF may increase. Under this reaction conditions, although, the increase in fructose conversion (76%) was observed, no significant HMF yield (51%) was attained. Later, the reaction carried out at higher temperature (185°C) showed poor yield of HMF (45%) with higher fructose conversion (92%). This eventually leads to lower HMF selectivity (49%) at 185°C. At higher temperature, lower HMF yields can be explained in terms of predominant formation of degradation products (black solid formation in reaction system). This might be due to formation of condensation product of sugar and HMF at higher temperature in presence of acid catalysts.[20,21] To reduce the degradation reactions at 185°C, dehydration reaction was carried out for shorter time (0.5 h) but the HMF yield (53%) was not so attractive. This study confirms that the best temperature to carry out fructose dehydration reaction was 175°C (1 h), yielding highest HMF formation (78%) with highest selectivity (88%).

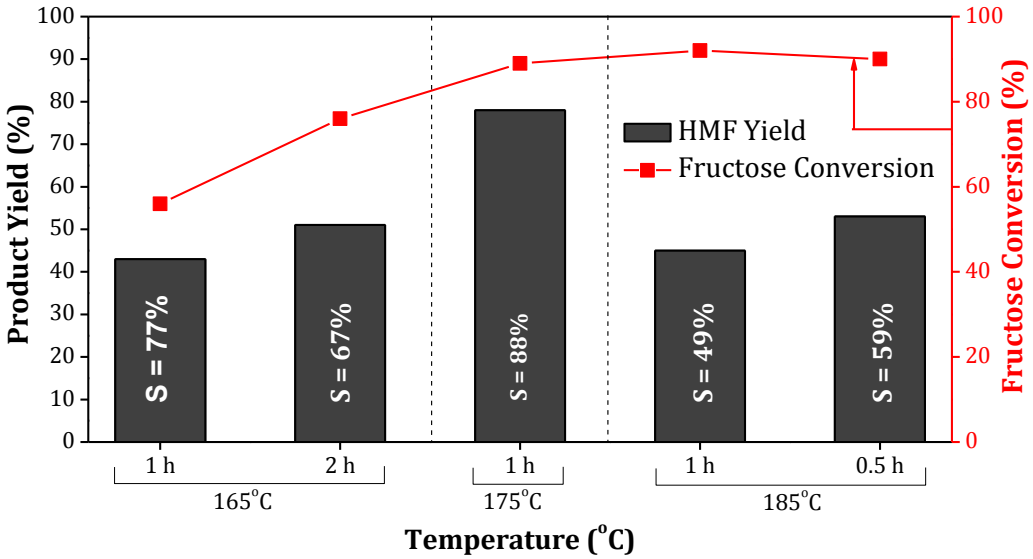

Fig. 5.2. Influence of reaction temperature on fructose conversion into HMF in presence of SAPO-44 catalyst. Reaction conditions: fructose (10 wt% with respect to water), SAPO-44 (0.143 g), water + MIBK = 30 mL (1:5 *v/v*).

Further, to know if reaction atmosphere has any effect on the fructose conversions and HMF yields, reactions were performed under nitrogen and air atmosphere. Over SAPO-44 catalyst, the reactions carried out in both the atmosphere at 175°C, 1 h showed similar results (fructose conversion = 88±2%, HMF yield = 78±2%, glucose yield = 6±1%). This data set confirmed that reaction atmosphere has no effect in this work. Hence, all the later reactions were carried out using SAPO-44 catalyst in air under atmospheric pressure.

5.2.1.3. Effect of Substrate Concentrations

To make sure the process to be operated on industrial scale successfully, it is necessary to develop a process with high substrate concentration. Hence reactions were carried out using 10 wt% and 30 wt% fructose solutions (with respect to water amount) keeping S/C ratio constant. Use of 10 wt% fructose solution for reaction showed excellent yields of HMF (78%) in water + MIBK solution. However, unfortunately, increase in concentration to 30 wt% decreased the HMF yield to 66% (selectivity = 73%) with slight increase in fructose conversion (91%). At very high substrate concentration, after certain interval of reaction, there is high amount of unreacted fructose and high amount of formed HMF in reactor which in presence of acid sites and high temperature may lead to formation of condensation products (humin) and thereby reduces HMF yields. So, 10 wt% fructose solutions were chosen as optimized substrate concentration in all reactions.

5.2.1.4. Influence of Solvent System and Biphasic Ratio

From literature reports it is understood that use of only water as a reaction media leads to formation of side products (humin) as well as it reduces HMF yield.[2,10,16,17] In addition, presence of acidic catalysts in water system accelerates the formation of rehydration products of HMF i.e. formic and levulinic acids.[10] Hence, to overcome formation of these by-products from HMF several organic solvents such as MIBK, 2-butanol, DMSO, ethyl acetate, THF etc. are reported in literature.[2,10,16,17] The purpose of using organic solvent in addition to water in reaction system is to extract HMF from water later to organic layer and thereby separating HMF from acid catalyst contact and hence to suppress further conversion of HMF. But the basic understanding on the earlier

reported solvent system such as water + 2-butanol, water + DMSO, water + ethyl acetate, water + THF etc. informs that those cannot be the good solvent system as these organic solvents are miscible with water and hence the purpose (separation of formed HMF from water containing catalyst and substrate) of using those may not be solved. Therefore, in this work, water + MIBK solvent system was used (Fig. 5.3). However, to compare the data, water only system and organic only system (ethanol; where both fructose and HMF can dissolve) was also used in this study (Fig. 5.3).

Reactions were carried out with fructose in presence of SAPO-44 catalyst at 175°C for 1 h. As expected, use of only water as a solvent forms lower HMF yields (39%) with lower HMF selectivity (59%). However, under similar reaction conditions, use of only ethanol (organic solvent) showed better HMF yield (56%) compared to water only solvent system. This emphasized that in absence of water, rehydration reaction of HMF is not possible. The same observation is also reported earlier where it is shown that change in solvent system from water to organic (DMSO) improves the HMF yield.[10,13,15,17,22,23] Later, biphasic (water + MIBK) system was found to be more suitable to achieve high yields of HMF (78%). This suggests that use of biphasic solvent system (water + MIBK) is more appropriate for this transformation.

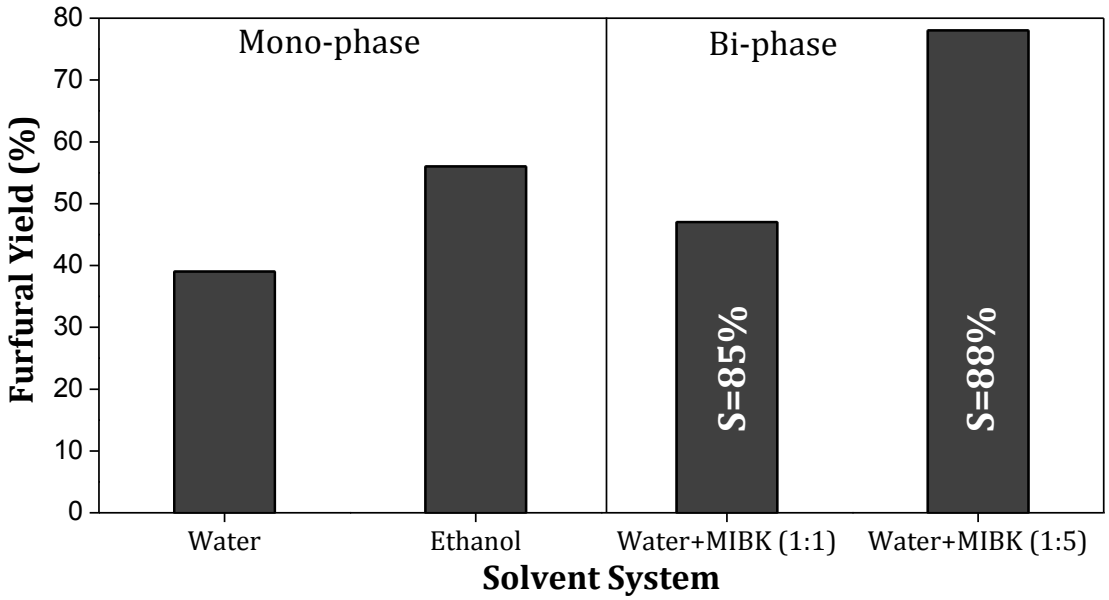

Fig. 5.3. Influence of solvent system and biphasic ratio of HMF synthesis from fructose. Reaction conditions: fructose (10 wt% with respect to water), SAPO-44 (0.143 g), solvent = 30 mL, 175°C, 1 h.

Although, from the above studies, it is understood that use of water + MIBK yields better amount of HMF from fructose however, my aim was to understand the effect of extracting solvent amount i.e. water/extracting solvent ratio on the formation of HMF. To check the effect of water + MIBK ratio on the HMF yield and selectivity, reactions were conducted with 1:1 (*v/v*) and 1:5 (*v/v*) solvent ratios (Fig. 5.3). It was observed that with 1:5 (*v/v*) ratio higher yield of HMF (78%) was seen compared to 1:1 (*v/v*) ratio (47%). Though, in both the reactions HMF selectivity was almost remained same (ca. 85%). Hence, it will be better to carry out reactions with 1:5 (*v/v*) biphasic ratio to obtain higher HMF yield and selectivity.

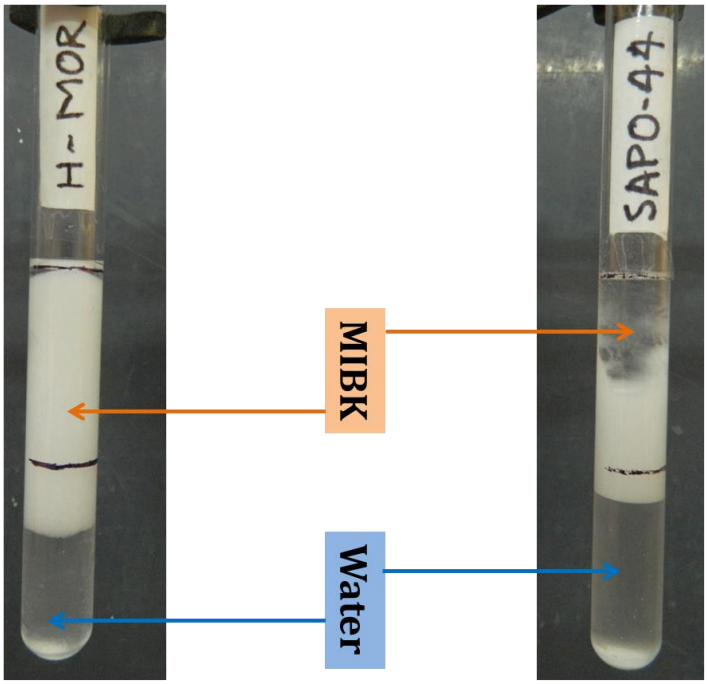

Fig. 5.4. Hydrophilicity-hydrophobicity of catalysts in water + MIBK solvent system.

5.2.1.5. Hydrophilicity-Hydrophobicity of Catalysts

As discussed in chapter 3 (section 3.2.1.3), hydrophilic property of SAPO-44 catalyst influences in the formation of desired product (furfural) by stay separated from furfural compared to less hydrophilic zeolites in water + toluene solvent system. To check whether this concept is valid for water + MIBK solvent system, a study was undertaken with SAPO-44 and HMOR. In a procedure, same amount of both the materials (~0.1 g) were placed in two test tubes and to it, 5 mL water (d = 0.997 g/mL at 25°C) was added.

Next, same amount of MIBK (5 mL, d = 0.802 g/mL at 25°C) was added to both the test tubes maintaining 1:1 *v/v* ratio of water + MIBK and mixed properly. From Fig. 5.4, it can be visible that MIBK occupied the upper layer in solvent system due to less density compared to water. Immediate after mixing, it can be seen that maximum of SAPO-44 came in the water layer (bottom) and very little amount of SAPO-44 remains at the interface of MIBK-water. This is because MIBK has some miscibility in water (16.6 g/L at 30°C, 12.2 g/L at 90°C).[24] On the other hand most of the HMOR remains in the MIBK layer (Fig. 5.4). This study once again proved that in presence of water + MIBK solvent system also SAPO-44 showed higher hydrophilicity compared to HMOR and thereby improves HMF yield.

5.2.1.6. Effect of Catalyst Acidity and Types

The study shown in Fig 5.1 used same amount of catalyst (weight) in all cases although their acid amount were different; this in turn provides different amount of acidity in the reaction system. Now to understand the actual catalytic effect with catalyst acid amount and types, the reactions were carried out keeping same acid amount in reaction system i.e. changing the catalyst amount (Fig. 5.5). Here purposefully, 2DCT (0.4 mmol/g, having only weak acidity) and SAPO-44 (1.2 mmol/g; having both weak + strong acidity) were taken for the study since both of them showed difference in activity (HMF yield = 60% and 78% respectively). Now, increase in 2DCT catalyst amount thrice in reaction allowed the total acid amount similar to the SAPO-44 catalyst system in reaction (1.2 mmol/g). However, even by increasing the charge of 2DCT catalyst the yields of HMF remained same (62%). It can be noted that although, the modified reaction system with 2DCT catalyst has the same total acid amount but the strong acid sites were absent in reaction. Additionally, surface area data shows that 2DCT has lower surface area (155 m^2/g) compared to SAPO-44 (369 m^2/g) and hence, it can be suggested that lower surface area of 2DCT material might influences in its catalytic activity. This emphasized that for boosting the HMF yields further, strong acid sites are required which are not present in 2DCT catalyst but present in SAPO-44. Again in case of HMOR, it can be seen that the presence of higher amount of strong acid sites (0.7 mmol/g) compared to that of SAPO-44 (0.5 mmol/g) reduces the HMF yield. Considering all the above discussions it is possible to say that in the formation of HMF

combined effect of catalyst properties like acid amount, ratio of weak and strong acid sites, hydrophobicity-hydrophilicity play an important role. Overall, SAPO-44 has optimum properties which are required to achieve higher HMF yield and selectivity.

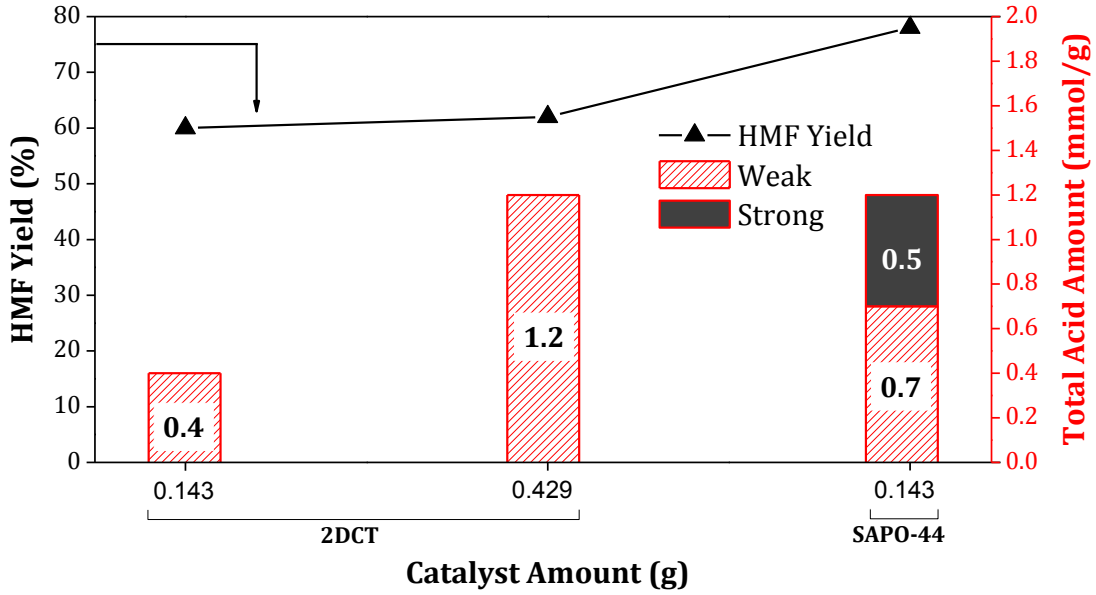

Fig. 5.5. Influence of acid amount and acid sites present in catalysts for HMF synthesis from fructose. Reaction conditions: fructose (10 wt% with respect to water), catalyst, water + MIBK = 30 mL (1:5 *v/v*), 175°C, 1 h.

5.2.1.7. Catalyst Recycle Study

To understand catalyst stability under the optimum reaction conditions [175°C, water + MIBK (1:5, *v/v*), 1 h], catalyst recycle study was carried out. It was discussed earlier in this chapter that fresh SAPO-44 catalyst showed 78% HMF yield from fructose. Now, the catalyst was recovered from the 1st run and after washing with water directly used in the next run. Direct use of recovered catalyst after simple washing with water showed decrease in the catalytic activity (50% HMF yield). This might be due to the adsorption of carbonaceous deposits on the catalytically active sites as a total of 94% carbon balance was observed in the reaction. The elemental analysis of catalyst also supports the presence of carbon (ca. 4%) on the spent catalyst. Later, the carbon deposition was removed from the catalyst by calcination at 550°C for 12 h and used in further reactions. After calcination of spent SAPO-44, its activity was seen to be increased (71% HMF yield) compared to un-calcined one (50% HMF yield). These results proved that

removal of carbonaceous deposits is must to achieve higher activity in recycle runs. Fig. 5.6 showed that with fresh catalyst 78% HMF yield was observed which slightly decreased to 71% in 2nd run and 66% in 3rd run. However, 3rd run onwards activity remained almost constant up to 5th run (4th run: 65%, 5th run: 65%). Noteworthy, in all five runs HMF selectivity remains almost similar (80-88%). The decrease in the activity in initial recycle runs can be attributed to the fact that SAPO-44 undergoes minor morphological changes (more details are discussed later in section 5.4 based on XRD, NMR, TPD-NH_3, ICP and N_2 sorption analysis data). Conversely, HMOR catalyst showed decrease in the activity in each consecutive runs up to 5th recycle run (HMF yield; 1st run: 63%, 2nd run: 40%, 3rd run: 34%, 4th run: 30%, 5th run: 28%). After 4th recycle run, HMOR catalyst showed activity similar to non-catalytic reaction (29% yields). This suggests that after 4th run HMOR catalyst is no more active to carry out fructose conversion reaction. This behaviour of HMOR catalyst is obvious since under the reaction conditions it undergoes morphological modifications to make the catalyst inactive as described in earlier report.[25] Recycle study of catalysts further confirmed the superiority of SAPO-44 catalyst compared to zeolite, HMOR.

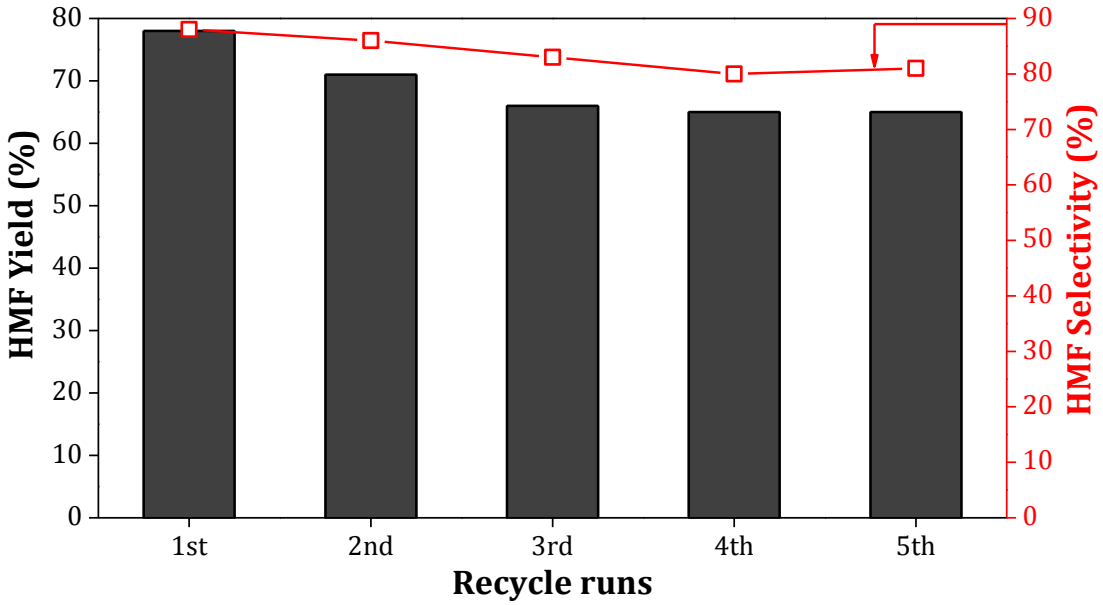

Fig. 5.6. Recycle activity of SAPO-44 catalyst in synthesis of HMF from fructose. Reaction conditions: fructose (10 wt%), SAPO-44 (approx. 0.143 g in all runs), water + MIBK = 30 mL (1:5 *v/v*), 175°C, 1h.

5.2.1.8. Isolation of HMF

Considering industrial applicability, it is essential to show the possibility of isolation of HMF from the reaction mixture and later to confirm the purity of HMF with NMR spectroscopy. The reaction mixture was collected after processing of fructose under the best reaction conditions (10 wt% fructose with respect to water, SAPO-44, water + MIBK (30 mL, 1:5 *v/v*), 175°C, 1 h). After separation of water and MIBK layer from each other, MIBK layer containing HMF was collected in a round-bottom flask. Now, MIBK was evaporated completely in rotary evaporator and the semi-solid mass obtained was directly taken for ^{1}H NMR analysis using D_2O solvent (Bruker Avence-200 MHz spectrometer) without further purification. NMR data is shown in Fig. 5.7 which confirmed that the semi-solid obtained after MIBK removal was actually pure form of HMF.[5] Based on the solid recovered, further the yield of isolated HMF was calculated and it was found to be 88% considering total HMF yield in the reaction as 100%.

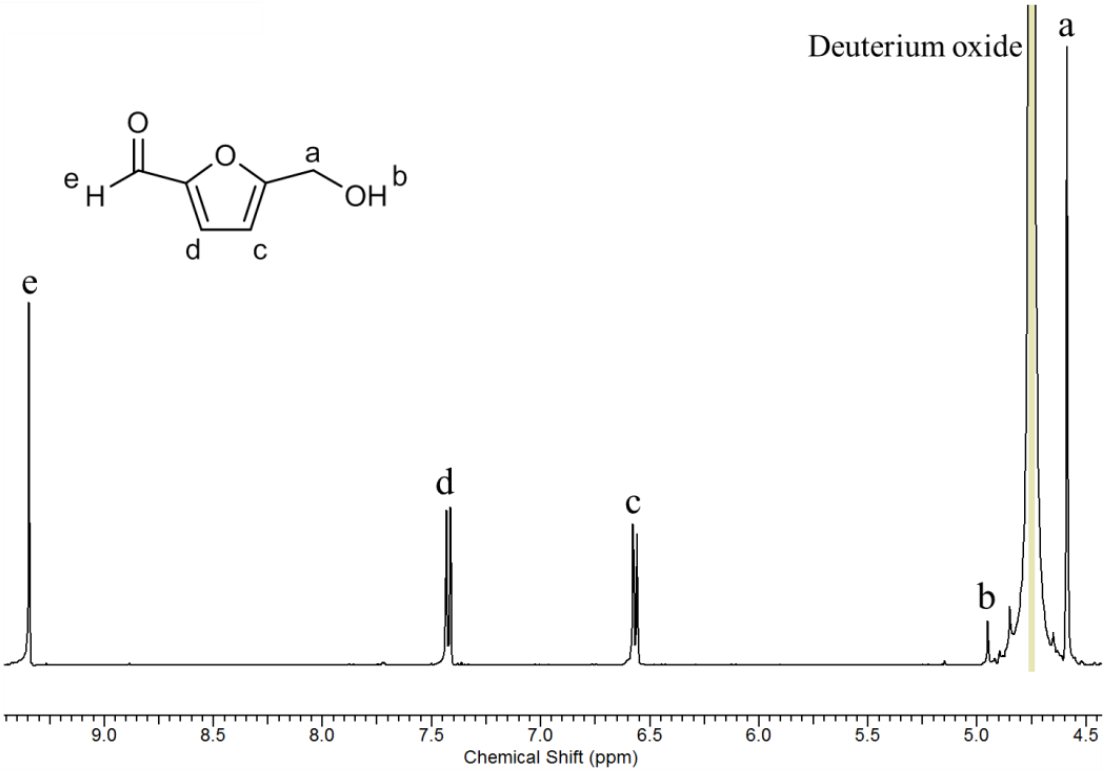

Fig. 5.7. ^{1}H NMR spectra for isolated HMF from reaction mixture.

5.2.2. One-Pot Conversion of Glucose into HMF via Fructose Formation

Although, it was shown that fructose can be converted into HMF with very high selectivity, but in terms of fructose availability, the process needs to be modified with the use of cheaply and abundantly available glucose. In presence of Lewis acid sites present in SAPO-44 catalyst first, glucose may isomerize into fructose and later, fructose is dehydrated into HMF[5] (Scheme 5.2).

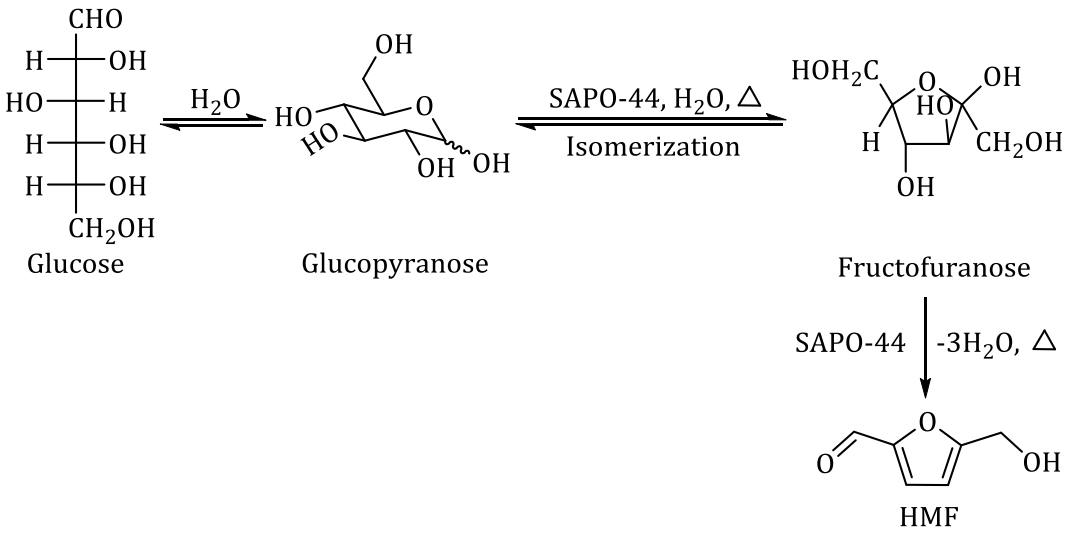

Scheme 5.2. Acid catalyzed direct conversion of glucose into HMF via fructose.

When SAPO-44 was used as a solid acid catalyst, it offered 67% HMF yield (81% selectivity) from 83% glucose conversion in one-pot method after 4 h at 175°C. In addition to HMF formation, the intermediate (isomerization) product, fructose (13%) in the reaction mixture was also observed. Combining these two product yields, a very good carbon balance of 96% was observed in presence of SAPO-44 catalyst. Further, HMOR catalyst was also checked for the glucose conversion under reaction conditions but a lower yield of HMF (49%) was evident compared to SAPO-44 catalyst. It is noteworthy to point out here that SAPO-44 could convert glucose efficiently into HMF without addition of any other catalyst (such as base). This data elucidates that presence of Lewis acid functionality in SAPO-44 isomerizes glucose into fructose through intramolecular 1,2 hydride shifting (Section 1.7.2; chapter 1) and further fructose dehydrates into HMF in presence of SAPO-44 acid sites.

5.2.3. Use of Di- and Poly-saccharides for HMF Synthesis

Use of glucose again is not a good option as it may create food crisis in society. Hence, it will be better if directly poly-saccharides of glucose (starch and cellulose) can be used as substrate for HMF synthesis since; those are profusely available in nature. However, in this work first di-saccharides of glucose (α-dimer: maltose and β-dimer: cellobiose) as substrate was tried and it can be expected that those di-saccharides may mimic their poly-saccharides. In this point of view, maltose and cellobiose were examined for HMF synthesis in presence of SAPO-44 catalyst (Scheme 5.3). Later, starch (glucose α-1,4-polymer) was also used as substrate for HMF synthesis in presence of SAPO-44 catalyst (Scheme 5.3).

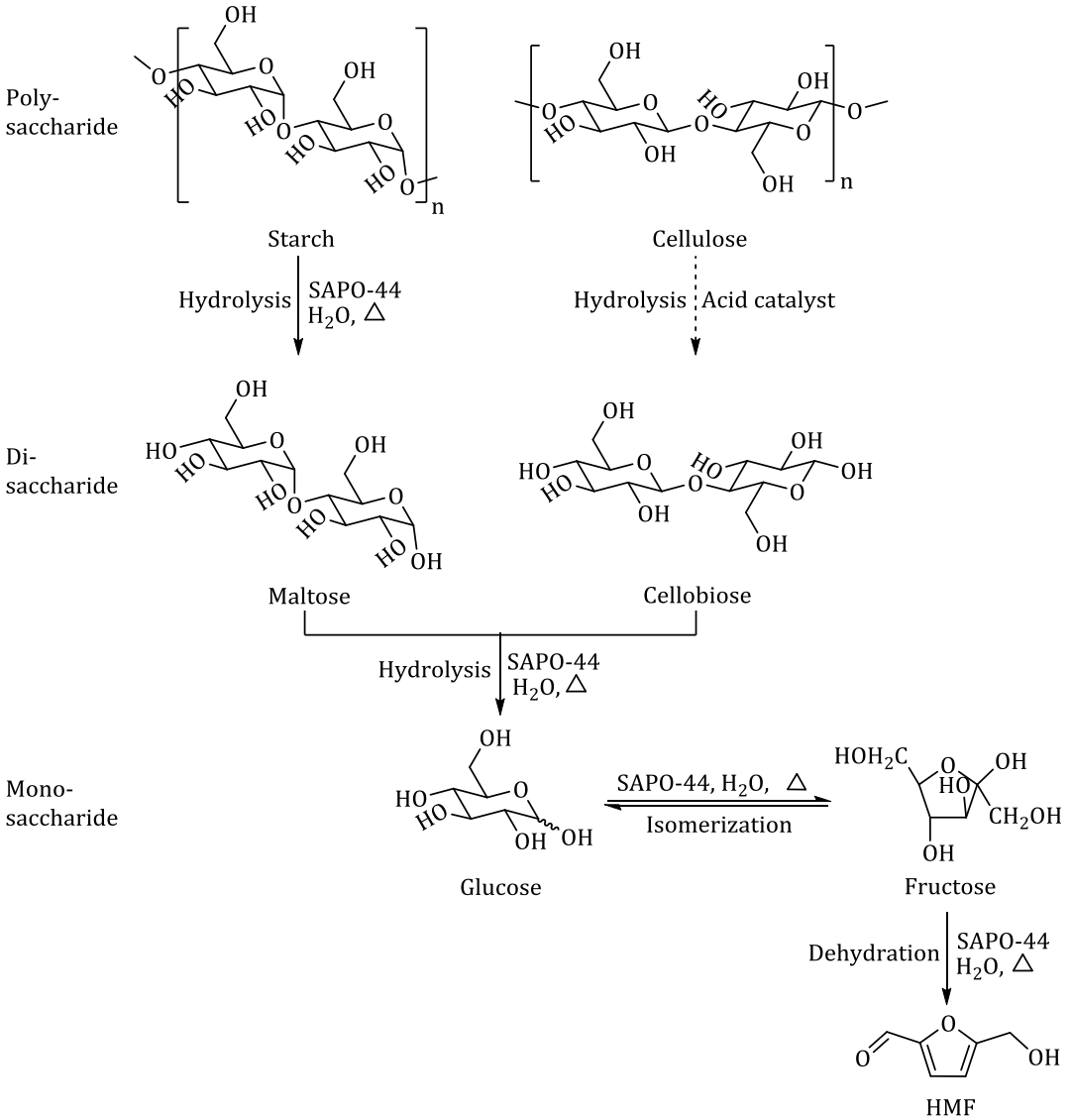

Scheme 5.3. One-pot conversion of poly- and di-saccharides into HMF using SAPO-44. The work shown by dotted arrow is not done by me.

SAPO-44 was used for the one-pot conversion of dimers of glucose such as maltose and cellobiose to yield HMF[5] and the results are summarized in Table 5.1. In all the reactions, complete conversion of substrates was observed. At 175°C, SAPO-44 converts maltose directly into HMF (57%) within 4 h reaction time. Along with HMF, 14% yield for glucose + fructose was obtained. Conversely, HMOR gave only 41% HMF yield under similar reaction conditions. When cellobiose is used as a substrate, 56% yield of HMF, along with 12% yield of glucose + fructose at 175°C within 6 h of reaction time was observed over SAPO-44. The HMOR catalyst gave 43% HMF yield under similar reaction conditions from cellobiose.

Table 5.1. One-pot conversion of di- and poly-saccharide of glucose into HMF.

Substrate	Reaction Time (h)	Catalyst	Glucose yield (%)	Fructose yield (%)	HMF yield (%)
Maltose	4	No-catalyst	17	8	22
Maltose	4	HMOR	1	2	41
Maltose	4	SAPO-44	5	9	57
Cellobiose	6	No-catalyst	21	9	15
Cellobiose	6	HMOR	2	3	43
Cellobiose	6	SAPO-44	7	5	56
Starch	6	No-catalyst	17	7	29
Starch	6	HMOR	10	8	41
Starch	6	SAPO-44	15	7	68

Reaction conditions: substrate (10 wt% with respect to water), 175°C, water + MIBK = 30 mL (1:5 *v/v*).

Later, glucose poly-saccharide, starch was used as a substrate for the synthesis of HMF in one-pot fashion.[5] SAPO-44 catalyst converts starch into higher yield of HMF (68%) at 175°C within 6 h reaction time (Table 5.1). Along with HMF, formation of glucose (15%) and fructose (7%) was also evident. Now, it was thought that increase in further reaction time may lead to higher HMF yield. However, when reaction was conducted for 8 h HMF yield decreased to 61%, which might be due to the occurrence of

side reactions leading to brown colour solid (humin) formation.[26] Under similar reaction condition HMOR has shown lower activity to yield less HMF (41%).

Similar phenomenon of humin formation from sugars and HMF in presence of absence of acid catalysts is reported in literature.[27-33] Humins are generally water insoluble brown coloured polymeric organic compounds formed by condensation reactions between furans and sugars. One report shows the elemental composition of humins as C = 61.2 wt%, H = 4.5 wt% and average particle size = 5-10 μm.[34] In another report humin elemental composition is shown as C = 55.7%, H = 4.5%, O = 30.4%.[32] One more report presents elemental composition of humin as O/C = 0.33-0.39, H/C = 0.68-0.79 and particle size = 1-8 μm.[33] Moreover, it is suggested that formation of humin and its structure is dependent on the substrate used, reaction temperature, reaction time, solvent etc. Furthermore, the GC-MS data confirms that in humin furans ring presents in higher amount (60%) compared to aliphatic chains (20%).[35] Later, using FT-IR (Furrier Transform Infra-red) analysis technique, the functional groups present in humin are determined as hydroxyl, carbonyl, C=C, aliphatic C-H, aromatic rings etc.[36] Additionally, UV-Vis (Ultra Violet Visible) absorption in the range of λ=330-500 nm assure the existence of conjugated π-bonded systems in humins.[36] In another report, the IR spectral analysis of humin approves the presence of C-O, C=O, C-C, C-H bonds in its structure.[33] The presence of various types of carbon environment *viz.* C=O, HC=O, COOH, COOR, C=C-O, C-C=C-C, C-C=C-O, C-OH, C-O-C, C-H, -CH_2-, -CH_3, C in humin is also proposed based on 2D Pass (two-dimensional phase-adjusted spinning sidebands) ^{13}C NMR spectroscopy.[33] Considering the above discussions, it can be said that the formation of humin and its structure is dependent on various factors as mentioned above and till now researchers are struggling to determine exact structure of humin.

5.3. Possible Degradation Pathways

Considering all the processes, it is understood that in presence of acid catalysts (SAPO-44 and HMOR) side reactions are also possible along with HMF formation reaction since carbon balance is less (SAPO-44: 94% and HMOR: 79%). Hence, it is important to know which catalyst allows more side reactions and how the side reactions are taking place.

Three pathways are possible for the formation of side products in fructose to HMF reactions[5] such as,

1. Conversion of HMF into degradation products
2. Conversion of fructose to unwanted products
3. Condensation reaction between fructose and HMF

To realize which of these reactions were playing a major role in decreasing the selectivity for HMF, first HMF stability study was undertaken at 175°C for 1 h with various catalysts such as SAPO-44, 4DCT, 2DCT, ZDCT, SAPO-5, SAPO-11, SAPO-46 and HMOR. Surprisingly, the results showed that HMF remained stable under the reaction conditions (175°C, 1 h) in presence of all catalysts and hence possibility of further degradation of HMF was ruled out.

The study on the second possibility of fructose conversion to unwanted products cannot be performed since in any case fructose will give rise to HMF and other products.

Third possibility is the formation of condensation products arising from fructose and HMF. To study this, reaction was carried out with a mixture of fructose and HMF as substrates at 175°C, 1 h in presence of SAPO-44 or HMOR in water + MIBK (1:5, *v/v*). Reaction was carried out with a mixture of 0.25 g fructose (half of fructose charged in all reactions; considering 50% reaction was already taken place) and 0.17 g HMF (50% of fructose will give 0.17 g HMF yield considering 88% selectivity). After reaction, analysis was done and the results are illustrated in Fig. 5.8.

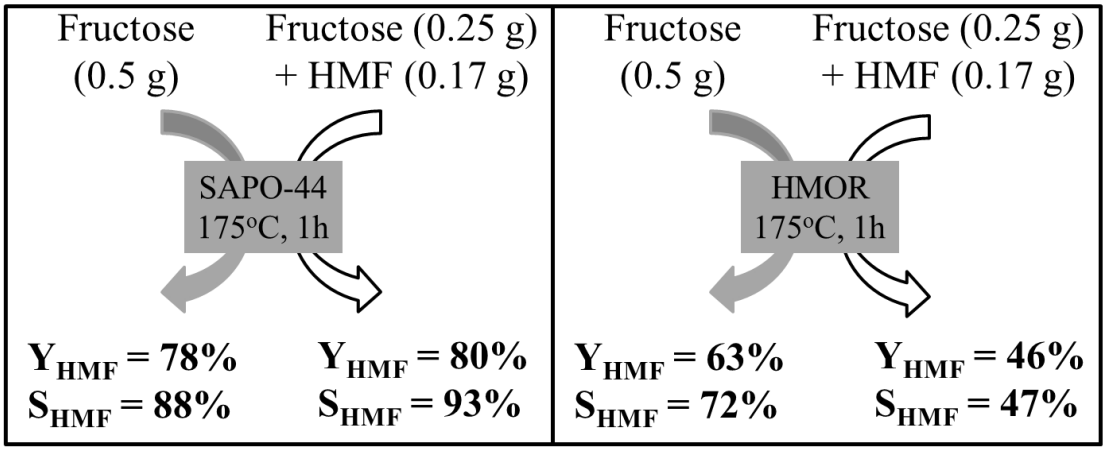

Fig. 5.8. Illustration of reaction system with single and mixture of substrates in presence of SAPO-44 and HMOR catalyst.

The data represented in Fig. 5.8 confirmed that over SAPO-44 catalyst almost similar HMF yield (78-80%) and selectivity (88-93%) was observed either with single substrate (fructose) or with mixture of substrates (fructose + HMF). However, use of HMOR catalyst reduces HMF yield (46%) and selectivity (47%) with mixture of substrate (fructose + HMF) compared to single fructose as substrate (HMF yield = 63%, selectivity = 72%). Hence, it is clear that in presence of HMOR catalyst, fructose and HMF undergoes condensation reactions leading to humin type by-product formation. This is possible since majority of strongly acidic HMOR remained in organic phase due to higher hydrophobicity (for details please see section 5.2.1.5.) and hence, come in contact with extracted HMF and remaining fructose to produce condensation products. The detail calculations were shown below.

Reaction with SAPO-44 as catalyst:

Initially charged fructose = 0.25 g

If 100% fructose conversion and 100% HMF selectivity is possible then it will produce 0.175 g HMF from 0.25 g fructose.

Fructose conversion = 89% i.e. 0.22 g fructose was converted.

Now, if, 0.22 g fructose was converted into HMF with 100% selectivity, a HMF yield of [(0.22 × 126) / 180] = 0.15 g will produce.

Initially we charged 0.17 g HMF and after reaction we obtained 0.31 g HMF.

Hence, (0.31-0.17 g) = 0.14 g HMF was formed under the reaction conditions (considering HMF does not undergo any conversion under reaction conditions; as was proved in HMF stability experiments).

So the additional formed HMF selectivity = [(0.14 × 100) / 0.15] = 93%.

Additional HMF yield = [(0.14 × 100) / 0.175] = 80%

Reaction with HMOR as catalyst:

Initially charged fructose = 0.25 g

If 100% fructose conversion and 100% HMF selectivity is possible then it will produce 0.175 g HMF from 0.25 g fructose.

Fructose conversion = 95% i.e. 0.24 g fructose was converted.

Now, if, 0.24 g fructose was converted into HMF with 100% selectivity, a HMF yield of [(0.24 × 126) / 180] = 0.17 g will produce.

Initially we charged 0.17 g HMF and after reaction we obtained 0.25 g HMF.

Hence, (0.25-0.17 g) = 0.08 g HMF was formed under the reaction conditions (considering HMF does not undergo any conversion under reaction conditions; as was proved in HMF stability experiments).

So the additional formed HMF selectivity = [0.08 × 100) / 0.17] = 47%

Additional HMF yield = [(0.08 × 100) / 0.175] = 46%

5.4. Catalyst Characterizations: Fresh and Spent SAPO-44

From the discussions on recycle experiment (section 5.2.1.7), it is understood that under the reaction conditions SAPO-44 might underwent morphological changes. To study this issue in detail, both fresh and spent SAPO-44 (recovered after 1st recycle run) catalysts were subjected to various physico-chemical characterizations. Spent SAPO-44 was calcined at 550°C for 12 h in presence of air (flow = 10 mL/min) before analysis.

5.4.1. XRD analysis

The XRD patterns for fresh and spent SAPO-44 catalysts (recovered after 1st recycle run) are presented in Fig. 5.9. The XRD pattern for fresh SAPO-44 catalyst was matches well with the literature report and confirms that SAPO-44 crystallized with CHA morphology.[37,38] In case of spent SAPO-44 material, XRD patterns were matching fine with the fresh SAPO-44 material however; peak intensities were decreased implying

that crystallinity of the SAPO-44 became lower. Careful observation of spent SAPO-44 XRD patterns resembled the XRD patterns for 4DCT material (Fig. 5.9). Moreover, it can be seen from recycle study that the catalytic results for spent SAPO-44 (HMF yield = 71%) was similar to that of 4DCT material (HMF yield = 67%). It is important to note here that though peak intensities in spent SAPO-44 catalyst was reduced but none of the peak(s) are completely vanished.

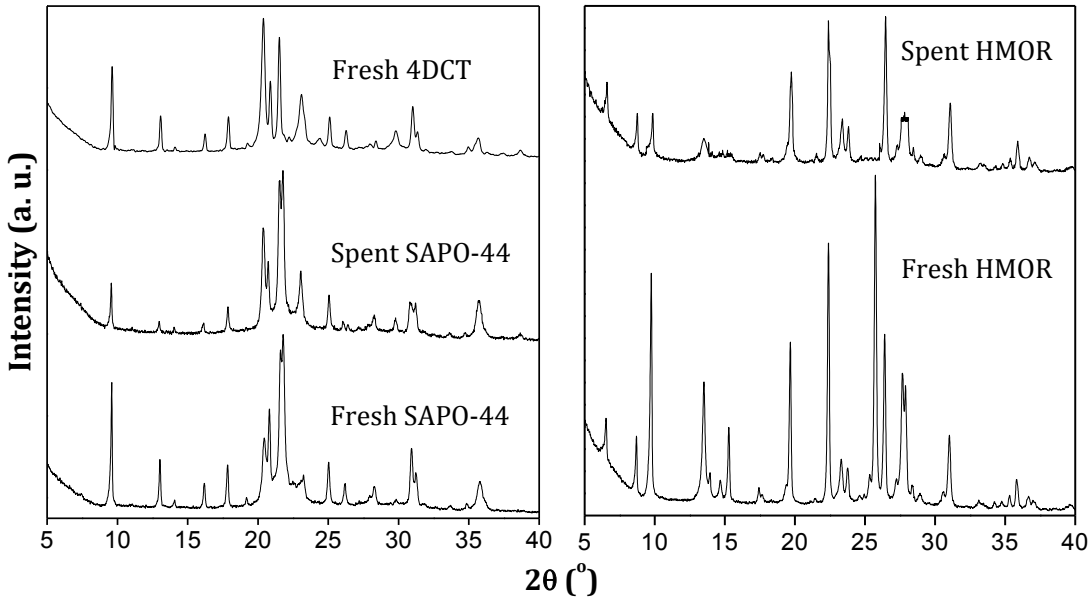

Fig. 5.9. XRD patterns for fresh and spent catalysts.

Fig. 5.9 showed the XRD patterns for the fresh and spent HMOR samples. In the XRD of spent HMOR sample compared to fresh HMOR sample lower peak intensity for all the peaks was observed. Moreover, it can be seen that the highest intense peak due to (202) at 2θ = 25.8° present in the fresh HMOR sample was absent in the spent HMOR sample. This clearly indicates that during the reaction HMOR catalyst undergoes serious morphological changes compared to SAPO-44. The similar morphological modification of HMOR catalyst is also proven earlier with the help of various physico-chemical techniques (XRD, NMR, TPD-NH_3, ICP etc.).[25]

5.4.2. Solid State NMR analysis

Solid state ^{31}P, ^{27}Al, and ^{29}Si MAS NMR spectra of fresh and spent SAPO-44 were recorded to understand the changes in the local environment of SAPO-44 after reaction. The NMR spectra of fresh SAPO-44 shown in Fig. 5.10 were well matches with the

literature report.[37] A more detail discussion on the local environment around P, Al and Si elements in fresh SAPO-44 is already discussed in section 2.5.2, chapter 2.

In ^{31}P MAS NMR spectra a sharp peak at -31.5 ppm in both fresh and spent SAPO-44 catalysts was observed [Fig. 5.10.A)]. This peak is characteristics of tetrahedrally co-ordinated phosphorous [P(4Al)] in SAPO-44 framework. Careful observation suggested that in spent catalyst the peak has broadened which may imply that few other P species are forming under reaction conditions.

^{27}Al MAS NMR spectrum showed major peak at 38.2 ppm which can be assigned to the presence of tetrahedrally coordinated aluminium in the framework of fresh and spent SAPO-44 [Fig. 5.10.B)]. Additionally, in both fresh and spent catalyst a minor peak was observed at ca. -15.0 ppm for octahedral Al species. The octahedral Al species is possible via coordination of water molecule to the tetrahedral $Al(OSi)_4$ species to form $Al(OSi)_3(H_2O)_3$ species.[39] Moreover, in fresh SAPO-44 catalyst, peak broadening was observed which may point out that few other Al (5-cordinated, distorted 4-cordinated) species may present.

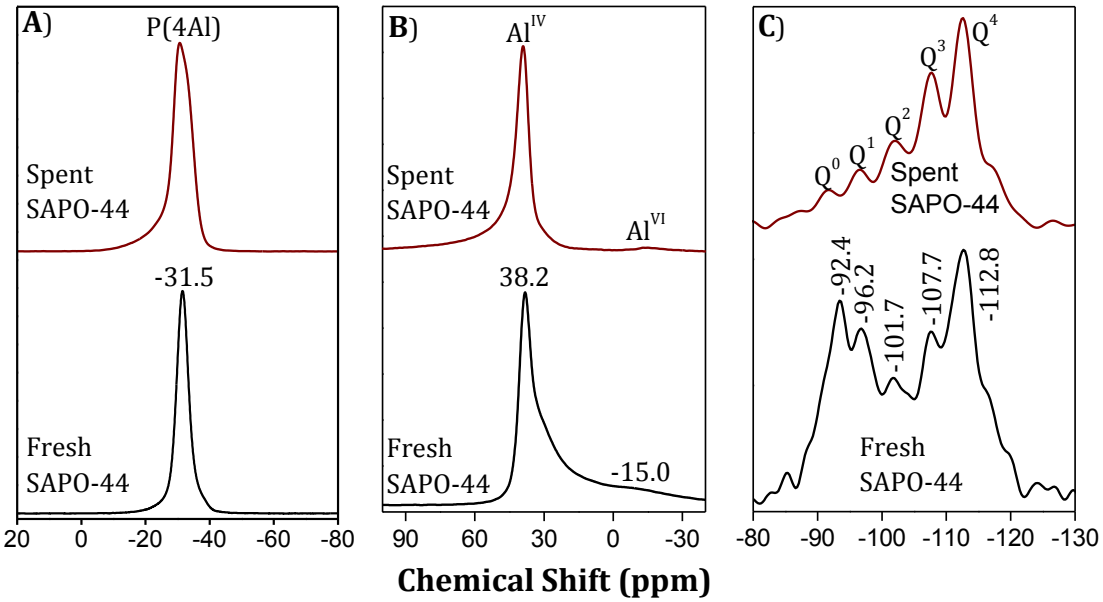

Fig. 5.10. Solid state NMR analysis of fresh and spent SAPO-44. A) ^{31}P NMR, B) ^{27}Al NMR, C) ^{29}Si NMR.

^{29}Si MAS NMR spectra for fresh and spent SAPO-44 catalyst showed multiple signals suggesting that Si is present in multiple environments. Fig. 5.10.C) showed the

presence of all the peaks corresponds to Q^0 (-92.4 ppm), Q^1 (-96.2 ppm), Q^2 (-101.7 ppm), Q^3 (-107.7 ppm) and Q^4 (-112.8 ppm) species in spent SAPO-44 as like fresh SAPO-44 catalyst. However, the change in intensity confirmed that SAPO-44 undergoes morphological modifications during the catalytic runs. It can be clearly seen from Fig. 5.10.C) that the intensity of Q^0 [Si(4Al)] and Q^1 [Si(3Al)] species are decreased with increase in intensity for Q^2 [Si(2Al)], Q^3 [Si(1Al)] and Q^4 [Si(0Al)] species. This suggests that some amount of silica comes out from the uniform composite framework of SiO_2, Al_2O_3 and P_2O_5 to make the framework non uniform. This may lead to formation of SAPO-44 framework along with some amount of ALPO framework and to it detached silica are attached. The same can be seen from the XRD pattern of spent SAPO-44 catalyst (Fig. 5.9) which clearly indicates the higher peak intensity for ALPO-44 (2θ = 20.5° and 21.7°) although, other peak intensities are less. Additionally, it is known that incorporation of Si in ALPO framework lead to generation of acidity in SAPO-44.[7] Hence, it can be expected that removal of silica from uniform composite framework may reduce acidity in spent SAPO-44 catalyst. The expected phenomenon is discussed more in next section.

5.4.3. TPD-NH_3, ICP-OES, N_2 Sorption and SEM analysis

To check the possibility of change in acid amount and acid sites present in SAPO-44 under the reaction conditions with the change in SAPO-44 structure later, TPD-NH_3 analysis was undertaken. The TPD-NH_3 profile for fresh and spent SAPO-44 catalysts is shown in Fig. 5.11. The data presented in Table 5.2 informs that lower total acid amount was available in spent SAPO-44 catalyst (0.5 mmol/g) compared to fresh SAPO-44 catalyst (1.2 mmol/g). Noteworthy, strong acid sites present in fresh SAPO-44 catalyst were completely vanished in spent SAPO-44 catalyst. This data further approved the morphological modification in SAPO-44 under reaction conditions.

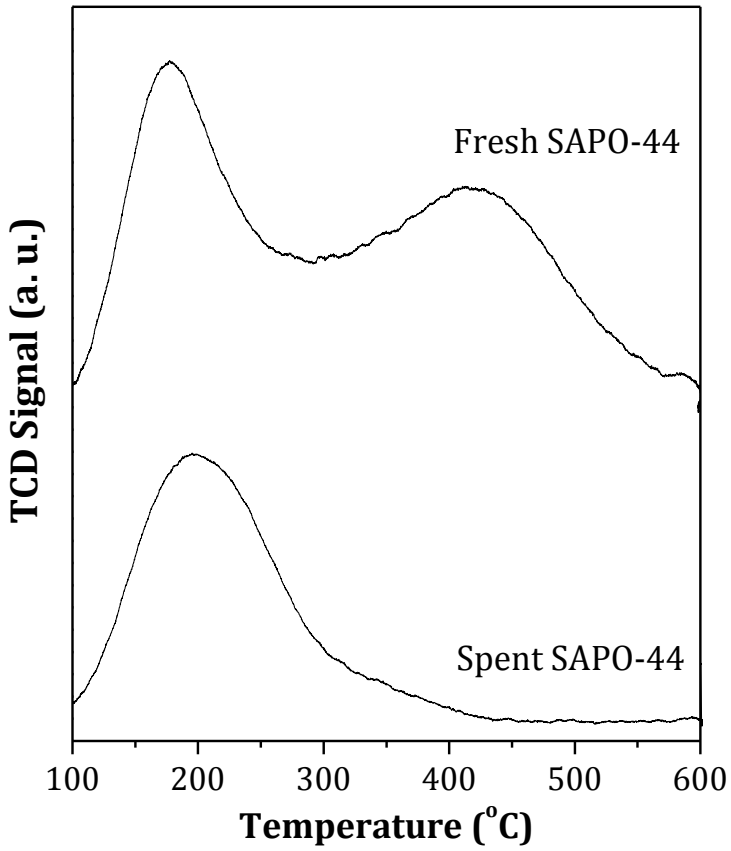

Fig. 5.11. TPD-NH_3 profile for fresh and spent SAPO-44 catalysts.

Furthermore, the ICP-OES analysis of both fresh and spent SAPO-44 was undertaken to know the amount of Al and P present in catalyst. The data shown in Table 5.2 confirmed that the amount of Al and P present in both fresh and spent SAPO-44 were similar. Moreover, the absence of Al and/or P in the reaction solution suggests that elements are not leached out during the reaction. Hence, from these analysis data it can be proposed that the local environment around Si, Al and P in SAPO-44 has altered without leaching out elements in solution under reaction conditions.

Table 5.2. Physico-chemical characterizations of fresh and spent SAPO-44.

Catalyst	Acid amount (mmol/g)[a]			Elemental analysis (ppm)[b]		Surface area (m^2/g)[c]
	Weak	Strong	Total	Al	P	
Fresh SAPO-44	0.7	0.5	1.2	22.5	24.6	369
Spent SAPO-44	0.5	0.0	0.5	21.7	25.3	133

[a]TPD-NH_3 analysis, [b]ICP-OES analysis, [c]N_2 sorption analysis

The specific surface area data of catalysts is summarized in Table 5.2. It was observed that after the catalytic run, surface area of SAPO-44 decreased from 369 m^2/g (fresh) to 133 m^2/g (spent). The decrease in surface area might be due to the fact that SAPO-44 undergoes some morphological changes during the reaction.

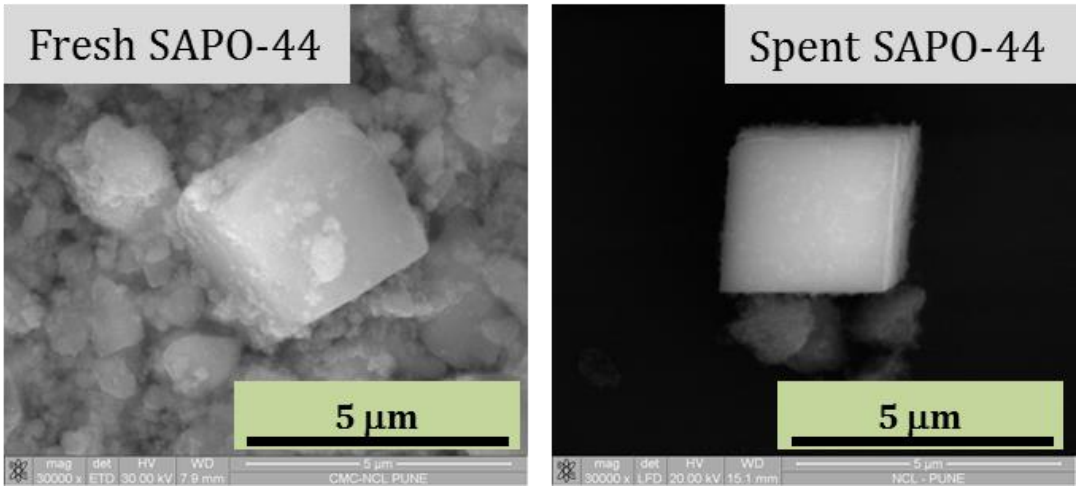

Fig. 5.12. SEM images of fresh and spent SAPO-44.

Fig. 5.12 represents the SEM images for fresh and spent SAPO-44 catalyst. SEM images of both fresh and spent SAPO-44 indicate the presence of cubic morphology with similar edge length (fresh = 2.79 µm, spent = 2.83 µm).

Combining the results of various physico-chemical characterizations (XRD, NMR, TPD-NH_3 and N_2 sorption) it is now confirmed that SAPO-44 catalyst undergoes slight morphological changes under the reaction conditions employed. However, ICP analysis data suggests that the change in spent SAPO-44 catalyst is not because of leaching of elements from catalyst. Moreover, SEM images of spent SAPO-44 catalyst inform that cubic morphology of SAPO-44 remains intact after use. This finally suggests that although, SAPO-44 catalyst morphological modification is evident however, the change is not huge as observed in case of HMOR catalyst. Hence, recycle activity with SAPO-44 catalyst is possible.

5.5. Conclusions

In this work, various structured SAPO catalysts having acid functionality were synthesized aiming that those might show better stability compared to zeolite catalysts. Among SAPO's (SAPO-44, SAPO-46, SAPO-5 and SAPO-11) and other catalysts (SiO_2, γ-Al_2O_3, HMOR), SAPO-44 showed the best activity for efficient synthesis of HMF (78%) from fructose at 175°C, 1 h. It was demonstrated that use of MIBK solvent in addition to water influences in selective formation of HMF. The high activity achieved may be attributed to the properties associated with the catalyst such as, hydrophilicity, phase purity, acid amount, strong to weak acid site ratio etc. Furthermore, the formed HMF was easily isolated in pure form from reaction mixture by simply evaporation of solvent. In the recycle study, marginal decrease in the SAPO-44 activity was observed until 3rd run however it remained constant up to 5th run. The SAPO-44 catalyst is also active in the one-pot conversions of other substrates *viz.* mono- (glucose), di- (maltose, cellobiose) and poly-saccharide (starch) directly into HMF indicating that separate reactor is not required to form fructose from these substrates. Precisely, the influence of Lewis acid sites present in SAPO-44 to carry out isomerization reaction of glucose into fructose is a key novelty of this work. This method allowed processing of poly-, di-saccharides and glucose directly into HMF in one-pot method. However, a thorough catalyst characterization study allowed to state that SAPO-44 catalyst undergoes slight morphological changes during the reaction.

5.6. References

(1) Bozell, J. J.; Petersen, G. R. *Green Chem.* **2010**, *12*, 539.
(2) Hu, L.; Zhao, G.; Hao, W.; Tang, X.; Sun, Y.; Lin, L.; Liu, S. *RSC Adv.* **2012**, *2*, 11184.
(3) Moliner, M.; Roman-Leshkov, Y.; Davis, M. E. *Proc. Nat. Acad. Sci.* **2010**, *107*, 6164.
(4) Takagaki, A.; Ohara, M.; Nishimura, S.; Ebitani, K. *Chem. Commun.* **2009**, 6276.
(5) Bhaumik, P.; Dhepe, P. L. *RSC Adv.* **2013**, *3*, 17156.
(6) Bhaumik, P.; Deepa, A. K.; Kane, T.; Dhepe, P. L. *J. Chem. Sci.* **2014**, *126*, 373.
(7) Lok, B. M.; Messina, C. A.; Patton, R. L.; Gajek, R. T.; Cannan, T. R.; Flanigen, E. M. *J. Am. Chem. Soc.* **1984**, *106*, 6092.
(8) Bhaumik, P.; Dhepe, P. L. *ACS Catal.* **2013**, *3*, 2299.
(9) Bhaumik, P.; Dhepe, P. L. *RSC Adv.* **2014**, *4*, 26215.
(10) Rosatella, A. A.; Simeonov, S. P.; Frade, R. F. M.; Afonso, C. A. M. *Green Chem.* **2011**, *13*, 754.

(11) Moreau, C.; Durand, R.; Razigade, S.; Duhamet, J.; Faugeras, P.; Rivalier, P.; Ros, P.; Avignon, G. r. *Appl. Catal. A: Gen.* **1996**, *145*, 211.
(12) Ordomsky, V. V.; Schaaf, J. V.; Schouten, J. C.; Nijhuis, T. A. *J. Catal.* **2012**, *287*, 68.
(13) Zhao, Q.; Wang, L.; Zhao, S.; Wang, X.; Wang, S. *Fuel* **2011**, *90*, 2289.
(14) Saha, B.; Abu-Omar, M. M. *Green Chem.* **2014**, *16*, 24.
(15) Gallezot, P. *Chem. Soc. Rev.* **2012**, *41*, 1538.
(16) Dutta, S. *RSC Adv.* **2012**, *2*, 12575.
(17) Karinen, R.; Vilonen, K.; Niemelä, M. *ChemSusChem* **2011**, *4*, 1002.
(18) Antal Jr, M. J.; Mok, W. S. L.; Richards, G. N. *Carbohydr. Res.* **1990**, *199*, 91.
(19) Villa, A.; Schiavoni, M.; Fulvio, P. F.; Mahurin, S. M.; Dai, S.; Mayes, R. T.; Veith, G. M.; Prati, L. *J. Energy Chem.* **2013**, *22*, 305.
(20) Huber, G. W.; Chheda, J. N.; Barrett, C. J.; Dumesic, J. A. *Science* **2005**, *308*, 1446.
(21) Chheda, J. N.; Dumesic, J. A. *Catal. Today* **2007**, *123*, 59.
(22) Zhu, H.; Cao, Q.; Li, C.; Mu, X. *Carbohydr. Res.* **2011**, *346*, 2016.
(23) Shimizu, K. I.; Uozumi, R.; Satsuma, A. *Catal. Commun.* **2009**, *10*, 1849.
(24) D. Mackay, W. Y. S., K. C. Ma, S. C. Lee; Second Edition ed.; CRC Press, Taylor & Francis Group: 2006; Vol. III.
(25) Sahu, R.; Dhepe, P. L. *ChemSusChem* **2012**, *5*, 751.
(26) Wang, J.; Xu, W.; Ren, J.; Liu, X.; Lu, G.; Wang, Y. *Green Chem.* **2011**, *13*, 2678.
(27) Kuster, B. F. M.; S. van der Baan, H. *Carbohydr. Res.* **1977**, *54*, 165.
(28) Sun, X.; Li, Y. *Angew. Chem. Int. Ed.* **2004**, *43*, 597.
(29) Yao, C.; Shin, Y.; Wang, L. Q.; Windisch, C. F.; Samuels, W. D.; Arey, B. W.; Wang, C.; Risen, W. M.; Exarhos, G. J. *J. Phy. Chem. C* **2007**, *111*, 15141.
(30) Titirici, M. M.; Antonietti, M.; Baccile, N. *Green Chem.* **2008**, *10*, 1204.
(31) Mi, Y.; Hu, W.; Dan, Y.; Liu, Y. *Mater. Lett.* **2008**, *62*, 1194.
(32) Patil, S. K. R.; Lund, C. R. F. *Energy Fuels* **2011**, *25*, 4745.
(33) van Zandvoort, I.; Wang, Y.; Rasrendra, C. B.; van Eck, E. R. H.; Bruijnincx, P. C. A.; Heeres, H. J.; Weckhuysen, B. M. *ChemSusChem* **2013**, *6*, 1745.
(34) Girisuta, B.; Janssen, L. P. B. M.; Heeres, H. J. *Green Chem.* **2006**, *8*, 701.
(35) Sumerskii, I. V.; Krutov, S. M.; Zarubin, M. Y. *Russ. J. Appl. Chem.* **2010**, *83*, 320.
(36) Hu, X.; Lievens, C.; Li, C. Z. *ChemSusChem* **2012**, *5*, 1427.
(37) Prakash, A. M.; Unnikrishnan, S.; Rao, K. V. *Appl. Catal. A: Gen.* **1994**, *110*, 1.
(38) Ashtekar, S.; Chilukuri, S. V. V.; Chakrabarty, D. K. *J. Phy. Chem.* **1994**, *98*, 4878.
(39) Bourgeat-Lami, E.; Massiani, P.; Di Renzo, F.; Espiau, P.; Fajula, F.; Des Courieres, T. *Appl. Catal.* **1991**, *72*, 139.

CHAPTER-6

SUMMARY & CONCLUSIONS

Summary & Novelty of Work

From the green chemistry perspective, for the synthesis of various society needed chemicals, it is desirable to use renewable and inexpensive feedstock, biomass as a replacement for non-renewable and expensive (increasing day-by-day) fossil feedstocks. Moreover, the utilization of biomass can protect our environment by reducing the global warming since it is a carbon neutral process. Hence, the use of biomass for the synthesis of various chemicals gains attraction. Considering these points, I have worked on the development of new catalytic systems for the conversion of mono- and poly-saccharides into furan compounds (furfural, HMF). The thesis is distributed into six chapters of which chapters 2, 3, 4 and 5 discusses the actual work carried out during my Ph.D. degree. The main points from each chapter are summarized below.

In chapter 1, general overview of the topic is described. The compulsion for use of biomass instead of fossil feedstocks is discussed. Later, the types and availability of biomass are summarized. The details on the structures of components of plant derived biomass are presented. This helps in deciding which biomass is preferable to use for the synthesis of desirable value-added chemicals such as furfural and HMF. Due to large availability and potentiality, plant-derived biomass is chosen as substrate in my work. Moreover, the available biomass conversion technologies with their pros and cons are discussed which further allowed me to decide the methodology for efficient biomass conversion into chemicals. Considering all the available methods, I chose to use chemical conversion method since; it converts biomass more efficiently into chemicals under relatively milder reaction conditions. By use of chemical conversion method (hydrolysis and dehydration), the possible products (sugars: xylose, arabinose, glucose, fructose and furans: furfural, 5-hydroxymethylfurfural) from plant-derived biomass are identified and later, the applications of these products are discussed. It is understood from literature that use of homogeneous acid catalysts (chemical method) are not good due to several drawbacks but heterogeneous catalysts (chemical method) can serve better. Hence, a list of commonly used heterogeneous acid catalysts (solid acid catalysts) with their properties (structure, acid amount, types of acid sites and surface area) are summarized. Next, to get a glimpse of available processes for plant-derived

biomass conversion into chemicals (sugars and furans) using solid acid catalysts, literature reports are scrutinized systematically. Based on the discussions of literature reports, it is understood that most of these processes have some drawbacks such as instability of catalysts under reaction conditions (structured catalysts morphology changes), use of edible sugars as substrate (may cause food crisis), low and non-selective yields for products (non-efficient catalytic process) and lack of efficient product isolation method (purification problem). Considering these drawbacks, I tried to develop a methodology for biomass conversion into chemicals using stable solid acid catalysts which may resolve all the issues with current processes and give a better way for the synthesis of chemicals. At the end of the chapter, the hypothesis of my work (for choosing substrate and catalyst) and point-by-point objectives of my work are summarized. It is proposed that SAPO type structured catalysts which are known from the literature as stable catalysts and amorphous metal oxide catalysts can serve the purpose of developing stable, recyclable catalysts in the conversion of poly-saccharides into furans (furfural and HMF).

In chapter 2, details on the catalysts synthesis, characterization methods, composition analysis of crop wastes are discussed. Additionally, experimental details on the catalytic reactions and analysis of reaction mixture are also described. The major findings of chapter 2 are summarized below.

- To develop stable catalysts, two strategies were undertaken; 1) use of hydrothermally stable structured silicoaluminphosphates (SAPO's) and 2) use of amorphous supported metal oxide catalysts which may be also stable since those doesn't have definite pore structure.
- Various methods [hydrothermal for SAPO's and wet-impregnation (WI) & sol-gel (SG) for supported metal oxides] were used for the synthesis of catalysts to understand their influence on catalytic activity.
- Variation of synthesis parameters (crystallization time, precursor concentration) during SAPO preparation were carried out to understand the role of these parameters on the catalytic activity.

- To get an insight on the various properties of catalysts several physico-chemical characterization methods were employed.

  - ☑ TGA analysis carried out with SAPO-44, WO_3/SiO_2 (SG) and Ga_2O_3/SiO_2 (SG) catalysts showed that those are thermally very stable (1000°C).

  - ☑ Phase purity in SAPO's (SAPO-44: CHA, SAPO-5: AFI, SAPO-11: AEL, SAPO-46: AFS) was confirmed with XRD and SEM analysis.

  - ☑ XRD patterns for silica supported metal oxide catalysts notify that SG method uniformly disperses the metal oxides on support and hence only amorphous peak for silica was detected. But, with WI synthesis method crystalline phase for metal oxides was visible in addition to amorphous silica peak. Furthermore, use of ZrO_2 support also showed crystalline phase for metal oxides although, those were synthesized by SG method. This directs that silica is a better support material compared to zirconia for the uniform dispersion of metal oxides.

  - ☑ Local environment around Si, Al and P (in SAPO-44) was confirmed with the help of solid state NMR analysis. The study suggested that Si is present in multiple environment *viz.* [Si(4Al/P)], [Si(3Al/P)(1Si)], [Si(2Al/P)(2Si)], [Si(1Al/P)(3Si)] and [Si(4Si)] however, Al and P are present mainly in tetrahedral environment with small fraction of octahedral environment.

  - ☑ IR analysis confirmed the presence of terminal M=O, M-O-M and O-M-O bonds in supported metal oxide catalysts.

  - ☑ Raman and UV-Vis spectroscopy analysis suggested that SG method produces smaller metal oxide particles but WI method forms bigger particles. Moreover, Raman analysis confirmed the presence of silicotungstic type species only in case of WO_3/SiO_2 (SG) catalyst. This phenomenon highlights that WO_3/SiO_2 (SG) might show better acidity/activity compared to other supported metal oxides.

  - ☑ XPS spectra informed the presence of W^{6+}, Mo^{6+}, Mo^{4+} and Ga^{3+} species in silica supported metal oxide catalysts (SG).

- ☑ TPD-NH_3 analysis showed that SAPO-44 has highest amount of acid sites as well as highest amount of strong acid sites than other SAPO's. Moreover, among supported metal oxide catalysts WO_3/SiO_2 (SG) has highest acid amount and highest strong acid sites. Hence, these two catalysts are expected to show better activity.

- ☑ Pyridine IR analysis confirmed the presence of both Brönsted and Lewis acid sites in SAPO's but mainly Lewis acid sites in supported metal oxides. The calculation of kinetic diameter of probe molecules explain why in SAPO-44 catalyst very low intensity peaks were observed when pyridine was used as probe molecule.

- ☑ Elemental composition of SAPO's was analyzed using ICP-OES method and the data suggested that almost similar concentrations of elements are present in synthesized material as used during synthesis. Further, ICP-OES analysis data illustrated that use of SG method and silica support accommodate higher amount of metals in catalysts than WI method or zirconia support.

- ☑ N_2 sorption analysis showed that SAPO-44 has highest surface area compared to other SAPO's. Moreover, it was found that use of silica as support and SG method for synthesis provides better surface area in supported metal oxide catalysts.

From these characterization data it is expected that SAPO-44 and WO_3/SiO_2 (SG) catalysts may show better catalytic activity since those have higher thermal stability, surface area, acid amount and strong acid sites.

- From a view point of using renewable, abundant and inexpensive feedstock, various plant-derived biomass substrates such as isolated xylans (derived from softwood and hardwood), crop wastes (bagasse, rice husk and wheat straw) and C_6 mono-, di, poly-saccharides (fructose, glucose, maltose, cellobiose, starch) were collected and used for chemical synthesis.

- Detail characterizations of crop wastes were carried out with the help of TAPPI method, TGA analysis and ICP-OES analysis to quantify their compositions. It was

found that pentosan concentration in bagasse and wheat straw are higher (21.4-30%) compared to rice husk (11.2-15.9%).

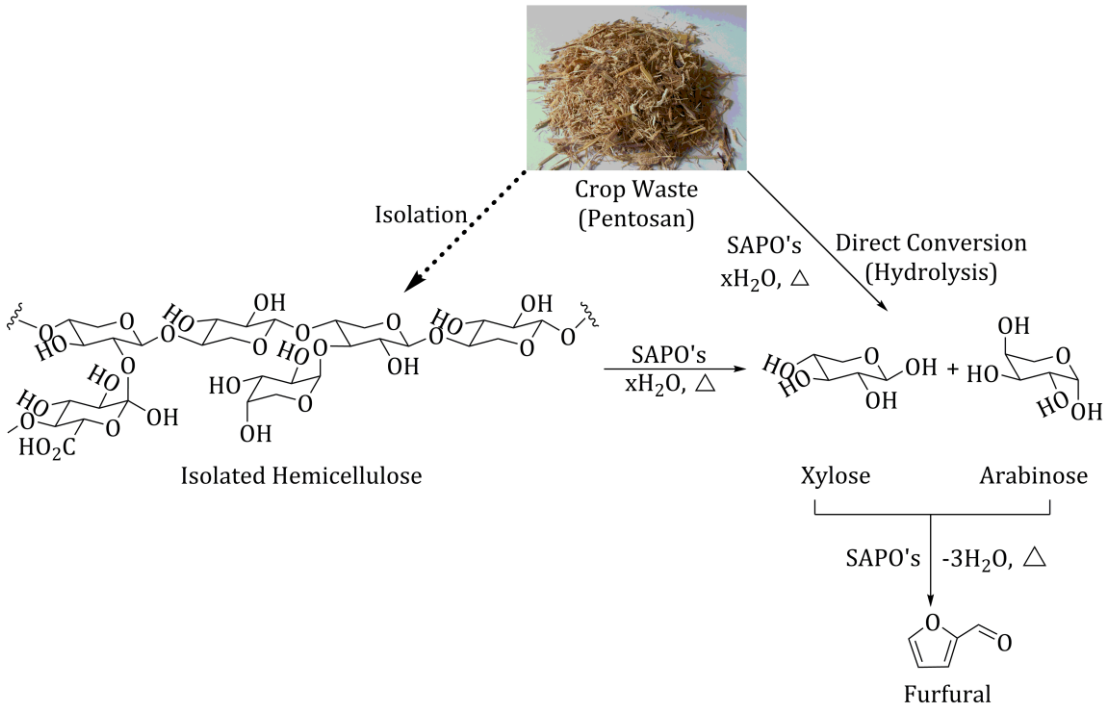

Scheme 6.1. Pathway for the synthesis of C_5 sugars (xylose and arabinose) and furfural from biomass using SAPO catalysts. The dotted arrow shown in this scheme is not my work.

Chapter 3 describes the synthesis of C_5 sugars (xylose, arabinose) and furfural from isolated xylans or pentosan part of crop wastes using structured SAPO catalysts (Scheme 6.1). The major findings from this chapter are briefed below.

- The catalytic activities of all the SAPO's were checked in addition to various other solid acid catalysts (zeolites and Amberlyst-15, Nafion SAC-13 and Nb_2O_5) in isolated xylan (softwood and hardwood) conversion reaction in water + toluene solvents. The results suggested that SAPO-44 is the best active catalyst. Next, to understand the stability of structured catalysts (SAPO-44, SAPO-46, HMOR, HUSY) under reaction conditions, those were reused and it was found that SAPO catalysts are stable but zeolites are not. The SAPO catalysts stability was also further confirmed with the help of XRD analysis. These data informs that, although SAPO catalysts are structured, their morphology remains intact even after use.

- The better catalytic activity of SAPO-44 catalyst compared to zeolites (HMOR) is explained in terms of hydrophilicity-hydrophobicity property (determined by water-organic solvent distribution and TGA analysis) of catalysts. It is suggested that due to higher hydrophilicity of SAPO-44, it tends to remain in water layer and efficiently catalyzes both, hydrolysis and dehydrocyclization reactions. Next, due to good extracting power of toluene to remove formed furfural from water layer where SAPO-44 catalyst is present, reduces the chances of contact between catalyst, furfural and C_5 sugar. This in turn prevents the condensation reaction between sugars and furfural. This helps in achieving higher furfural yields with SAPO-44. But, in case of HMOR catalysts, due to its lower hydrophilicity it distributes itself in both water-toluene layers, which enhances the chances of condensation reactions between furfural and C_5 sugars. This eventually, lowers the furfural yields.
- Since, SAPO-44 was observed as a best catalyst later, the influence of various synthesis parameters (precursor composition, crystallization time, silica concentration) of SAPO-44 was studied. The catalytic results illustrate that precursor composition and crystallization time has influence on the catalytic activity of synthesized catalyst. In Fig. 6.1 effects of precursor composition, silica molar ratio and crystallization time on furfural yields are summarized. It is observed that SAPO-44 catalyst having composition of Si, Al and P precursors, silica concentration of 1.0 molar ratio and treated for 7 days crystallization time showed the best activity.

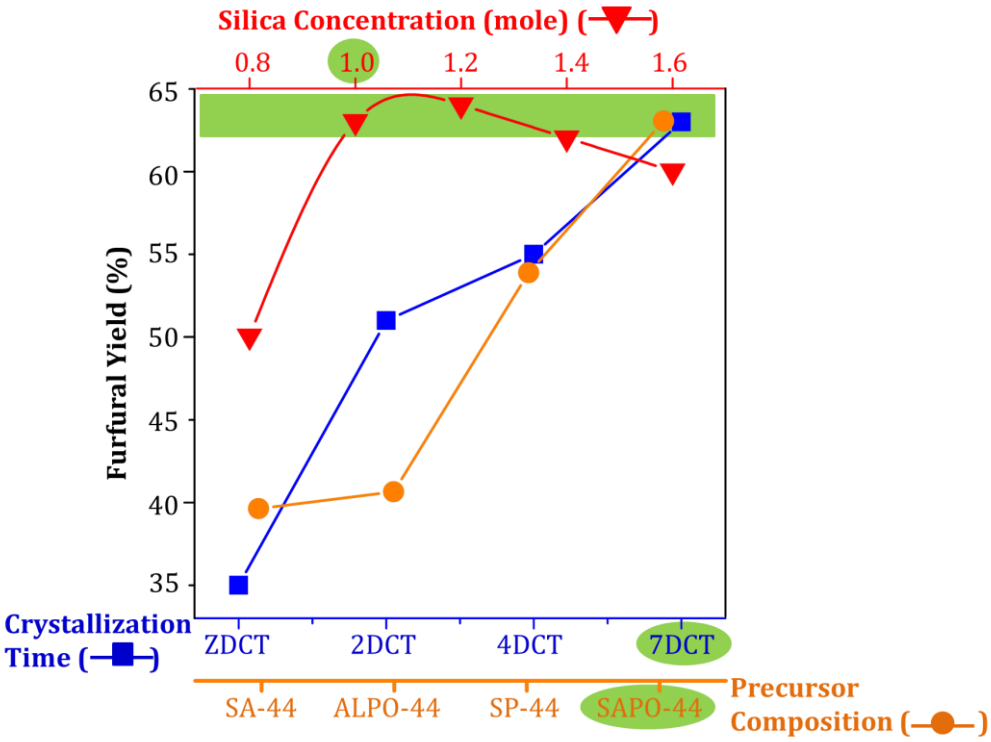

Fig. 6.1. Comparison between variation in catalytic activity (furfural yields) and precursor composition, crystallization time, and silica concentration in SAPO-44. Reaction conditions: xylan (0.3 g), catalyst (0.075 g), water + toluene = 60 mL (1:1 *v/v*), 2 bar N_2 at *RT* (~9 bar at 170°C), 170°C, 8 h.

- pH measurement of various solid acid catalysts dispersed in water proposes that some of the labile protons from catalyst surface travels in water to form hydronium ions (H_3O^+) which can carry out hydrolysis reaction of bigger xylan molecule to form smaller sugars. Next, these sugar molecules are converted /dehydrocyclized into furans over acidic sites.

- It is shown that by modifying the water + toluene solvent ratio to 1:2 (*v/v*) a maximum possible amount of furfural (82%) was formed from isolated xylan in one-pot method.

- All the crop wastes (bagasse, rice husk, wheat straw) were processed under the optimized reaction conditions using SAPO-44 catalyst to yield an extraordinary amount of furfural (86-93%). Moreover, it was shown that mainly pentosan part of crop wastes are converted selectively under the operating conditions.

- Importantly, isolation method for furfural from reaction mixture was shown to separate out furfural in pure form (confirmed with NMR).
- Stability of the SAPO-44 catalyst used in the conversion of variety of substrates under the reaction conditions was approved with the help of several physico-chemical characterizations (XRD, NMR, TPD-NH_3, N_2 sorption, ICP-OES, SEM). Due to higher stability SAPO-44 catalyst showed similar activity in minimum 8 recycle runs for all the substrates.

In chapter 4, various amorphous (no definite pore structure) supported metal oxide catalysts having acidic properties were used for the synthesis of C_5 sugars (xylose, arabinose) and furfural from isolated xylans or pentosan part of crop wastes. For the synthesis of supported metal oxide catalysts, two methods were used namely, wet-impregnation (WI) and sol-gel (SG). Moreover, silica and zirconia supports were used in the synthesis. Below the major findings of this work are summarized.

- The catalytic data informed that SG synthesis method is better compared to WI method in terms of catalyst stability (leaching of metal in WI catalysts) and activity. Moreover, use of silica as support showed better catalytic activity compared to zirconia support.
- Pyridine IR analysis approved that supported metal oxide catalysts mainly have Lewis acid sites and the catalytic results informed that these acid centers are active for both hydrolysis and dehydration reactions. Based on these observations, mechanism for hydrolysis-dehydration reaction was drawn.
- Among all the catalysts, WO_3/SiO_2 (SG) yielded better amount of products (sugars and furfural) from xylan due to higher acid amount (TPD-NH_3), presence of silicotungstic species (Raman), higher acid strength (Hammett acidity), higher surface area and smaller particle size (XRD, UV-Vis and TEM).
- Optimization of reaction parameters allows observance of maximum of 71% furfural yield directly from isolated xylans using WO_3/SiO_2 (SG) catalyst.
- All the crop wastes are also used for the conversion of their pentosan part into very high yields of furfural (72-83%) in presence of WO_3/SiO_2 (SG) catalyst.

- Importantly, it was shown that WO_3/SiO_2 (SG) catalyst is stable under the reaction conditions (XRD, TPD-NH_3, N_2 sorption, TEM) and hence, shows minimum 8 times recycle activity (Fig. 6.2).

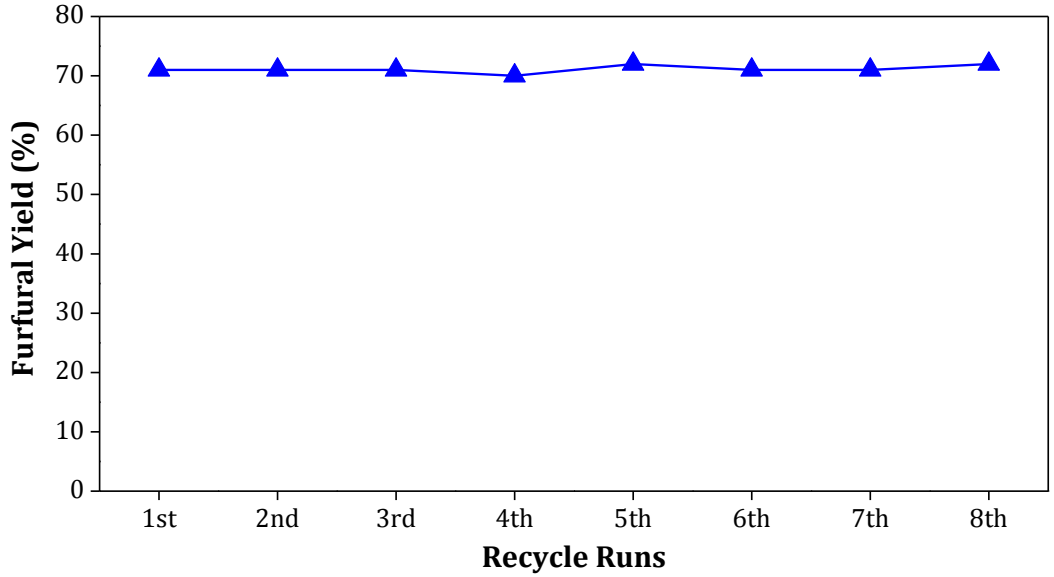

Fig. 6.2. Recycle activity of WO_3/SiO_2 (SG). Reaction cond.: oat spelt xylan (1.0 g), catalyst (0.25g), water + toluene = 60 mL (1:2 *v/v*), 2 bar N_2 at *RT*, 170°C, 10 h.

Chapter 5 deals with the one-pot synthesis of important furan chemical, 5-hydroxymethylfurfural (HMF) from mono-, di- and poly-saccharides (fructose, glucose, maltose, cellobiose and starch) using structured SAPO catalysts (Scheme 6.2). Structured SAPO catalysts were chosen in this work since those have high acid amount and proven as stable catalysts in chapter 3. Below the major findings of this work are summarized.

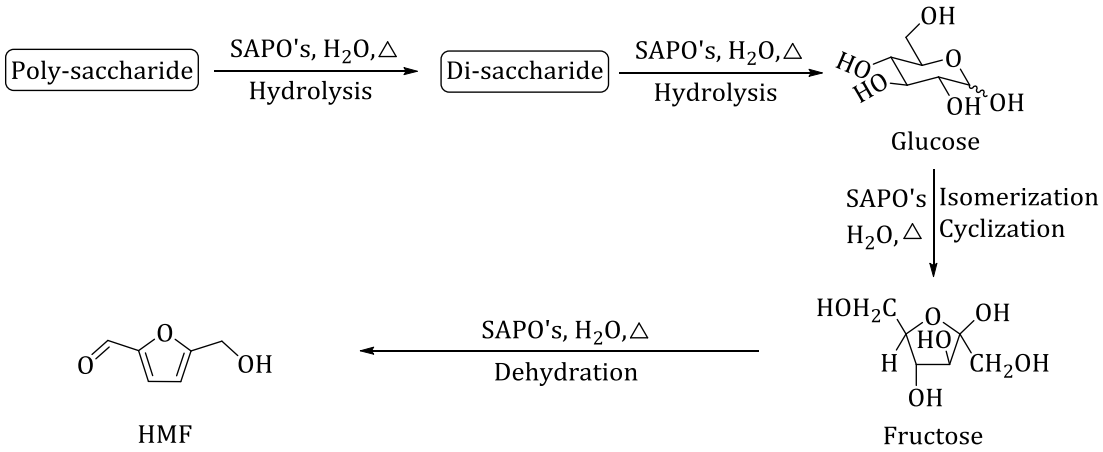

Scheme 6.2. One-pot conversion of poly-, di and mono-saccharides into HMF using SAPO catalysts.

- According to literature, for the conversion of poly-saccharides into HMF three processes are operated namely, hydrolysis (acid catalyzed), isomerization (base catalyzed) and dehydration (acid catalyzed). So, to carry out the complete process, combined use of acid + base catalyst is required in a single-pot which eventually may neutralize the catalytic system to show lower activity. To sort out this issue in my work, SAPO catalysts were used which have both Brönsted and Lewis acid property. It is proposed that the presence of Lewis acid sites in catalysts can isomerize glucose into fructose via 1, 2-hydride shift (section 1.7.2, chapter 1) and both hydrolysis-dehydration reactions can happen in presence of Brönsted acid sites. Hence, one-pot processing of poly-, di- and mono-saccharides into HMF is possible in presence of SAPO catalysts.

- The catalytic results suggested that SAPO-44 is the best active catalyst than other SAPO's since it has higher acid amount, higher strong acid sites, higher surface area and CHA morphology.

- It is observed that some catalysts (zeolite) showed lower furfural formation compared to SAPO-44 catalyst. So, to understand the phenomenon, study on identification of possible degradation reaction pathway was done. When a reaction was carried out using a mixture of substrate having composition of fructose + HMF (1:1 *wt/wt*) in presence of HMOR catalyst, condensation reactions are prominent but SAPO-44 didn't allow condensation reaction (section 5.3, chapter 5).

- Under the optimized reaction conditions, SAPO-44 is well active for the formation of HMF (56-78%) from all the substrates (fructose, glucose, maltose, cellobiose and starch).

- Next, to check SAPO-44 stability, it was recycled in presence of fructose (substrate). The data showed a marginal decrease in HMF yields up to 3rd run and afterwards constant activity up to 5th run in presence of SAPO-44 catalyst. However, in all runs HMF selectivity remains almost similar (80-88%).

- To understand the decrease in catalytic activity, SAPO-44 catalyst (fresh and spent) was subjected to various physico-chemical characterizations. XRD, NMR

and N_2 sorption analysis of fresh and spent SAPO-44 catalysts suggests that SAPO-44 undergoes slight morphological modification under reaction conditions. Due to this modification in SAPO-44 structure, it losses strong acid sites completely hence, total acid amount decreases. However, ICP-OES data suggested that Al and/or P were not leached out in the solution indicating that change in local environment around elements leads to structure change. Moreover, SEM images display similar cubic morphology for both fresh and spent SAPO-44 catalysts. Finally, it can be said that though, structural modification in SAPO-44 catalyst was happening under reaction conditions but the change is not enough to reduce catalytic activity drastically as observed in case of zeolite catalysts.

Finally, in chapter 6 all the major outcome of my work is summarized and later, the novelty of work is discussed.

The novelty of my work is discussed below.

- First time very stable solid acid catalysts are introduced for the synthesis of furans (furfural and HMF) from isolated xylans, crop wastes (lignocelluloses) and various C_6 carbohydrates.
  - ☑ Structured SAPO's and amorphous supported metal oxides
- Detailed crop waste composition analysis by TAPPI and ICP-OES method
  - ☑ 3 types of bagasse, 3 types of rice husk and 1 type of wheat straw
- Extraordinary high and stable yields for furfural from lignocelluloses
  - ☑ Isolated xylans and crop wastes
- One-pot conversion of mono-, di- and poly-saccharides into high yields of HMF
  - ☑ Fructose, glucose, maltose, cellobiose and starch
- Excellent amount of furans isolation in pure form
  - ☑ Furfural = 79%, HMF = 88%
- Detailed characterizations for fresh & spent catalyst to understand catalyst properties and to draw catalyst structure-activity correlation
  - ☑ XRD, NMR, IR, Raman, XPS, UV-Vis, TPD-NH_3, ICP-OES, N_2 sorption, TGA, SEM, TEM

Research Publications

1. Bhaumik, P.; Dhepe, P. L. Influence of properties of SAPO's on the one-pot conversion of mono-, di- and poly-saccharides into 5-hydroxymethylfurfural. *RSC Advances* **2013,** *3* (38), 17156-17165.

2. Bhaumik, P.; Dhepe, P. L. Efficient, stable, and reusable silicoaluminophosphate for the one-pot production of furfural from hemicellulose. *ACS Catalysis* **2013,** *3* (10), 2299-2303.

3. Bhaumik, P.; Deepa, A. K.; Kane, T.; Dhepe, P. L. Value addition to lignocellulosics and biomass-derived sugars: an insight into solid acid-based catalytic methods. *Journal of Chemical Sciences* **2014,** *126* (2), 373-385.

4. Bhaumik, P.; Dhepe, P. L. Exceptionally high yields of furfural from assorted raw biomass over solid acids. *RSC Advances* **2014,** *4* (50), 26215-26221.

5. Bhaumik, P.; Kane, T.; Dhepe, P. L. Silica and zirconia supported tungsten, molybdenum and gallium oxide catalysts for the synthesis of furfural. *Catalysis Science & Technology* **2014,** *4* (9), 2904-2907.

6. Bhaumik, P.; Dhepe, P. L. Effects of careful designing of SAPO-44 catalysts on the efficient synthesis of furfural. *Catalysis Today* **2014,** DOI:10.1016/j.cattod.2014.10.042.

7. Bhaumik, P.; Dhepe, P. L. Solid Acid Catalyzed Synthesis of Furans from Carbohydrates (Review). *Manuscript under revision,* **2014**.

8. Bhaumik, P.; Dhepe, P. L. From Lignocellulosic Biomass to Furfural: Catalytic Insight on Supported Metal Oxides. *Manuscript under Preparation* **2014**.

9. Bhaumik, P.; Dhepe, P. L. Conversion of Biomass into Sugars (Book chapter for RSC Green Chemistry Series). *Manuscript under Preparation* **2015**.

Work Presented

1. Poster presented entitled "Hemicellulose hydrolysis using new solid acid catalysts" during *"15th National Workshop on the Role of Materials in Catalysis (2011)"* held at IIT-Madras, Chennai, India.

2. Poster presented entitled "Conversion of hemicellulose using metal oxide catalysts" during *"National Seminar on Current Trends in Industrial Catalysts (2012)"* held at CSIR-NCL, Pune, India.

3. Poster presented entitled "Conversion of hemicellulose using solid acid catalysts" during *"National Science Day Celebration (2012)"* held at CSIR-NCL, Pune, India.

4. Poster presented entitled "Conversion of hemicellulose using solid acid catalysts" during *"21st National Symposium on Catalysis (2013)"* held at IICT, Hyderabad, India.

5. Poster presented entitled "Efficient and re-usable SAPO catalysts for the selective production of furans from biomass" during *"2nd International Congress on Catalysis for Bio-refineries (2013)"* held at Dalian Institute of Chemical Physics (DICP), Dalian, China.

6. Poster presented entitled "Efficient and re-usable SAPO catalysts for the selective production of furans from biomass" and "Conversion of hemicellulose using supported metal oxides" during *"National Science Day Celebration (2014)"* held at CSIR-NCL, Pune, India.

List of Award Received

1. **Chinese Journal of Catalysis Best Poster Award:** *"2nd International Congress on Catalysis for Bio-refineries (CatBior 2013)"* held at Dalian Institute of Chemical Physics (DICP), Dalian, China.

2. **NCL-RF Agnimitra Memorial Best Poster Award:** *"National Science Day 2014 Celebration"* held at CSIR-National Chemical Laboratory (NCL), India.